THERMODYNAMICS AND MECHANISMS OF SORPTION FOR HYDROPHOBIC ORGANIC COMPOUNDS ON NATURAL AND ARTIFICIAL SORBENT MATERIALS

By

KENT BENSON WOODBURN

A DISSERTATION PRESENTED TO THE GRADUATE SCHOOL
OF THE UNIVERSITY OF FLORIDA IN
PARTIAL FULFILLMENT OF THE REQUIREMENTS
FOR THE DEGREE OF DOCTOR OF PHILOSOPHY

UNIVERSITY OF FLORIDA

1985

ACKNOWLEDGMENTS

My sincere and heartfelt thanks go to my advisor, Dr. Joseph Delfino, whose guidance, scientific insight, and encouragement were instrumental in the completion of this project. I would also like to thank Dr. Suresh Rao, Dr. Peter Nkedi-Kizza, and Dr. Arthur Hornsby for their generous assistance and helpful comments and criticisms. Special thanks go to Dr. Rao for his guidance and support over the past two years and Dr. John Dorsey for technical assistance and guidance in the liquid chromatography experiments.

I would like to thank the students and staff of the Environmental Engineering Sciences Department and the Soil Science Department for their kind support and assistance. I would especially like to thank Ms. Linda Lee and Mr. Sture Edvardsson of the Soil Science Department for their able technical assistance in many aspects of this work. Special thanks must go to Mr. Ron Jessup of the Soil Science Department for assistance in statistical and mathematical operations and for his insight and guidance in the understanding of thermodynamic processes. My sincere thanks also go to

Ms. Barbara Smerage for her expert typing and proofreading of this dissertation.

Finally, this work would never have been possible without the support of my wife, Janet, whose love and friendship have tempered the pains of research during the past three years. My thanks and loving appreciation go to my parents and family, who have shown unfailing support during my many years of graduate study.

This research was funded by the United States Environmental Protection Agency, cooperative agreement #CR-811144. This financial support is gratefully acknowledged.

TABLE OF CONTENTS

LIST OF TABLES

LIST OF FIGURES

Abstract of Dissertation Presented to the Graduate School
of the University of Florida in Partial Fulfillment of
the Requirements for the Degree of
Doctor of Philosophy

THERMODYNAMICS AND MECHANISMS OF SORPTION FOR
HYDROPHOBIC ORGANIC COMPOUNDS ON NATURAL
AND ARTIFICIAL SORBENT MATERIALS

By

Kent Benson Woodburn

August 1985

Chairman: Professor Joseph J. Delfino
Major Department: Environmental Engineering Sciences

Reversed-phase liquid chromatography (RPLC) was used to investigate the thermodynamics and mechanisms of sorption for hydrophobic organic chemicals retained on C-2, C-4, C-8, and C-18 RPLC supports in polar solvent mixtures. The mobile phase consisted of methanol or acetonitrile in binary combinations with water, and the test solutes were various alkylbenzenes, polycyclic aromatic hydrocarbons (PAHs), and the mono-substituted halobenzenes.

The mechanism of retention for hydrophobic organic compounds in the soil or groundwater environment is currently a topic of considerable interest. An enthalpy-entropy compensation model was used to study sorption interactions on a carbonaceous surface soil compared to the RPLC stationary phases. For a methanol/water solution of three PAH solutes on the surface soil material, the measured

compensation temperature (β) was 573°K. This temperature compares favorably with β values obtained for PAH compounds in methanol/water RPLC systems. This indicates that the mechanism of retention is the same in both systems. This finding should facilitate the study of soil sorption interactions, as RPLC is an effective surrogate for studying the sorption of hydrophobic compounds in a soil environment.

The standard sorption enthalpy and entropy changes, ΔH^{o} and ΔS^{o}, respectively, decreased as the water content of the eluent and the hydrocarbonaceous surface area (HSA) of the solute molecules were increased in methanol/water and acetonitrile/water RPLC systems. A single linear regression line described the relationship of ΔH^{o} to solute HSA in both eluent systems. However, plots of ΔS^{o} vs. solute HSA produced separate linear regression lines for the alkylbenzenes compared with PAH and halobenzene compounds.

In methanol/water and acetonitrile/water mobile phases, the thermodynamics and mechanisms of RPLC retention were different for the alkylbenzene solutes compared with PAH and halobenzene compounds. The occurrence of two distinct RPLC retention mechanisms is a unique finding of this work.

The solvophobic theory of RPLC retention provided an excellent model for describing the solute sorption data in acetonitrile/water RPLC systems based on known solvent properties. The results indicate that solute-stationary phase interactions change considerably as one progresses from the C-2 to C-18 stationary phase carbon chains.

CHAPTER I
INTRODUCTION

The contamination of subsurface water supplies is a topic of considerable scientific and public interest. Much of the recent concern centers on the presence of a variety of hydrophobic organic chemicals in these water supplies. The sources of these chemicals include agricultural and silvicultural practices (pesticides), accidental spills and leaks, as well as surface and subsurface disposal of organic wastes. Research has established that sorption and degradation (biotic and abiotic) are the two major processes attenuating the transport of organic chemicals in soils. The high potential sorption capacity of soils thus allows the sorption process to play an important role in the potential for groundwater contamination due to these compounds. A thorough understanding of sorption mechanisms and thermodynamics would greatly improve our ability to model and predict solute transport in the soil and groundwater environment.

Historically, most of the sorption data for hydrophobic organic chemicals have been collected in batch systems, which do not easily lend themselves to thermodynamic experimentation. Recent advances in reversed-phase liquid

chromatography (RPLC) suggest that this technique may be a model system for the study of sorption of hydrophobic organic chemicals on soil materials. The RPLC technique involves the use of a chemically bonded nonpolar stationary phase and a polar mobile phase of water mixed with a water-miscible organic solvent, such as methanol. This form of liquid chromatography offers a well-tested experimental technique and a sound theoretical background for obtaining data on solute-sorbent interactions. The method is less cumbersome than traditional batch techniques and may be easily modified for the collection of thermodynamic sorption data.

This dissertation presents a detailed discussion of the application of RPLC as a technique for investigating the thermodynamics and mechanisms of sorption for hydrophobic organic chemicals on nonpolar surfaces. The sorptive behavior of such solutes was also studied in a natural soil environment to compare and contrast the solute-sorbent interactions in the RPLC and soil systems.

CHAPTER II
OBJECTIVES

The main objectives of this study were

(1) To examine the thermodynamics and mechanisms of sorption for a variety of hydrophobic solutes on RPLC surfaces;

(2) To examine the thermodynamics of sorption for several hydrophobic compounds on a highly carbonaceous soil surface; and

(3) To apply the solvophobic model of Horvath et al. (1976) to solute retention on RPLC surfaces and to examine solute-sorbent interactions using this retention model.

CHAPTER III
LITERATURE REVIEW

3.1 Introduction

This chapter will present a review of the pertinent literature for each of the major subject areas covered in this work: the solvophobic theory of hydrophobic interactions; the thermodynamics of sorption processes; and enthalpy-entropy compensation effects.

3.2 Overview

The contamination of subsurface water supplies is currently a topic of considerable concern among scientists, legislators, and the general public. Nearly one-half of the population of the United States use groundwater as its primary source of drinking water. Approximately 35 percent of the municipal drinking water supplies come from groundwater, and 75 percent of major U.S. cities currently depend on groundwater as their principal water source (Pye and Patrick, 1983; Todd, 1980). Although groundwater contamination has occurred for centuries, population demands, agricultural activities, and increased industrialization have greatly exacerbated the problem in some areas. As our

dependence on groundwater increases, its quality becomes an increasingly important issue.

Much of the concern over groundwater quality centers on the presence of anthropogenic organic compounds in these systems. The route of entry for such compounds may include agricultural practices, accidental spills, and surface and subsurface disposal of chemical wastes. In response to this problem, there exists a need for better understanding of the transport of organic chemicals in the unsaturated soil zone. Research has established the phenomenon of adsorption onto soil materials as a principal attenuation mechanism in the transport of organic solutes. Historically, adsorption and desorption data have been determined by batch equilibrium experiments using single solvent-single sorbate systems. Solute leaching data have been obtained primarily by the use of two methods: soil thin-layer chromatography or STLC (Helling, 1971) and miscible displacement (MD) through soil columns. Each technique has its own inherent strengths and weaknesses. While STLC is less complicated to perform than soil column experiments, the results do not adequately reflect the dynamic conditions present in a natural soil system. Miscible displacement techniques reflect actual soil conditions better; however, a considerable amount of time and experience are required to produce reproducible results.

High-performance liquid chromatography (HPLC) is a chemical separation technique which exploits the differential distribution of sample components between two distinct physical phases. One of these phases is a stationary support or sorbent, while the other is a liquid mobile phase percolating through the column bed. The chromatographic separation process occurs due to repeated sorption-desorption steps during solute transport through the stationary support. Separation of sample components is due to differences in their distribution activities between the two phases.

There are numerous subgroups of HPLC. In general, the divisions are based on the nature of the stationary phase and the separation process. One of the most popular modes of separation, reversed-phase liquid chromatography, involves a stationary phase which is nonpolar in nature and a mobile phase composed of a polar liquid, such as water or a water/methanol mixture. Thus, the more nonpolar a solute, the longer it will be retained on the nonpolar stationary support.

Recent advances in reversed-phase liquid chromatography (RPLC) suggest that this technique may be applicable as a model for natural soil systems, given the appropriate selection of the sorbent/solvent system. This particular form of modern liquid chromatography may best simulate the natural sorption conditions present in soils. Adsorption and

thermodynamic data determined by RPLC may be more representative of the conditions present in soil than batch equilibrium techniques. It is worth noting at this time that the term "sorption" is often used interchangeably with "adsorption" when speaking of solute retention on soils or RPLC supports. The fundamental processes of solute retention on RPLC and soil surfaces are not well understood; hence, the term "sorption" indicates our lack of knowledge over whether adsorptive, absorptive, or partitioning mechanisms control retention. Mingelgrin and Gerstlz (1983) recently reviewed this topic in considerable depth.

The evidence supporting the use of reversed-phase columns as models of varying soil environments may be found in the recent chromatographic literature. Veith et al. (1979) demonstrated the relationship between a chemical's corrected retention time (k') on an octadecylsilane RPLC column and its octanol/water partition coefficient (K_{ow}). The work of Karickhoff et al. (1979) and Kenega and Goring (1980) showed the excellent correlation which exists between K_{ow} and K_{oc}, the carbon-normalized soil sorption coefficient. Swann et al. (1979) and Rao and Nkedi-Kizza (1983) reported on the correlation between measured K_{oc} and octadecylsilane retention time for selected organic solutes. Finally, the research of McCall et al. (1981) presented a solute mobility classification system based on a compound's RPLC retention time. A linear correlation was observed

between soil column leaching distance and RPLC retention time.

Although sorption onto soil material is critically important in attenuating the transport of organic solutes, little is known of the thermodynamics of the sorption process(es). Chromatographic techniques are well suited to thermodynamic studies, and this approach may be applicable for examining liquid-phase sorption reactions in soils and chromatographic media. The following sections will outline the use of RPLC as a model for solute transport in aqueous and mixed-solvent conditions. The focus of this chapter will be the thermodynamic basis of sorption and how the energetics of the sorptive process may be studied and evaluated.

3.3 Solvophobic Model of Hydrophobic Sorption

One of the most widely accepted models used to describe solute retention on hydrophobic surfaces (RPLC packings, pyrocarbon, etc.) is termed the solvophobic or hydrophobic theory (Horvath and Melander, 1977; Horvath et al., 1976). Among all the theories put forward to describe nonpolar interactions in polar solvents, only the solvophobic model treats such processes in terms of the bulk solvent properties, such as surface tension and the dielectric constant, and solute properties, such as surface area and dipole moment. These properties are generally available from the

literature or may be estimated from structure-activity relationships or molecular models.

According to the solvophobic model, the hydrophobic interaction between a solute molecule and the surface of the nonpolar RPLC packing material is considered a reversible association between the solute molecule, S, and the hydrocarbonaceous ligand, L, resulting in a complex, LS

$$S + L \rightleftharpoons LS \tag{3-1}$$

Three important parameters govern the strength of association between L and S and hence the retention of solute S:

(1) the hydrocarbonaceous surface area of the solute, HSA_s;

(2) the hydrocarbonaceous surface area of the ligand, HSA_l;

(3) the surface tension, γ, of the bulk solvent.

In dissolving a hydrophobic compound in a solvent mixture, the original solvent structure must be disrupted and a cavity formed for the hydrophobic or nonpolar portion of the molecule that cannot interact significantly with the polar solvent. The energy required for cavity formation ($\Delta G^o{}_{cav}$) is proportional to the surface tension (γ) of the solvent and to the hydrocarbonaceous surface area of the solute molecule (HSA_s). The surface tension is used here as an indication of intermolecular solvent forces, which

increase as a direct function of γ. Additionally, the larger the HSA_s value, the greater will be the $\Delta G^o{}_{cav}$ required for the molecule.

The driving force for the dispersive interactions between the hydrophobic solute and the hydrocarbonaceous ligand is thought to be the tendency of the polar solvent (water, water/methanol mixture, etc.) to minimize the hydrophobic surface created about the solute-ligand complex (HSA_{sl}). Quite simply, the polar mobile phase "drives" the hydrophobic solute toward the stationary phase rather than any inherently strong attraction existing between S and L. The net energy of interaction is determined largely by the hydrophobic contact area, ΔA, of the LS complex ($\Delta A = HSA_s + HSA_l - HSA_{sl}$), and the solvent surface tension, γ. Higher values of ΔA or γ lead to more energy being liberated during the association of L and S and subsequently cause the retention of S to be stronger.

In applying this theory to chromatography with nonpolar reversed-phase supports, it is necessary to relate the measured solute retention factor, k', to the ΔG^o for the binding process

$$k' = \phi K \tag{3-2}$$

where K is the thermodynamic equilibrium binding constant and ϕ is the phase ratio or the volume ratio of the

stationary and mobile phases. The solvophobic theory may now be used to establish a quantitative relationship between k' and the properties of the solvent and solute.

To evaluate the equilibrium constant, K, K must be related to the free energy change for the chromatographic binding process. Recall that

$$\ln K = -\Delta G^o/RT \tag{3-3}$$

where R is the universal gas constant and T is the absolute temperature (°K). Since the value of ΔG^o for the binding process is independent of the path taken, we may now write the association reaction as follows:

$$\begin{tikzcd}
S(g) \arrow[d, shift left] & + & L(g) \arrow[d, shift left] \arrow[rr, rightleftharpoons, "\Delta G_{vdw,assoc}"'] & & SL(g) \arrow[d, shift left] & (3\text{-}4) \\
S(l) \arrow[u, shift left, "\Delta G^o_s"] & + & L(l) \arrow[u, shift left, "\Delta G^o_l"] \arrow[rr, rightleftharpoons, "\Delta G^o_{assoc}"'] & & SL(l) \arrow[u, shift left, "\Delta G^o_{sl}"] & (3\text{-}5)
\end{tikzcd}$$

where g and l represent the gaseous and liquid phases, respectively. The molecular associations in solution can be conceptually broken down into two processes. One is the interaction of S and L to yield SL in a hypothetical gas

phase without interaction of the solvent. The second, more involved process entails the interaction of all species with the solvent. The free energy of the binding process in solution is merely the difference between these respective terms.

The association of S and L in the gas phase is assumed to occur by van der Waals forces only, and the free energy change is denoted by $\Delta G_{vdw,assoc}$. The standard free energy change associated with bringing each component (S, L, and SL) from the hypothetical gas phase into the solvent is considered mathematically as the sum of two parts. The first part corresponds to the free energy, ΔG_{cav}, required to prepare a solvent cavity of suitable size and shape for the solute. The second term, ΔG_{int}, expresses the interaction energy between the solute and solvent. This latter expression also contains a term which accounts for the entropy of mixing which arises upon mixing the solute and solvent. The entropic term accounts for the distance a solvent molecule can freely move before striking another solvent molecule. These processes and the associated terms are shown in Figure 3-1. In summary, the total standard free energy change for the solvation of species i is given by

$$\Delta G^{o}_{i} = \Delta G_{cav,i} + \Delta G_{int} + RT\ln(RT/P_{o}V) \qquad (3\text{-}6)$$

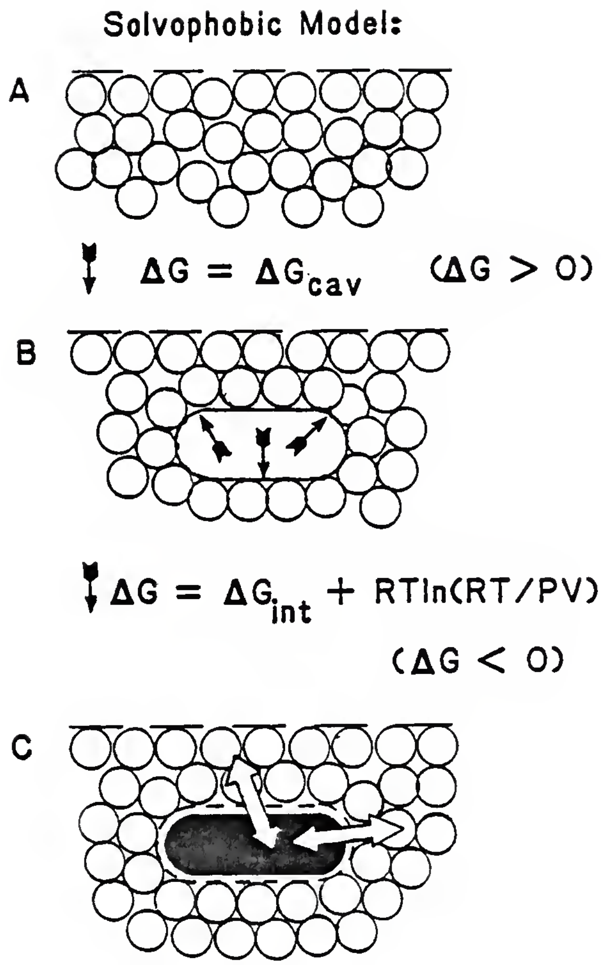

Figure 3-1. Schematic illustration of dissolving a hydrophobic solute into a polar solvent. The free energy change involved in formation of a suitable cavity, depicted in A to B, is ΔG_{cav}. The magnitude of ΔG_{cav} is determined by the cavity surface area and the surface tension of the solvent and is greater than zero. In B to C, the solute is placed in the cavity and interacts with the solvent. The free energy change of interaction is ΔG_{int} and the free energy change of mixing is $T(R \ln(RT/PV))$, where $R \ln(RT/PV)$ is the entropy change of mixing. The total free energy change of interaction is less than zero.

where V is the molar volume (cm^3/mole) of the solvent and P_o is the standard atmospheric pressure (1 atm).

The overall standard free energy change for the association of S and L in solution, ΔG^o_{assoc}, is given by

$$\Delta G^o_{assoc} = \Delta G_{vdw,assoc} + (\Delta G^o_{sl} - \Delta G^o_{s} - \Delta G^o_{l}) \qquad (3\text{-}7)$$

which can be expanded to

$$\Delta G^o_{assoc} = \Delta G_{vdw,assoc} + (\Delta G_{cav,sl} + \Delta G_{int,sl}) - (\Delta G_{cav,s} + \Delta G_{int,s}) - (\Delta G_{cav,l} + \Delta G_{int,l}) - RT\ln(RT/P_oV) \qquad (3\text{-}8)$$

The individual terms have been evaluated (Horvath and Melander, 1977; Horvath et al., 1976; Sinanoglu, 1968). The free energy of cavity formation for any species is given approximately by

$$\Delta G_{cav,i} = K^e_i HSA_i \, \gamma(1 - W_i)N \qquad (3\text{-}9)$$

where HSA_i is the hydrocarbonaceous surface area of species i, γ is the surface tension (dyne/cm) of the bulk solvent, N is Avogadro's number, and

$$W_i = (1 - K^s_i/K^e_i)(d\ln\gamma/d\ln T + 2/3A_iT) \qquad (3\text{-}10)$$

where A_i is the coefficient of thermal expansion for species i. The term $K^e{}_i$ is the ratio between the energy required for formation of a suitably shaped cavity of surface area HSA_i and the energy required to expand the planar surface of the solvent by the same amount, which is approximately $(HSA_i\gamma)$. In other words, because the cavity surface has a small radius of curvature, the surface tension of the cavity will differ from that of the bulk solvent by a proportionality factor, $K^e{}_i$. The term $K^s{}_i$ is the corresponding function for the entropy produced upon formation of the solute cavity. The K^e values have been computed and tabulated for a number of pure solvents (Halicioglu and Sinanoglu, 1969; Horvath et al., 1976). The $K^e{}_i$ value for species i may be estimated (Horvath et al., 1976) by

$$K^e{}_i = 1 + (K^e - 1)(V/V_i)^{2/3} \tag{3-11}$$

where K^e is evaluated for the pure solvent, and V and V_i are the molar volumes (cm^3/mole) of the solvent and species i, respectively. A similar relationship may be developed for $K^s{}_i$. Both $K^e{}_i$ and $K^s{}_i$ approach unity as the size of the solute molecule increases with respect to the size of the solvent molecules.

The second term in Eqn. (3-6) expresses the interaction of species i with the solvent. It is generally

assumed to be the sum of a van der Waals component, $\Delta G_{vdw,i}$, and electrostatic free energy term, $\Delta G_{es,i}$

$$\Delta G_{int,i} = \Delta G_{vdw,i} + \Delta G_{es,i} \tag{3-12}$$

The van der Waals contribution has been estimated by Sinanoglu (1968). These calculations suggest that the van der Waals free energy can be reliably estimated by

$$\Delta G_{vdw,i} = Y + aHSA_i \tag{3-13}$$

where Y and a are solvent-dependent parameters and HSA_i is the hydrocarbonaceous surface area of the species of interest. Therefore, the contribution to the binding energy from van der Waals forces may be expressed as

$$\Delta G_{vdw,assoc} = -Y - a\Delta A \tag{3-14}$$

where all terms are as denoted earlier.

The electrostatic free energy change, $\Delta G_{es,i}$, has been evaluated for a number of cases (Horvath et al., 1976; Sinanoglu, 1968). In the case of simple dipoles, this energy has been approximated using the following expression:

$$\Delta G_{es,i} = -N \mu_i^2 \Gamma P/2 v_i \tag{3-15}$$

where μ_i is the static dipole moment of species i, v_i is the molecular volume of i, and Γ is a function of the static dielectric constant of the solvent, ε, as given by

$$\Gamma = 2(\varepsilon - 1)/(2\varepsilon + 1) \tag{3-16}$$

The term P depends on the polarizability of species i, α_i, as

$$P = [4\pi\varepsilon_o(1 - \Gamma\alpha_i/v_i)]^{-1} \tag{3-17}$$

where ε_o is the permittivity constant. The term P is essentially independent of solvent composition (Horvath and Melander, 1977).

Upon combining Eqns. (3-8), (3-9), (3-12), and (3-15), an expression is generated for the standard free energy change for the overall binding process

$$\begin{aligned}\Delta G^o_{assoc} = {} & \Delta G_{vdw,assoc} + [\Delta G_{vdw,sl} - N\mu_{sl}^2\ \Gamma P/2v_{sl} \\ & K^e_{sl}HSA_{sl}\ \gamma(1 - W_{sl})N] - [\Delta G_{vdw,s} \\ & - N\mu_s^2\ \Gamma P/2v_s + K^e_s HSA_s\ \gamma)1 - W_s)N] \\ & - [\Delta G_{vdw,l} - N\mu_l^2\ \Gamma P/2v_l \\ & + K^e_l HSA_l \gamma(1 - W_l)N] - RT\ln(RT/P_oV)\end{aligned} \tag{3-18}$$

In most chromatographic systems, the solvent molecules (water, methanol, etc.) are much smaller than the solute molecules of interest. Hence, the following assumptions appear to be quite reasonable

$$W_{sl} = W_s = W_l = 0 \tag{3-19}$$

$$\Delta G_{vdw,sl} = \Delta G_{vdw,l} \tag{3-20}$$

$$\mu_{sl} = \mu_s \tag{3-21}$$

$$\mu_l = 0 \tag{3-22}$$

and

$$K^e_{sl} = K^e_l = 1 \tag{3-23}$$

An assessment of the molecular volume of the complex (v_{sl}) is necessary for the model, and for convenience this volume is assumed to be a multiple of the molecular volume of the solute (v_s)

$$v_{sl} = \lambda v_s \tag{3-24}$$

where λ is a proportionality constant. The total hydrophobic surface area of the complex (SL) is expressed by

$$HSA_{sl} = HSA_s + HSA_l - \Delta A \tag{3-25}$$

where ΔA is once again the contact surface area of the associated species. Combining the assumptions from Eqns. (3-19)-(3-25) with Eqn. (3-18) yields

$$\Delta G^o_{assoc} = \Delta G_{vdw,assoc} - \Delta G_{vdw,s} + N(\lambda - 1)\mu_s^2 \ \Gamma P/2\lambda v_s$$
$$- N\Delta A\gamma - N(K^e_s - 1)HSA_s\gamma$$
$$- RT\ln(RT/P_oV) \tag{3-26}$$

Substituting the expression for K^e_s from Eqn. (3-11) produces the final expression for ΔG^o_{assoc}

$$\Delta G^o_{assoc} = \Delta G_{vdw,assoc} - \Delta G_{vdw,s} + N(\lambda - 1)\mu_s^2 \ \Gamma P/2\lambda v_s$$
$$- N\Delta A\gamma - N\gamma(K^e - 1)HSA_s(V/V_s)^{2/3}$$
$$- RT\ln(RT/P_oV) \tag{3-27}$$

It is now possible to relate the measured solute retention factor, k', to the standard free energy of the binding process, ΔG^o_{assoc}. Combining Eqns. (3-2), (3-3), and (3-27) produces the following expression for the solute retention factor:

$$\ln k' = \ln \phi - 1/RT[\Delta G_{vdw,assoc} - \Delta G_{vdw,s} + N(\lambda - 1)\,\mu_s^{\,2}\,\Gamma P/2\lambda v_s - N\Delta A\gamma - N\gamma(K^e_s - 1)HSA_s(V/V_s)^{2/3} - RT\ln(RT/P_oV)] \quad (3\text{-}28)$$

The above expression may be further simplified by assuming that the solute, ligand, and complex all have spherical shapes. Following Sinanoglu (1968) and Horvath et al. (1976), it is possible to calculate the nonpolar surface area of the solute by

$$HSA_s(cm^2) = 4.836v_s^{\,2/3} = 4.836(V_s/N)^{2/3} \quad (3\text{-}29)$$

where V_s(cm^3/mole) is the solute's molar volume. Combining Eqns. (3-9), (3-11), and (3-29) with the assumption of W = 0 (Eqn. 3-19) yields

$$\Delta G_{cav,s} = NHSA_s\gamma + 4.836N^{1/3}(K^e - 1)V^{2/3}\gamma \quad (3\text{-}30)$$

The combination of Eqns. (3-2), (3-3), (3-8), (3-11), (3-12), (3-15), and (3-30), with the assumption of Eqns. (3-19) to (3-23), yields the following expression for the retention factor, k'

$$\ln k' = \ln\phi - 1/RT[\Delta G_{vdw,assoc} - \Delta G_{vdw,s}$$
$$+ N(\lambda - 1)\ \mu_s^2\ \Gamma P/2\lambda\ v_s - N\Delta A\gamma$$
$$- 4.836N^{1/3}(K^e - 1)V^{2/3}\gamma - RT\ln(RT/P_oV) \quad (3\text{-}31)$$

The expression for the solute retention factor as given in Eqn. (3-31) may now be simplified for certain chromatographic situations. For any given solute/sorbent combination, the temperature and flow rate may be considered constant while solvent composition may be easily changed. Under these conditions, solute and ligand properties may be considered constant, as well as $\Delta G_{vdw,assoc}$. Hence, Eqn. (3-31) may be rewritten as

$$\ln k' = (A + E) + B\Gamma + C\gamma + D(K^e - 1)V^{2/3}\gamma$$
$$+ \ln(RT/P_oV) \quad (3\text{-}32)$$

where the terms are defined as

$$A = \ln\phi - \Delta G_{vdw,assoc}/RT \quad (3\text{-}33)$$

$$B = (1 - \lambda)\ \mu_s^2\ NP/2\lambda RTv_s \quad (3\text{-}34)$$

$$C = N\Delta A/RT \quad (3\text{-}35)$$

$$D = 4.836N^{1/3}RT = 1.67 \times 10^7\ \text{mole}^{2/3}/\text{l-atm} \quad (3\text{-}36)$$

$$E = \Delta G_{vdw,s}/RT \quad (3\text{-}37)$$

Rearranging terms, Eqn. (3-32) becomes

$$\ln k' - D(K^e - 1)V^{2/3}\gamma - \ln(RT/P_oV) = (A + E) + B\Gamma + C\gamma \tag{3-38}$$

The K^e terms for cavity formation may be determined (Horvath et al., 1976) from the molar volume (V), the heat of vaporization (ΔE_{vap}), and surface tension (γ) of the solvent at the temperature of interest, in addition to the temperature derivative of the surface tension and the thermal coefficient of expansion (A_i) by

$$K^e = \frac{N^{1/3} \quad \Delta E_{vap}}{V^{2/3}\gamma\ (1 - \frac{d \ln \gamma}{d \ln T} - \frac{2}{3} A_i T)} \tag{3-39}$$

These physicochemical properties are generally known for solvents of chromatographic interest or can be reliably estimated (Horvath et al., 1976).

There are literature data on density (Carr and Riddick, 1951; Timmermans, 1960), dielectric constant (Akerlof, 1932; Douhert and Morenas, 1967), surface tension (Horvath et al., 1976), and K^e (Horvath et al., 1976; Wells, 1981). Using such data, all terms except (A + E), B, C, and ln k' may be calculated for a given solvent composition in which k' is experimentally determined. A linear regression of the terms on the left side of Eqn. (3-38) versus Γ and γ will produce

values of (A + E), B, and C as regression coefficients. Once these terms are evaluated, estimates of k' are possible at any solvent composition.

A number of researchers have validated the "solvophobic effect" and its importance in the retention of nonpolar solutes on reversed-phase supports (Colin et al., 1983; Horvath and Melander, 1977; Horvath et al., 1976; Miller et al., 1982; Wells and Clark, 1982; Wells and Clark, 1984), and hydrophobic soils and sediments (Karickhoff, 1981; Karickhoff et al., 1979; McCall et al., 1980; Rao and Nkedi-Kizza, 1983). Additionally, Horvath et al. (1977) have successfully applied the solvophobic theory to describe the retention of weak acids, weak bases, and ampholytes in reversed-phase systems.

The solvophobic theory will be utilized in the following chapters to clarify and enhance our understanding of the hydrophobic retention of nonpolar solutes in polar solvent systems. The model and related theory have been presented here to aid the reader in that process. The above description should be considered an overview, however, and the reader is directed to Horvath et al. (1976, 1977) for more detailed discussions.

3.4 Thermodynamics of Sorption

3.4.1 Overview

The theory supporting the chromatographic determination of free energy, enthalpy, and entropy evolved from the classical equation for chromatography developed by Martin and Synge (1941). The work of Greene and Pust (1958) resulted in a relationship between chromatographic retention time (k') and the heat of adsorption (ΔH^o). The later work of Gale and Beebe (1964) examined equilibrium adsorption models and developed a concise expression for the measurement of heat of adsorption by chromatographic techniques.

The fundamental expression associated with equilibrium sorption on chromatographic supports is Eqn. (3-2), $k' = \phi K$. The solute retention factor is easily obtained from $k' = (t_R - t_o)/t_o$, where t_R and t_o are the retention times for the solute under study and an unretained compound, respectively. The retention factor may be related to $\Delta H^o{}_{sorp}$ and $\Delta S^o{}_{sorp}$ by combining Eqn. (3-3) with the free energy relationship

$$\Delta G^o = \Delta H^o - T\Delta S^o \qquad (3\text{-}40)$$

Substituting Eqn. (3-40) into Eqn. (3-3) yields

$$\ln k' = -\Delta H^o/RT + \Delta S^o/R + \ln \phi \qquad (3\text{-}41)$$

The determination of these thermodynamic parameters for selected organic compounds on RPLC supports and soils may be of great usefulness in understanding and predicting solute retention in RPLC and soil environments. For many hydrophobic compounds in RPLC systems, the enthalpy term dominates the entropy term in the free energy expression in Eqn. (3-40) (Colin et al., 1978; Melander et al., 1978). However, for many of the ubiquitous and carcinogenic polycyclic aromatic hydrocarbons (PAHs), entropic processes may control RPLC sorption (Chmielowiec and Sawatzky, 1979). It is noteworthy that enthalpy-entropy effects have not been extensively researched for hydrophobic solutes in natural soil/water systems. For example, Mills and Biggar (1969) measured the ΔH^o for sorption of aqueous hexachlorocyclohexane onto organic and inorganic surfaces, while Wauchope et al. (1983) determined ΔH^o_{sorp} and ΔS^o_{sorp} for aqueous naphthalene sorbing onto a sandy loam soil.

3.4.2 Evaluation of Enthalpy and Entropy Changes

If the heat capacity change upon the binding of the solute to the stationary phase is zero and the phase ratio (ϕ) is independent of temperature, then a plot of ln k' versus T^{-1}(°K^{-1}) is linear, according to Eqn. (3-41). With such a diagram (termed a van't Hoff plot), the ΔH^o can be obtained directly from the slope of the regression line. Departure from linearity can occur if the heat capacities of

the bound and free forms of the solute are different. Generally, most van't Hoff plots of RPLC data are linear and allow easy determination of ΔH^o_{sorp}. Typical values of ΔH^o_{sorp} for hydrophobic solutes range from -2 to -12 kcal/mole on RPLC and pyrocarbon LC supports (Colin et al., 1978; Melander et al., 1978).

A number of authors have successfully correlated the enthalpy of binding in RPLC to a numerical description of solute molecular structure. Hirata and Sumiya (1983) reported that the ΔH^o_{sorp} of p-nitrobenzyl esters of fatty acids on octadecylsilane (C-18) increases almost linearly with the number of carbon atoms in the molecule. Hornsby and Rao (1983) employed a more complex description of solute structure, the HSA, and found that ΔH^o_{sorp} increases linearly with the HSA of the sorbate molecule. The results of these studies agree with the solvophobic model of RPLC retention, as described by Horvath et al. (1976).

As discussed previously, a plot of ln k' vs. T^{-1} ($°K^{-1}$), will yield the ΔH^o_{sorp} from the slope of the regression line (Eqn. 3-41). The evaluation of the corresponding entropy change, ΔS^o_{sorp}, from the intercept is difficult because the phase ratio (ϕ) is usually not known. When using RPLC bonded phase supports (C-4, C-8, C-18, etc.), the "volume" or an equivalent property of the stationary phase is not clearly defined, thus a standard method for determining ϕ does not exist. Melander et al. (1980) suggested

expressing ϕ as the ratio of the surface area of the sorbent (m^2) to the column void volume (cm^3). Alternatively, Davydov et al. (1981) have used the ratio of mass of column material (g) to column void volume (cm^3). Other authors have defined the volume of stationary phase as the fraction of the column not occupied by the mobile phase (Chmielowiec and Sawatzky, 1979; Jandera et al., 1982a). These latter two assumptions appear to be particularly flawed, for they assume the total mass or volume of solid support to consist exclusively of the chemically bonded stationary phase. This ignores the fact that the stationary phase occupies only a small fraction of the total surface area of the silica gel particle (Kikta and Grushka, 1976). Typical surface coverage values for C-8 and C-18 alkanes are 5 to 20% (Kikta and Grushka, 1976; Sander and Wise, 1984).

Given the difficulties associated with experimentally measuring a value of ϕ, a number of authors have instead concentrated on determining this constant from the physical properties of the packing material. Knox and Vasvari (1973) estimated ϕ for a C-18 column to be 0.04, while Sander and Field (1980) calculated ϕ to be 0.38 for their octadecylsilane column. In neither case did the authors detail their method for computing the phase ratio.

The problems encountered in calculating ϕ stem from estimating the volume of stationary phase from the physical properties of the sorbent. Only recently have researchers

begun to explore the explicit character of the n-alkane stationary phases commonly found in RPLC (Engelhardt et al., 1982; Gilpin and Gangoda, 1984; Sander and Wise, 1984; Wise and May, 1983). Wise and May (1983) have proposed a simple expression for calculating the surface concentration (C_s) of the bonded alkylsilane

$$C_s(\mu mol/m^2) = \%C(10^6)/1200\ N_C S_{BET} \qquad (3\text{-}42)$$

where %C is the percent carbon (w/w) from elemental analysis, N_C is the total number of carbon atoms in the bonded silane molecule, and S_{BET} is the specific surface area (m^2/g) of the chemically modified silica as determined by the BET nitrogen adsorption method (Brunauer et al., 1938).

Equation (3-42) may now be modified (Dorsey, 1984) to yield an expression for the volume of stationary phase (V_{SP}) present on an RPLC column

$$V_{SP}(cm^3) = C_s(\mu mol/m^2) S_{BET}(MW/D)10^{-6}M \qquad (3\text{-}43)$$

where MW is the molecular weight (g/mole) of the bonded alkane, D is the density (g/cm^3) of the bonded alkane, and M is the mass (g) of packing material in the RPLC column. Combining Eqns. (3-42) and (3-43) yields

$$V_{SP}(cm^3) = \%C(MW)M/1200\ N_cD \tag{3-44}$$

Hence, with some knowledge of the physical properties of the packing material (%C, N_c, M) and bonded alkane (MW, D), it is possible to estimate the volume of stationary phase present on a given RPLC column. If the column void volume, $V_o(cm^3)$, is also known, the phase ratio may be expressed as

$$\phi = \%C(MW)M/1200\ N_cDV_o \tag{3-45}$$

Equation (3-45) was used in the following chapters to estimate ϕ for the RPLC columns under study. This allowed the value of $\Delta S^o{}_{sorp}$ to be calculated from ln k' versus $T^{-1}(°K^{-1})$ regression plots (Eqn. 3-41). It should be noted, however, that Eqn. (3-45) assumes that the molecular weight, density, and number of alkyl carbons is the same for a bonded alkylsilane as for the bulk alkyl liquid, i.e., C-8 is physico-chemically similar to liquid n-octane. Alkyl ligands are rotationally and vibrationally restricted compared to their unbonded counterparts (Gilpin and Gangoda, 1984), and polymeric stationary phases may diverge considerably from simple n-alkyl groups on a silica surface (Sander and Wise, 1984). Still, Eqn. (3-45) should represent an improved technique for determining the phase ratio of an RPLC column.

3.4.3 Enthalpy-Entropy Compensation Effects

In many physico-chemical interactions which are governed by the same basic mechanism, the overall free energy change is proportional to the change in enthalpy (Leffler and Grunwald, 1963; Melander and Horvath, 1980). This is indeed the case in RPLC, as ln k' (a measure of ΔG^{o}) is linearly related to the enthalpy of binding (Colin et al., 1978; Knox and Vasvari, 1973; Melander et al., 1978). From Eqn. (3-41), one would expect the slope of ln k' versus $-\Delta H^{o}$ to be approximately 1/RT. In actual practice, however, the increase in the natural logarithm of the retention factor with the enthalpy is much less than expected, as seen in Figure 3-2. The data for Figure 3-2 were taken from Chmielowiec and Sawatzky (1979); similar regressions could be developed from Appendices A and C.

In Figure 3-2, the slope ($\pm$95% confidence limits) of the ln k' versus $-\Delta H^{o}$ regression lines is 0.00034 ($\pm$4.8E-5) (mole/cal) for the collected PAH compounds. This value is significantly less than the 1/RT value at 298°K, that is, 0.00169 (mole/cal). This difference is attributed to changes in the binding enthalpy which are accompanied by corresponding changes in the binding entropy (Melander et al., 1978; Melander et al., 1980). The changes in the binding entropy are believed to be due to structural modifications of the sorbate molecule or changes in solvent entropy (Melander and

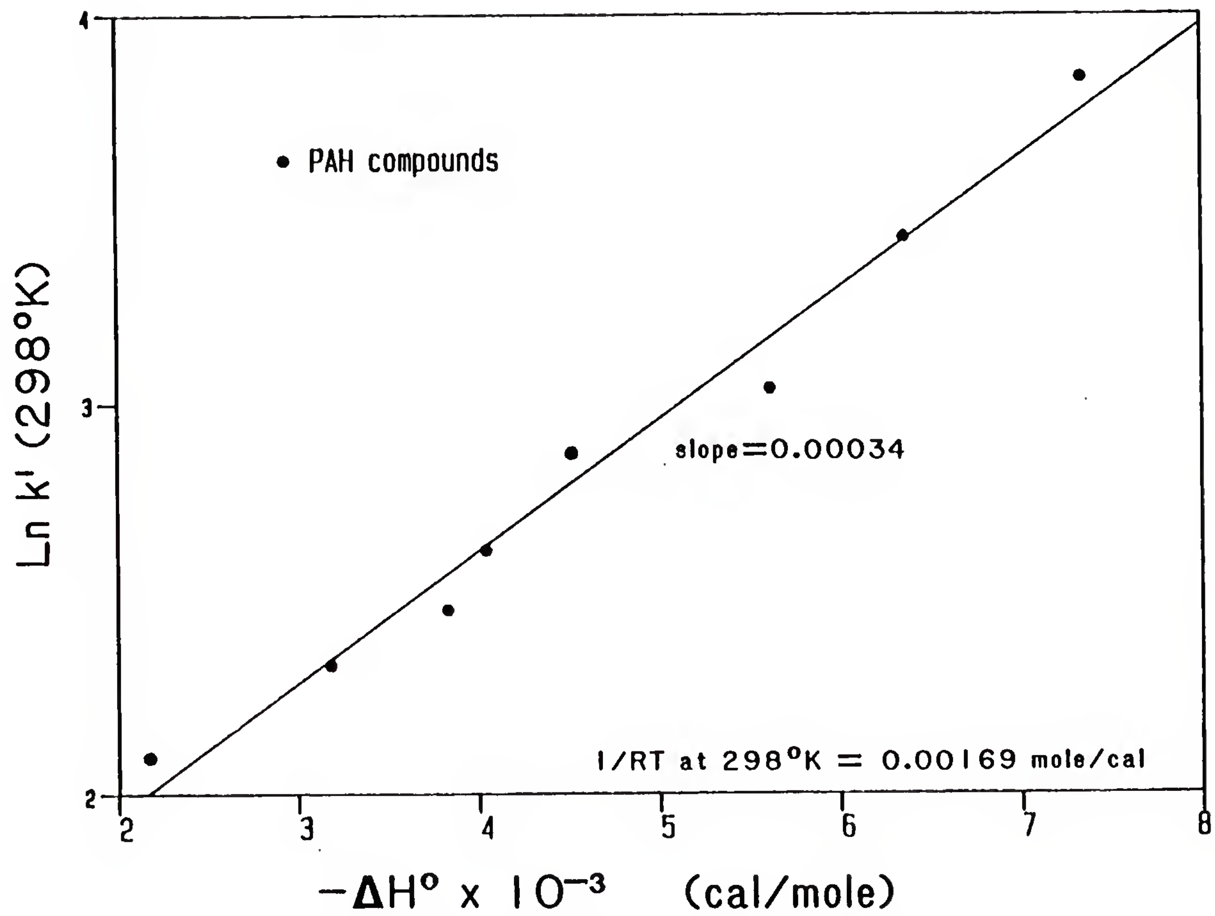

Figure 3-2. Ln k' at 298°K vs. $-\Delta H^{o}$ (cal/mole) for PAH sorption in RPLC, taken from Chmielowiec and Sawatzky (1979).

Horvath, 1980; Sander and Field, 1980). This effect is termed enthalpy-entropy compensation and has been observed on RPLC supports (Jinno and Ozaki, 1984; Melander et al., 1978; Melander et al., 1979; Melander et al., 1980; Sander and Field, 1980) and pyrocarbon LC columns (Colin et al., 1978).

The use of an enthalpy-entropy compensation model in this work should allow for greater insight into the energetics of solute binding. Compensation effects may be conveniently expressed by the relationship

$$\Delta H^{o} = \beta \Delta S^{o} + \Delta G^{o}_{\beta} \tag{3-46}$$

where ΔG^{o}_{β} denotes the change in free energy of sorption at the temperature β and β is a proportionality constant termed the compensation temperature (°K). Comparison of "compensation temperatures" obtained from thermodynamic data can be used to investigate whether the intrinsic mechanism of retention for one chromatographic system is identical to that found on another system (Melander et al., 1978). Substituting Eqn. (3-40) into Eqn. (3-46) and rearranging yields

$$\Delta G^{o}_{T} = \Delta H^{o}(1 - T/\beta) + T\Delta G^{o}_{\beta}/\beta \tag{3-47}$$

where ΔG^{o}_{T} is the standard free energy change at temperature T. Equation (3-41) may now be rewritten as

$$\ln k'_{T} = -(\Delta H^{o}/R)(1/T - 1/\beta) - \Delta G^{o}_{\beta}/R\beta + \ln \phi \quad (3\text{-}48)$$

where k'_{T} is the solute retention factor at temperature T.

According to Eqn. (3-48), a plot of the natural logarithm of the retention factor vs. the standard enthalpy changes obtained on a constant RPLC system by various solutes yields a straight line when compensation occurs, i.e., when solute/sorbent binding is due to an essentially identical mechanism for all solutes. The compensation temperature, β, may be evaluated from the slope of the regression line. If similar measures of β (°K) are obtained for varying solvent/sorbent systems, one may infer that the major mechanisms of the sorptive process are identical for those systems (Jinno and Ozaki, 1984; Melander et al., 1978; Melander et al., 1980).

Knox and Vasvari (1973) examined the retention of various substituted benzenes by RPLC supports and reported enthalpy-entropy compensation effects in a 40/60 (v/v) methanol/water eluent. Compensation effects have also been reported by Melander et al. (1978) for buffered and ionized aromatic acids on C-18 material in 100% aqueous and in acetonitrile/water systems (up to 30% acetonitrile), and by Jinno and Ozaki (1984) for alkylbenzenes on C-8 and C-18

phases in various methanol/water mixtures. Similar compensation temperatures of 500 to 700°K were calculated for each of these RPLC systems. Melander et al. (1978) hypothesized that the mechanism of hydrophobic sorption is essentially the same, regardless of the nature and concentration of the organic solvent present and the chemical nature of the sorbate molecules. Further support for this conclusion comes from the data of Kikta and Grushka (1976). Compensation temperatures of 593 and 512°K may be computed from their data concerning alkylphenone retention on two different types of nonylsilica stationary phases in 50/50 (v/v) methanol/water eluent. These β values are similar to those detailed above.

It is interesting to note that in chromatographic systems employing polar stationary phases and nonpolar eluents (normal-phase chromatography), the calculated compensation temperature, 140°K, was markedly lower than those obtained in RPLC (Knox and Vasvari, 1973). The lower β value suggests that the retention mechanism in normal-phase chromatography is different from that operating in RPLC.

3.4.4 <u>Enthalpy-Entropy Compensation with Changing Solvent Composition</u>

The work of Melander et al. (1978, 1979, 1982), Colin et al. (1983), and Martire and Boehm (1983) suggests the presence of a rigorous mathematical relationship between the

effect of temperature and solvent composition on solute retention in RPLC. The following presentation will outline a thermodynamic model for this relationship and is taken primarily from research performed by C. Horvath and W. Melander of Yale University.

Enthalpy-entropy compensation effects have been observed in RPLC by numerous authors (Boumahraz et al., 1983; Colin et al., 1978; Knox and Vasvari, 1973; Melander et al., 1978). This behavior was reviewed in Section 3.4.3, and it suggests that the change in the enthalpy of solute binding to the stationary phase as solvent composition changes is proportional to a change in the corresponding entropy; the proportionality constant is termed the compensation temperature. This relationship may be expressed as the derivative of Eqn. (3-46) with respect to solvent composition

$$d\Delta H^{o}(\theta)/d\theta \quad = \quad \beta \; d\Delta S^{o}(\theta)/d\theta \tag{3-49}$$

where $d\Delta H^{o}(\theta)$ and $d\Delta S^{o}(\theta)$ are the incremental changes in enthalpy and entropy at solvent composition θ, upon change in composition, $d\theta$ (as measured by volume fraction of organic modifier), and β is the compensation temperature (°K).

Integrating Eqn. (3-49) from a reference solvent composition, $\theta = 0$, to a final composition, θ, yields

$$\Delta H^{o}(\theta) - \Delta H^{o}(0) = \beta\Delta S^{o}(\theta) - \beta\Delta S^{o}(0) \tag{3-50}$$

The dependence of the change of entropy of binding on solvent composition may be eliminated by combining Eqns. (3-41) and (3-50), with the result that

$$\ln k' = \frac{\Delta H^{o}(\theta)}{RT} + \frac{\Delta H^{o}(\theta) - \Delta H^{o}(0)}{R\beta} + \frac{\Delta S^{o}(0)}{R} + \ln \phi \tag{3-51}$$

Equation (3-51) relates the natural logarithm of the retention factor, ln k', at a particular solvent composition and temperature to the change in the standard enthalpy of binding at that composition and the change in the standard binding enthalpy and entropy at the reference composition, taken to be 100% water ($\theta = 0$). It is now useful to relate $\Delta H^{o}(\theta)$ to the enthalpy at the reference state, $\Delta H^{o}(0)$, where $\Delta H^{o}(0)$ is the standard enthalpy change for solute binding in 100% water.

3.4.4.1 Enthalpy as a function of solvent composition

The dependence of the change in standard binding enthalpy upon solvent composition may be expressed in several ways. The simplest relationship is given by

$$\Delta H^{o}(\theta) = \Delta H^{o}_{c}(0)f(\theta) \tag{3-52}$$

where $\Delta H^{o}_{c}(0)$ is the standard enthalpy change in 100% water which exhibits complete enthalpy-entropy compensation, and $f(\theta)$ is the solvent compensation function which is unity for 100% aqueous solutions.

When some portion of the standard binding enthalpy change does not undergo compensation, the relationship may be written as

$$\Delta H^{o}(\theta) = \Delta H^{o}_{n}(0) + \Delta H^{o}_{c}(0)f(\theta) \qquad (3\text{-}53)$$

where $\Delta H^{o}_{n}(0)$ is the noncompensated portion of the total standard enthalpy change (in 100% water). This relationship is commonly observed in RPLC systems exhibiting enthalpy-entropy compensation effects (Melander and Horvath, 1984; Melander et al., 1978).

Equations (3-51) and (3-52) may be combined to yield an expression for solutes undergoing complete enthalpy-entropy compensation

$$\ln k' = \frac{-\Delta H^{o}_{c}(0)f(\theta)}{RT} + \frac{[\Delta H^{o}_{c}(0)(f(\theta) - 1)]}{R} + \frac{\Delta S^{o}(0)}{R} + \ln \phi \qquad (3\text{-}54a)$$

Likewise, a relationshp may be developed for the partially compensated binding enthalpy change by combining Eqns. (3-51) and (3-53)

$$\ln k' = \frac{-\Delta H^{\circ}_{c}(0)f(\theta) - \Delta H^{\circ}_{n}(0)}{RT} + \frac{\Delta H^{\circ}_{c}(0)(f(\theta) - 1)}{R\beta} + \frac{\Delta S^{\circ}(0)}{R} + \ln \phi \tag{3-54b}$$

A linear relationship between the natural logarithm of the retention factor ($\ln k'$) and the solvent composition (θ) is frequently observed with water-miscible organic eluents (Abbott et al., 1976; Horvath et al., 1976). Since θ is the volume fraction of organic solvent, the value of $f(\theta)$ is unity with a 100% aqueous eluent. The mathematical expression for this simple case is

$$f(\theta) = 1 + \alpha\theta \tag{3-55}$$

where α is a constant and will have a negative value. For example, a 30/70 (v/v) acetonitrile/water eluent ($\theta = 0.30$), where α may be -2.0, has a $f(\theta)$ value of 0.40.

Karger et al. (1976), on the other hand, noted a marked deviation from linearity for $\ln k'$ vs. θ plots of straight-chain alcohols in acetonitrile/water mobile phases. Schoenmaker et al. (1978) studied the retention of aromatic solutes in methanol/water, ethanol/water, and n-propanol/water mobile phases and suggested a quadratic relationship for the dependence of $\ln k'$ on solvent composition

$$f(\theta) = 1 + \alpha\theta + \Psi\theta^2 \qquad (3\text{-}56)$$

where α and Ψ are constants.

If the simple linear model for $f(\theta)$ is considered, the following relationship results from combining Eqns. (3-54a) and (3-54b) with (3-55)

$$\ln k' = A_1\theta(1 - \beta/T) + A_2/T + A_3 \qquad (3\text{-}57)$$

Similarly, using Eqn. (3-56) for the quadratic $f(\theta)$ expression

$$\ln k' = A_1\theta(1 - \beta/T) + A_2/T + A_3 + A_4\theta^2(1 - \beta/T) \qquad (3\text{-}58)$$

The mathematical expressions for A_1, A_2, A_3, and A_4 for fully compensated (Eqn. 3-54a) and partially compensated (Eqn. 3-54b) standard binding enthalpy changes are given in Table 3-1.

3.4.4.2 Model evaluation

3.4.4.2.1 Solvent compensation function, $f(\theta)$

To properly discriminate between the linear and quadratic forms of the solvent compensation function, it is generally convenient to examine the dependence of ln k' on solvent composition, θ. A linear or quadratic model is

Table 3-1. Mathematical description of parameters A_1. A_2, A_3, and A_4 in Eqns. (3-57) and (3-58).

Parameter	Full enthalpy compen-tion according to Eqn. (3-54a)	Partial enthalpy compen-sation according to Eqn. (3-54b)
A_1	$\alpha \Delta H^o{}_c(0)/R\beta$	$\alpha \Delta H^o{}_c(0)/R\beta$
A_2	$-\Delta H^o{}_c(0)/R$	$-(\Delta H^o{}_c(0) + \Delta H^o{}_n(0))/R$
A_3	$\Delta S^o(0)/R + \ln \phi$	$\Delta S^o(0)/R + \ln \phi$
A_4	$\Psi \Delta H^o{}_c(0)/R\beta$	$\Psi \Delta H^o{}_c(0)/R\beta$

The parameters $\Delta H^o{}_c(0)$ and $\Delta H^o{}_n(0)$ are the compensating and noncompensating portions of the standard binding enthalpy change in a 100% aqueous mobile phase, and $\Delta S^o(0)$ is the standard binding entropy change in 100% water. R, β, ϕ, α, and Ψ are the gas constant, compensation temperature (°K), column phase ratio, and the coefficient for the first- and second-order solvent dependence of the natural logarithm of the solute retention factor, ln k', respectively.

selected by statistical fit of experimental data to Eqn. (3-57) or (3-58), respectively.

3.4.4.2.2 Full versus partial enthalpy compensation

An examination of the coefficients in Table 3-1 reveals that A_1, A_3, and A_4 are identical for the two enthalpy compensation models, Eqns. (3-52) and (3-53). The physical interpretation of A_2 is different for each model, however, and this fact permits selection of the proper compensation model based on the chromatographic data. If full enthalpy-entropy compensation occurs (Eqn. 3-52), then from Table 3-1

$$A_2 = -\beta A_1/\alpha \tag{3-59}$$

However, if enthalpy compensation is incomplete, then from Table 3-1

$$A_2 = -\Delta H^{o}{}_{n}(0)/R - \beta A_1/\alpha \tag{3-60}$$

Upon comparing Eqns. (3-59) and (3-60), it is clear that the behavior of the A_2/A_1 ratio for a given chromatographic system may be used to select the appropriate enthalpy compensation function. The ratio of A_2 to A_1 will remain constant only if full enthalpy-entropy compensation

is exhibited by the test solutes. A homologous series of solutes is preferred for such an investigation.

The research of Melander et al. (1979, 1982) explored the application of the above thermodynamic model to the RPLC retention of n-alkylbenzenes in binary mobile phases of methanol, acetonitrile, dioxane, tetrahydrofuran, and isopropanol in water. They found that Eqn. (3-57) best fit the retention data. Additionally, the A_2/A_1 ratio was found to generally increase with chain length of the n-alkylbenzene solute, indicating incomplete enthalpy-entropy compensation effects (Eqn. 3-53). Therefore, Melander et al. (1979, 1982) suggested that Eqn. (3-57) best described the dependence of n-alkylbenzene retention on solvent composition and temperature and that the expressions for A_1, A_2, and A_3 given in Table 3-1 are for partial enthalpy compensation.

Further research by Melander et al. (1985) examined the application of Eqns. (3-57) and (3-58) for describing the octadecylsilane retention of 54 polar and nonpolar sorbates in acetonitrile/water solvent mixtures. They found that the average relative errors in predicting solute retention were 7.8% and 6.0% for the four-parameter (Eqn. 3-58) and three-parameter (Eqn. 3-57) equations, respectively. In view of the small decrease in error, but considerable increase in complexity and in number of data points associated with use of the four-parameter equation, Melander et

al. (1985) recommended that the three-parameter equation, Eqn. (3-57), be applied in general use.

The results obtained with the enthalpy-entropy compensation model compare favorably with attempts by Colin et al. (1983), Grant et al. (1979), and Martire and Boehm (1983) to model RPLC retention dependence on solvent composition and temperature. The model has a further advantage in that it may allow greater insight into the energetics and mechanisms of the sorptive process. The dependence of the regression parameters A_1, A_2, and A_3 on the carbon number in n-alkylbenzenes (Melander et al., 1982) suggests a close relationship between the model parameters and solute molecular structure. Additionally, Melander and Horvath (1984) have used this model to examine three proposed mechanisms of RPLC retention. It is the broad range of applications that makes this thermodynamic approach a useful technique for contrasting and comparing sorption processes on reversed-phase LC supports and natural soil surfaces. In the following chapters, thermodynamic and retention data will be interpreted with the aid of the enthalpy-entropy compensation model and the solvophobic theory of hydrophobic sorption.

CHAPTER IV
MATERIALS AND METHODS

4.1 Introduction

This chapter will discuss the materials and experimental methods employed in all the experiments performed during this study. The guidelines for selecting model sorbents, natural sorbents, organic solvents, and hydrophobic solutes will initially be presented, followed by a description of reagents, equipment, and the experimental design for model and natural sorbent studies.

4.2 Selection of Model Sorbents

The choice of RPLC packing material, which was to serve as a surrogate sorbent for a soil, was a critical component of the model chromatographic system. The factors that influence the sorption and selective attenuation of solutes by a sorbent include the surface loading of the bonded alkyl phase (Sadek and Carr, 1984), the n-alkyl chain length of the bonded phase (Berendsen and DeGalan, 1980), and the extent of cross-linkage or polymerization of the stationary phase (Scott and Simpson, 1980). The wide range of RPLC packing materials currently available made it possible to select almost any combination of sorbent properties.

It is worth noting that the n-alkyl stationary phases usually found in RPLC systems are covalently bonded to the parent silica surface. The resulting n-alkyl bonded film is retarded both in rotational and vibrational degrees of freedom when compared to organic matter adsorbed onto soil mineral surfaces. The sorptive capacity of RPLC stationary phases is much greater than that of soil materials (including organic soils and peat), due to their higher organic loading and bonded attachment to the silica gel support. Four RPLC stationary phases were selected for investigation because of interest in the effect of RPLC chain length on sorptive interactions of hydrophobic solutes. For this reason, the following 10 μm (outside particle diameter), reversed-phase, polymeric stationary phases on silica gel (Analytichem International Inc.) were chosen for study:

(1) C-2 (ethyl), 5.57% carbon

(2) C-4 (n-butyl), 7.92% carbon

(3) C-8 (n-octyl), 12.05% carbon

(4) C-18 (n-octadecyl), 14.73% carbon.

4.3 Selection of Natural Sorbents

The principal natural sorbent used in this study was a Webster sandy clay loam surface soil, collected in Iowa at 0-30 cm depth from a profile classified as a Typic Haplaquoll. The physical and chemical properties of this

soil are listed in Table 4-1. The Webster soil has been used extensively in earlier studies of sorption and leaching of hydrophobic pesticides (Nkedi-Kizza et al., 1983; Nkedi-Kizza et al., 1985). This soil was chosen for study since it represents a highly carbonaceous, hydrophobic surface soil. The high organic carbon content (3.9%) allowed an evaluation to be made of hydrophobic sorption on a natural soil surface. The Webster soil was air-dried and passed through a 2 mm sieve to remove stones and root fragments prior to use.

4.4 Selection of Organic Solvents

The interactions occurring between the solute and the solvent can greatly affect solute retention and transport in a soil system or chromatographic column. The four major interactions are dispersion forces, dipole interactions, hydrogen bonding, and dielectric interactions (Snyder and Kirkland, 1979). The organic solvents chosen for intensive study were methanol (CH_3OH) and acetonitrile (CH_3CN), which represent two distinct classes of organic solvents. These solvents were used in binary combinations with water in order to provide a wide range of solute-solvent interactions.

Table 4-1. Physical and chemical properties of Webster soil.*

Soil	Mechanical analysis			pH	OC[a]	CEC[b]	Major clay minerals
	sand	silt	clay	1:1 .01N$CaCl_2$	%	meq/100g	
Webster	55	20	25	7.3	3.9	21.8	smectites

*Taken with permission from Nkedi-Kizza et al. (1985).

[a]Percent organic carbon.

[b]Cation exchange capacity.

4.5 Selection of Hydrophobic Compounds

The hydrophobic organic solutes chosen for investigation were compounds of general environmental concern. Chemicals that were distinctly different in their molecular conformations were studied to examine the effect of solute structure on retention thermodynamics. One of the classes of compounds studied was the polycyclic aromatic hydrocarbons (PAHs), which have been the focus of numerous studies concerning their fate and sorption in the aqueous environment (Dzombak and Luthy, 1984; Karickhoff, 1981; Means et al., 1980; Waters and Luthy, 1984). Members of this class of ubiquitous environmental pollutants have been found widely distributed in air (Handa et al., 1984; Harkov et al., 1984), rainwater (Pankow et al., 1984), freshwater (Hase and Hites, 1976), wastewater (Adams and Giam, 1984), and sediments and soils (Boehm and Farrington, 1984; Prahl et al., 1984). The environmental sources of PAHs include anthropogenic inputs such as petroleum spills and energy production (Hase and Hites, 1976) and natural inputs such as the combustion of organic material (Kamens et al., 1985; Mast et al., 1984). A number of the PAHs are potent carcinogens (Neff, 1979). Reversed-phase liquid chromatography is one of the techniques generally used in the analysis of environmental samples containing PAHs. Due to their extensive aromaticity and lack of substituent groups, the PAHs are generally rigid, planar molecules with little or no

internal degrees of movement. Recent research has concentrated on developing a mathematical relationship between the molecular structure of PAHs and their RPLC retention factors (Hanai and Hubert, 1984; Hasan and Jurs, 1983; Jinno and Kawasaki, 1983a; Wise et al., 1981).

Another class of compounds studied was the substituted benzenes. In particular, the alkylbenzenes were selected for study since members of this series of compounds have been the subject of considerable thermodynamic and RPLC retention research (Jinno and Kawasaki, 1983b; Melander and Horvath, 1984; Melander et al., 1982) and have been discovered in landfill leachate plumes (Reinhard et al., 1984). The alkylbenzenes are also of interest by way of structural contrast when compared to the rigid, planar PAHs. The alkyl-chain portion of a molecule in the solid state has been observed to exist in a fully extended form (Mizushima, 1954). The extended form is also a stable conformation in the liquid state, but it may not predominate because its statistical weight is small compared with the sum of other possible conformers (Testa, 1979). When placed in aqueous solution, the C_1-C_4 n-alkanes are suggested to exist predominately in an extended conformation (Nemethy and Scheraga, 1962), while the C_5 and large aliphatic hydrocarbons are proposed to exist in folded or coiled conformations (Edward, 1970; Nemethy and Scheraga, 1962; Herman, 1972). It is these coiled and folded conformations which

present the smallest amount of hydrophobic surface area for contact with water molecules.

The space inside a coiled or folded alkyl-chain may consist of a nonsolvated, empty interior volume stabilized by intramolecular interactions (Edward, 1970; Nemethy and Scheraga, 1962), or the hydrocarbon chains may be separated by one or more layers of solvent molecules (Herman, 1972). An RPLC retention study encompassing a number of straight chained and branched alkylbenzenes, as well as the rigid PAHs, may therefore provide useful information for determining the importance of solute conformation upon the mechanisms and energetics of hydrophobic sorption.

Nitrobenzene and the monohalobenzenes were chosen for study because of their structural simplicity and concern over their environmental fate (Chiou, 1985). A listing of the solute compounds used in experiments reported in this dissertation and their respective hydrocarbonaceous surface area (HSA) values is shown in Table 4-2. Except for nitrobenzene, it was assumed that the total surface area (TSA) was equivalent to HSA. The HSA value for nitrobenzene was calculated using a modification of the surface area model proposed by Herman (1972). The actual HSA value for nitrobenzene was calculated by Dr. G. Belfort of Rensselaer Polytechnic Institute (Belfort, 1982).

Table. 4-2. List of hydrophobic compounds used in chromatographic studies and their respective hydrocarbonaceous surface area (HSA) values.

Compound	HSA (Å^2)	Compound	HSA (Å^2)
A. Polycyclic aromatics[a]		C. Halobenzenes[a]	
Benzene	110	Fluorobenzene	114
Naphthalene	156	Chlorobenzene	127
Biphenyl	182	Bromobenzene	133
Phenanthrene	198	Iodobenzene	142
Anthracene	202		
Pyrene	213		
Fluoranthene	218		
Chrysene	241		
B. Alkylbenzenes[a]		D. Substituted Benzenes[b]	
Toluene	127	Nitrobenzene	86
Ethylbenzene	145		
n-Propylbenzene	163		
n-Butylbenzene	181		
n-Hexylbenzene	217		
o-Xylene	147		
p-Xylene	150		
m-Diethylbenzene	180		
1,2,4-Trimethyl-benzene	161		

[a]HSA values taken from Herman (1972),Valvani et al. (1976), Yalkowsky and Valvani (1979), and Yalkowsky et al. (1979).

[b]HSA value computed using a modified Herman (1972) model by Dr. G. Belfort of Rensselaer Polytechnic Institute.

4.6 Reagents

A listing of the reagent chemicals used in the discussed experiments and their respective industrial sources is shown in Table 4-3. The solvents (water, acetonitrile, and methanol) used in the RPLC and soil experiments were HPLC-grade and were obtained from Fisher Scientific Co.

4.7 Equipment

The isocratic elution of the hydrophobic solutes through packed columns of the RPLC sorbents was performed using a modular liquid chromatography system consisting of two Gilson Model 302 metering pumps, a Gilson 1.5 mL analytical mixer, and two Gilson Model 802 manometric modules interfaced with an Apple IIe microcomputer system. The absorbance of the column effluent was monitored at 254 nm using a Waters 450 variable wavelength UV detector, with the chromatograms recorded with a Hewlett-Packard 3390A reporting integrator. Batch soil studies employed a Gilson Model 121 filter fluorometer as a detector for the solution phase solute, with excitation and emission filters of 305-395 and 430-470 nm, respectively. In the RPLC retention studies, injections of the hydrophobic solutes onto the RPLC supports were made using a Rheodyne 7161 switching valve with a 20 μL injection loop. For quantitative analysis of the solution phase in soil batch studies, however, a 200 μL

Table 4-3. List of reagent chemicals and their respective sources.

Compound/Class	Source/Purity
Polycyclic aromatic hydrocarbons	Aldrich Chemical Co.--98+% pure
Biphenyl	Fisher Scientific Co.--Reagent grade
Benzene	Mallinckrodt Inc.--Nanograde, 99+% pure
n-Butylbenzene and n-Hexylbenzene	Aldrich Chemical Co.--99+% pure
Remaining alkylbenzenes and substituted benzenes	Eastman Kodak Inc.--Reagent grade

injection loop was required. All RPLC sorbate mixtures were 5-500 mg/L in 100% methanol. The flow rate for RPLC thermodynamic retention experiments was set at 1.0 mL/min; the actual flow rate was measured using a 10 mL graduated cylinder and a stopwatch and found to be within 5% of this value. All RPLC experiments were performed at least in triplicate.

All column packings were purchased from Analytichem International Inc. (Harbor City, CA). The precolumn packing material was 40 μm Sepralyte unbonded silica gel. As discussed in Section 4.2, the reversed-phase stationary phases consisted of porous, irregularly shaped, 10 μm diameter silica gel particles chemically bonded with the following trichloroalkylsilanes: C-2, C-4, C-8, and C-18. A listing of these stationary phases and their physicochemical properties is shown in Table 4-4. These stationary phases were slurry-packed into 5 cm x 4.6 mm (i.d.) x 1/4" (o.d.) stainless steel HPLC columns, equipped with 2 μm frits at each end. The unbonded silica gel was dry-packed into a similar column for use as a precolumn; however, the outlet end of this column contained a 0.5 μm frit to prevent fines from clogging the injection valve and downstream tubing.

Both the precolumn and analytical HPLC column were thermostated by circulating water jackets. The precolumn was filled with unbonded silica gel and was placed before

Table 4-4. Physical and chemical properties of reversed-phase, 10 μm diameter particle size, stationary phases used in chromatographic studies.

Stationary phase	Percent carbon	Alkyl ligand	Alkyl group molecular wt. (g/mole)	Density (20°K) of parent n-alkane (g/cm^3)
C-2	5.57	$-CH_2CH_3$	29	0.5235
C-4	7.92	$-(CH_2)_3CH_3$	57	0.5788
C-8	12.05	$-(CH_2)_7CH_3$	113	0.7025
C-18	14.73	$-(CH_2)_{17}CH_3$	253	0.7768

the injection valve to assist in bringing the mobile phase to the required temperature while also saturating the solvent mixture (water/methanol, etc.) with dissolved silica. The former effect is desired to avoid differential temperature bands in the analytical column while the latter minimized the loss of silica support from the downstream analytical column. The circulating water bath was a Brinkman Model RC-20T, capable of operating over a temperature range of -15 to 100°C, with an accuracy of $\pm$ 0.2°C. The temperature of the water bath was monitored with a Bailey Model BAT-8 digital thermocouple thermometer. This instrument has a stated range of 0 to 100°C and a maximum sensor error of $\pm$ 0.1°C at 100°C. The RPLC retention studies were routinely done at temperatures of 298, 308, 318, and 328°K for a single isocratic solvent mixture. In some experiments, the temperature 288°K was substituted for 328°K to avoid possible heat capacity effects in the hydrophobic sorption reaction.

A Shandon HPLC packing pump (courtesy of Dr. J. Dorsey) was used to slurry-pack the RPLC sorbent materials into the HPLC columns. Approximately 2 mL of the selected sorbent material was slurried in 20 mL of chloroform (Reagent grade, Fisher Scientific Co.). This slurry was shaken and placed in an ultrasonic bath for 20 minutes to insure adequate distribution of the 10 m material. The sorbent-chloroform slurry was then poured into the packing reservoir

and packed at 6000 psi with a succession of increasingly viscous solvent mixtures: 50/50 (v/v) chloroform/methanol, 100% methanol, and 50/50 (v/v) methanol/water. The first two solvent mixtures were run for 1-2 minutes, with the methanol/water mixture then packing the column for 10-15 minutes. Following the packing procedure, the column was removed and installed on the Gilson HPLC system.

A constant temperature room (courtesy of Dr. D. Silvia) was used to perform all soil thermodynamic sorption experiments. The room was manufactured by the Electric Hotpak Co. (Philadelphia, PA) and had an operating range of 0 to 40°C. The observed temperature variability was $\pm$1.0°C in studies from 5 to 35°C.

4.8 Experimental Techniques

4.8.1 General RPLC Experiments

A typical RPLC experiment involved the isocratic elution of all compounds from a given RPLC sorbent at a known solvent composition. For any given methanol/water or acetonitrile/water eluent, retention studies were performed at a minimum of four temperatures, e.g., 298 to 328°K in increments of 10°K. The solvent composition was then changed, usually by steps of θ = 0.10, and the temperature studies repeated. Four to five methanol/water or acetonitrile/water solvent systems were studied in this manner for each RPLC material. Solute retention factor (k')

data were collected as functions of solvent composition (θ) and temperature (T) on C-2, C-4, and C-8 stationary phases in methanol/water and acetonitrile/water mobile phases. To explore further the importance of stationary phase chain length in hydrophobic sorption reactions, isothermal retention data were collected on a C-18 sorbent in various acetonitrile/water solvent systems at 298°K. The collected ln k' data for all sorbent/solvent combinations may be found in Appendix A.

All RPLC experiments were performed on the Gilson HPLC unit using a 1.0 mL/minute flow rate. Measured flow rates agreed with this value within a 95% confidence limit. Isocratic solvent systems prepared using 250 mL burets gave identical solute retention as eluents prepared by the Apple IIe/analytical mixer system; i.e., k' values agreed within 1% of mean values. All retention studies were run at least in triplicate, and triplicate analyses typically agreed to within ±1-4% of the mean k' value.

4.8.2 Chromatographic Data Analysis

The coefficients for Eqns. (3-57) and (3-58) were obtained from multiple linear regression analyses of retention factor-composition-temperature data for each solute using the GLM package in SAS (Statistical Analysis System, Inc., Box 8000, Cary, NC) on an IBM 3081D/3033N/4341 computer at the Northeast Regional Data Center (Gainesville, FL). A

similar GLM analysis of retention factor-dielectric constant-surface tension data resulted in the regression coefficients for Eqn. (3-38).

4.8.3 Determination of Column Void Volume, V_o

In the previous discussions, the solute retention factor (k') was described by $k' = (t_R - t_o)/t_o$, where t_R and t_o are the retention times of the compound under study and an unretained solute, respectively. It is evident that proper evaluation of retention factors requires a knowledge of the chromatographic void volume (t_o or V_o) of the column, i.e., the mobile phase volume that is experienced by the solute in the course of the chromatographic process. Ideally, the column void volume is represented by the elution volume of an inert or ionic solute that explores the available mobile phase volume but does not interact with the stationary phase.

Recently, the problem of determining column void volume has received considerable attention in the RPLC literature. The investigative approach to this problem has taken several fronts. Some researchers used the linearity of solute retention for homologous series to determine V_o (Berendsen et al., 1980; Krstulovic et al., 1982; Tchapla et al., 1984). McCormick and Karger (1980) have made a convincing case for the use of D_2O, while others used various organic

and ionic solutes for V_o determination (Jinno et al., 1983; Wells and Clark, 1981).

Melander et al. (1983) examined both the theory and empirical determination of the void volume. They concluded that the nitrate ion (as in $NaNO_3$ or KNO_3) was an adequate V_o indicator, if the mobile phase contained between 25 and 75% methanol or between 25 and 95% acetonitrile and if the ionic strength of the eluent was sufficiently high to avoid the effect of Donnan salt-exclusion (Donnan, 1924). This strategy is in agreement with the research of Wells and Clark (1981), who found that the column void volume could be best estimated by an injection of approximately 3×10^{-6} mole or more of $NaNO_3$ in an unbuffered methanol/water system. The large amount of $NaNO_3$ was recommended to avoid Donnan salt-exclusion effects that may occur in an unbuffered mobile phase.

The $NaNO_3$ salt was chosen for use as the void volume indicator in the RPLC chromatographic studies. Since unbuffered solutions of methanol/water and acetonitrile/water were used, it was necessary to study the effect of $NaNO_3$ concentration upon measured void volume. The results are shown in Figure 4-1. The effect of increasing salt concentration upon measured retention volume was attributed to Donnan ion-exclusion. A concentration of 25 g/L was selected for use in V_o determinations for methanol/water and acetonitrile/water systems. If an injection volume of

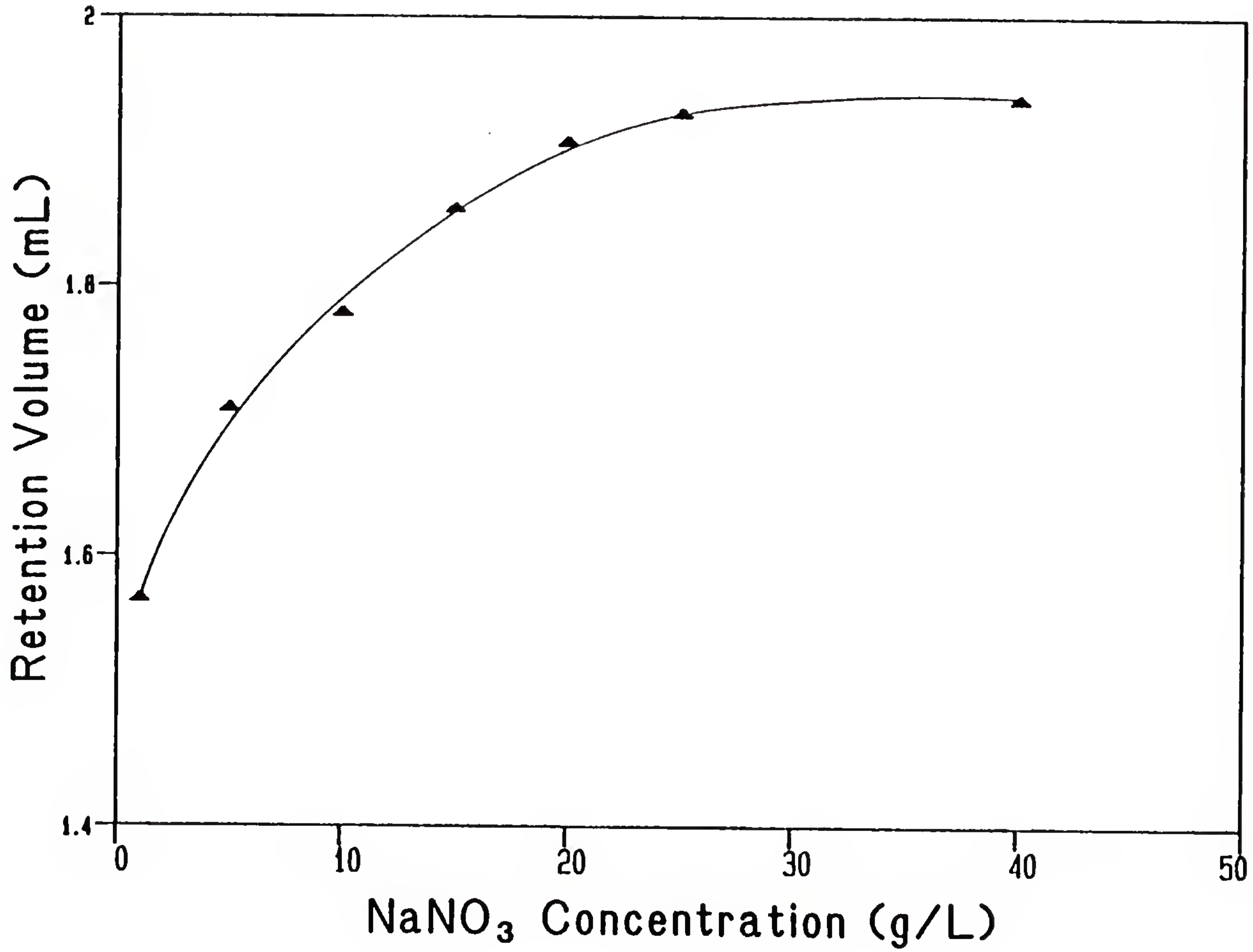

Figure 4-1. Retention volume vs. $NaNO_3$ concentration on a C-4 column in 70/30 methanol/water at 298°K.

20×10^{-6} L is assumed, this corresponds to an injection of approximately 6×10^{-6} mole of $NaNO_3$. This exceeds the 3 μmoles suggested by Wells and Clark (1981) to avoid exclusion effects in unbuffered methanol/water eluents.

The Donnan ion-exclusion effect has also been documented by Buytenhuys and van der Maeden (1978), who investigated the use of sodium heparin as a void volume indicator for silica gel columns. The effect they noted was quite similar to that described by Wells and Clark (1981) and similar to that shown in Figure 4-1.

4.8.4 Equilibrium Experiments with RPLC Materials

It is an implicit assumption in RPLC thermodynamic studies that a dynamic equilibrium is established between the sorbed and solution phases of the solute of interest. To investigate this assumption for the RPLC systems used in my studies, two experiments were performed:

(1) The solute retention factor, k', was examined as a function of column flow rate. On the C-8 sorbent, in a 60/40 (v/v) acetonitrile/water mobile phase, the k' of pyrene at 298°K was recorded at flow rates of 0.10 to 1.0 mL/min. If solution-phase kinetics were a limiting factor, one would expect some differentiation of k' as flow rate is changed over a significant range.

(2) Individual batch equilibrium sorption isotherms of biphenyl and pyrene were performed on RPLC material

dissolved in a 50/50 or 60/40 (v/v) acetonitrile/water solvent system. The linear equilibrium sorption coefficients for these systems were then calculated and compared to the column k' values for an identical system. When corrected for column mass and dead volume, the equilibrium sorption coefficient should be equivalent to k' measured on the column. The sorbent/solvent mixtures were shaken for 24 hours prior to centrifugation and analysis and are therefore assumed to represent equilibrium systems.

Approximately 0.1 to 0.4 g of the RPLC material was weighed into eight 25 mL glass centrifuge tubes with Teflon-backed rubber stoppers. Five milliliters each of four solute standards were then added to the tubes for duplicate analysis. The tubes were shaken at ambient temperature ($22 \pm 3°C$) for 24 hours and centrifuged for 30 minutes at 1000 rpm. Quantitative HPLC analysis of the solution phase employed a 15 cm, 10 μm, C-8 Zorbax column (DuPont column, via Fisher Scientific Co.) with a 60/40 (v/v) acetonitrile/water mobile phase at 298°K and 1.5 mL/min flow rate. Column effluent was monitored by the Waters 450 variable wavelength UV detector set at 254 nm. The solution phase concentration (C_e) of the solute of interest was determined from a four or five point standard curve; the standards were prepared in similar tubes and solutions and had been taken through the entire procedure. The sorbed solute concentration (S_e) was calcualted from

$$S_e = V/m\,(C_o - C_e) \qquad (4\text{-}1)$$

where S_e is the sorbed solute concentration (μg/g), C_e is the solution phase solute concentration (μg/mL), V is the volume (mL) of standard added initially to the tube, m is the mass (g) of sorbent present, and C_o is the standard solute concentration (μg/mL) added to the tube.

The batch equilibrium isotherm data were interpreted with the aid of the Freundlich equation, which expresses the equilibrium relationship between the solute in solution (C_e) and the sorbed solute (S_e) as

$$S_e = K\,C^N_e \qquad (4\text{-}2)$$

and

$$\ln S_e = \ln K + N \ln C_e \qquad (4\text{-}3)$$

where K is the thermodynamic equilibrium sorption coefficient, and N is a constant. The linear version of the Freundlich equation, where N = 1.0, was used by a number of investigators to describe the sorption of organic pesticides onto soil (Davidson and McDougal, 1973; Kay and Elrick, 1967). Other researchers have indicated that the linear Freundlich equation is inappropriate under certain soil conditions (Rao and Davidson, 1979). Since linear sorptive behavior is generally assumed to occur in RPLC (Snyder and Kirkland, 1979), the linear form of the Freundlich equation

was used to interpret the results of these RPLC batch equilibrium studies.

4.8.5 Soil Thermodynamic Sorption Studies

To properly study the thermodynamics of the sorption of hydrophobic solutes onto soils, the sorption of three hydrophobic solutes in a natural soil/solvent mixture was studied at several temperatures using the batch equilibrium sorption technique outlined in Section 4.8.4. The solutes chosen were biphenyl, anthracene, and pyrene, which were dissolved in a 30/70 methanol/water solvent mixture. Four standards of each solute were prepared, and 5 mL of each were individually applied to 1 g samples of Webster soil in glass centrifuge tubes with Teflon-lined caps. The samples were then shaken for 24 hours and then centrifuged for 1 hour at 1000 rpm in the constant temperature room. Four temperatures were used: 5, 15, 25, and 35°C, with an observed room temperature variation of ±1°C. Aliquots (50 μL) of the solution phase were removed from the tubes in the constant temperature room, and then were analyzed using the same HPLC conditions outlined in Section 4.8.4. However, a 65/35 acetonitrile/water (v/v) mobile phase was used for most analyses. In addition, for the solutes anthracene and pyrene, the Gilson Model 121 filter fluorometer (excitation and emission filters of 305-395 and 430-470 nm, respectively) was required for analyzing the low solution

phase concentrations of these solutes. The collected soil solution data were then analyzed using the nonlinear form of the Freundlich equation (Eqn. 4-2).

CHAPTER V
RESULTS AND DISCUSSION

5.1 Introduction

This chapter will review the results of all reversed-phase liquid chromatography (RPLC) and soil experiments that were performed and presents an extensive discussion of those results. The initial section outlines the experimental data and indicates their placement in the appendices. The discussion and interpretation of the data comprise the remainder of the chapter. The chapter will present an analysis of the thermodynamics of hydrophobic sorption on both RPLC materials and the Webster soil, the application of the enthalpy-entropy compensation model for RPLC retention, and use of the solvophobic model for examining the mechanisms of hydrophobic sorption.

5.2 Results

This section outlines the experimental and statistical results developed during this study and identifies the location of those results in Appendices A to I.

Sorption data in the form of ln k' as a function of temperature and solvent content were obtained for all experimental solutes retained on C-2, C-4, and C-8 sorbents

in methanol/water and acetonitrile/water solvent systems. Similar data were generated at a single temperature (298°K) for the solutes on a C-18 sorbent in an acetonitrile/water mobile phase. The collected retention data may be found in Appendix A. The HSA value for each solute is supplied for reference.

The ln k' data collected for each solute-sorbent system of interest have been linearly regressed against the inverse of absolute temperature, as presented in Eqn. (3-41). The regression coefficients for these individual van't Hoff plots are tabulated in Appendix B, where the correlation coefficient, slope, and intercept are listed, in addition to the 95% confidence limits for the latter two regression parameters.

The van't Hoff regression data (Appendix B) were mathematically modified to represent the mean ΔH^o and ΔS^o values for solute sorption in the RPLC systems under study. The ΔH^o_{sorp} data are presented in Appendix C, while the ΔS^o_{sorp} values, corrected for the column phase ratio, are listed in Appendix D.

The results of the RPLC retention experiments in methanol/water and acetonitrile/water eluents were analyzed using the enthalpy-entropy compensation model outlined in Chapter III, Section 3.4.3. Both the three-parameter (Eqn. 3-57) and four-parameter (Eqn. 3-58) models were studied, and the respective regression coefficients and

correlation coefficients are listed in Appendix E. The three-parameter model was applied to methanol/water and acetonitrile/water systems, while the nonlinear response of ln k' to acetonitrile content (θ_{ACN}) suggested the additional application of the four-parameter model to all acetonitrile/water systems for comparison purposes. To examine the importance of the compensation temperature upon the calculated thermodynamic parameters ($\Delta H^{o}_{n}(O)$, α, and Ψ), the β value was varied for the C-8 stationary phase material in the methanol/water and acetonitrile/water solvent systems. The results of these calculations also appear in Appendix E.

The data for the physicochemical properties of methanol/water and acetonitrile/water solvent systems, respectively, appear in Appendices F and G. These properties include density, refractive index, dielectric constant, molar volume, surface tension, and K^{e}; all data are at 25°C.

The physicochemical data tabulated in Appendices F and G may be used in conjunction with the ln k' data of Appendix A to examine the applicability of the solvophobic model (Horvath et al., 1976) to the RPLC systems under study. The solvophobic model (Eqn. 3-38) has been applied to the C-2, C-4, C-8, and C-18 stationary phases in an acetonitrile/water solvent system at 25°C (298°K). The

calculated regression parameters and correlation coefficients are shown in Appendix H.

The experimental data and statistical analyses of the Webster soil thermodynamic solute sorption studies are listed in Appendix I. Data for each of the three solutes involved in the experiments (biphenyl, anthracene, and pyrene) are detailed for each system temperature.

5.3 Hydrophobic Retention on RPLC Materials

An initial objective of the RPLC studies was to examine differences in sorptive behavior between structurally distinct classes of chemicals, i.e., the PAHs and the alkylbenzenes. To properly evaluate differences in hydrophobic retention, the compounds of interest must be described and differentiated on the basis of chemical properties or molecular structure. Parameters that are commonly used in such studies on RPLC or soil materials include topological descriptors such as the molecular connectivity index (Bojarski and Ekiert, 1982; Hanai and Hubert, 1984; Sabljic, 1984; Wells et al., 1982), and measures of hydrophobicity such as aqueous solubility (Chiou et al., 1979; Chiou et al., 1983) and the octanol/water partition coefficient (Chiou et al., 1983; Hammers et al., 1982; Harnisch et al., 1983; Karickhoff, 1981; Koopmans and Rekker, 1984; Rao and Nkedi-Kizza, 1981; Veith et al., 1979; Wells and Clark, 1984). Geometric descriptors such as the length/breadth

ratio (Wise et al., 1981) or the van der Waals volume (Jinno and Kawasaki, 1983b; Hanai and Hubert, 1984), along with chemical properties such as molecular polarizability (Jinno and Kawasaki, 1984b; Lamparcz et al., 1983) and the solubility parameter (Hafkenscheid and Tomlinson, 1983) are also commonly used to describe solute sorption in RPLC systems. Jinno and Kawasaki (1984a) reported that although the sorption of PAHs and alkylbenzenes is dominated by hydrophobic interactions, the size and shape of these molecules are of considerable importance in determining overall RPLC rentention.

The natural logarithm of the solute retention factor (ln k') was linearly regressed against the logarithm of the octanol/water partition coefficient (log K_{ow}) for sorption on C-8 material in 60/40 methanol/water and 50/50 acetonitrile/water. These plots are shown in Figures 5-1 and 5-2, respectively. The log K_{ow} is generally considered a measure of the solute's hydrophobic nature (Leo et al., 1971). The log K_{ow} values for the solutes used in the regression are listed in Table 5-1. In both the methanol/water and acetonitrile/water mobile phase systems, there is a difference in overall sorptive behavior between the PAH compounds and alkylbenzenes, based on a measure of their respective hydrophobicities. The regression parameters for both classes of compounds, taken from the data in Figures

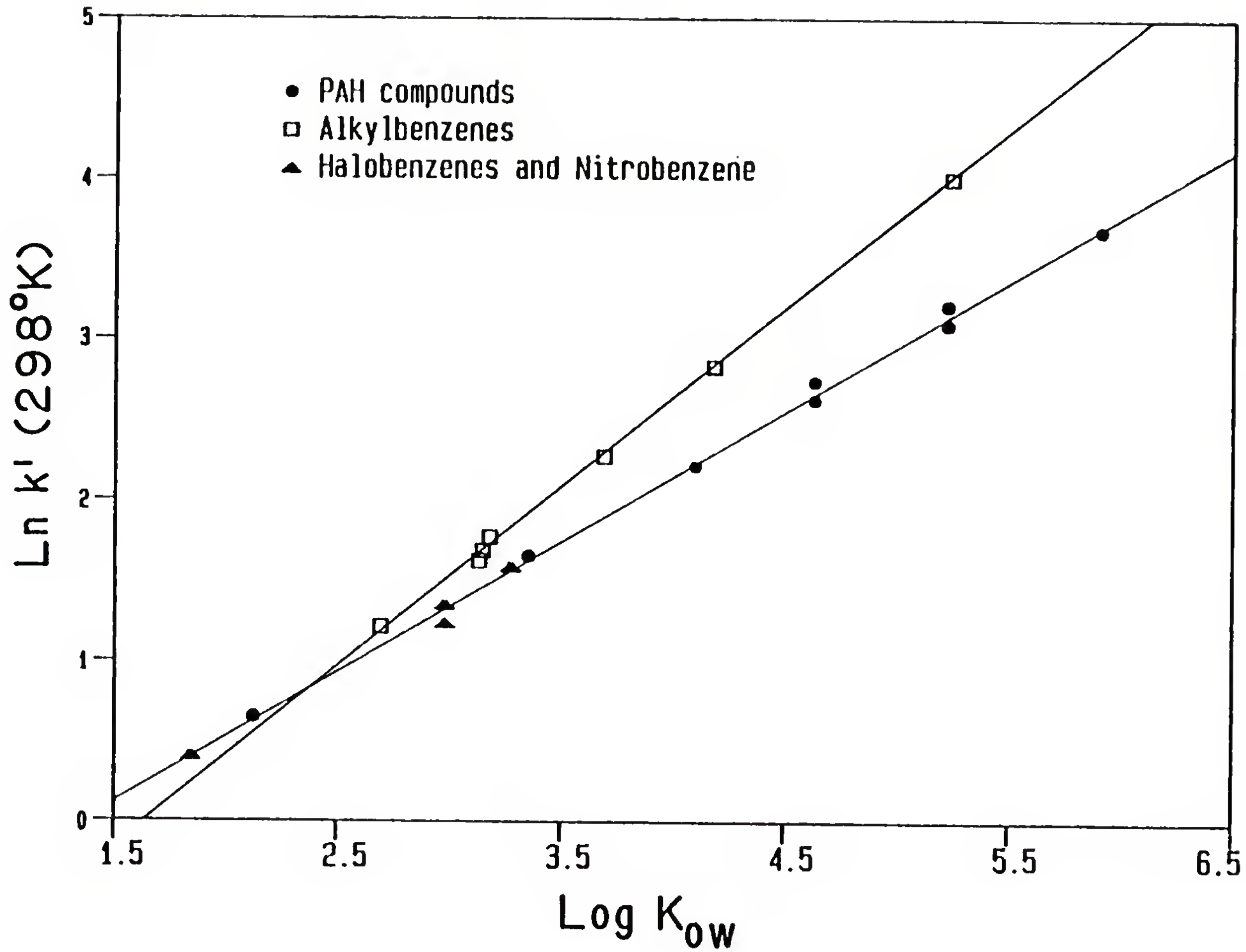

Figure 5-1. Ln k' vs. log K_{ow} for the hydrophobic solutes on C-8 material in a 60/40 methanol/water eluent at 298°K.

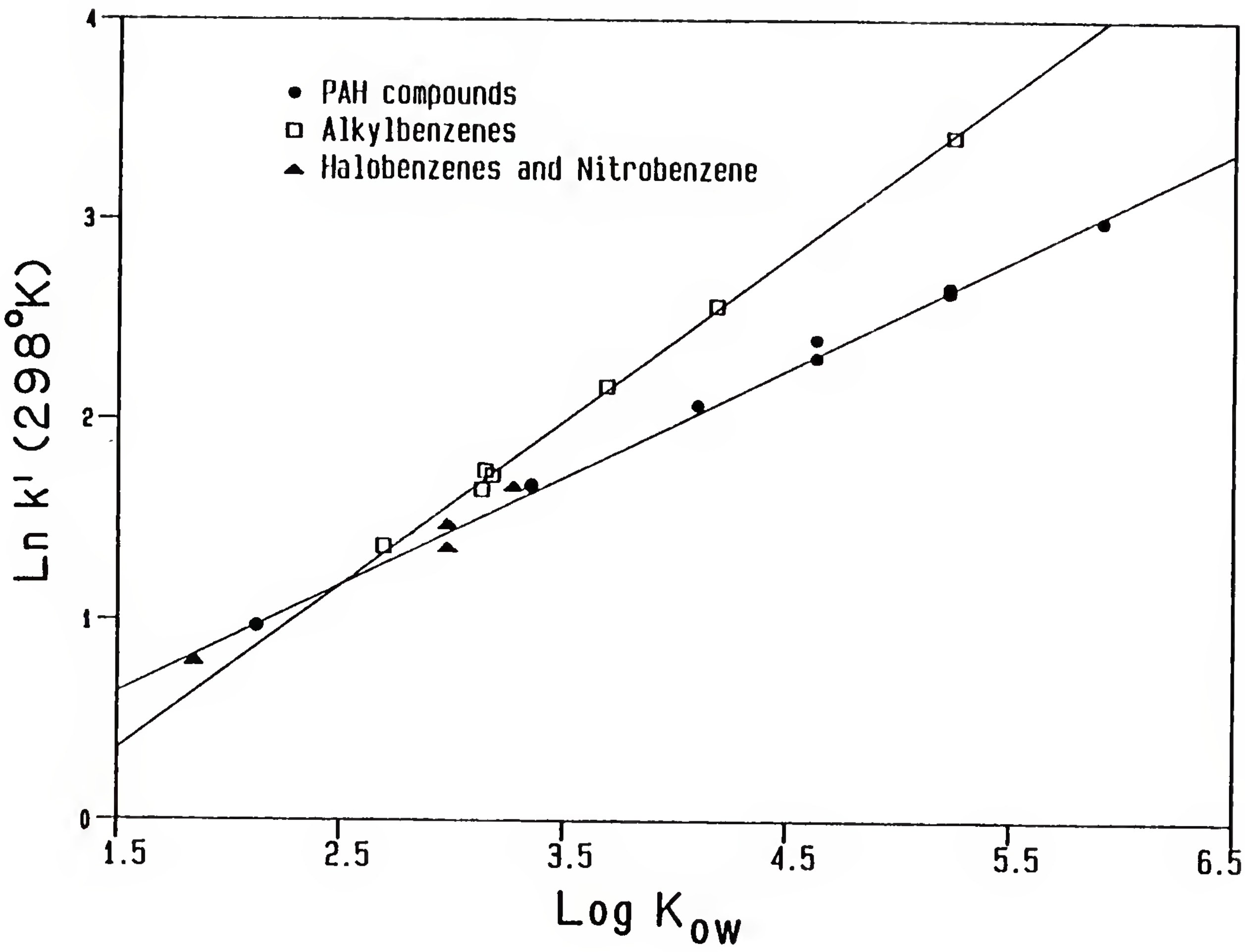

Figure 5-2. Ln k' vs. log K_{ow} for the hydrophobic solutes on C-8 material in 50/50 acetonitrile/water at 298°K.

Table 5-1. Octanol/water partition coefficients (K_{ow}) of the hydrophobic solutes used in the RPLC retention studies.

Compound	Log K_{ow}	Reference
Biphenyl	4.10	Bruggeman et al., 1982
Naphthalene	3.55	Bruggeman et al., 1982
Phenanthrene	4.63	Bruggeman et al., 1982
Anthracene	4.63	Bruggeman et al., 1982
Pyrene	5.22	Bruggeman et al., 1982
Chrysene	5.91	Bruggeman et al., 1982
Fluoranthene	5.22	Bruggeman et al., 1982
Benzene	2.13	Leo et al., 1971
Toluene	2.69	Nys and Rekker, 1973
Ethylbenzene	3.15	Nys and Rekker, 1973
n-Propylbenzene	3.69	Wasik et al., 1981
n-Butylbenzene	4.18	Bruggeman et al., 1982
n-Hexylbenzene	5.24	Bruggeman et al., 1982
p-Xylene	3.18	Wasik et al., 1981
o-Xylene	3.13	Wasik et al., 1981
Chlorobenzene	2.98	Wasik et al., 1981
Bromobenzene	2.98	Wasik et al., 1981
Iodobenzene	3.28	Wasik et al., 1981
Nitrobenzene	1.85	Wasik et al., 1981

5-1 and 5-2, are listed in Table 5-2 for the two RPLC systems.

Also shown in Table 5-2 are data for similar ln k' vs. log K_{ow} correlations on the C-2 sorbent in various methanol/water and acetonitrile/water mobile phases. Overall, there appears to be little to no difference in sorptive behavior as the alkyl chain of the stationary phase is increased in length. These findings differ considerably from those of Jinno and Kawasaki (1983b), who found that the size and shape of a solute molecule are the dominant factors controlling retention on a C-2 stationary phase, with hydrophobic interactions becoming more important as stationary phase chain length is increased. Their conclusions were not supported for the RPLC sorbents used in this study.

The hydrocarbonaceous surface area (HSA) is a useful descriptor of the solute area available for hydrophobic interactions (Horvath and Melander, 1977; Horvath et al., 1976; Nkedi-Kizza et al., 1985; Rao et al., 1985; Woodburn et al., 1985). It has been used extensively by Horvath et al. (1976) in their solvophobic model of hydrophobic retention and by Rao et al. (1985) and Woodburn et al. (1985) as a tool in modeling solute sorption in soil systems containing organic solvent/water mobile phases. The excellent linear correlation between the HSA and the classic hydrophobicity parameter, log K_{ow}, is shown in Figure 5-3, where a single regression line was found to fit the PAHs, alkylbenzenes,

Table 5-2. Regression parameters from linear correlation of ln k' (298°K) vs. log K_{ow} in various RPLC systems.

Column	Solvent system	Regression parameters ($\pm$95% conf. limit) from ln k' (298°K) vs. log K_{ow}
C-2	60/40 MeH/H_2O[a]	(1) PAHs, Benzene, Halobenzenes, and Nitrobenzene
		n = 12, R = 0.9967
		Slope = 0.52 $\pm$ 0.03
		Intercept = -1.83 $\pm$ 0.12
		(2) Alkylbenzenes
		n = 7, R = 0.9995
		Slope = 1.85 $\pm$ 0.03
		Intercept = -2.68 $\pm$ 0.11
C-8	60/40 MeOH/H_2O	(1) PAHs, Benzene, Halobenzenes, and Nitrobenzene
		n = 12, R = 0.9989
		Slope = 0.81 $\pm$ 0.03
		Intercept = -1.09 $\pm$ 0.11
		(2) Alkylbenzenes
		n = 7, R = 0.9997
		Slope = 1.11 $\pm$ 0.03
		Intercept = -1.80 $\pm$ 0.11
C-2	50/50 ACN/H_2O[b]	(1) PAHs, Benzene, Halobenzenes, and Nitrobenzene
		n = 12, R = 0.9959
		Slope = 0.34 $\pm$ 0.02
		Intercept = -0.52 $\pm$ 0.09
		(2) Alkylbenzenes
		n = 7, R = 0.9991
		Slope = 0.57 $\pm$ 0.03
		Intercept = -1.10 $\pm$ 0.10

Table 5-2. Continued

Column	Solvent system	Regression parameters ($\pm$95% conf. limit) from ln k' (298°K) vs. log K_{ow}
C-8	50/50 ACN/H_2O	(1) PAHs, Benzene, Halobenzenes, and Nitrobenzene
		n = 12, R = 0.9981
		Slope = 0.54 $\pm$ 0.02
		Intercept = -0.14 $\pm$ 0.12
		(2) Alkylbenzenes
		n = 7, R = 0.9994
		Slope = 0.82 $\pm$ 0.03
		Intercept = -0.87 $\pm$ 0.12

[a]Methanol/water solvent system

[b]Acetonitrile/water solvent system

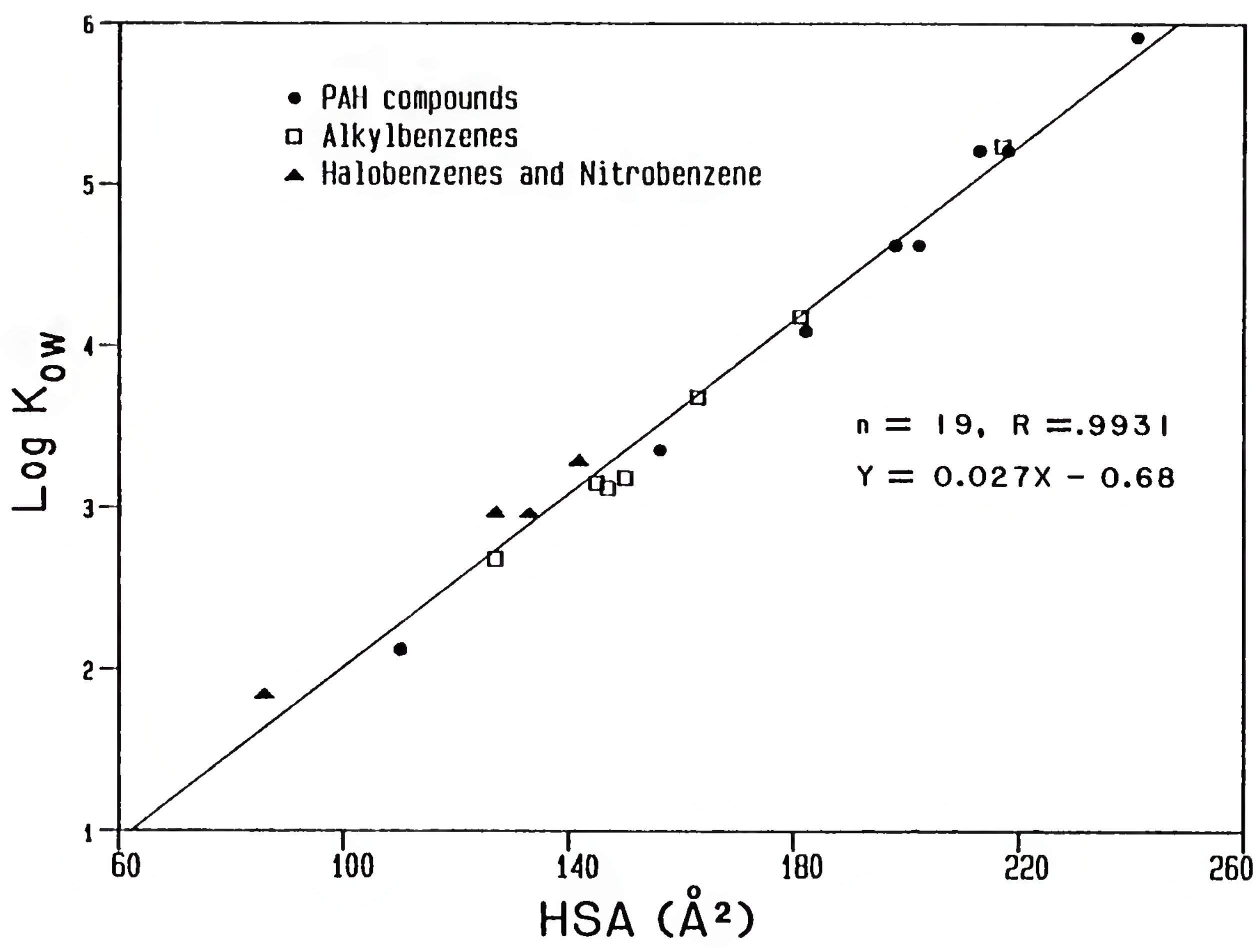

Figure 5-3. Log K_{ow} vs. solute HSA for 19 hydrophobic solutes.

and substituted benzenes. As a result, it is not surprising that ln k' vs. HSA plots are similar to those developed for ln k' vs. log K_{ow}. Plots of ln k' vs. HSA are shown in Figures 5-4 and 5-5 for the C-8 stationary phase with 60/40 methanol/water and 60/40 acetonitrile/water eluents, respectively. The solute nitrobenzene has been omitted from any linear regressions involving HSA because it exhibits unusually strong retention relative to its small HSA value (86 $\mathring{A}^2$). This behavior is believed related to the interaction of the polar nitro group with the available silanol groups on the RPLC surface. Tanaka et al. (1978) reported similar behavior for nitrobenzene and attributed it to preferential polar interactions with the silanol groups still present on the RPLC surface.

The difference in retention behavior for the PAH and alkylbenzene solutes is again quite distinct in the ln k' vs. HSA plots for C-8 sorption in the two solvent systems (Figures 5-4 and 5-5). The pertinent regression parameters for the linear correlation of ln k' vs. HSA in several sorbent/solvent systems are listed in Table 5-3. As in the ln k' vs. log K_{ow} relationships, stationary phase chain length does not appear to affect the quality of the correlation of retention to solute structure.

The molecular connectivity index, or chi factor, is an easily computable topological parameter devised by Randic (1975) and extended by Kier and Hall (1976) for describing

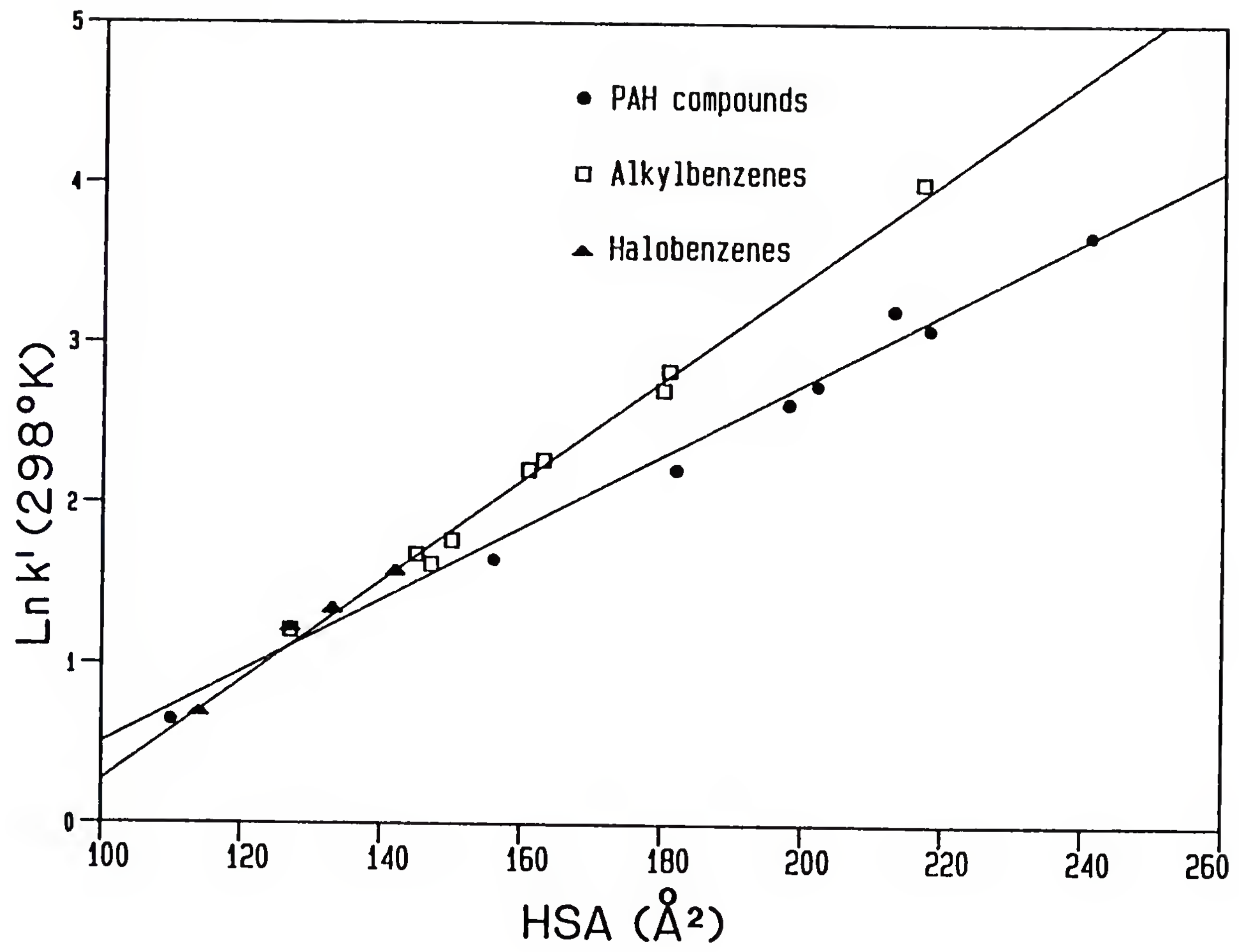

Figure 5-4. Ln k' vs. solute HSA for the hydrophobic solutes on C-8 material in 60/40 methanol/water at 298°K.

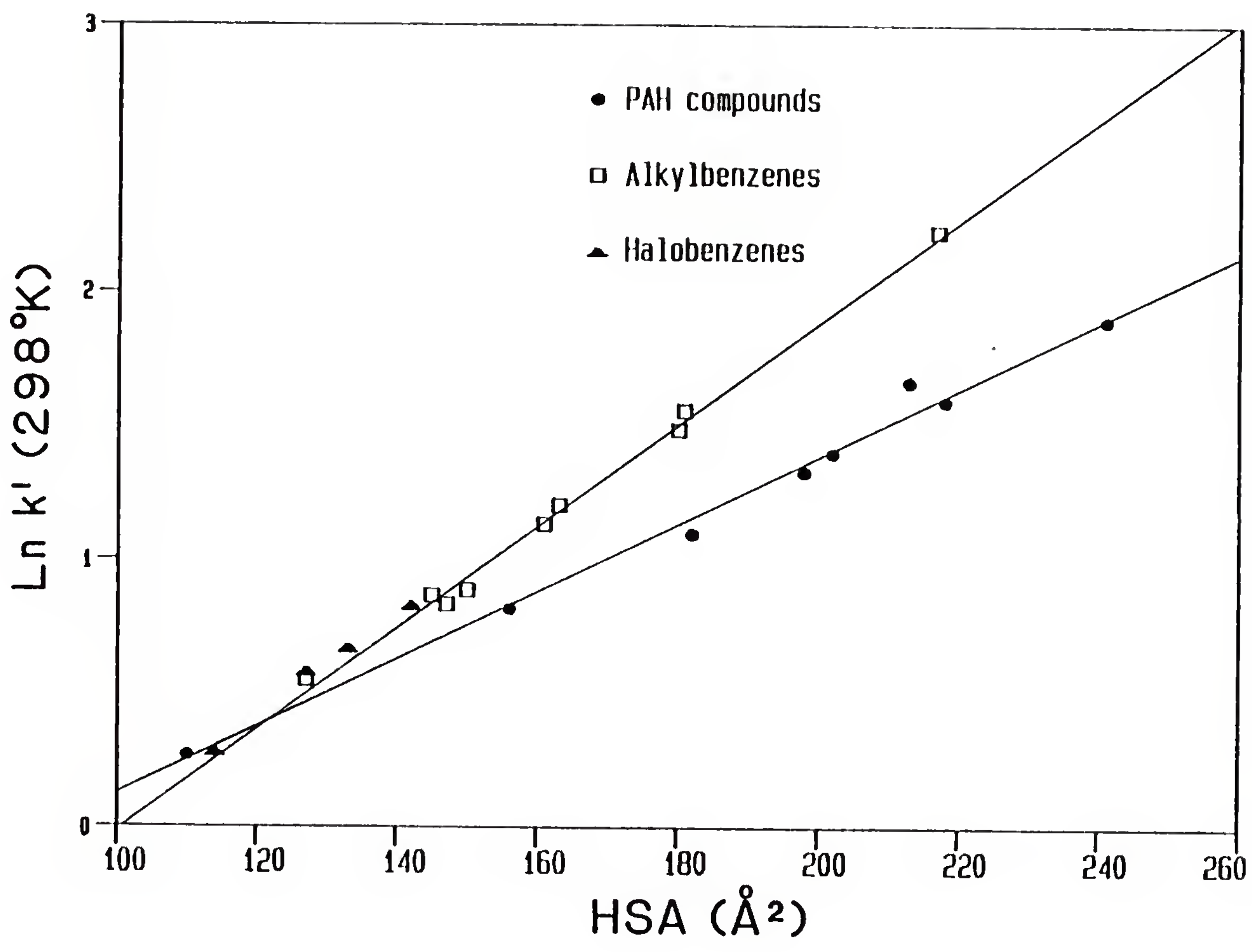

Figure 5-5. Ln k' vs. solute HSA for the hydrophobic solutes on C-8 material in 60/40 acetonitrile/water at 298°K.

Table 5-3. Regression parameters from linear correlation of ln k' (298°K) vs. HSA in various RPLC systems

Column	Solvent system	Regression parameters (±95% conf. limit) from ln k' (298°K) vs. HSA
C-2	60/40 $MeOH/H_2O$[a]	(1) PAHs, Benzene, and Halobenzenes n = 12, R = 0.9941 Slope = 0.0141 ± 0.0010 Intercept = -2.21 ± 0.19
		(2) Alkylbenzenes n = 9, R = 0.9955 Slope = 0.0245 ± 0.0021 Intercept = -3.58 ± 0.34
C-8	60/40 $MeOH/H_2O$	(1) PAHs, Benzene, and Halobenzenes n = 12, R = 0.9975 Slope = 0.0224 ± 0.0018 Intercept = -1.74 ± 0.31
		(2) Alkylbenzenes n = 9, R = 0.9975 Slope = 0.0313 ± 0.0018 Intercept = -2.86 ± 0.29
C-2	50/50 ACN/H_2O[b]	(1) PAHs, Benzene, and Halobenzenes n = 12, R = 0.9944 Slope = 0.0094 ± 0.0007 Intercept = -0.77 ± 0.12
		(2) Alkylbenzenes n = 9, R = 0.9945 Slope = 0.0160 ± 0.0014 Intercept = -1.61 ± 0.22
C-8	50/50 ACN/H_2O	(1) PAHs, Benzene, and Halobenzenes n = 12, R = 0.9940 Slope = 0.0149 ± 0.0012 Intercept = -0.59 ± 0.20
		(2) Alkylbenzenes n = 9, R = 0.9948 Slope = 0.0236 ± 0.0022 Intercept = -1.73 ± 0.35

[a]Methanol/water solvent system

[b]Acetonitrile/water solvent system

molecular shape and the degree of molecular branching. A large number of studies have demonstrated that many physicochemical and biological properties depend upon the topology of a molecule, which may be related to the connectivity index. These properties include water solubility and boiling point (Hall et al., 1975), the octanol/water partition coefficient (Murray et al., 1975), the activity of general anesthetics (DiPaolo et al., 1977), solute retention in RPLC and GC systems (Bojarski and Ekiert, 1982; Hanai and Hubert, 1984; Jinno and Kawasaki, 1983a, 1983b, 1984a; Kaliszan and Lamparczyk, 1978; Wells et al., 1982) and solute sorption on soil material (Sabljic, 1984).

The first-order connectivity index, ^{1}X, may be computed from the expression

$$^{1}X = \Sigma\ (\delta_i \delta_j)^{-1/2} \tag{5-1}$$

where the sum is over all bonds in the molecule. Atoms i and j are directly bonded; δ is a number assigned to each atom reflecting the number of nonhydrogen atoms bonded to it. The ^{1}X values for the PAH compounds and alkylbenzenes are listed in Table 5-4, which includes a sample ^{1}X calculation for ethylbenzene.

Chromatographic data (ln k') from Appendix A were used to develop linear correlations between ln k' and ^{1}X for the PAHs and alkylbenzenes in methanol/water and acetonitrile/

Table 5-4. First-order molecular connectivity indices of $^1\chi$ of the PAHs and alkylbenzenes. A sample calculation for the $^1\chi$ value of ethylbenzene is shown.

Compound	Calculated $^1\chi$ value
Biphenyl	4.071
Naphthalene	3.405
Phenanthrene	4.815
Anthracene	4.809
Pyrene	5.559
Chrysene	6.226
Fluoranthene	5.565
Benzene	2.000
Toluene	2.411
Ethylbenzene	2.971
n-Propylbenzene	3.471
n-Butylbenzene	3.971
n-Hexylbenzene	4.971
o-Xylene	2.827
p-Xylene	2.821
m-Diethylbenzene	3.943
1,2,4-Trimethylbenzene	3.238

Sample $^1\chi$ calculation for ethylbenzene:

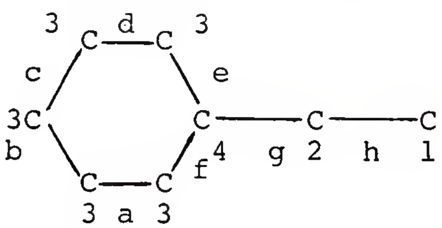

$$^1\chi = \underset{a}{\frac{1}{(3\times3)^{1/2}}} + \underset{b}{\frac{1}{(3\times3)^{1/2}}} + \underset{c}{\frac{1}{(3\times3)^{1/2}}} + \underset{d}{\frac{1}{(3\times3)^{1/2}}} + \underset{e}{\frac{1}{(3\times4)^{1/2}}} + \underset{f}{\frac{1}{(3\times4)^{1/2}}} +$$

$$+ \underset{g}{\frac{1}{(4\times2)^{1/2}}} + \underset{h}{\frac{1}{(2\times1)^{1/2}}}$$

$$^1\chi = 2.971$$

water eluents. The resulting correlations are shown in Figures 5-6 and 5-7 for sorption on C-8 material in 60/40 methanol/water and 40/60 acetonitrile/water solvent systems, respectively. The distinction between PAH and alkylbenzene retention as a function of molecular shape is evident from the figures and from the ln k' vs. ${}^{1}X$ regression data, presented in Table 5-5. As the data in Table 5-5 demonstrate, stationary phase chain length does not significantly affect the correlation of retention behavior to molecular topology. This conclusion differs from that of Jinno and Kawasaki (1983b), who reported that the correlation of solute retention to molecular shape (${}^{1}X$) improved considerably as the stationary phase chain length was decreased.

The explanation for the different conclusions reached in these two retention studies may lie in the steric distinction between the "brush-type" stationary phases used by Jinno and Kawasaki (1983b), and the "polymeric type" RPLC phases employed in my experiments. The brush-type reversed-phases are prepared by reacting dried silica gel with a monohalosilane, producing one bonded hydrocarbon chain per available silanol group. The polymeric or bulk-type phase, on the other hand, is prepared from silica reacting with a trichlorosilane in the presence of water, forming a cross-linked polymeric structure upon reaction (Scott and Simpson, 1980). The findings of Jinno and Kawasaki (1983b) may be in agreement with the finding that shorter (C-2) brush-type

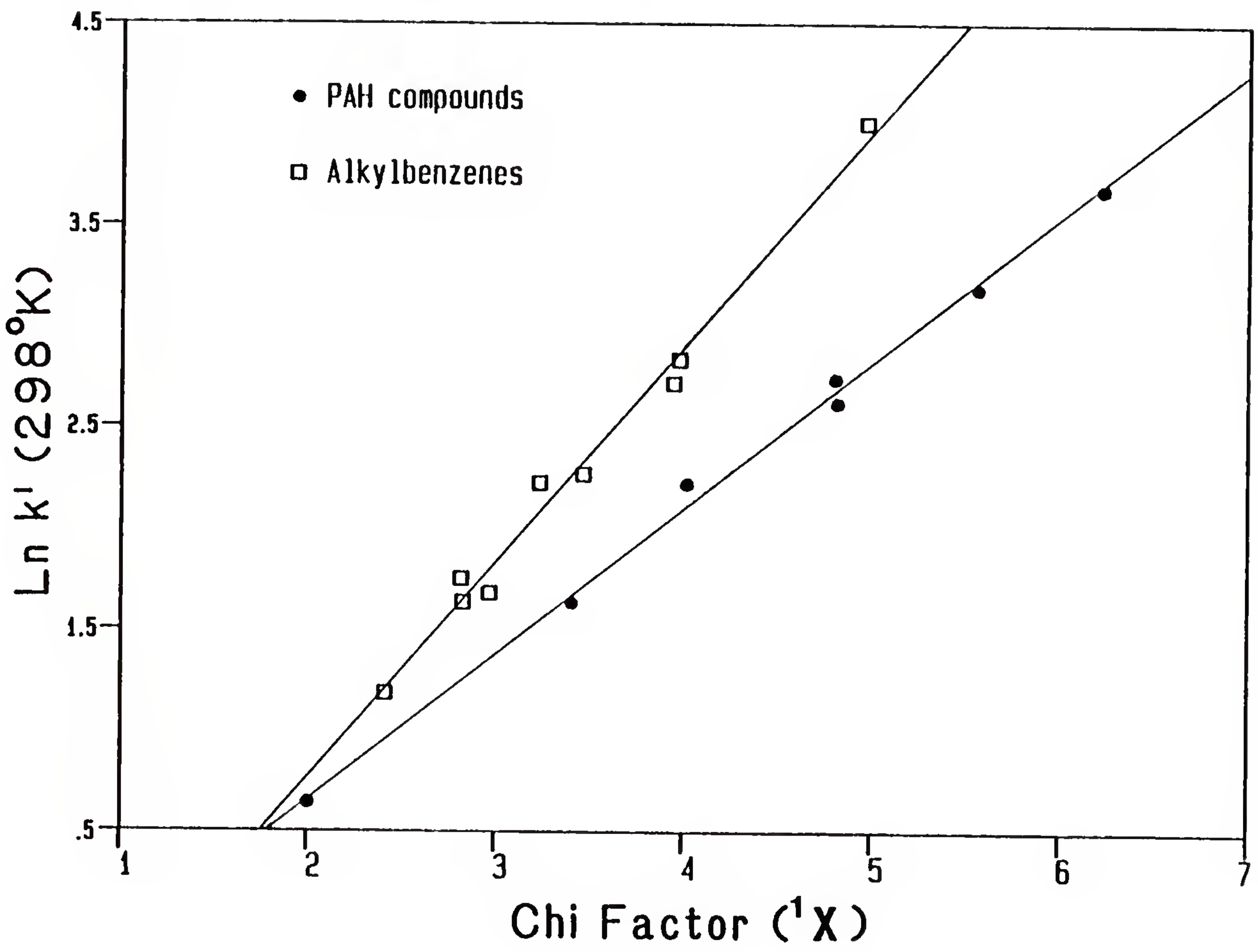

Figure 5-6. Ln k' vs. ^{1}X for the hydrophobic solutes on C-8 material in 60/40 methanol/water at 298°K.

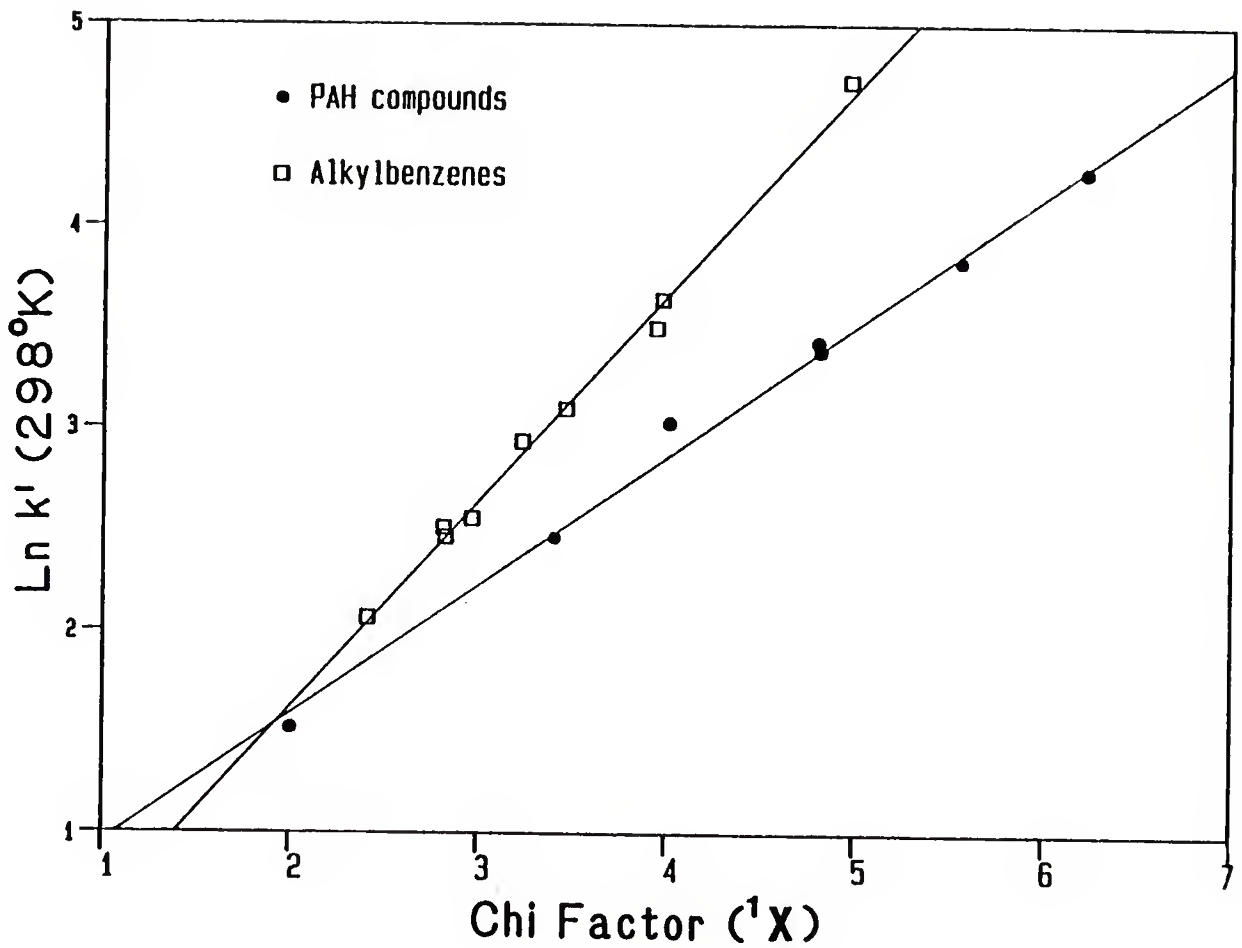

Figure 5-7. Ln k' vs. ^{1}X for the hydrophobic solutes on C-8 material in 40/60 acetonitrile/water at 298°K.

Table 5-5. Regression parameters from linear correlation of ln k' (298°K) vs. ^{1}X in various RPLC systems.

Column	Solvent system	Regression parameters ($\pm$95% conf. limit) from ln k' (298°K) vs. ^{1}X
C-8	60/40 MeOH/H_2O	(1) PAHs and Benzene n = 7, R = 0.9988 Slope = 0.72 $\pm$ 0.04 Intercept = -0.78 $\pm$ 0.19
		(2) Alkylbenzenes n = 9, R = 0.9940 Slope = 1.07 $\pm$ 0.11 Intercept = -1.38 $\pm$ 0.37
C-2	60/40 MeOH/H_2O	(1) PAHs and Benzene n = 7, R = 0.9918 Slope = 0.42 $\pm$ 0.09 Intercept = -1.45 $\pm$ 0.46
		(2) Alkylbenzenes n = 9, R = 0.9959 Slope = 0.82 $\pm$ 0.07 Intercept = -2.37 $\pm$ 0.23
C-2	40/60 ACN/H_2O	(1) PAHs and Benzene n = 7, R = 0.9880 Slope = 0.45 $\pm$ 0.08 Intercept = 0.09 $\pm$ 0.37
		(2) Alkylbenzenes n = 9, R = 0.9974 Slope = 0.78 $\pm$ 0.05 Intercept = -0.61 $\pm$ 0.18
C-8	40/60 ACN/H_2O	(1) PAHs and Benzene n = 7, R = 0.9980 Slope = 0.64 $\pm$ 0.05 Intercept = 0.29 $\pm$ 0.21
		(2) Alkylbenzenes n = 9, R = 0.9976 Slope = 1.02 $\pm$ 0.06 Intercept = -0.42 $\pm$ 0.22

RPLC phases appear to function as separate alkyl chains, while longer brush-type chains (C-8 and C-18) may aggregate together, thereby producing a hydrophobic "layer" for solute retention. Polymeric phases appear to be more consistent in their hydrophobic nature and chromatographic properties (Scott and Kucera, 1977; Scotto and Simpson, 1980).

Upon combining Eqns. (3-2) and (3-3), one may develop the following relationship

$$\ln k' = -\Delta G^{o}_{sorp}/RT + \ln \phi \qquad (5\text{-}2)$$

where ΔG^{o}_{sorp} is the standard free energy change for the sorption process. It is quite clear that ln k' is a direct measure of the standard free energy change for the solute retention process. The distinct relationship of ln k' to hydrophobicity (log K_{ow}), molecular size (HSA), and shape (^{1}X) for the PAHs and alkylbenzenes may therefore be seen as energetic differences in the overall sorptive behavior of these two classes of compounds. The basis of these thermodynamic differences will be explored in much greater detail later in this chapter.

In addition to the results presented here, a number of other researchers have noted the differences in retention behavior for PAHs and alkylbenzenes in a variety of RPLC systems. Hanai and Hubert (1984) examined sorption of PAHs and alkylbenzenes on octadecylsilane as a function of

molecular connectivity, log K_{ow}, and van der Waals volume (Bondi, 1964) in acetonitrile/water and tetrahydrofuran/water mobile phases. For each of the three parameters under study, there were distinct differences in solute retention for the PAHs and alkylbenzenes. Similar distinctions were noted by Hammers et al. (1982) for C-18 retention in a methanol/water eluent and by Jinno and Kawasaki (1983a, 1983b) for sorption on C-8 and C-18 columns in acetonitrile/water solvent systems. Hence, regardless of the parameters used to describe solute properties or molecular structure, it appears that the thermodynamic differences in hydrophobic retention for PAHs and alkylbenzenes are quite real. The results presented in this dissertation and the work of other researchers (Hanai and Hubert, 1984; Hammers et al., 1982) are in agreement with the suggestion of Jinno and Kawasaki (1983a, 1983b, 1984a) that molecular size, shape, and hydrophobicity are the dominant factors controlling RPLC retention of PAHs and alkylbenzenes.

5.4 Thermodynamics of Hydrophobic Sorption

The theory and supporting equations concerning the thermodynamics of hydrophobic sorption were extensively reviewed in Chapter III, Section 3.4. The following discussion will focus on the thermodynamic behavior of hydrophobic solutes in the RPLC systems under study: C-2, C-4, and C-8 stationary phases in acetonitrile/water and

methanol/water eluents. The thermodynamic properties ln k', ΔH^{o}_{sorp}, ΔS^{o}_{sorp} will now be examined as functions of eluent composition (θ) and molecular size (HSA).

5.4.1 Effects of Eluent Composition on Solute Retention, ln k'

The ln k' values of the solutes under study are listed in Appendix A for all sorbent systems in methanol/water and acetonitrile/water solvent systems. The effect of organic solvent content upon solute retention is a topic of considerable interest to chromatographers (Dorsey et al., 1983; Horvath et al., 1976; Jandera et al., 1982b; Karger et al., 1976; Schoenmakers et al., 1983; Snyder et al., 1979; Wells and Clark, 1984) and environmental scientists (Nkedi-Kizza et al., 1985; Rao et al., 1985; Woodburn et al., 1985). Horvath et al. (1976) and Karger et al. (1976) demonstrated a linear relationship for ln k' vs. solvent composition over the entire range of the methanol/water system for substituted aromatics retained on a C-18 column. Nkedi-Kizza et al. (1985) report a similar linear plot for the natural logarithm of the soil sorption coefficient vs. methanol content for several aromatic solutes on a wide variety of surface soils. It has been proposed by Snyder et al. (1979) and Rao et al. (1985) that a linear expression is valid over a wide range of k' values and solvent compositions.

$$\ln k' = \ln k_w - S\,\theta \qquad (5\text{-}3)$$

where k_w is the retention factor in pure water, θ is the volume fraction of organic solvent under isocratic conditions, and S is a parameter related to the "strength" of the pure organic solvent and the hydrophobic nature of the solute of interest. Values of the parameter S have been tabulated by Snyder et al. (1979) and Rao et al. (1985) for a number of organic solvents in RPLC and soil systems.

A number of researchers have reported a curvilinear response of ln k' to volume fraction organic solvent content, θ (Karger et al., 1976; Schoenmakers et al., 1983; Wells and Clark, 1984; Wells et al., 1982). Schoenmakers et al. (1983) studied the retention of a number of aromatic solutes in mixtures of methanol, acetonitrile, and tetrahydrofuran in water on a C-18 support. Their work suggested that a quadratic rather than a linear function of eluent composition was a better fit of ln k' vs. solvent composition plots

$$\ln k' = \ln k_w + A\theta^2 + B\theta \qquad (5\text{-}4)$$

where A and B are constants and all other terms are as defined previously. In soil systems, Nkedi-Kizza et al. (1985) found that a quadratic expression better described anthracene sorption (K) from acetone/water solutions on several soil types than a simple linear ln K vs. θ equation. Melander and Horvath (1980) suggested that the

nonlinearity may be due to the solvent-mediated formation of a conformer of the solute molecule which binds to the stationary phase differently than the solute present in 100% water.

The ln k' values for naphthalene, n-butylbenzene, and iodobenzene at different eluent compositions are plotted in Figures 5-8, 5-9, and 5-10, respectively. The figures represent the C-8 retention for these compounds at 298°K in methanol/water and acetonitrile/water mixtures. Retention data were collected on the C-8 support down to a methanol content of 50% by volume in methanol/water eluents and an acetonitrile content of 30-40% by volume in acetonitrile/water mobile phases. Below these solvent compositions, solute retention became so strong that collection of k' data was not practical on a routine basis.

The methanol ln k' data in Figures 5-8 to 5-10 were linearly regressed against the organic solvent content (θ), while the retention data in acetonitrile/water required the use of a quadratic ln k' vs. θ expression. The calculated ln k_w values for all tested solutes on the C-8 stationary phase in methanol and acetonitrile mixtures with water are listed in Table 5-6. Data from acetone/water eluents on C-8 for five PAH compounds are also included in the table for comparison purposes. The excellent agreement among calculated ln k_w values from the different solvent systems suggest that a linear ln k' vs. θ regression (Eqn. 5-3) is

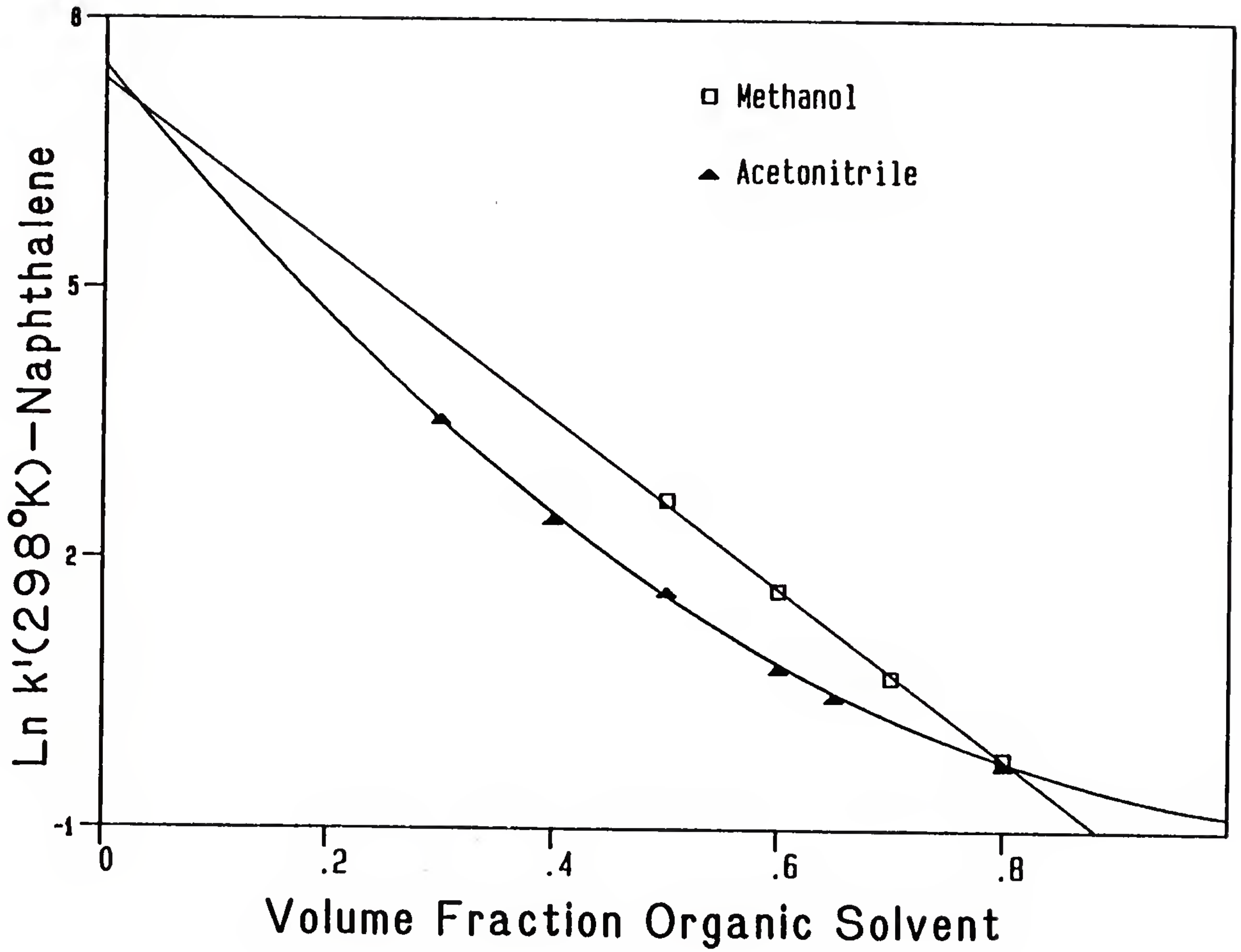

Figure 5-8. Ln k' of naphthalene vs. volume fraction of organic solvent on C-8 material at 298°K.

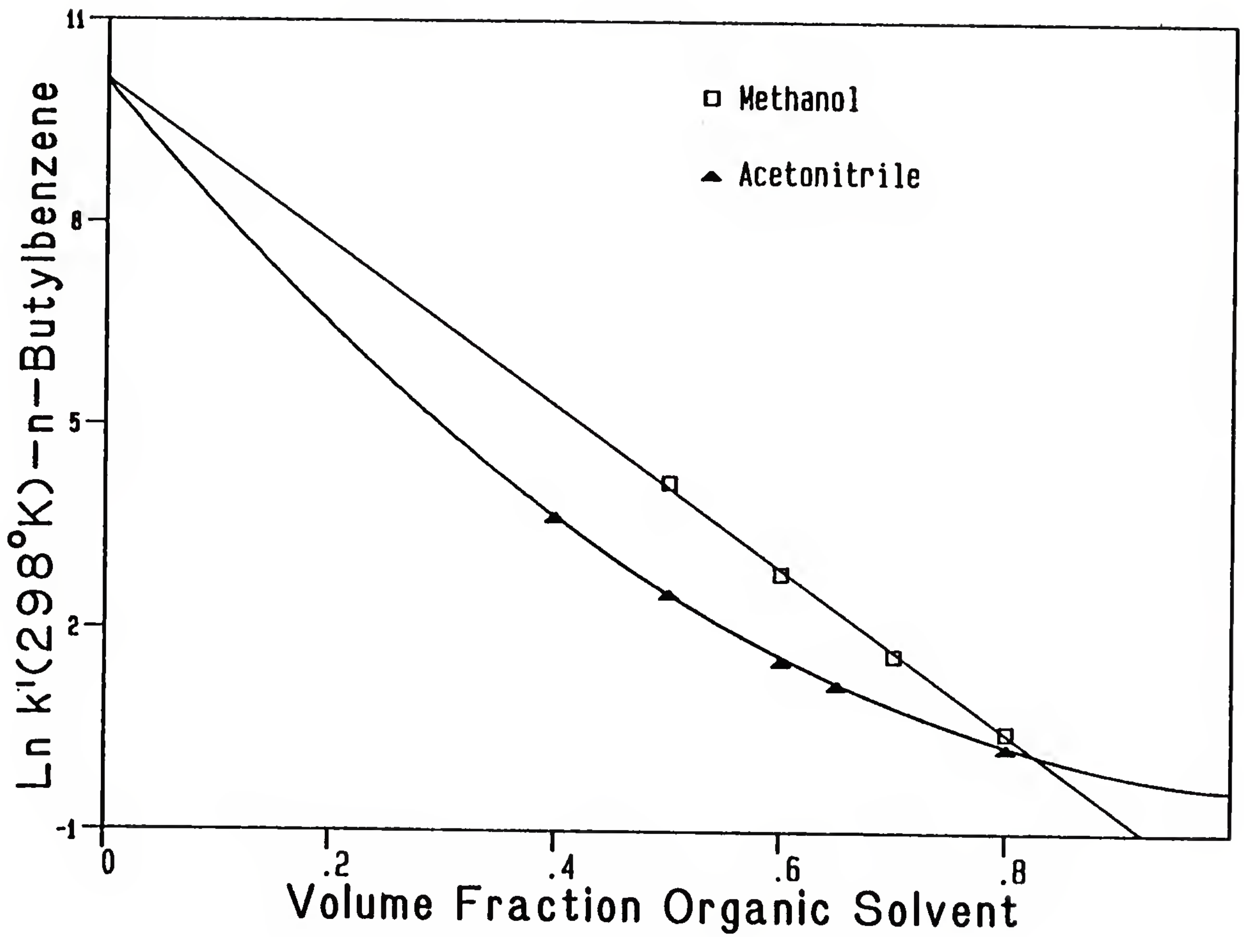

Figure 5-9. Ln k' for n-butylbenzene vs. volume fraction of organic solvent on C-8 material at 298°K.

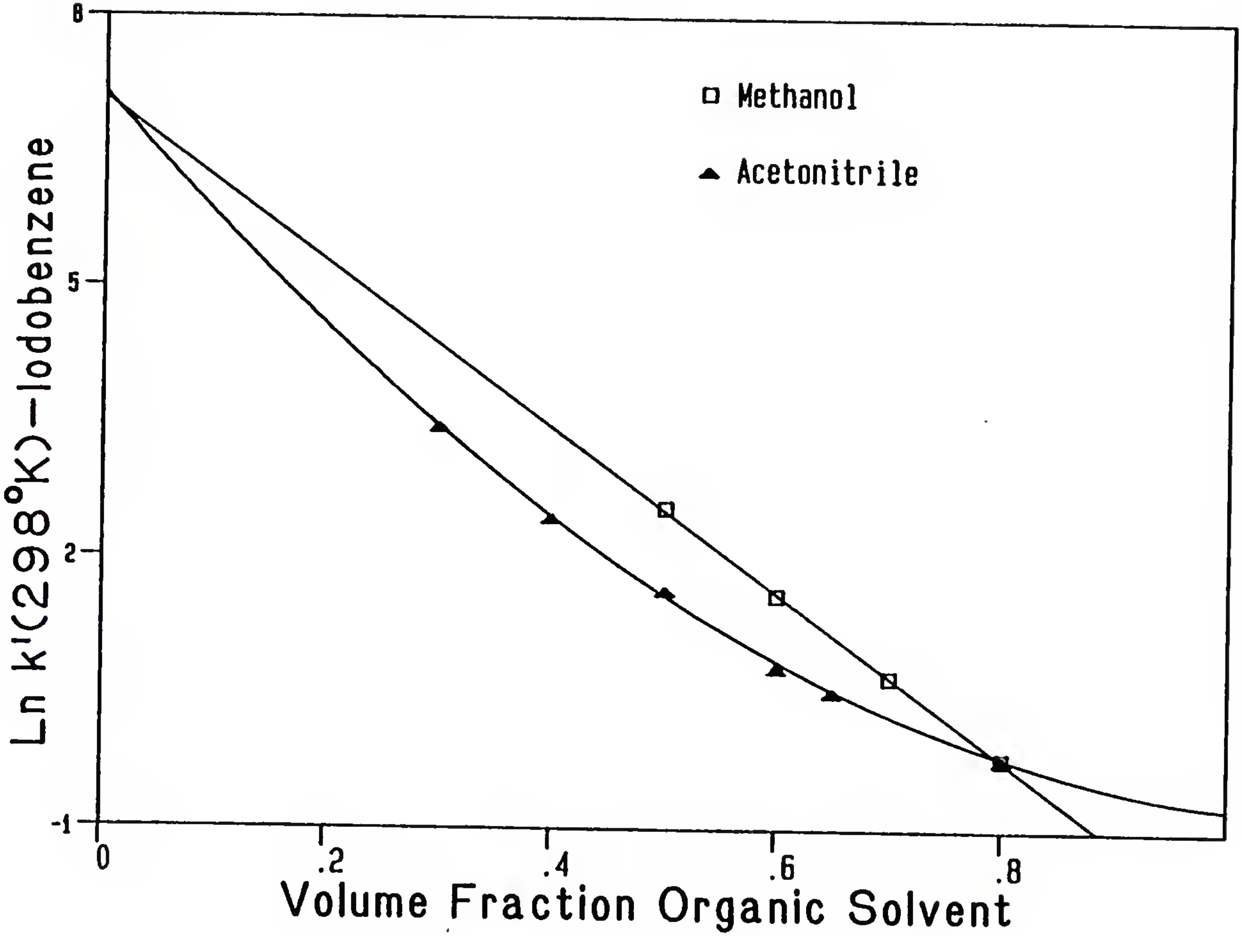

Figure 5-10. Ln k' of iodobenzene vs. volume fraction of organic solvent on C-8 material at 298°K.

Table 5-6. Calculated $\ln k_w$ values for the PAHs, alkylbenzenes, and substituted benzenes on the C-8 column at 298°K for several solvent systems.

Compound	Organic Solvent[a]	ln k' vs.	n^b	R^c	$\ln k_w{}^d$	$\ln k_w{}^{expt}$
Biphenyl	MeOh	Linear	4	-0.999	8.97	
	ACN	Quadratic	6	-0.999	9.13	
Naphthalene	MeOH	Linear	4	-0.999	7.31	7.22
	ACN	Quadratic	6	-0.999	7.47	
Phenanthrene	MeOH	Linear	4	-0.999	9.75	
	ACN	Quadratic	5	-0.999	9.72	
	ACT	Quadratic	4	-0.999	10.93	
Anthracene	MeOH	Linear	4	-0.999	10.02	
	ACN	Quadratic	5	-0.999	9.57	
	ACT	Quadratic	4	-0.999	10.74	
Pyrene	MeOH	Linear	4	-0.999	10.92	
	ACN	Quadratic	5	-0.999	10.60	
	ACT	Quadratic	4	-0.999	10.54	
Chrysene	MeOH	Linear	3	-0.999	11.70	
	ACN	Quadratic	5	-0.999	11.70	
	ACT	Quadratic	4	-0.999	11.09	
Fluoranthene	MeOH	Linear	3	-0.999	11.27	
	ACN	Quadratic	5	-0.999	10.60	
	ACT	Quadratic	4	-0.999	11.87	
Benzene	MeOH	Linear	4	-0.999	4.78	3.94
	ACN	Quadratic	6	-0.999	4.74	
Toluene	MeOH	Linear	4	-0.999	6.06	
	ACN	Quadratic	6	-0.999	5.97	
Ethylbenzene	MeOH	Linear	4	-0.999	7.32	
	ACN	Quadratic	6	-0.999	7.20	
n-Propylbenzene	MeOH	Linear	4	-0.999	8.70	
	ACN	Quadratic	6	-0.999	8.61	
n-Butylbenzene	MeOH	Linear	4	-0.999	10.11	
	ACN	Quadratic	5	-0.999	10.08	

Table 5-6. Continued.

Compound	Organic Solvent[a]	ln k' vs. θ	n^b	R^c	$\ln k_w{}^d$	$\ln k_w{}^{expt}$
n-Hexylbenzene	MeOH	Linear	3	-0.999	12.59	
	ACN	Quadratic	5	-0.999	11.23	
p-Xylene	MeOH	Linear	4	-0.999	7.26	
	ACN	Quadratic	6	-0.999	7.26	
o-Xylene	MeOH	Linear	4	-0.999	7.02	
	ACN	Quadratic	6	-0.999	6.97	
m-Diethyl-benzene	MeOH	Linear	4	-0.999	9.72	
	ACN	Quadratic	6	-0.999	9.51	
1,2,4-Trimethyl-benzene	MeOH	Linear	4	-0.999	8.28	
	ACN	Quadratic	6	-0.999	8.25	
Fluorobenzene	MeOH	Linear	4	-0.999	5.16	
	ACN	Quadratic	6	-0.999	5.22	
Chlorobenzene	MeOH	Linear	4	-0.999	6.24	5.40
	ACN	Quadratic	6	-0.999	6.31	
Bromobenzene	MeOH	Linear	4	-0.999	6.55	
	ACN	Quadratic	6	-0.999	6.55	
Iodobenzene	MeOH	Linear	4	-0.999	7.09	
	ACN	Quadratic	6	-0.999	7.15	
Nitrobenzene	MeOH	Linear	4	-0.999	4.56	4.49
	ACN	Quadratic	6	-0.999	4.87	

[a] MeOH = methanol; ACN = acetonitrile; ACT = acetone.

[b] Number of data points involved in regression equation.

[c] Correlation coefficient for the regression equation.

[d] Calculated $\ln k_w$ value from: $\ln k' = \ln k_w - S\theta$
or $\ln k' = \ln k_w + A\theta + B\theta^2$

[e] Experimental $\ln k_w$ values on C-18 material from Schoenmakers et al. (1983).

acceptable for methanol, while acetonitrile and acetone require the use of a quadratic ln k' vs. θ relationship (Eqn. 5-4). These relationships were used to develop the appropriate $f(\theta)$ functions for the enthalpy-entropy compensation models (Chapter III, Section 3.4.4) in methanol/water and acetonitrile/water mobile phases.

5.4.2 Effect of Eluent Composition on ΔH^{o}_{sorp}

The effect of organic solvent composition upon the sorptive enthalpy change has not been a subject of extensive research. Sander and Field (1980) reported that the ΔH^{o}_{sorp} value of isopropylbenzene retained on a C-18 support increased with the volume fraction of methanol in the mobile phase. Similar results were reported by Melander and Horvath (1984) for retention of n-alkylbenzenes on C-18 material in mobile phases of methanol, isopropanol, dioxane, and tetrahydrofuran in water.

The ΔH^{o}_{sorp} values of benzene, ethylbenzene, n-propylbenzene, and pyrene on a C-4 support are plotted in Figure 5-11 as a function of the eluent methanol content. The change in the standard enthalpy of sorption for each of the four solutes increases linearly with the volume fraction of methanol in the mobile phase. Similar results are demonstrated in Figure 5-12 for solute retention on the C-4 column with an acetonitrile/water solvent system. The trend of linearly increasing standard sorptive enthalpy change

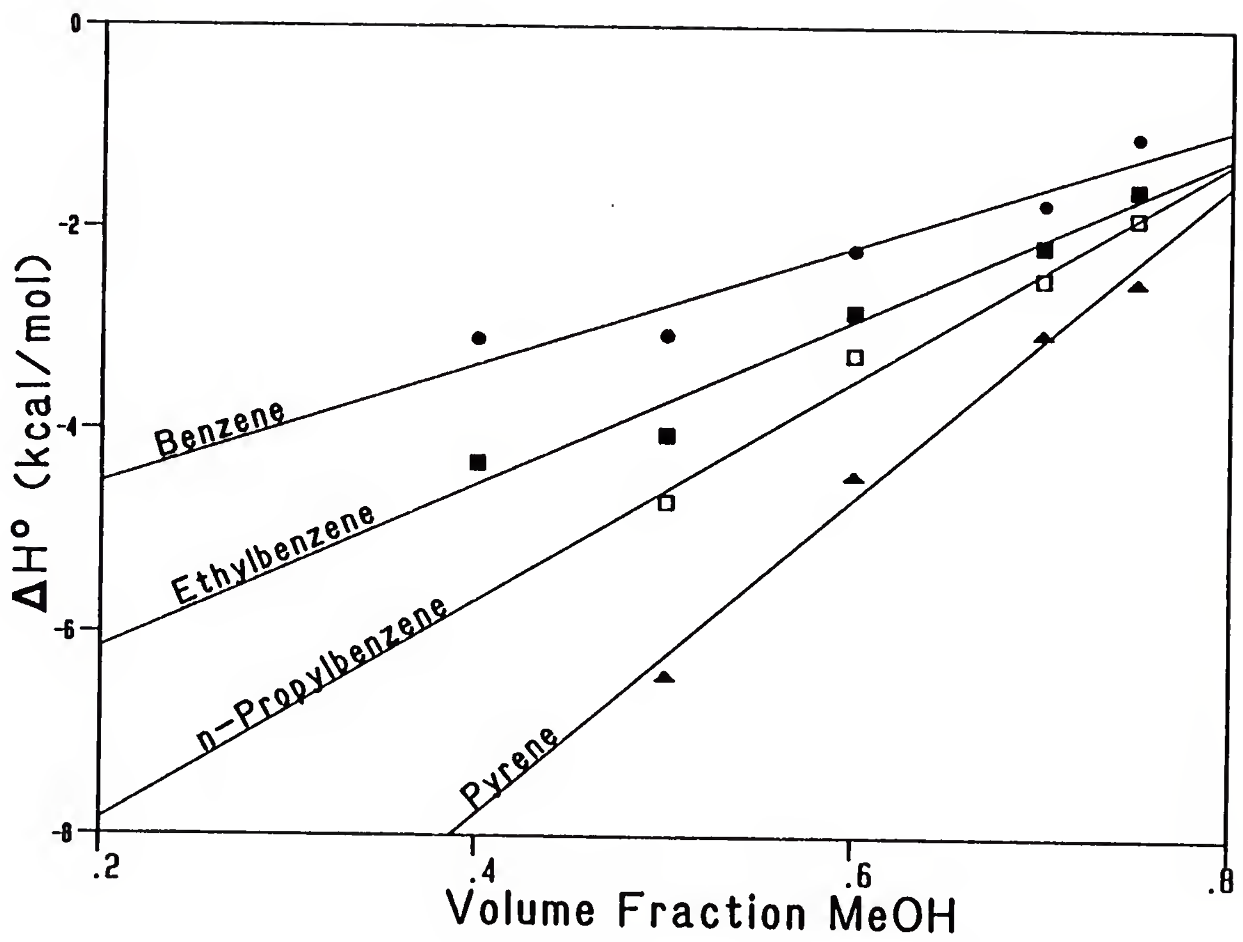

Figure 5-11. ΔH^{o} for sorption vs. volume fraction methanol content for four aromatic solutes on the C-4 support.

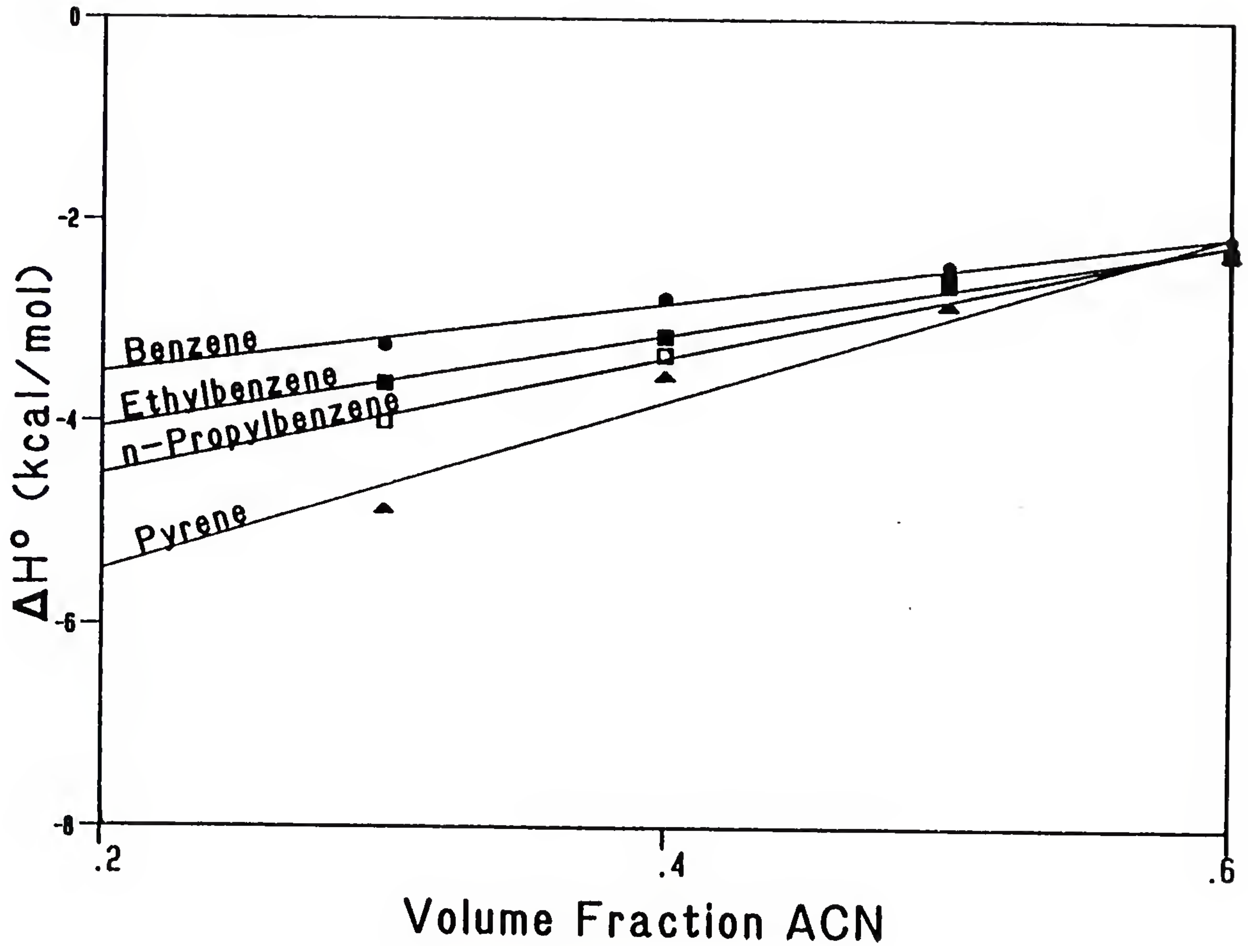

Figure 5-12. ΔH^{o} for sorption vs. volume fraction acetonitrile content for four aromatic solutes on the C-4 support.

with increasing organic solvent content was generally observed on all three stationary phases (C-2, C-4, and C-8) with both methanol/water and acetonitrile/water mobile phases. These results are in agreement with the data of Sander and Field (1980) and Melander and Horvath (1984). The collected ΔH^o_{sorp} values may be found in Appendix C.

More careful interpretation of the data in Figures 5-11 and 5-12 reveals several trends. In each figure, the standard sorption enthalpy changes are negative and become increasingly positive as the organic solvent concentration is increased. Thus, the transfer of solute from the mobile phase to the stationary phase becomes less favored, based on enthalpy considerations, at higher solvent concentrations. This results in an observed decrease in solute retention at higher solvent contents. Additionally, the slopes of the ΔH^o_{sorp} vs. θ plots in Figures 5-11 and 5-12 increase with the hydrophobicity of the solute molecules. These trends are in agreement with the solvophobic model of hydrophobic retention (Horvath et al., 1976). Based on a review of the solvophobic theory in Chapter III, Section 3.3, recall Eqn. (3-9), which relates the cavitization free energy change for solute i to the surface tension of mobile phase (γ) and the HSA of the solute molecule by

$$\Delta G_{cav,i} = K^e_i \text{ HSA } \gamma \, (1 - W_i)N \qquad (5\text{-}5)$$

where $\Delta G_{cav,i}$ is the change in free energy required to create a solvent cavity for solute i, K^e_i is a proportionality constant correcting the surface tension for the curvature of the solute's solvation sphere, γ is the solution surface tension, W is a complex function of K^e_i and γ, and N is Avogadro's number.

For many hydrophobic solutes retained on an RPLC column, enthalpic processes are thought to control the overall sorptive free energy change (Colin et al., 1978; Melander et al., 1978). From Eqn. (5-5), it may be theorized that for a given solute molecule, a decrease in organic modifier content, i.e., an increase in surface tension, will produce a greater $\Delta G_{cav,i}$ value. Since sorption may be viewed as a reversal of the cavitization process, the ΔG^o_{sorp} (and therefore ΔH^o_{sorp}) should become more exothermic as the surface tension of the mobile phase is increased. This is indeed the trend observed in Figures 5-11 and 5-12.

Similarly, from Eqn. (5-5), for a specific change in surface tension, the change in the $\Delta G_{cav,i}$ term is largely controlled by the solute's HSA value. That is, the slope of a ΔH^o_{sorp} vs. θ plot should be a function of the HSA value for the solute molecule and the relative change in surface tension for a given change in θ. Within a single solvent system, the solute's HSA value should dictate the magnitude of the slope. The thermodynamic behavior of the solutes in

Figures 5-11 and 5-12 agrees with Eqn. (5-5), with solutes of higher HSA values having more exothermic sorptive enthalpy changes and greater slopes for the individual ΔH^{o}_{sorp} vs. θ plots. The relationship of ΔH^{o}_{sorp} to HSA will be discussed in greater detail in a later section. Nkedi-Kizza et al. (1985), Rao et al. (1985), and Woodburn et al. (1985) have applied the solvophobic relationship expressed by Eqn. (5-5) to model soil sorption coefficients for hydrophobic organic chemicals in soil/water/organic solvent systems.

It is worth noting in Figures 5-11 and 5-12 that, for a given change in solvent composition ($\Delta\theta$), the corresponding change in ΔH^{o}_{sorp} for a given solute is greater in the methanol/water system (Fig. 5-11) than in the acetonitrile/water mixture (Fig. 5-12). This difference may be correlated to the relative change in surface tension for the two solvent systems over the θ range studied. The dependence of eluent surface tension upon methanol and acetonitrile content is demonstrated in Figures 5-13 and 5-14, respectively. The surface tension of the methanol/water system decreases nearly linearly with increasing methanol content. In an acetonitrile/water system, however, surface tension initially decreases almost exponentially with increasing solvent composition, then producng only a slight decline in the γ value from a θ_{ACN} of 0.40 to 1.0. Therefore, it is not surprising that the ΔH^{o}_{sorp} values in

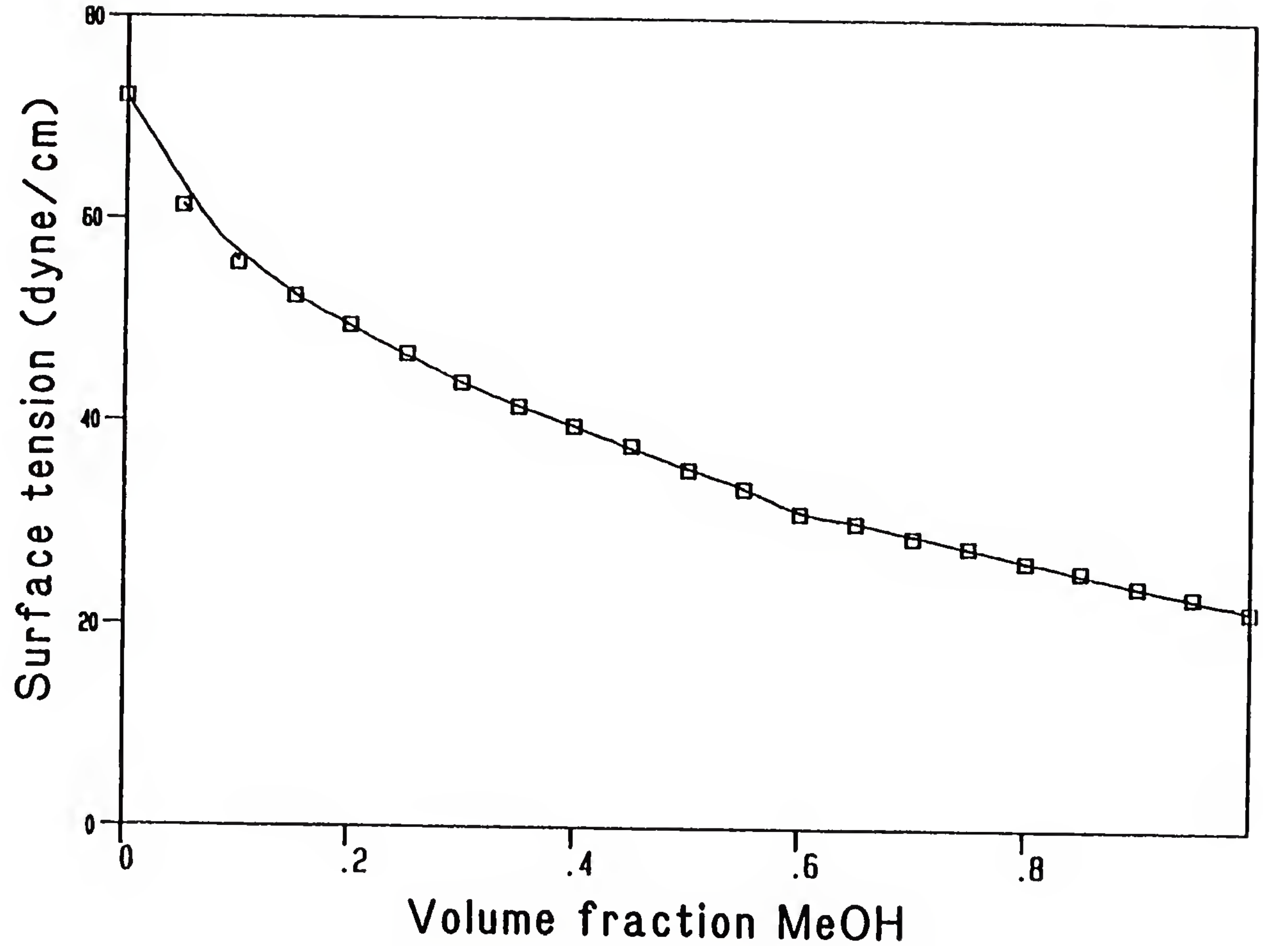

Figure 5-13. Surface tension vs. volume fraction methanol content at 25°C.

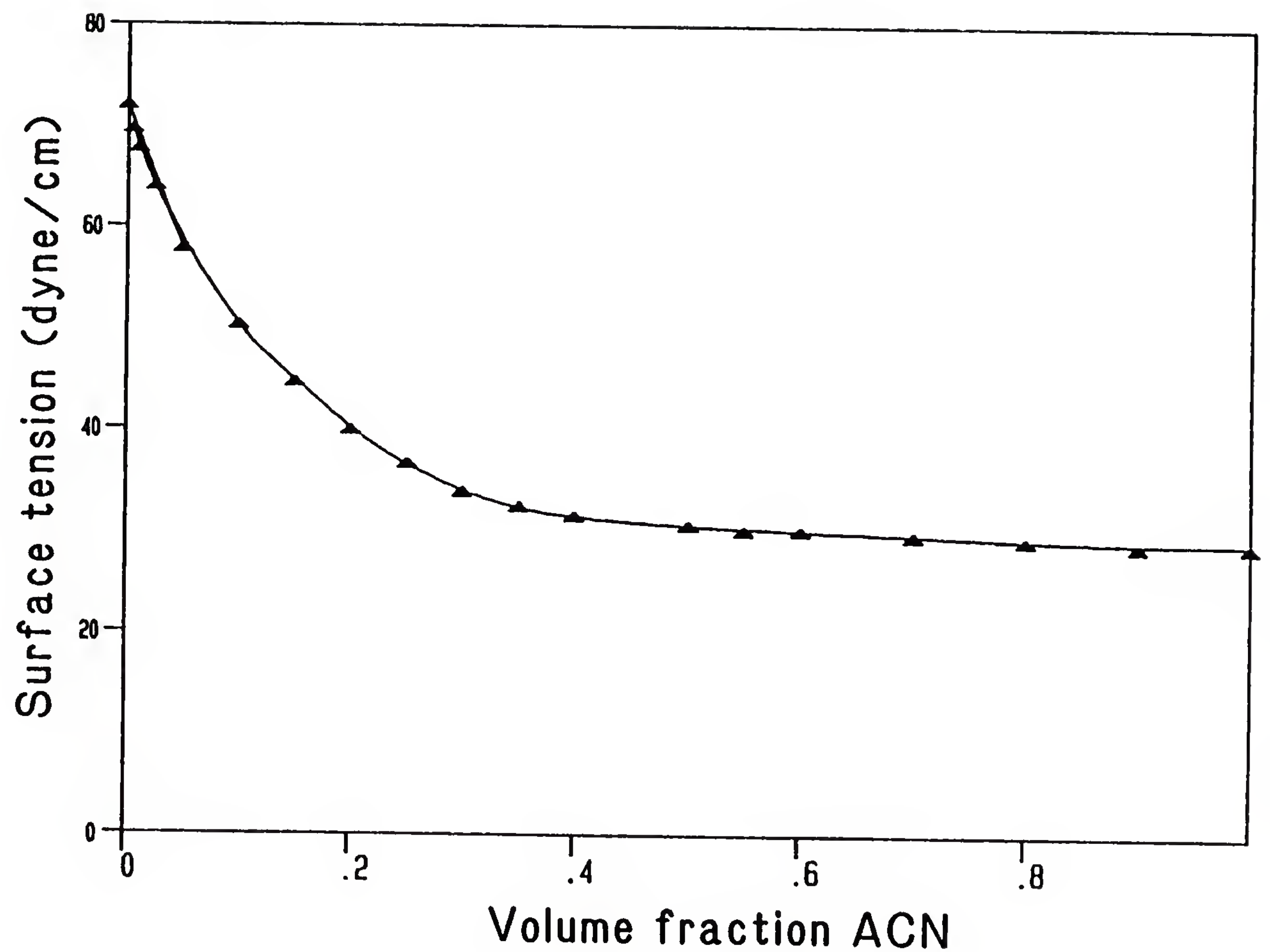

Figure 5-14. Surface tension vs. volume fraction acetonitrile content at 25°C.

Figure 5-12 show only a small change as the acetonitrile content in water is varied from a volume fraction of 0.30 to 0.60.

The effect and importance of solvent surface tension may perhaps best be seen from the slopes of ΔH^{o}_{sorp} vs. θ plots for the two eluent systems. A comparison of Figures 5-11 and 5-12 finds that higher slope values exist in the methanol/water system, for a given solute. This difference in solvent behavior is believed related to changes in surface tension for the two solvents over the θ range studied. The ΔH^{o}_{sorp} vs. θ regression equations for the four solutes retained on C-4 material in the two solvent systems are listed in Table 5-7. The data clearly show that for the θ range examined, slopes of ΔH^{o}_{sorp} vs. θ plots for a given solute are significantly greater in the methanol/water eluent.

In summary, the observed linear response of ΔH^{o}_{sorp} values with changing organic solvent content agrees with previous RPLC data (Sander and Field, 1980; Melander and Horvath, 1984) and also with the solvophobic theory of hydrophobic retention (Horvath et al., 1976). Melander and Horvath (1984) reported that the linear dependence of ΔH^{o}_{sorp} on organic solvent content supports the proposal of a "well-mixed" model for describing RPLC sorption. The following section will analyze the relationshp between the

Table 5-7. Correlation of ΔH^o values for C-4 sorption with fractional organic solvent content, θ. Comparison of methanol/water and acetonitrile/water systems for four aromatic solutes.

Compound	Regression Equation for ΔH^o vs. θ (MeOH)[a]	Regression Equation for ΔH^o vs. θ (ACN)[b]
Benzene	n = 5, R = 0.9662 Y = 5.88X - 5.70	n = 4, R = 0.9916 Y = 3.45X - 4.21
Ethylbenzene	n = 5, R = 0.9850 Y = 8.12X - 7.78	n = 4, R = 0.9914 Y = 4.62X - 4.99
n-Propylbenzene	n = 4, R = 0.9903 Y = 10.86X = 10.02	n = 4, R = 0.9905 Y = 5.78X = 5.68
Pyrene	n = 4, R = 0.9929 Y = 15.62X - 14.04	n = 4, R = 0.9768 Y = 8.34X - 7.13

[a] θ range for methanol/water system = 0.40 to 0.75; n is the number of data points used in the regression equation; R is the correlation coefficient.

[b] θ range for acetonitrile/water system = 0.30 to 0.60; n is the number of data points used in the regression equation; R is the correlation coefficient.

experimental ΔS^{o} sorption values and the eluent organic solvent content, θ.

5.4.3 Effect of Eluent Composition on ΔS^{o}_{sorp}

In considering the standard entropy changes for the transfer of a solute molecule from the mobile phase to the stationary phase, one must consider the relative degree of disorder existing for the solute in both systems. It seems logical that the solute molecule may be in a more ordered state in the stationary phase than in solution, i.e., the sorption process should produce negative ΔS^{o} values. This is indeed what is observed in the RPLC systems under study; the collected ΔS^{o}_{sorp} values are listed in Appendix D.

It is important to note that ΔH^{o}_{sorp} values are independent of the column phase ratio, ϕ. Any uncertainty in the evaluation of ϕ affects ΔS^{o}_{sorp}, and all ΔS^{o}_{sorp} values are affected equally for a given RPLC column. For this reason, any uncertainty in the calculation of the column phase ratio affects only the exact ΔS^{o}_{sorp} values, and thus trends in ΔS^{o}_{sorp} as a function of θ, HSA, etc. will not be affected. It is estimated from the computed phase ratios that uncertainty in the ϕ values would result in a maximum offset of ± 3.8 cal/mole-°K in observed ΔS^{o}_{sorp} trends.

In general, it is more difficult to identify trends in the behavior of ΔS^{o}_{sorp}, due to the limited thermodynamic data set and consequent high degree of uncertainty

concerning the ΔS^o values, expressed in units of cal/mole-°K. For example, a typical ΔS^o_{sorp} value of -3.00 cal/mole-°K might easily have a 95% confidence limit of $\pm$1 to 4 cal/mole-°K. This makes the interpretation of the ΔS^o_{sorp} data somewhat tenuous. Nevertheless, we shall proceed with our scientific curiosity intact.

The observed ΔS^o values for the sorption process are negative, as expected, and this supports the hypothesis that the solute is more ordered on the stationary phase than in solution. Interestingly, the ΔS^o_{sorp} values appear to become more negative as the organic modifier content is decreased; this trend is especially marked in methanol/water systems. For the moment, we will restrict our discussion of ΔS^o_{sorp} to methanol/water eluents.

In Figure 5-15, the ΔS^o_{sorp} values on the C-4 support for nitrobenzene, naphthalene, n-butylbenzene, and chrysene are plotted as a function of the methanol content of the mobile phase. In general, the ΔS^o_{sorp} values appear to be a linear function of the methanol content, θ, with the ΔS^o_{sorp} values declining as the fraction of water in the mobile phase is increased. Sander and Field (1980) reported similar results for the retention of isopropylbenzene and N,N-diethylaniline on a C-18 support in methanol/water eluents. The decrease in ΔS^o values with increasing water content is initially perplexing, for it argues that the entropy change for sorption of the solute molecule is a

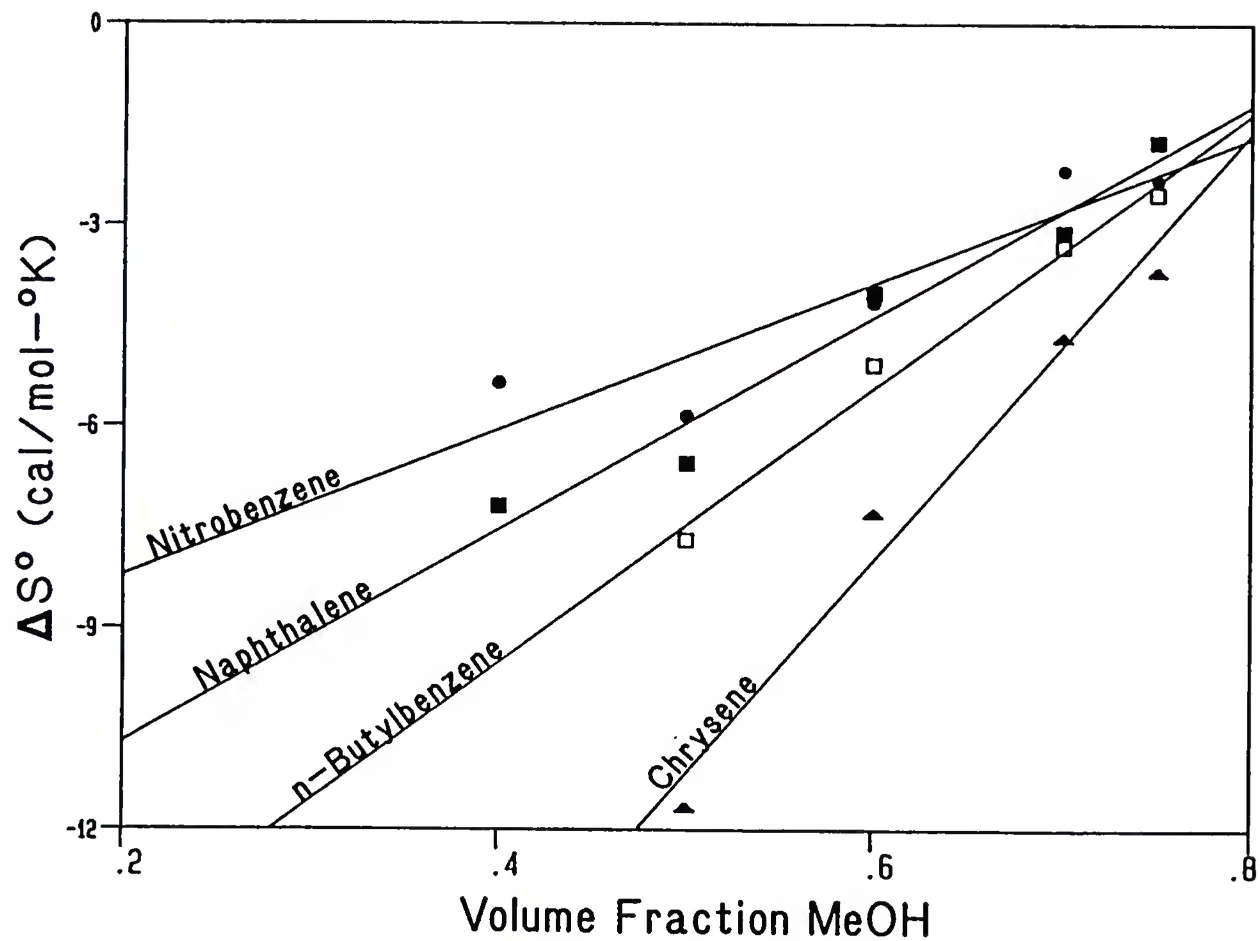

Figure 5-15. ΔS^{o} for sorption vs. volume fraction methanol content for four aromatic solutes on the C-4 support.

function of eluent composition. Perhaps the phenomenon of solute sorption may be considered as the sum of two related processes: (1) the actual sorption of the solute molecule; and 2) the release of organic solvent and water molecules acting as a solute's solvation sphere back into the bulk solution. These processes, and their relative contributions to the overall ΔS^{o}_{sorp} value, will now be considered.

Recall that a ΔS^{o}_{sorp} value represents the standard change in entropy for the entire system in which solute sorption is occurring. The change in entropy for the solute molecule moving from a solution phase to a sorbed state is most certainly negative, and the process would not appear to be a strong function of solution surface tension. However, when sorption of a solute does occur, there is a concomitant release of solvated organic solvent and water molecules from their ordered state about the solute back to the bulk solution. Evidence for this release of ordered solvent molecules may be found in the research literature on solution thermodynamics. Nemethy and Scheraga (1962) reported that aqueous solutions of nonpolar compounds have a large negative entropy change associated with the solubilization of such compounds. The negative entropy change was attributed to the ordered structure of water molecules about the hydrophobic solute. Therefore, the sorption of nonpolar compounds should produce a positive entropy change associated with the "relaxation" of the solvation sphere.

By definition, surface tension is the rate of increase in system free energy per unit increase in interfacial area (Lewis and Randall, 1961). Surface tension is attributed to the relative strength of intermolecular forces in solution (Castellan, 1971). The lower the surface tension, the lower the extent of intermolecular attractive forces and greater the degree of disorder of the solution phase. Thus, it would seem logical that for systems of low surface tension, i.e., high organic solvent content, that the ΔS^o for the release of solvent and water molecules from the solvation sphere would be positive and increase in magnitude as surface tension declines. That is, the release of "ordered solvation sphere" molecules back to the bulk solvent is a process of positive entropy change, and it becomes more positive as the surface tension of the bulk solution declines.

The ΔS^o values for solute sorption may therefore be viewed as the sum of two opposing effects: (1) the sorption of the solute molecule, producing a negative entropy change, termed ΔS^o_1; and (2) the release of the solvation sphere back to the bulk solution when solute sorption occurs. The latter process produces a positive ΔS^o, termed ΔS^o_2, and the magnitude of ΔS^o_2 depends upon the relative degree of order of the bulk solution, which may be indicated by the solution's surface tension. Since $\Delta S^o_{sorp} = \Delta S^o_1 + \Delta S^o_2$, the value of ΔS^o_{sorp} should become more negative as the surface

tension of the bulk solution is increased. This is because the intermolecular attractive forces between solvent and water molecules increase with surface tension. As the attractive forces increase and the degree of order of the bulk solvent improves, the magnitude of the positive ΔS^{o}_{2} will decline, producing a more negative value of ΔS^{o}_{sorp}. This theory, explaining the trend of the ΔS^{o}_{sorp} values with solution composition, agrees with the observed data.

It was suggested previously that a plot of ΔG^{o}_{sorp} vs. θ should produce a slope that is a function of the solute's HSA value (Eqn. 5-5). This trend was observed for the ΔH^{o}_{sorp} vs. θ plots in Figures 5-11 and 5-12. The ΔS^{o}_{sorp} vs. θ regression lines shown in Figure 5-15 show a similar dependence of the slope value upon the hydrophobicity of the solute molecule. It seems logical that larger, more hydrophobic molecules exhibit greater ordering during sorption, i.e., their ΔS^{o}_{sorp} values should be more negative than those of smaller, less hydrophobic molecules. This behavior has been observed for PAH solutes by Chmielowiec and Sawatsky (1979). If, as suggested, ΔS^{o}_{2} values decline toward zero with increasing eluent water content, then ΔS^{o}_{1} values will become dominant factors in determining overall ΔS^{o}_{sorp} values. This may explain the behavior of the slopes of the ΔS^{o}_{sorp} vs. θ regression lines in Figure 5-15.

With this introduction to the importance of both solute HSA and eluent surface tension to ΔS^{o}_{sorp} in methanol/water

solvent systems, we may now investigate the ΔS^{o}_{sorp} trends in acetonitrile/water. The dependence of eluent surface tension upon acetonitrile content was shown in Figure 5-14; notice again that surface tension decreases only slightly over a θ_{ACN} range of approximately 0.40 to 1.0. The above discussion would suggest that an appreciable change in ΔS^{o}_{sorp} values with respect to θ_{ACN} might not occur until an acetonitrile content of 30% by volume or lower was reached. Data showing ΔS^{o}_{sorp} vs. θ plots for biphenyl, pyrene, m-diethylbenzene, and bromobenzene retained on a C-2 support are given in Figure 5-16. The data seem to agree with the suggestion that sizeable changes in ΔS^{o}_{sorp} do not occur until acetonitrile contents of 30% by volume and lower. This ΔS^{o}_{sorp} vs. θ effect appears directly related to solution surface tension. The curves drawn through the data points in Figure 5-16 are not calculated regression lines; these lines merely illustrate the nonlinear behavior of ΔS^{o}_{sorp} with respect to acetonitrile content.

The collected ΔS^{o}_{sorp} data in acetonitrile/water systems on the C-4 and C-8 RPLC materials (Appendix D) support the trends observed on the C-2 material. The ΔS^{o} values decline or remain generally constant as acetonitrile content is lowered to 0.30. At and below a θ_{ACN} of 0.30, the ΔS^{o} values decline much more rapidly with changing acetonitrile content. The C-2 data best demonstrate this trend, for only on this support were ΔS^{o} values collected in mobile phases

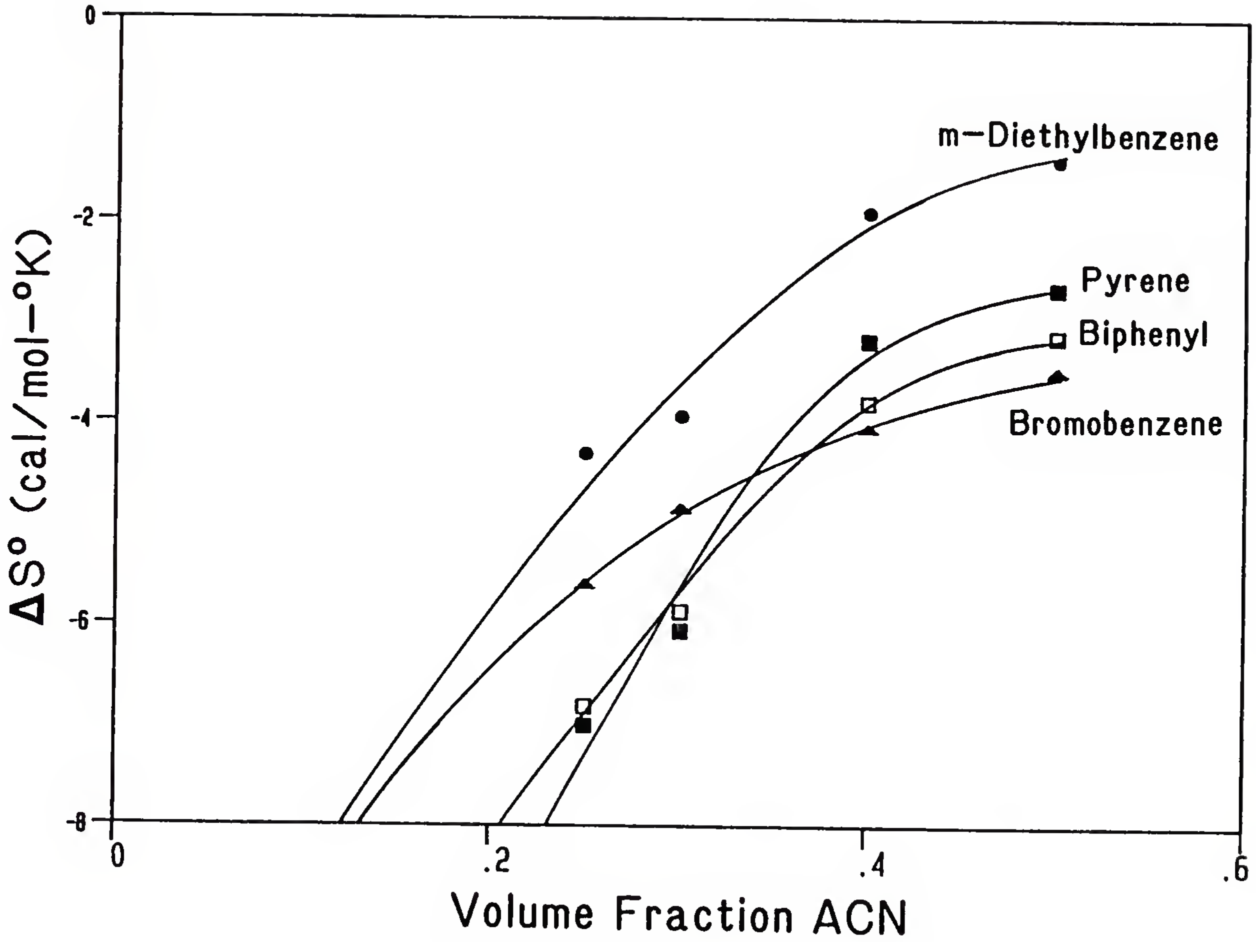

Figure 5-16. ΔS^{o} for sorption vs. volume fraction acetonitrile content for four aromatic solutes on the C-2 support.

of less than 30% acetonitrile by volume (Fig. 5-16). A more extensive data set is required, particularly at low acetonitrile compositions, to verify the effect of acetonitrile content on ΔS^{o}_{sorp}.

Summarizing, the trends exhibited by the ΔS^{o}_{sorp} data are quite similar to those noted in the ΔH^{o}_{sorp} vs. θ plots. In a methanol/water eluent, ΔS^{o}_{sorp} values decline linearly with increasing water content, and the slopes of the regression lines appear to be a function of the solute's hydrophobic nature (Figure 5-15). The linearity of the ΔS^{o} vs. θ plots in methanol/water systems may be related to the steady change in solution surface tension with methanol content (Figure 5-13). The observed decrease in ΔS^{o}_{sorp} values with increasing water content may be due to the decline in the positive entropy change (ΔS^{o}_{2}) associated with the highly ordered solvation sphere returning to the bulk solution upon solute sorption. Similar linear behavior of ΔS^{o}_{sorp} vs. θ plots is not observed in acetonitrile/water eluents (Figure 5-16). The data suggest a slight decline in ΔS^{o}_{sorp} values with acetonitrile contents greater than 30% by volume, followed by a sharp decrease in ΔS^{o}_{sorp} below a θ_{ACN} of 0.30. This change in entropic behavior is believed related to the rapid increase in surface tension for acetonitrile/water systems when the acetonitrile content falls below 30% by volume (Figure 5-14).

5.4.4 Effect of Solute Size on ΔH^{o}_{sorp}

In RPLC, solutes with longer retention volumes have larger k' values and, consequently, larger ΔG^{o}_{sorp} values. Since retention in RPLC was suggested to be enthalpically controlled (Colin et al., 1978; Melander et al., 1978), the larger, more hydrophobic, and more strongly retained solutes are expected to have more exothermic ΔH^{o}_{sorp} values. The solvophobic model (Horvath et al., 1976; Horvath and Melander, 1977) presents a theoretical expression relating ΔG^{o}_{sorp} to the nonpolar contact area (ΔA) occurring between the solute and stationary phase. This relationship is expressed in Eqn. (3-31). Since ΔA is directly related to the solute's HSA value (Eqn. 3-25), it would seem logical to investigate the relationship between measured ΔH^{o}_{sorp} values and solute molecular structure. This course of research has been pursued by a number of scientists.

Melander et al. (1979, 1982) reported a linear relationship between ΔH^{o}_{sorp} and the number of carbon atoms in the side chain of n-alkylbenzenes retained on C-18 material in acetonitrile/water and methanol/water eluents. A similar relationship was found by Hirata and Sumiya (1983) between ΔH^{o}_{sorp} and the number of carbon atoms in the fatty acid moiety of p-nitrobenzyl esters for C-18 sorption in 70/30 acetonitrile/water. Snyder (1979) reported a correlation between the size and compactness of PAH molecules and their ΔH^{o}_{sorp} values on a C-18 column in 80/20 methanol/water.

Finally, Hornsby and Rao (1983) employed the HSA as a descriptor of solute structure and found a linear relationship between ΔH^{o}_{sorp} and HSA values for aromatic solutes retained on C-8 and C-18 columns in a methanol/water mobile phase.

The ΔH^{o}_{sorp} values listed in Appendix C were linearly regressed against the solute HSA values (Table 4-2) for a number of the RPLC systems under study. The ΔH^{o} data have been plotted vs. HSA in Figure 5-17 for sorption of the hydrophobic solutes on the C-8 material in a 60/40 methanol/water solvent system; the linear regression line demonstrates the excellent correlation between ΔH^{o}_{sorp} and HSA. This behavior is generally observed in all methanol/water eluents for the C-2, C-4, and C-8 stationary phases. The data in Table 5-8 demonstrate that the slopes of the ΔH^{o}_{sorp} vs. HSA regression lines do not differ greatly on the three RPLC supports.

A ΔH^{o} vs. HSA plot for the sorption of aromatic solutes in an acetonitrile/water eluent on the C-4 support is shown in Figure 5-18. Once again, the linear relationship between ΔH^{o}_{sorp} and solute HSA is quite evident. Additional data in Table 5-9 suggest that the three RPLC supports do not cause a significant variance in the correlation of ΔH^{o}_{sorp} to HSA in acetonitrile/water systems.

In general, a single linear regression line best describes the relationship of standard sorption enthalpy

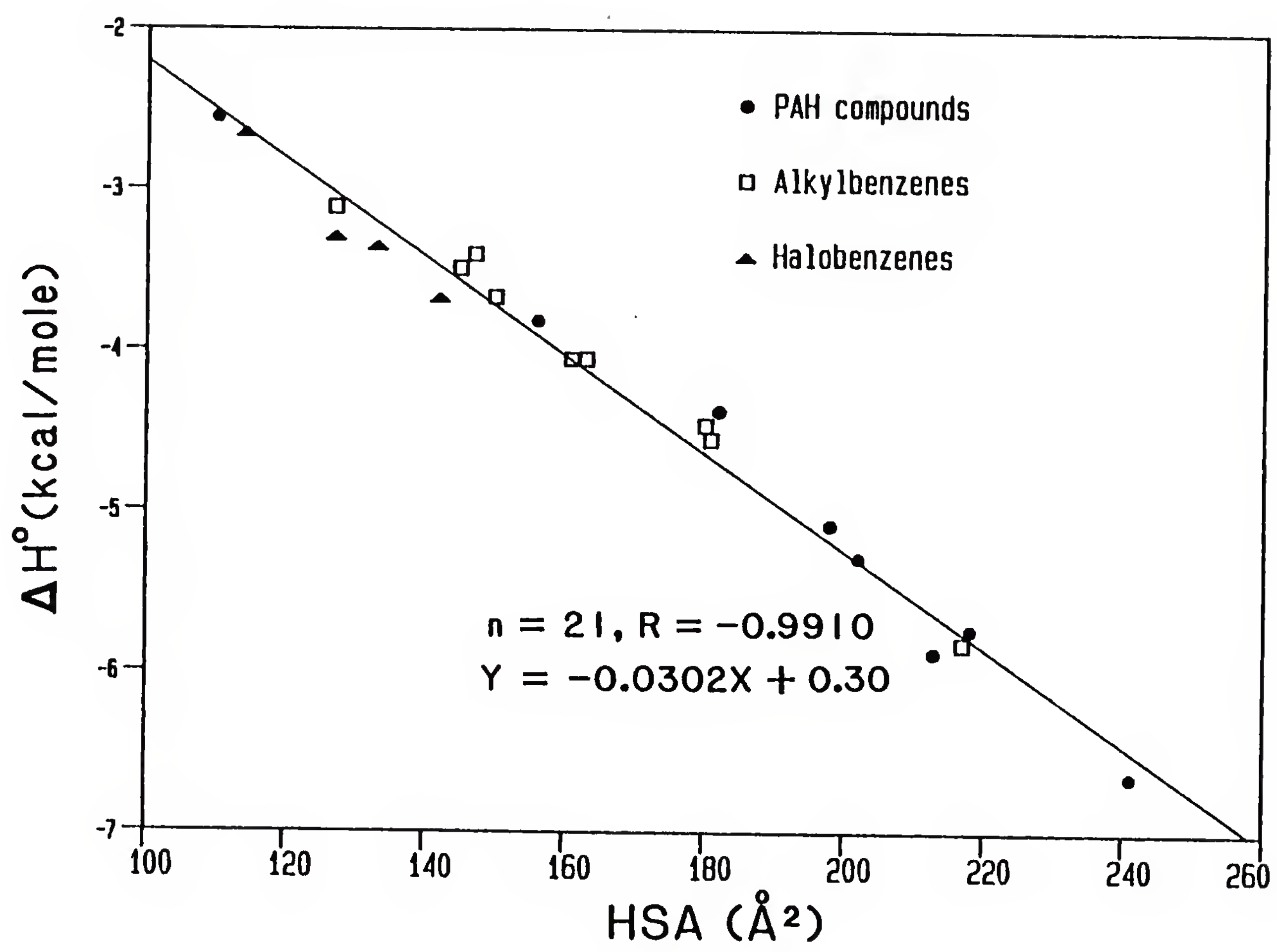

Figure 5-17. ΔH^{o} vs. solute HSA for sorption of the hydrophobic solutes on C-8 material in 60/40 methanol/water.

Table 5-8. Correlation of ΔH^{o} vs. HSA for the sorption of hydrophobic solutes in a methanol/water mobile phase on three RPLC sorbents.

RPLC Support	θ(MeOH)[a]	ΔH^{o} vs. HSA[b]
C-2	0.50	n = 22, R = -0.9628 Slope = -0.0255 ± 0.0033 Intercept = -0.07 ± 0.56
C-4	0.50	n = 20, R = -0.9673 Slope = -0.0274 ± 0.0036 Intercept = -0.26 ± 0.58
C-8	0.50	n = 19, R = -0.9849 Slope = -0.0378 ± 0.0034 Intercept = 1.41 ± 0.56

[a]Methanol/water (v/v) mixture = 50/50.

[b]n is the number of data points used in the regression; R is the correlation coefficient; slope and intercept values represent mean values ±95% confidence limits.

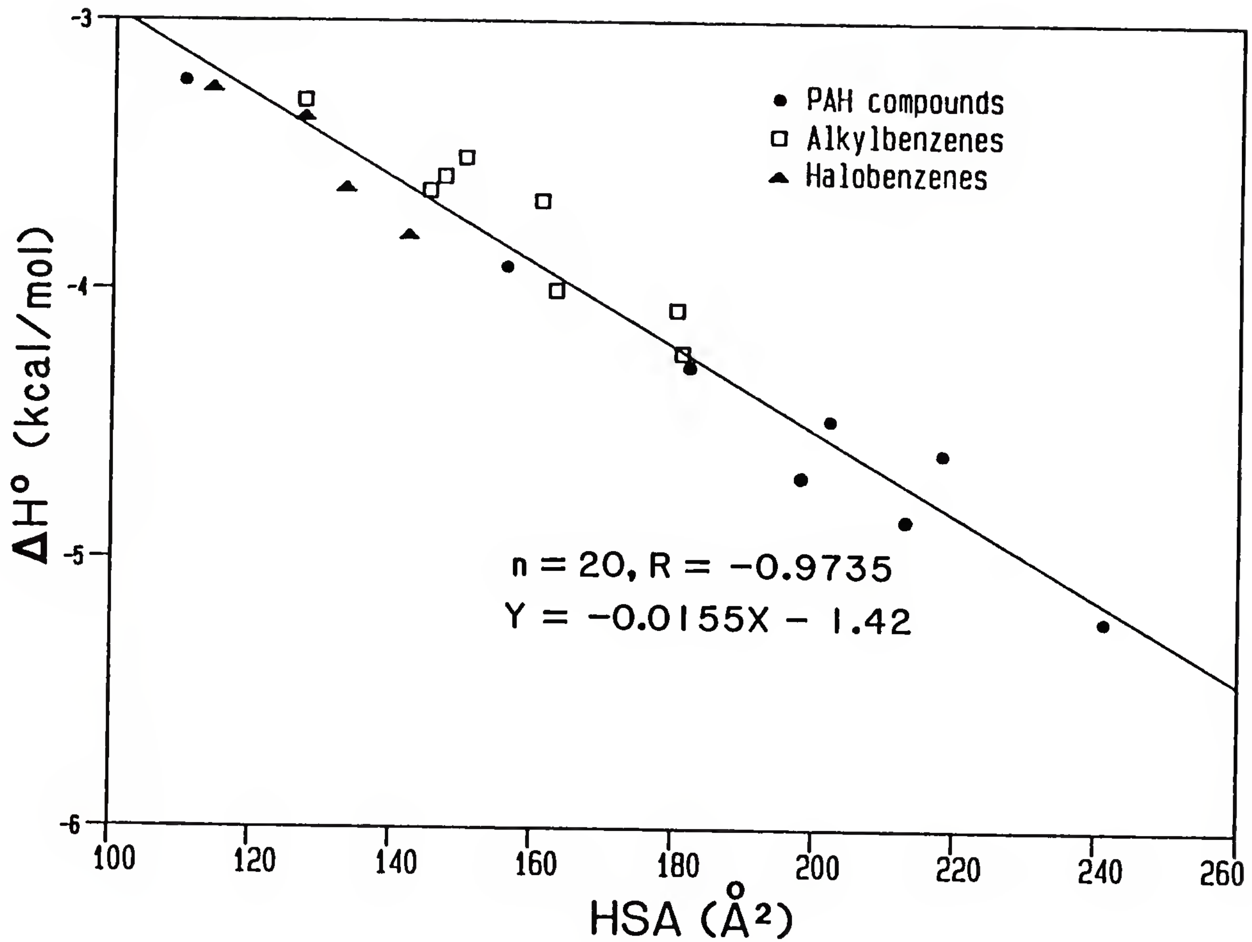

Figure 5-18. ΔH^{o} vs. solute HSA for sorption of the hydrophobic solutes on the C-4 material in 30/70 acetonitrile/water.

Table 5-9. Correlation of ΔH^{o} vs. HSA for the sorption of hydrophobic solutes in an acetonitrile/water mobile phase on three RPLC sorbents.

RPLC Support	θ(ACN)[a]	ΔH^{o} vs. HSA[b]
C-2	0.30	n = 20, R = -0.9700 Slope = -0.0168 $\pm$ 0.0021 Intercept = -1.79 $\pm$ 0.35
C-4	0.30	n = 20, R = -0.9735 Slope = -0.0155 $\pm$ 0.0018 Intercept = -1.42 $\pm$ 0.30
C-8	0.30	n = 12, R = -0.9406 Slope = -0.0197 $\pm$ 0.0050 Intercept = -0.99 $\pm$ 0.74

[a]Acetonitrile/water (v/v) mixture = 30/70.

[b]n is the number of data points used in the regression; R is the correlation coefficient; slope and intercept values represent mean values $\pm$ 95% confidence limits.

change to solute HSA values. This relationship was found in both methanol/water and acetonitrile/water eluents on the C-2, C-4, and C-8 RPLC stationary phases. Stationary phase chain length did not have a noticeable effect on ΔH^{o}_{sorp} vs. HSA correlations.

In work discussed earlier in Section 5.3, differences in overall RPLC retention were noted for the alkylbenzenes and PAH compounds. It was then argued that since ln k' is directly related to ΔG^{o}_{sorp}, these two classes of chemicals may be significantly different in their overall sorption thermodynamics. It appears from the ΔH^{o}_{sorp} vs. HSA data that alkylbenzenes and PAHs do not differ considerably in their relationship of standard sorptive enthalpy change to molecular size, as described by solute HSA. This behavior suggests that the entropic portion of the retention process may account for the observed differences in sorption behavior exhibited by the PAHs and alkylbenzenes. The relationship of ΔS^{o}_{sorp} to molecular size (HSA) will now be investigated.

5.4.5 Effect of Solute Size on ΔS^{o}_{sorp}

Previously in Section 5.3, it was discussed how the ΔS^{o} for the sorption process may be conceptually viewed as consisting of two entropy terms: (1) the entropy change involved in the actual solute sorption process, ΔS^{o}_{1}, which should have a negative value and become increasingly

negative as the hydrophobic portion of the molecule is increased in size; and (2) the entropy change associated with the release of organic solvent and water molecules from the highly ordered solvation sphere back to the bulk solution, termed ΔS^o_2. The value of ΔS^o_2 is positive and should decrease as the surface tension of the bulk solvent is increased. The magnitude of ΔS^o_2 should increase with the surface area of the hydrophobic molecule, since the size of the solvation sphere would also increase. In theory, each of the entropy change terms, ΔS^o_1 and ΔS^o_2, contributes to ΔS^o_{sorp}. The actual value of ΔS^o_{sorp} is a complex function of solution surface tension and the size of the hydrophobic portion of the solute molecule.

The initial discussion of ΔS^o_{sorp} as a function of solute HSA will be presented for the methanol/water solvent system. A plot of ΔS^o vs. HSA for solute retention on the C-2 support in 35/65 methanol/water is shown in Figure 5-19. The ΔS^o_{sorp} values are negative and decrease as the hydrophobic solutes increase in hydrophobic surface area. The negative ΔS^o_{sorp} values result from increased molecular order due to sorption. The solutes with larger HSA values demonstrate greater ordering during sorption than the smaller compounds, as seen from the ΔS^o_{sorp} values. Additionally, the PAH and alkylbenzene data result in different linear regression lines when ΔS^o_{sorp} is plotted versus

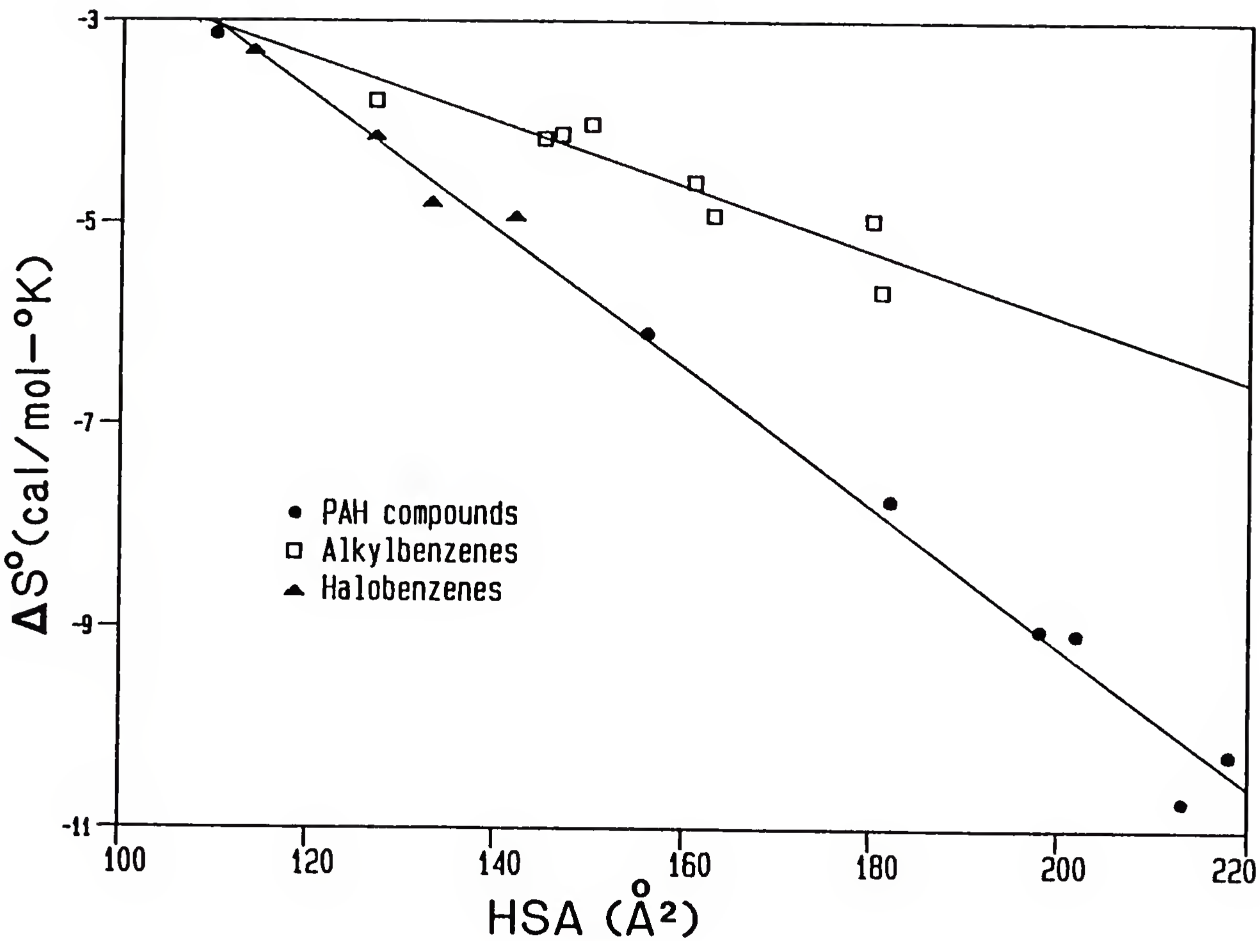

Figure 5-19. ΔS^{o} vs. solute HSA for sorption of the hydrophobic solutes on C-2 material in 35/65 methanol/water.

solute HSA. Similar entropic behavior was reported by Chmielowiec and Sawatzky (1979) for PAH and phenyl-substituted compounds retained on C-18 material in 80/20 methanol/water.

Plots of ΔS^{o}_{sorp} vs. solute HSA are presented in Figures 5-20 and 5-21 for solute retention on the C-8 material in 50/50 and 60/40 methanol/water eluents, respectively. The PAHs and alkylbenzenes consistently show differences in their standard sorptive entropy changes with increasing molecular size. The ΔS^{o}_{sorp} values of the alkylbenzenes do not decrease as rapidly with increasing solute size as do the halobenzenes and the rigid PAH molecules.

The distinct trends present in the ΔS^{o}_{sorp} vs. HSA plots of Figures 5-19 to 5-21 do not appear to change appreciably with RPLC chain length (C-2 to C-8) and methanol content (0.35 to 0.60 by volume). The ΔS^{o}_{sorp} data of Appendix D support these observations. Data collected in Table 5-10 demonstrate that the correlation of ΔS^{o} to solute HSA remains essentially constant with RPLC chain length; separate correlations were developed for the PAHs and alkylbenzenes. Although the actual slopes of the ΔS^{o}_{sorp} vs. HSA regression lines change with methanol content (see Section 5.4.3), Figures 5-19 to 5-21 show that the relative difference between PAH and alkylbenzene entropic behavior remains unchanged with methanol composition of the solvent.

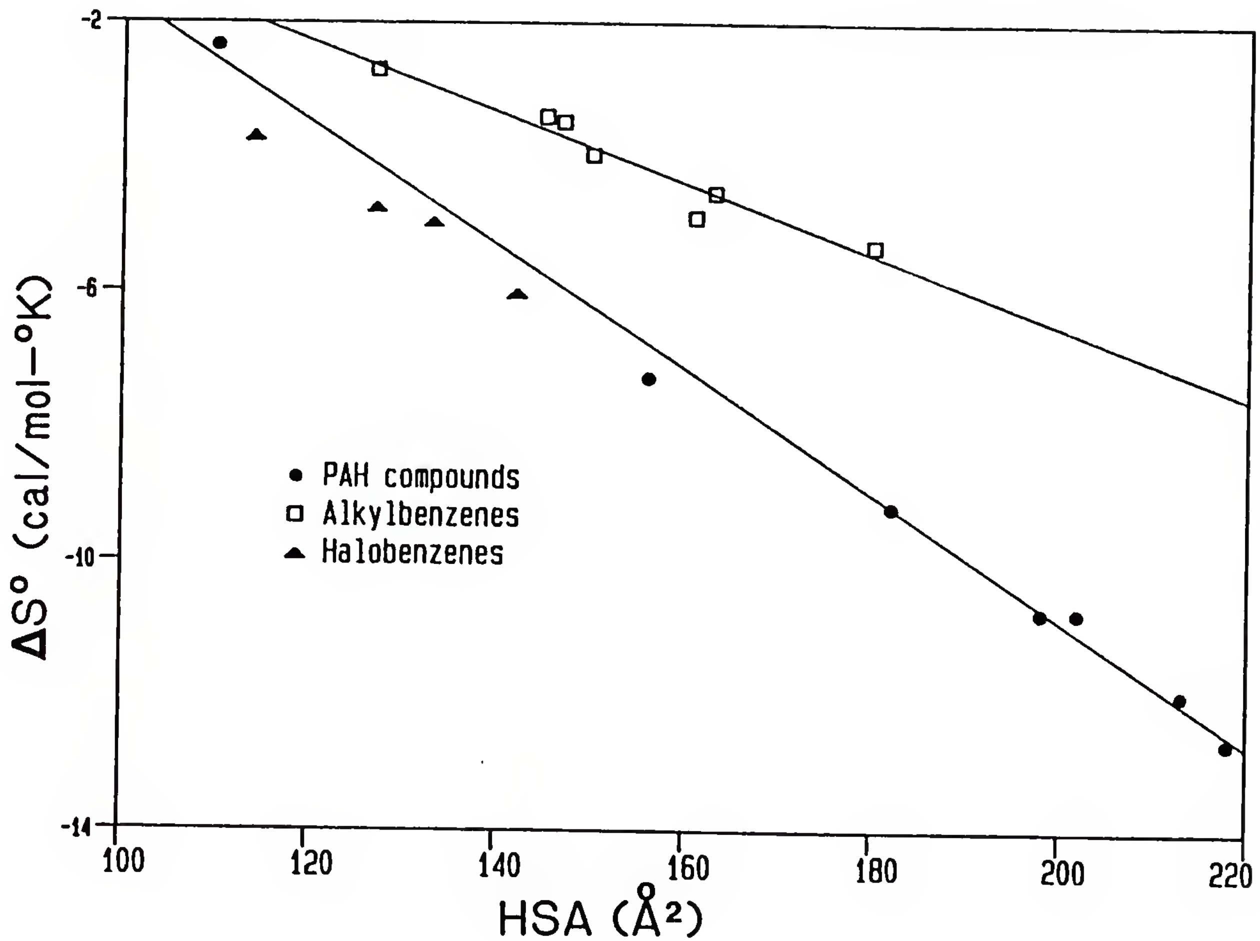

Figure 5-20. ΔS^{o} vs. solute HSA for sorption of the hydrophobic solutes on C-8 material in 50/50 methanol/water.

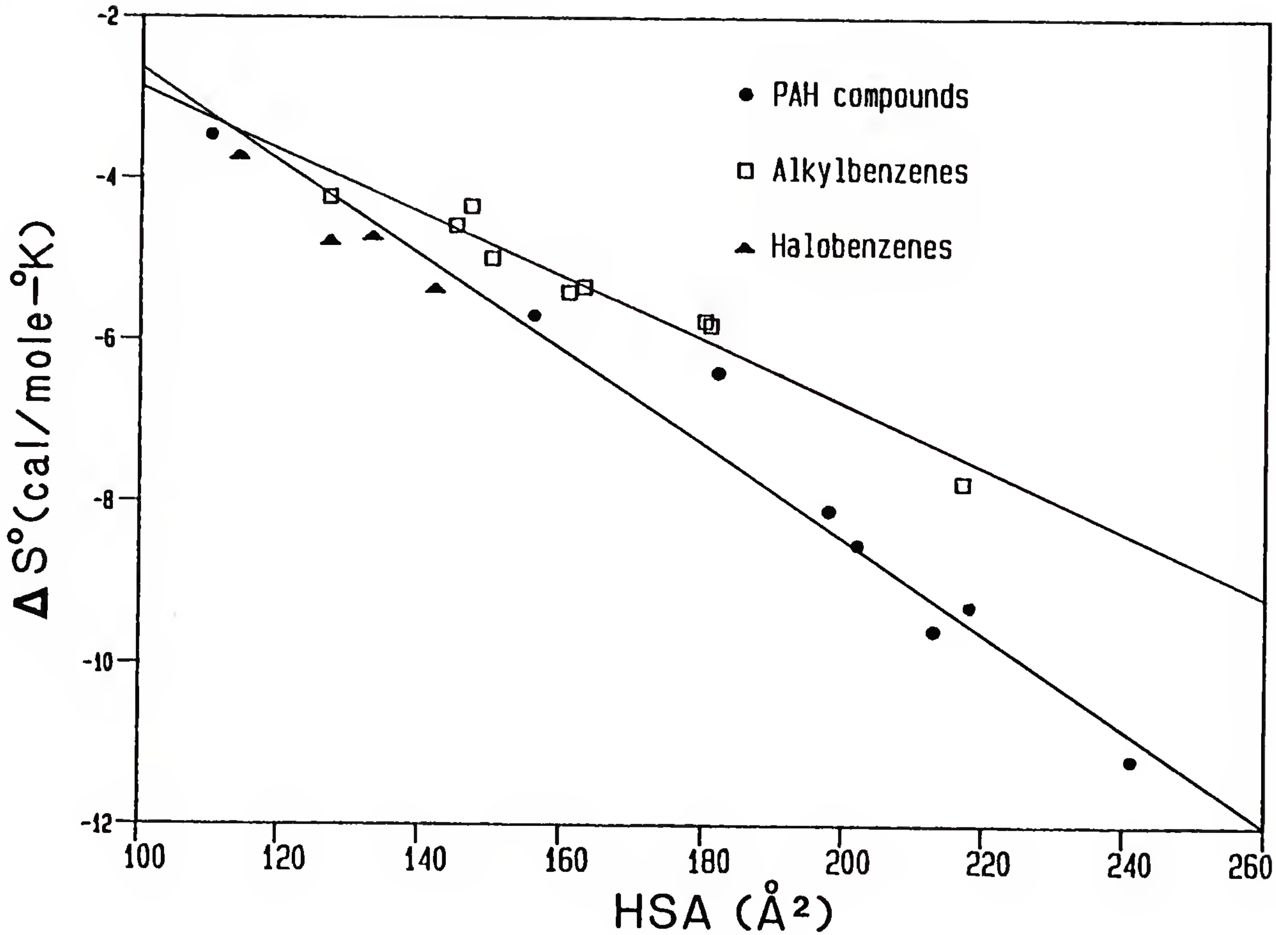

Figure 5-21. ΔS^{o} vs. solute HSA for sorption of the hydrophogic solutes on C-8 material in 60/40 methanol/water.

Table 5-10. ΔS^o vs. HSA for the sorption of PAH compounds and alkylbenzenes from a 50/50 methanol/water mobile phase on three RPLC sorbent materials.

RPLC Support	ΔS^o vs. HSA[a] PAH compounds & Benzene	ΔS^o vs. HSA[a] Alkylbenzenes
C-2	n = 8, R = -0.9968 Slope = -0.0501 ± 0.0040 Intercept = 1.56 ± 0.78	n = 8, R = -0.9553 Slope = -0.0344 ± 0.0120 Intercept = -0.13 ± 1.89
C-4	n = 7, R = -0.9916 Slope = -0.0586 ± 0.0088 Intercept = 2.48 ± 1.67	n = 7, R = -0.9439 Slope = -0.0366 ± 0.0140 Intercept = -0.026 ± 2.27
C-8	n = 7, R = -0.9930 Slope = -0.0686 ± 0.0093 Intercept = 4.52 ± 1.74	n = 8, R = -0.9279 Slope = -0.0320 ± 0.0128 Intercept = 0.47 ± 2.02

[a]Correlation of ΔS^o vs. HSA developed independently for (1) the PAHs and benzene and (2) the alkylbenzenes; n is the number of data points used in the correlation; R is the correlation coefficient; slope and intercept values represent mean values ± 95% confidence limits.

Summarizing the ΔS^{o}_{sorp} vs. HSA trends in methanol, the ΔS^{o}_{sorp} values are negative for the hydrophobic solutes and decrease as the amount of hydrophobic surface area available for hydrophobic interactions increases. The PAH and alkylbenzene data clearly yield independent linear regression lines in the ΔS^{o}_{sorp} vs. HSA plots; the monohalobenzenes appear to act in a manner similar to the PAHs and their data are shown for comparison purposes. The entropic distinction between the PAHs and alkylbenzenes appears to be independent of eluent methanol content and RPLC chain length.

The reason for the slower rate of ΔS^{o} decline with increasing size of the alkylbenzenes may be related to the size of the solvation sphere for these compounds. As discussed in Chapter IV, Section 4.5, the alkyl chain of the alkylbenzene molecules may exist in a variety of conformational states (Edward, 1970; Nemethy and Scheraga, 1962). This is in contrast to the rigid, planar structure of the PAH compounds. For this reason, it is conceivable that an alkylbenzene molecule may require a more extended solvation sphere than a PAH compound with a comparable HSA value. The standard entropy change associated with release of the alkylbenzene's solvation sphere, ΔS^{o}_{2}, will consequently be of greater magnitude, and the resulting ΔS^{o}_{sorp} value will be higher than that of the PAH molecule. This theory of greater solvation effects for the alkylbenzenes generally agrees with the experimental data. However, our lack of

knowledge concerning the RPLC retention mechanisms and entropic processes in solution limits our ability to precisely explain the thermodynamic results.

With the discussion of ΔS^{o}_{sorp} vs. HSA for selected solute classes in methanol/water mixtures now complete, the acetonitrile/water eluent system for RPLC will be covered next. A plot of ΔS^{o} vs. HSA for solute retention on the C-2 stationary phase in 25/75 acetonitrile/water is shown in Figure 5-22. The same general trends observed in the methanol/water eluent are noted here: (1) the ΔS^{o}_{sorp} data are negative and decline with increasing solute HSA; and (2) the PAHs and alkylbenzenes each form a distinct ΔS^{o}_{sorp} vs. solute HSA linear regression; the halobenzenes seem to follow the behavior of the PAH compounds. The limited data set for the halobenzenes prevents any definitive conclusion being drawn concerning their behavior, and the data are presented for comparison purposes. The acetonitrile/water solvent system initially behaves in a manner similar to the methanol/water mobile phase.

There is a considerable change in entropic behavior, however, upon the addition of a small amount of acetonitrile to the 25/75 acetonitrile/water mixture of Figure 5-22. The ΔS^{o}_{sorp} vs. HSA data for C-2 retention in 30/70 acetonitrile/water are shown in Figure 5-23 for the PAHs, alkylbenzenes, and halobenzenes. In this slightly less polar eluent system, the alkylbenzenes show a slight

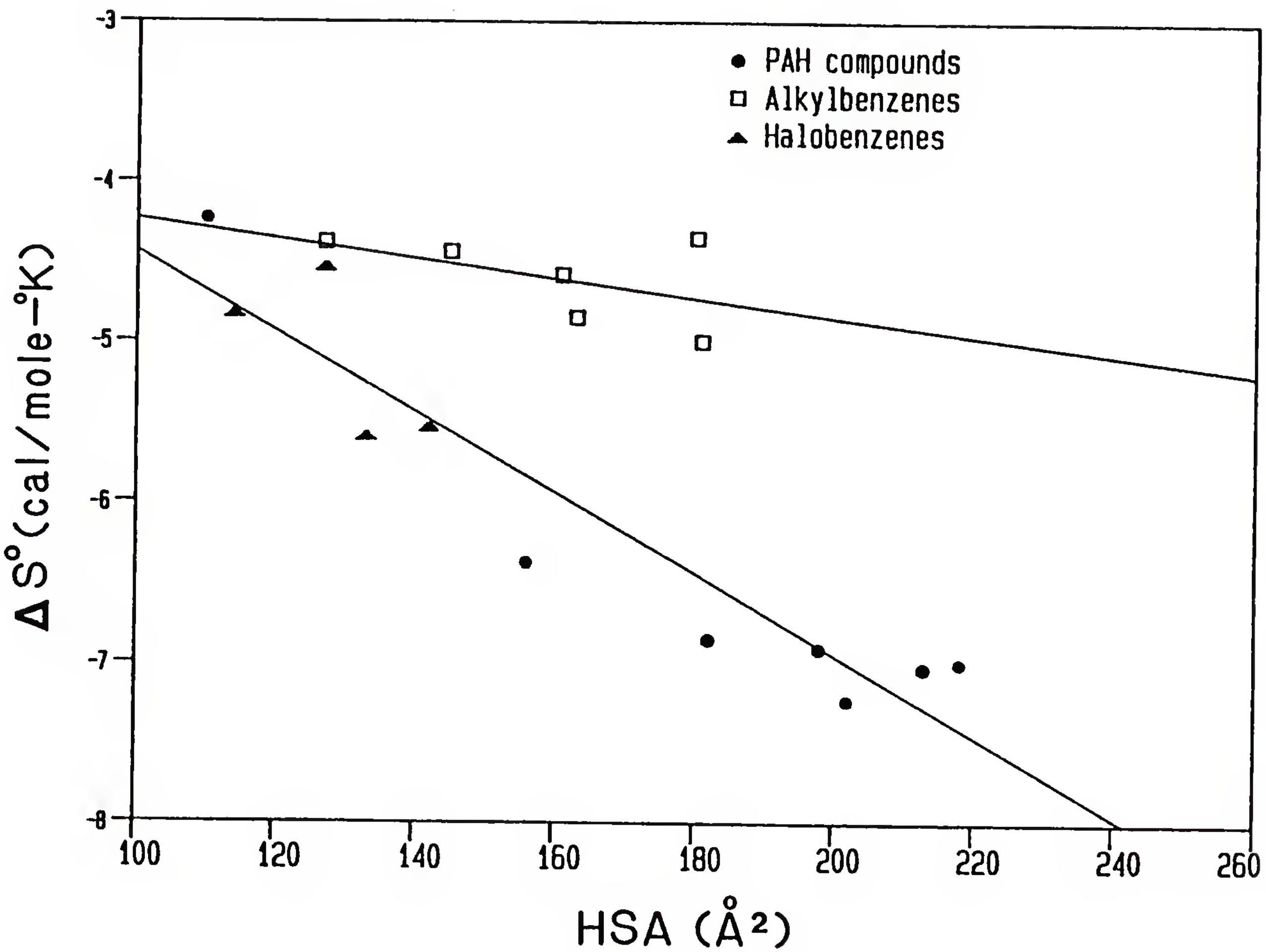

Figure 5-22. ΔS^{o} vs. solute HSA for sorption of the hydrophobic solutes on the C-2 support in 25/75 acetonitrile/water.

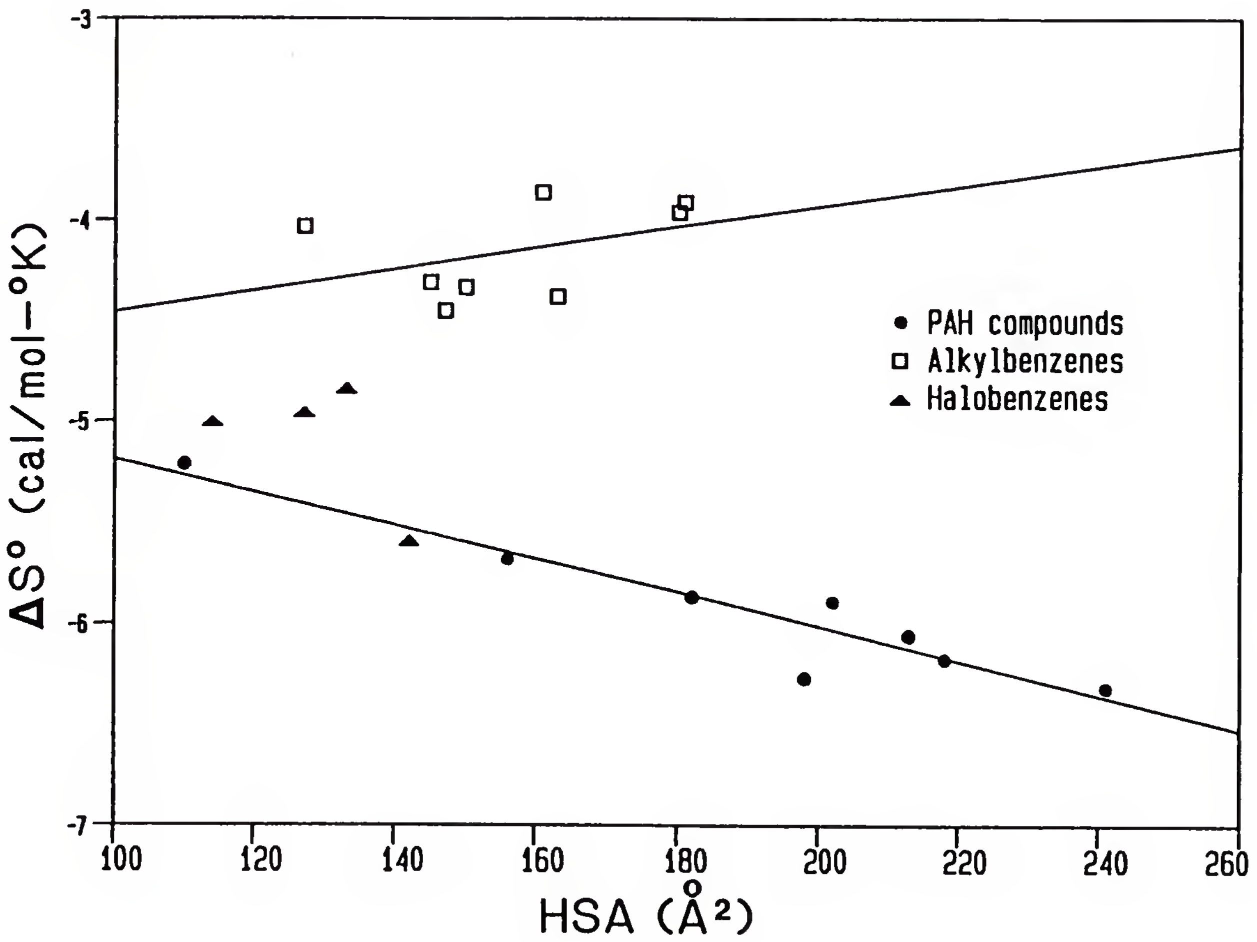

Figure 5-23. ΔS^{o} vs. solute HSA for sorption of the hydrophobic solutes on the C-2 support in 30/70 acetonitrile/water.

increase in ΔS^o_{sorp} with increasing solute HSA, while the slope of the PAH regression line has shifted towards zero. These changes in the ΔS^o_{sorp} vs. HSA trends may be related to the drop in solution surface tension upon changing the acetonitrile content from 25% to 30% by volume (see Fig. 5-14). The decrease in solution surface tension correlates with a decline of intermolecular attractive forces in the bulk solution (Castellan, 1971). This greater solution disorder suggests larger standard entropy changes associated with relaxation of the solute's solvation sphere, termed ΔS^o_2. The magnitude of ΔS^o_2 increases directly with solute HSA, with larger solutes exhibiting greater entropy effects upon relaxation of the solvation sphere. This relationship of surface tension to ΔS^o_2 could well explain the ΔS^o_{sorp} vs. HSA plots of Figure 5-23.

The ΔS^o vs. HSA plots shown in Figure 5-24 are for solutes sorbed on the C-4 support in a 40/60 acetonitrile/ water mobile phase system. The regression line for the PAH compounds has now shifted to a positive slope, with both the alkylbenzenes and PAHs/halobenzenes showing an increase in ΔS^o_{sorp} with higher solute HSA values.

The change in solute behavior from Figure 5-22 to Figure 5-24 may again be related to the decline in solution surface tension as the volume fraction of acetonitrile is increased from 0.25 to 0.40. It is believed that the increase in ΔS^o_{sorp} values with increasing solute HSA is due

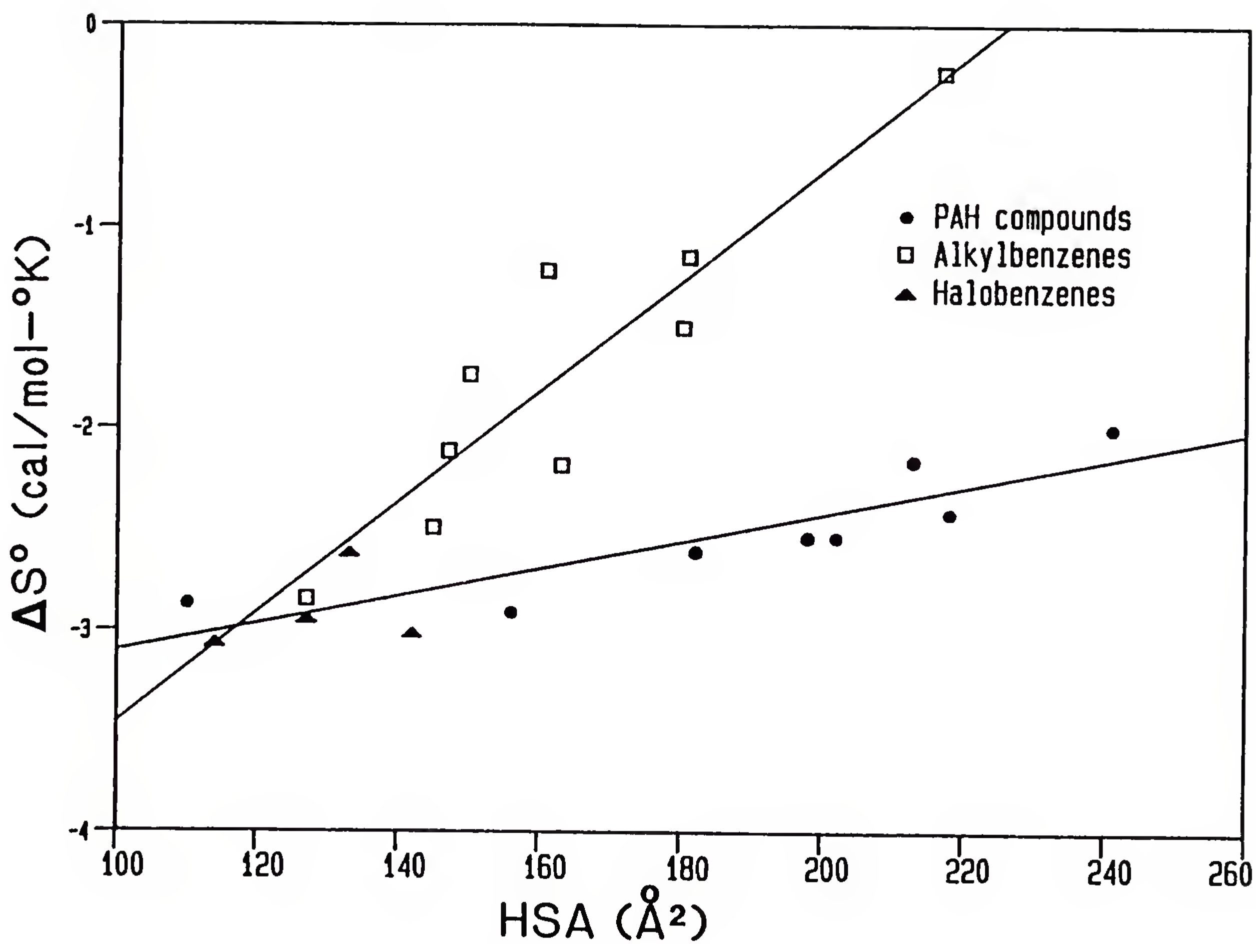

Figure 5-24. ΔS^{o} vs. solute HSA for sorption of the hydrophobic solutes on the C-4 support in 40/60 acetonitrile/water.

to greater ΔS^{o}_{2} values associated with an acetonitrile content of 40% by volume. The lower surface tension of this eluent will allow for greater ΔS^{o}_{2} values upon release of the solute's solvation sphere. The magnitude of ΔS^{o}_{2} is directly related to solute HSA. Larger ΔS^{o}_{2} values should become dominant factors in determining ΔS^{o}_{sorp}, with the standard sorptive entropy change consequently increasing in value with solute HSA. If the alkylbenzenes, as suggested, do have significantly larger solvation spheres than PAH molecules of comparable HSA, then the ΔS^{o}_{sorp} values of alkylbenzenes will increase more rapidly with HSA than PAH compounds. The experimental data generally agree with this proposed solvation sphere effect.

Finally, the standard entropy changes associated with solute sorption on the C-8 support in a 60/40 acetonitrile/water eluent are plotted versus solute HSA in Figure 5-25 for the solutes of interest. The ΔS^{o}_{sorp} vs. HSA plots are nearly identical to those in Figure 5-24 for a 40/60 acetonitrile/water mobile phase. This similarity is not particularly surprising, as the solution surface tension is virtually unchanged from a θ_{ACN} of 0.40 to 0.60. Consequently, the ΔS^{o}_{2} terms in 60/40 acetonitrile/water will increase only marginally for a given solute relative to the 40/60 mixture, and the relative behavior of PAHs and alkylbenzenes will be similar in both solvent systems.

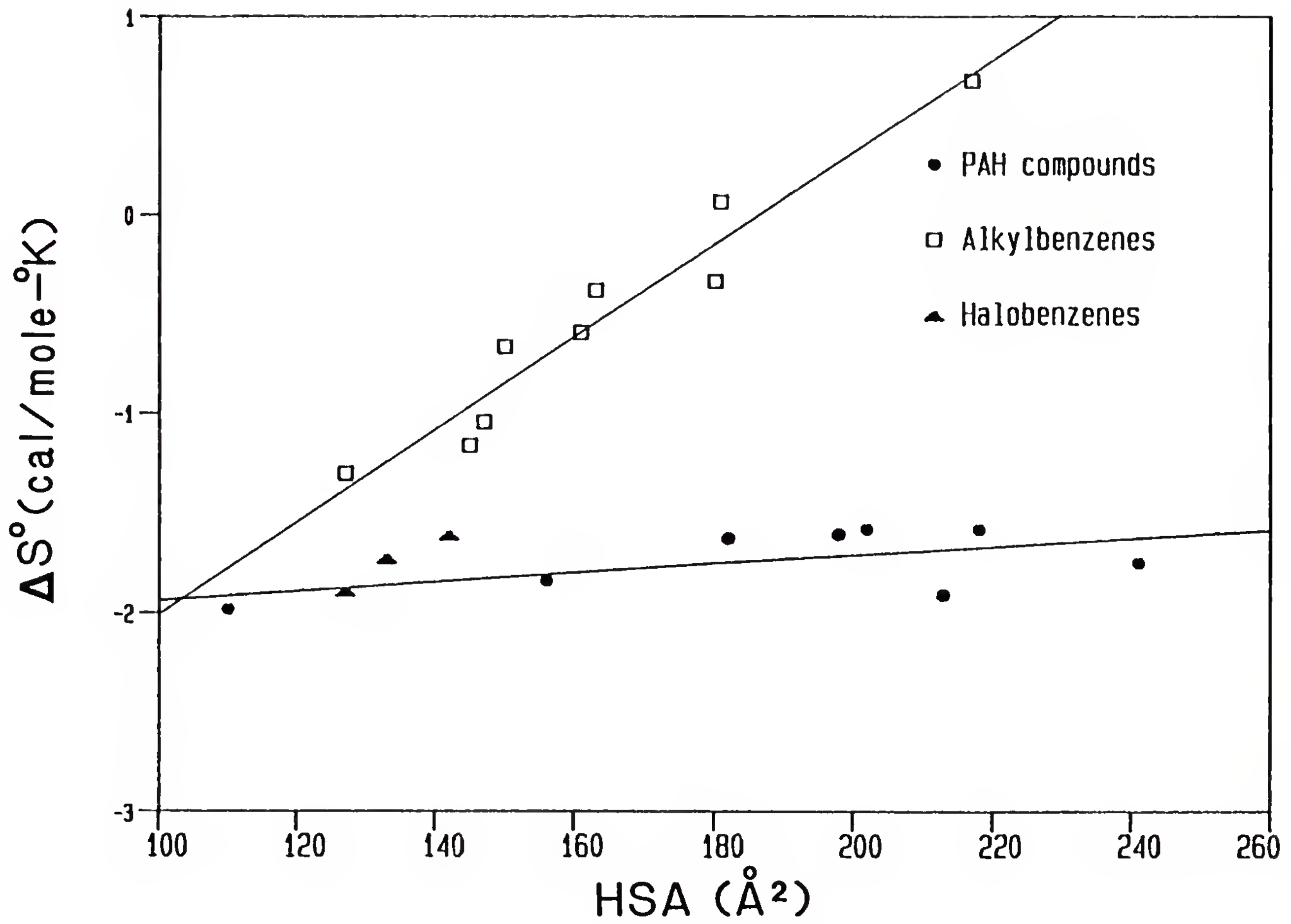

Figure 5-25. ΔS^{o} vs. solute HSA for sorption of the hydrophobic solutes on the C-8 support in 60/40 acetonitrile/water.

In summary, it appears that the ΔS^o_{sorp} vs. HSA trends in acetonitrile water solvent systems are dramatically different from the behavior of the solutes in methanol/water mixtures. Changes in solution surface tension appear to play a major role in the entropy effects of solute retention and the effect of solute size upon ΔS^o_{sorp}. For acetonitrile/water mixtures of 25% or less, the ΔS^o_{sorp} vs. HSA behavior is similar to that of methanol/water eluents. At higher acetonitrile contents, however, the decreased surface tension causes considerable changes in the entropic behavior of the solutes. As in the methanol/water mixtures, the PAHs and alkylbenzenes maintain their individually distinct entropic behavior, and the halobenzenes act in a manner similar to the PAH compounds. The RPLC chain length seems to have minimal effect upon the ΔS^o_{sorp} vs. HSA trends of PAHs and alkylbenzenes in acetonitrile/water. The data collected in Table 5-11 are for ΔS^o_{sorp} vs. HSA correlations of PAHs and alkylbenzenes retained on the three RPLC supports in 40/60 acetonitrile/water. The correlations are less strong than those seen in methanol/water eluents, but RPLC chain length does not have a systematic effect on the relationship of ΔS^o_{sorp} to solute HSA.

5.4.6 Effect of RPLC Chain Length Upon ΔH^o_{sorp}

The solvophobic theory of hydrophobic retention (Horvath et al., 1976) relates the natural logarithm of the

Table 5-11. ΔS^o vs. HSA for the sorption of PAH compounds and alkylbenzenes from a 40/60 acetonitrile/water mobile phase on three RPLC sorbent materials.

	ΔS^o vs. HSA[a]	
RPLC Support	PAH compounds & Benzene	Alkylbenzenes
C-2	n = 8, R = 0.7873 Slope = 0.0079 ± 0.0062 Intercept = -5.08 ± 1.19	n = 9, R = 0.9025 Slope = 0.0180 ± 0.0080 Intercept = -5.54 ± 1.27
C-4	n = 8, R = 0.8740 Slope = 0.0067 ± 0.0037 Intercept = -3.78 ± 0.72	n = 9, R = 0.9177 Slope = 0.0276 ± 0.0100 Intercept = -6.23 ± 1.76
C-8	n = 5, R = -0.9308 Slope = -0.0095 ± 0.0068 Intercept = -1.11 ± 1.37	n = 9, R = 0.8995 Slope = 0.0247 ± 0.0100 Intercept = -5.08 ± 1.78

[a]Correlation of ΔS^o vs. HSA developed independently for (1) the PAHs and benzene and (2) the alkylbenzenes; n is the number of data points used in the correlation; R is the correlation coefficient; slope and intercept values represent mean values ± 95% confidence limits.

solute retention factor to the contact surface area, ΔA, between the solute and the RPLC alkyl chain. This relationship is detailed in Eqn. (3-31). The contact surface area was defined earlier (Eqn. 3-25) as the HSA of the solute-ligand complex minus the individual HSA values of the solute and alkyl ligand. As the RPLC chain length is increased, the solvophobic model predicts larger k' values, i.e., greater solute retention. The retention data in Appendix A show that ln k' values definitely increase with stationary phase chain length for the hydrophobic solutes retained on the RPLC supports in the methanol/water and acetonitrile/ water eluents.

A number of researchers have suggested that enthalpic processes control sorption interactions in RPLC (Colin et al., 1978; Melander et al., 1978). If this is the case for the RPLC system under study, then, recalling Eqn. (3-41)

$$\ln k' = -\Delta H^{o}/RT + \Delta S^{o}/R + \ln \phi$$

the ΔH^{o}_{sorp} values for a given solute should be directly related to RPLC chain length. A plot of ΔH^{o}_{sorp} vs. RPLC chain length for pyrene, chrysene, n-butylbenzene, and n-hexylbenzene in a 60/40 methanol/water solvent system is shown in Figure 5-26. As suggested, the ΔH^{o}_{sorp} values are a function of RPLC chain length. Examination of the methanol/water data in Appendix C reveals that the ΔH^{o}_{sorp}

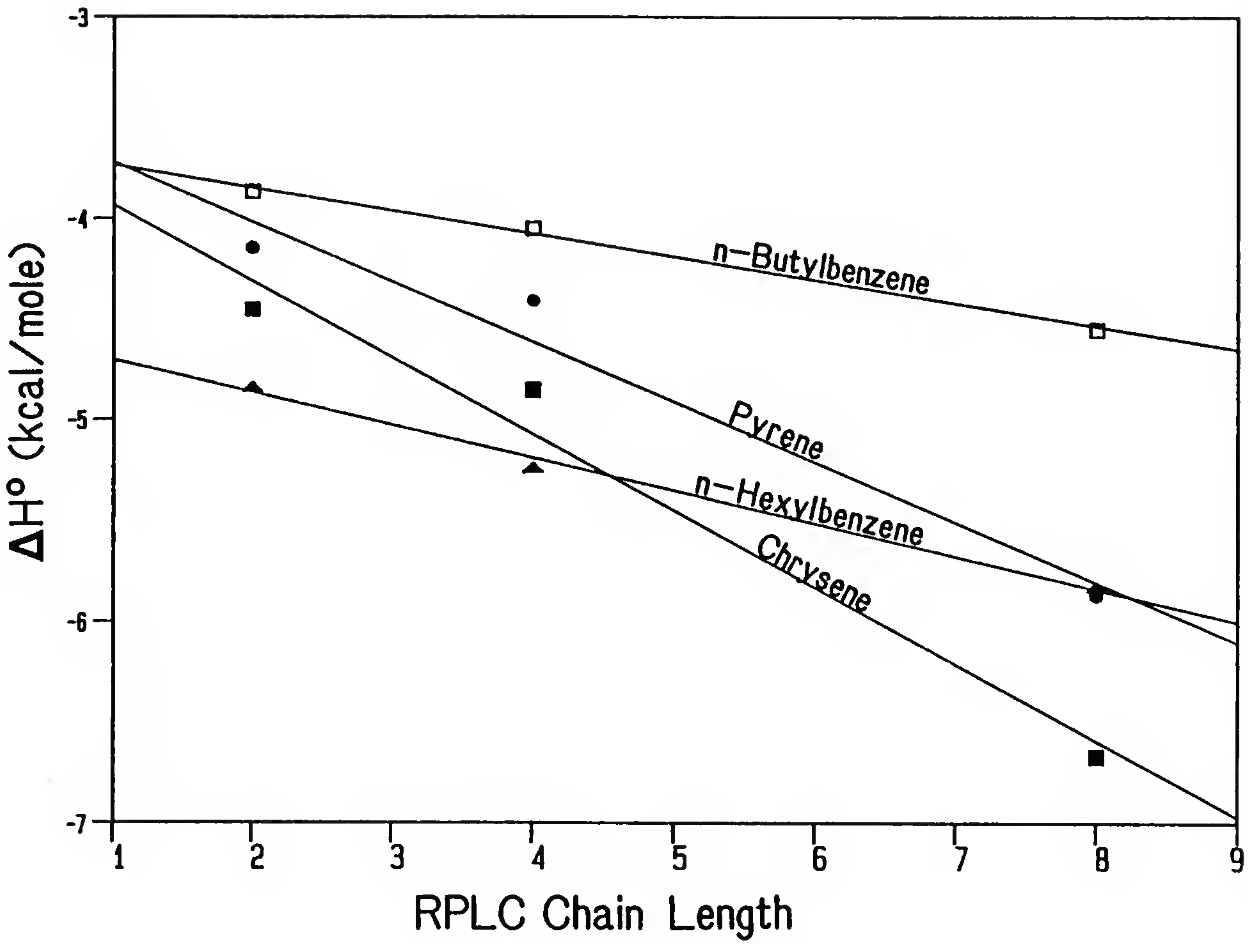

Figure 5-26. ΔH^{o} vs. RPLC chain length for sorption of pyrene, chrysene, n-butylbenzene, and n-hexylbenzene in 60/40 methanol/water.

values of a given solute generally decline with increasing stationary phase chain length. In both the 50/50 and 60/40 methanol/water eluents, the ΔH^{o}_{sorp} values for nearly all the solutes are considerably more exothermic on the C-8 support than their respective values on the C-2 sorbent. The data indicate that the observed increase in solute retention with RPLC chain length is due principally to enthalpic effects in the methanol/water system. Next, the dependence of ΔH^{o}_{sorp} upon RPLC chain length in acetonitrile/water eluent systems will be examined.

In the acetonitrile/water solvent system, the ΔH^{o}_{sorp} values were not found to be a function of RPLC chain length. For only a very few compounds were the ΔH^{o}_{sorp} values on C-8 material lower than their respective values on the C-2 support; the differences were typically small, in the range of 0.3-0.5 kcal/mole. None of the hydrophobic solutes exhibited the linear correlation of ΔH^{o}_{sorp} to RPLC chain length noted in Figure 5-26 for the methanol/water system. Therefore, although solute retention factors in acetonitrile/water systems increase considerably with RPLC chain length, a decline in ΔH^{o}_{sorp} values is apparently not the critical factor driving the increase in ln k'. This suggests that entropic effects play an important role in the increase of solute retention with RPLC chain length in acetonitrile/water systems.

5.4.7 Effect of RPLC Chain Length on ΔS^{o}_{sorp}

The discussion of RPLC chain length to this point has centered upon its influence upon ΔH^{o}_{sorp} for the hydrophobic compounds in methanol/water and acetonitrile/water mobile phases. The difference between ΔH^{o}_{sorp} values measured on the C-2 vs. C-8 stationary phases in methanol/water are typically 0.5-2.0 kcal/mole. This decrease in the standard sorption enthalpy change is generally sufficient to explain the differences in solute retention on these two RPLC supports (see Eqn. 3-41), if the respective column phase ratios are considered. However, in the acetonitrile/water systems, the decline in ΔH^{o}_{sorp} values with increasing RPLC chain length is either very small (0.2-0.4 kcal/mole) or non-existent. Hence, the increase in ln k' with RPLC chain length in acetonitrile/water mobile phases is most likely due to entropic effects rather than the enthalpic processes noted in methanol/water eluents.

An examination of the ΔS^{o}_{sorp} data in Appendix D for methanol/water eluents reveals fairly constant ΔS^{o}_{sorp} values grading from the C-2, to C-4, to C-8 stationary phases within a given solvent mixture. The data indicate that entropy effects do not play an important role in the observed increase in ln k' with RPLC chain length for the methanol/water systems studied.

The situation is considerably different for the acetonitrile/water RPLC systems. As shown in Figure 5-27,

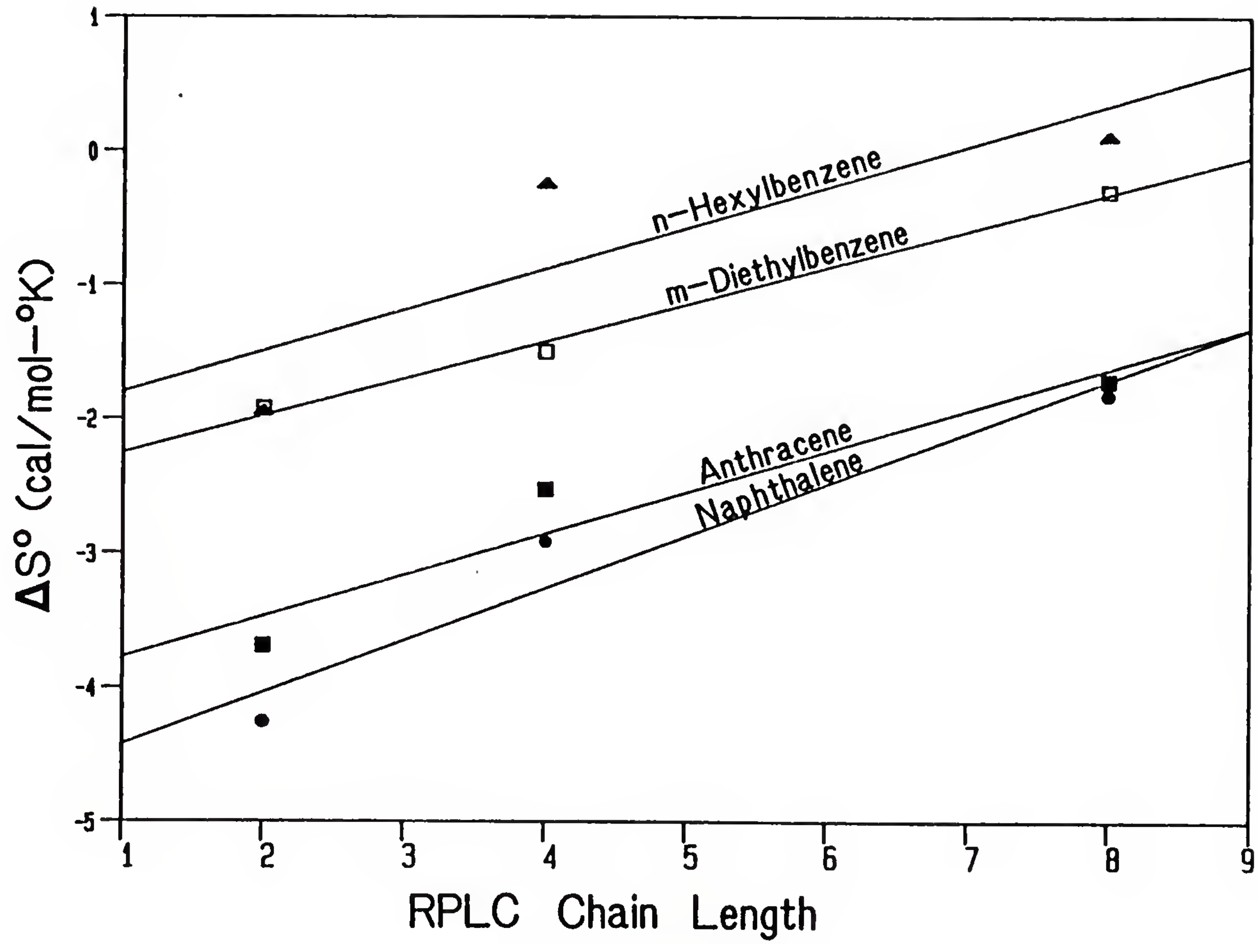

Figure 5-27. ΔS^{o} vs. RPLC chain length for sorption of anthracene, naphthalene, n-hexylbenzene, and m-diethylbenzene in 40/60 acetonitrile/water.

the ΔS^{o}_{sorp} values of n-hexylbenzene, m-diethylbenzene, anthracene, and naphthalene all increase with RPLC chain length in a 40/60 acetonitrile/water solvent mixture. This trend is generally repeated for most of the hydrophobic solutes in this solvent system, with differences in ΔS^{o}_{sorp} between the C-2 and C-8 stationary phases of approximately 1-3 cal/mole-°K. This change in ΔS^{o}_{sorp}, combined with the respective column phase ratios, is sufficient to account for most of the observed increase in solute retention (ln k') when going from the C-2 to C-8 RPLC support. For this calculation, Eqn. (3-41) may be used, with ΔH^{o}_{sorp} held constant for a given solute.

An examination of the ΔS^{o}_{sorp} data for acetonitrile/water systems in Appendix D reveals that ΔS^{o}_{sorp} values generally increase with RPLC chain length, as shown in Figure 5-27. This indicates that the solute molecules are more ordered on the C-2 support than on the longer stationary phases, C-4 and C-8. In Chapter IV, Section 4.2, it was proposed that the longer alkyl stationary phases have greater degrees of freedom for translational and rotational movement than shorter RPLC phases. If this is the case, the C-8 sorption of a solute molecule would produce a more positive standard entropy change than retention on the C-2 support. The restricted motion of a C-2 alkyl chain yields a more negative ΔS^{o}_{sorp} upon sorption of the hydrophobic chemical. This proposed distinction between the behavior of

RPLC supports with differing alkyl chain lengths agrees with the experimental data for the acetonitrile/water systems.

The thermodynamic sorptive behavior of solutes in methanol/water and acetonitrile/water systems are distinctly different with respect to RPLC chain length. The reason for this may be found in the fundamental interactions of these organic solvents with the RPLC supports. Stahlberg and Almgren (1985) reported that methanol and acetonitrile showed considerably different interactions with RPLC surfaces. Their data indicate that methanol molecules initially enter between the alkyl chains of the stationary phase and hydrogen bond to the free silanol groups on the silica gel surface. Since the methyl group is turned away from the surface, the polarity of the surface decreases. The addition of more methanol to the solvent mixture produces no real increase in surface polarity, suggesting that the concentration of methanol molecules freely moving between the alkyl chains is quite low.

In acetonitrile/water mixtures, the addition of a low concentration of acetonitrile to the RPLC stationary phase produces a decrease in surface polarity. This indicates that acetonitrile molecules hydrogen bond to available silanol groups, turning their methyl groups away from the surface, just as in the methanol/water eluents. However, the addition of more acetonitrile to the solvent produces an increase in surface polarity. This change in polarity

suggests that the additional acetonitrile molecules move freely among adjacent RPLC alkyl chains, leading to the observed increase in the polarity of the surface.

Therefore, the results of Stahlberg and Almgren (1985) indicate that methanol/water and acetonitrile/water mixtures vary considerably in their fundamental interactions with RPLC surfaces. The presence of freely moving acetonitrile molecules among the RPLC alkyl chains may produce greater differences in the rotational and translational movement of the C-2, C-4, and C-8 supports. These differences in alkyl chain "movement" may explain the greater solute ordering observed on C-2 as opposed to C-8 RPLC surfaces. The absence of this solvent effect in methanol/water systems may explain the similar ΔS^{o}_{sorp} response of the three RPLC supports in this eluent system.

5.4.8 Summary of Thermodynamic Behavior

The thermodynamic behavior of the hydrophobic solutes as a function of solvent composition and solute hydrophobicity occurred as predicted by the solvophobic theory of Horvath et al. (1976). The value of ΔH^{o}_{sorp} for a given solute varied as a linear function of θ and solute HSA. The ΔS^{o}_{sorp} values in methanol/water eluents showed a similar linear dependence on θ and HSA, but this was not true for acetonitrile/water mixtures. The nonlinear relationship of ΔS^{o}_{sorp} with acetonitrile content is due to the surface

tension behavior of acetonitrile/water solutions (see Fig. 5-14). The surface tension of acetonitrile/water mixtures may also play a crucial role in the relationship of ΔS^{o}_{sorp} to solute HSA.

Finally, the methanol/water and acetonitrile/water solvent systems showed fundamental differences in their relationship of ΔH^{o}_{sorp} and ΔS^{o}_{sorp} to stationary phase chain length. Decreases in ΔH^{o}_{sorp} control the increase in solute retention with RPLC chain length in methanol/water solutions, while increases in ΔS^{o}_{sorp} with RPLC chain length dictate solute retention changes in acetonitrile/water mixtures. The distinct behavior of these solvents may be related to differences in the interactions of methanol and acetonitrile with bonded RPLC alkyl phases.

5.5 Enthalpy-Entropy Compensation Effects

5.5.1 Compensation Temperatures in RPLC Systems

Enthalpy-entropy compensation effects, as applied to an understanding of thermodynamic interactions, were outlined in Chapter III, Section 3.4. A comparison of system compensation temperatures may be used to determine if the intrinsic mechanism of interaction in one system is identical to that found in another. The enthalpy-entropy compensation effects have been reported in methanol/water and acetonitrile/water (up to 30% by volume) RPLC systems (Melander et al., 1979, 1980; Sander and Field, 1980), with

an average reversed-phase compensation temperature of 625°K for substituted benzenes (Melander et al., 1978, 1979).

Enthalpy-entropy compensation effects may be easily investigated for solute retention in HPLC systems through an expression relating ln k', ΔH^o_{sorp}, and β. From Chapter III, recall Eqn. (3-48)

$$\ln k' = -(\Delta H^o/R)(1/T - 1/\beta) - \Delta G^o_\beta/R\beta + \ln \phi$$

where ΔH^o is the standard enthalpy change for solute sorption, β is the system's compensation temperature, and ΔG^o_β is the standard free energy change at temperature β (°K) for the sorption process. The tabulated ln k' (Appendix A) and ΔH^o (Appendix C) data for sorption of the hydrophobic solutes were examined for enthalpy-entropy compensation effects using Eqn. (3-48). The RPLC systems examined were the C-2, C-4, and C-8 sorbents with the methanol/water and acetonitrile/water mobile phases.

The ln k' and ΔH^o data for solute retention on the C-8 support in 60/40 methanol/water are presented in Figure 5-28, with ln k' plotted vs. $-\Delta H^o/R$. The solutes included in Figure 5-28 are the PAH compounds, alkylbenzenes, and halobenzenes. The reference temperature for the solute retention factor, k', was chosen as the geometric mean of the experimental temperatures used in the evaluation of the ΔH^o_{sorp} value (Melander et al., 1978). Nitrobenzene

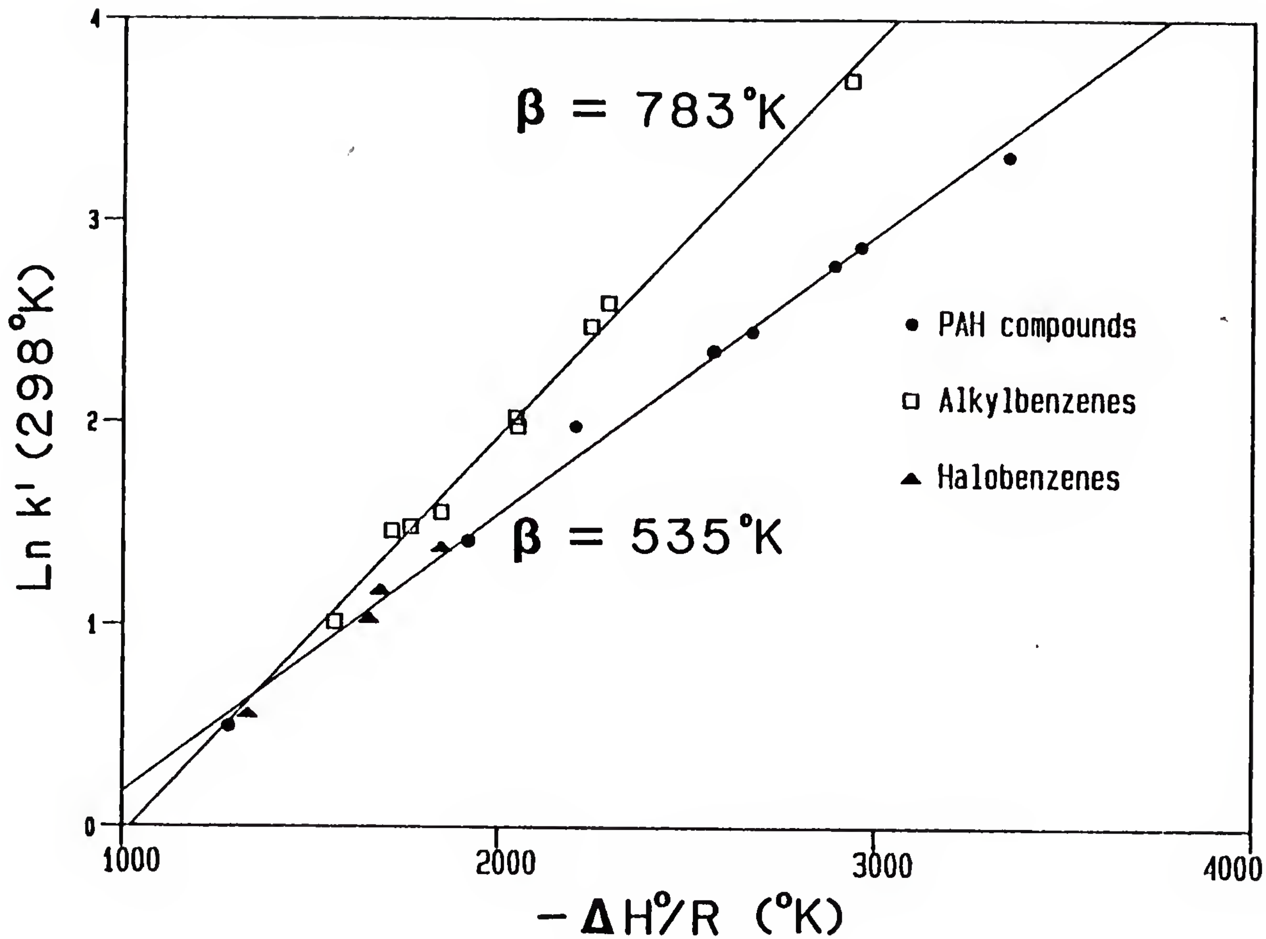

Figure 5-28. Ln k' at 298°K vs. $-\Delta H^{o}/R$ for sorption of the hydrophobic solutes on C-8 material in 60/40 methanol/water.

exhibited anomalous thermodynamic behavior compared to the other solutes and was excluded from the compensation studies. Nitrobenzene showed unusually low ΔH^o_{sorp} values, as this behavior was due to interaction of the polar nitro moiety with free silanol groups on the RPLC surface. Tanaka et al. (1978) reported that nitrobenzene deviated considerably from solvophobic behavior in their RPLC studies and suggested that this behavior was due to preferential polar interactions.

From a plot of ln k' vs. - $\Delta H^o/R$ (Figure 5-28), the system compensation temperature may be calculated from the slope of the linear regression line (see Eqn. 3-48). The PAH compounds and halobenzenes exhibit different compensation effects than did the alkylbenzenes, as seen from the separate regression lines in Figure 5-28. The β values ($\pm$95% confidence limits) for the PAHs/halobenzenes and the alkylbenzenes in Figure 5-28 were calculated as 535 ($\pm$22)°K and 783 ($\pm$97)°K, respectively. This plot successfully demonstrates the thermodynamically distinct behavior of the PAHs and alkylbenzenes in a C-8 methanol/water system. The observed difference in compensation effects for the PAHs/halobenzenes and alkylbenzenes indicates that these two compound groups differ in their hydrophobic retention mechanisms on the C-8 support using the methanol/water system. This distinction may be related to the conformational differences between alkylbenzenes and PAHs, or in the

manner that the alkyl chain(s) of alkylbenzenes may or may not preferentially interact with the C-8 stationary phase.

The ln k' and $-\Delta H^{o}_{sorp}/R$ data for the remaining C-2, C-4, and C-8 methanol/water systems were examined using the chromatographic enthalpy-entropy compensation model, Eqn. (3-48). In each system, the distinct difference in energetic behavior was noted for the alkylbenzenes and the PAHs/halobenzenes, as indicated by separate linear regression lines and β values. These β values ($\pm$95% confidence limits) were calculated for each methanol/water RPLC system and are listed in Table 5-12. It is clear from the data in Table 5-12 that the compensation temperatures of the PAHs/halobenzenes are significantly different from those of the alkylbenzenes in most RPLC systems. Additionally from Table 5-12, the β values for each group of compounds are not apparently affected by methanol content of the mobile phase or stationary phase chain length.

In summary, enthalpy-entropy compensation effects exist for the hydrophobic solutes on C-2, C-4, and C-8 supports in methanol/water eluents. The PAH and monohalobenzene compounds are thermodynamically distinct in their RPLC retention behavior from the alkylbenzenes. This energetic difference is evident in the separate ln k' vs. $-\Delta H^{o}_{sorp}/R$ linear regression lines and compensation temperature for these two groups of compounds. The compensation temperatures of the PAHs/halobenzenes and alkylbenzenes are

Table 5-12. Comparison of compensation temperatures (β) collected on three RPLC supports in a methanol/water mobile phase system.

RPLC Phase	θ(MeOH)[a]	β(°K) ± 95% C.L. for PAHs, Benzene, & Halobenzenes[b]	β(°K) ± 95% C.L. for Alkylbenzenes[c]
C-2	0.60	762 ± 248	820 ± 330
	0.50	554 ± 10	657 ± 115
	0.40	521 ± 12	695 ± 365
	0.35	517 ± 16	725 ± 125
C-4	0.75	541 ± 65	696 ± 64
	0.70	699 ± 25	886 ± 135
	0.60	563 ± 23	650 ± 165
	0.50	532 ± 17	745 ± 88
	0.40	516 ± 25	780 ± 120
C-8	0.80	471 ± 20	623 ± 59
	0.70	504 ± 27	774 ± 167
	0.60	535 ± 22	783 ± 97
	0.50	547 ± 22	1034 ± 176

[a]Volume fraction methanol in methanol/water mobile phase.

[b]Compensation temperature (°K) ± 95% confidence limits for the PAH compounds, benzene, and the halobenzenes.

[c]Compensation temperature (°K) ± 95% confidence limits for the alkylbenzenes.

independent of the RPLC chain length and methanol content. The β values found for the alkylbenzenes compare favorably with the 639°K reported by Melander et al. (1978) for the retention of substituted benzenes on octadecylsilane in 60/40 (v/v) methanol/water. The difference in observed enthalpy-entropy compensation effects for the alkylbenzenes and PAHs/halobenzenes indicates that these two groups of compounds have different mechanisms of retention to RPLC supports (Melander et al., 1978, 1979). A more detailed discussion of the differing enthalpy-entropy compensation effects for the alkylbenzenes and PAHs/halobenzenes in a methanol/water eluent will follow in a later section.

Following this examination of enthalpy-entropy compensation effects in methanol/water eluents, the presence of such effects in acetonitrile/water RPLC systems can now be discussed. A plot of ln k' vs. $-\Delta H^{o}/R$ for the sorption of the hydrophobic solutes on the C-8 support in a 60/40 acetonitrile/water system is shown in Figure 5-29. The compensation temperatures and separate linear regression lines again suggest the presence of different hydrophobic retention mechanisms for the alkylbenzenes and PAHs/halobenzenes. However, the correlation of the alkylbenzene data with the compensation equation (Eqn. 3-48) is much weaker than in methanol/water mixtures, and the compensation temperatures are distinctly different from those reported in Table 5-12 for methanol/water eluents.

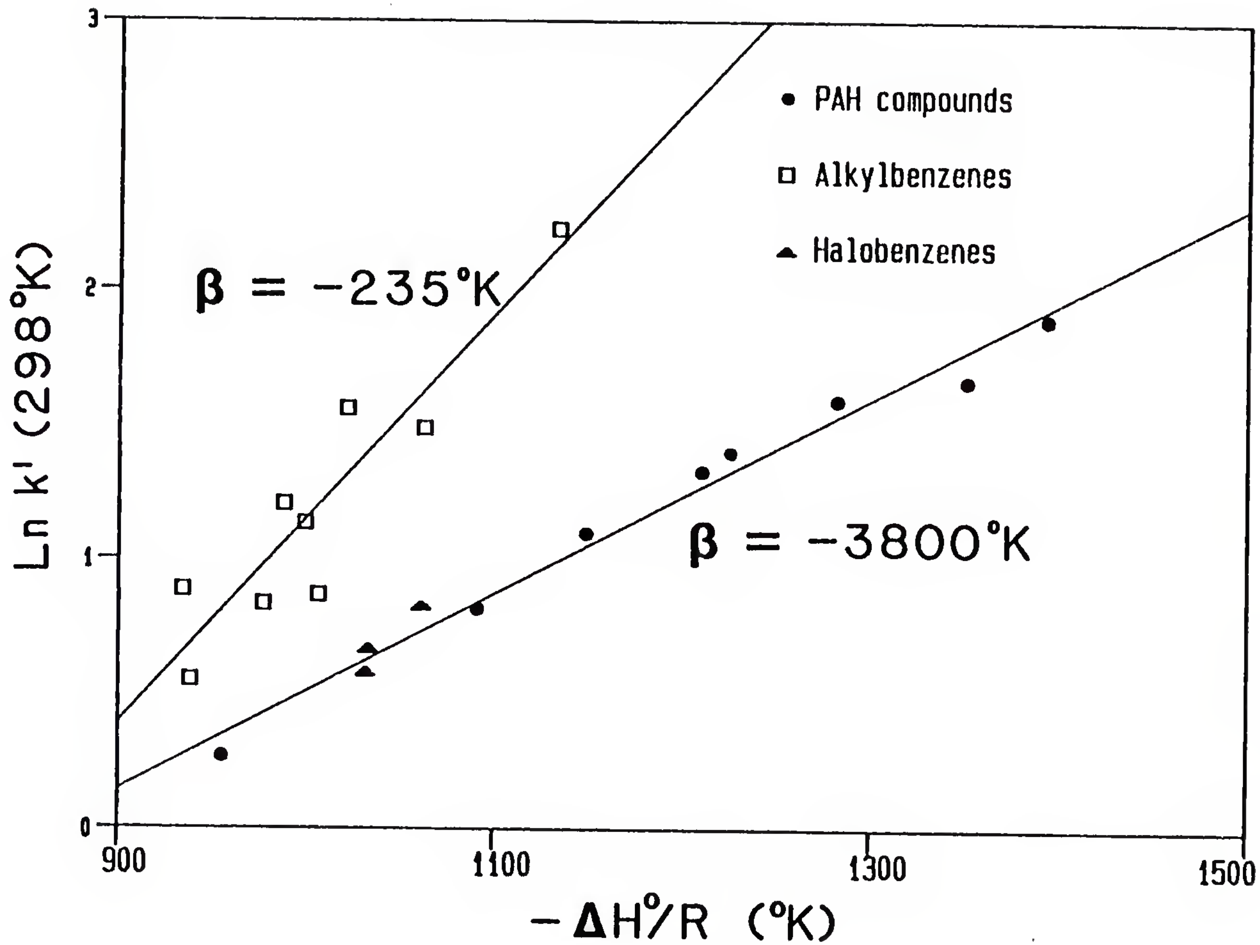

Figure 5-29. Ln k' at 308°K vs. $-\Delta H^{o}/R$ for sorption of the hydrophobic solutes on C-8 material in 60/40 acetonitrile/water.

The ln k' vs. $-\Delta H^{o}_{sorp}/R$ data for the remaining C-2, C-4, and C-8 acetonitrile/water systems were examined using Eqn. (3-48) and separate linear regression lines developed for the alkylbenzenes and PAHs/halobenzenes in each acetonitrile/water eluent. The respective compensation temperatures for the PAHs/halobenzenes and alkylbenzenes were calculated and are listed in Table 5-13. Although the β values for the two groups are statistically different in almost all RPLC systems, there are significant variations in β for each group of compounds. The consistent β values observed in methanol/water mixtures, approximately 550-750°K, are generally absent in the acetonitrile/water RPLC systems.

The correlation of solute hydrophobic surface area with the standard sorptive entropy change, ΔS^{o}_{sorp}, was discussed in Section 5.4.5. The effect of acetonitrile content on ΔS^{o}_{sorp} vs. HSA plots was shown at that time to be considerable. When the acetonitrile content exceeded 25% by volume, the ΔS^{o}_{sorp} vs. HSA regression lines for PAHs/halobenzenes and alkylbenzenes deviated significantly from the relatively constant entropic behavior of the solutes in methanol/water eluents. This deviation was attributed to surface tension effects in acetonitrile/water solvent systems.

Upon examining the β values in Table 5-13 more closely, it appears that the only system in which compensation temperatures approach those noted in methanol/water eluents

Table 5-13. Comparison of compensation temperatures (β) collected on three RPLC supports in an acetonitrile/water mobile phase.

RPLC Phase	θ(ACN)[a]	β(°K) ± 95% C.L. for PAHs, Benzene, & Halobenzenes[b]	β(°K) ± 95% C.L. for Alkylbenzenes[c]
C-2	0.50	-409 ± 253	-646 ± 338
	0.40	-1038 ± 510	-436 ± 145
	0.30	1433 ± 491	-1398 ± 745
	0.25	877 ± 182	1340 ± 667
C-4	0.60	-609 ± 1570	-653 ± 675
	0.50	-317 ± 64	-180 ± 140
	0.40	-1186 ± 426	-466 ± 250
	0.30	2190 ± 950	-1508 ± 740
C-8	0.65	-1045 ± 344	-302 ± 145
	0.60	-3800 ± 2400	-235 ± 488
	0.50	9367 ± 7310	-665 ± 470
	0.40	1250 ± 443	-640 ± 325
	0.30	912 ± 323	-2256 ± 1680

[a]Volume fraction acetonitrile in acetonitrile/water mobile phase.

[b]Compensation temperature (°K) ± 95% confidence limits for the PAH compounds, benzene, and the holobenzenes.

[c]Compensation temperature (°K) ± 95% confidence limits for the alkylbenzenes.

is the 25/75 acetonitrile/water system with the C-2 stationary phase. The compensation temperatures for the PAHs/halobenzenes and the alkylbenzenes in this RPLC system are 877°K and 1340°K, respectively. A plot of ln k' vs. $-\Delta H^{o}/R$ for solute sorption on the C-2 support in 25/75 acetonitrile/water is shown in Figure 5-30. The similarity of compensation temperatures in methanol/water mixtures and 25/75 acetonitrile/water suggests that the retention mechanism for a given compound is approximately the same in the two eluent systems. This suggestion is supported by the trends in ΔH^{o}_{sorp} vs. HSA and ΔS^{o}_{sorp} vs. HSA observed for these systems in Section 5.4. However, based on their compensation temperatures, RPLC systems with acetonitrile contents of greater than 25% by volume apparently involve hydrophobic retention mechanisms that are thermodynamically distinct from those operating in methanol/water mixtures and 25/75 acetonitrile/water. This difference may involve a significantly greater contribution of solvation sphere entropy changes (ΔS^{o}_{2}) to the overall sorptive free energy change (ΔG^{o}_{sorp}) for RPLC systems with elevated acetonitrile contents.

The compensation temperatures for alkylbenzenes and PAHs/halobenzenes appear to follow a consistent trend on a given RPLC support as the water content of the solvent is increased: (1) the ß values initially decrease; (2) suddenly become posiive; and then (3) decline to the

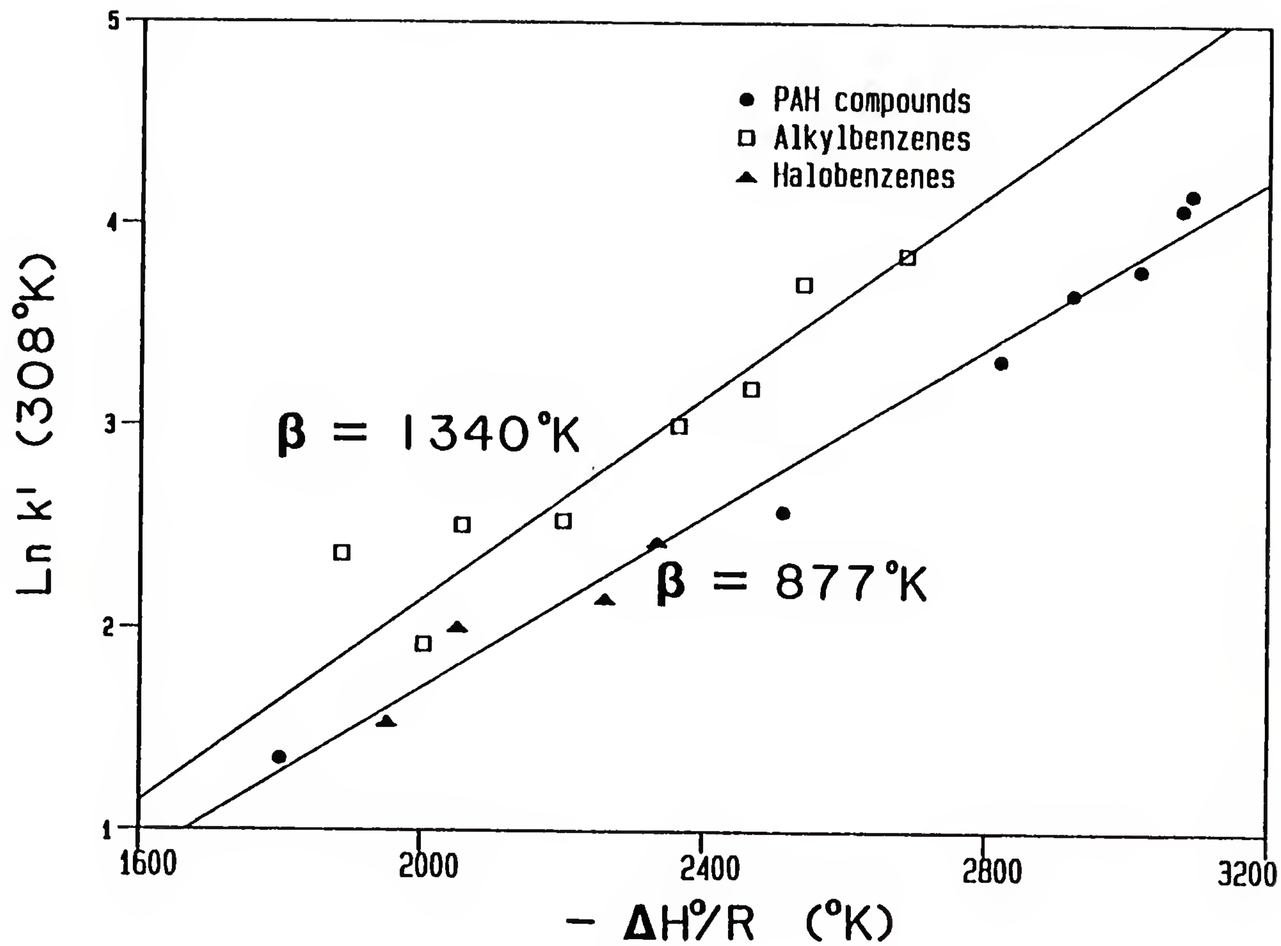

Figure 5-30. Ln k' at 308°K vs. $-\Delta H^{o}/R$ for sorption of the hydrophobic solutes on the C-2 support in 25/75 acetonitrile/water.

approximate β values observed in methanol/water mixtures. The acetonitrile content at which the β values convert from negative to positive is 0.40-0.30 for PAHs/halobenzenes and 0.30-0.25 for alkylbenzenes. This transformation point for enthalpy-entropy compensation effects is most likely related to solution surface tension and the entropy changes associated with release of the solute's solvation sphere. As surface tension increases, the ΔS^{o}_{2} entropy changes decline in importance and a shift occurs in enthalpy-entropy compensation effects towards the dominance of enthalpic retention processes. In this way, the enthalpy-entropy compensation effects in acetonitrile/water RPLC systems appear to slowly approach those in methanol/water eluents as solution acetonitrile content is decreased.

Chang and Huang (1985) reported a similar dependence of the solute retention mechanism on mobile phase composition. Their study involved the enthalpy-entropy compensation model as applied to the retention of substituted anilines on amino- and diamine-bonded phases with a variable eluent of 2-propanol in n-heptane. The system β values varied considerably as a function of 2-propanol content, and the authors attributed negative β values to the presence of multiple retention mechanisms for a given RPLC system.

Summarizing, enthalpy-entropy compensation effects are present for hydrophobic solute retention in acetonitrile/

water solvent systems of C-2, C-4, and C-8 RPLC sorbents. The correlation of experimental data with the chromatographic compensation model, Eqn. (3-48), is generally weaker than in similar methanol/water RPLC systems. The PAHs and halobenzenes form a ln k' vs. $-\Delta H^{o}_{sorp}/R$ linear regression relationship that is independent of a similar line for the alkylbenzenes. The compensation temperatures for these chemicals indicate the presence of thermodynamically distinct hydrophobic retention mechanisms for the two groups of compounds. Only for the C-2, 25/75 acetonitrile/water system were the β values similar to those determined for the methanol/water RPLC system (Table 5-12) and measured by Melander et al. (1978). At higher acetonitrile contents, the enthalpy-entropy compensation effects were different from those observed in the methanol/water eluent systems, with entropic solution processes perhaps assuming greater thermodynamic importance. The data suggest that the thermodynamic basis of the hydrophobic retention mechanism in acetonitrile/water RPLC systems is a function of solvent content. There are similar solute retention mechanisms at work in methanol/water systems and in solutions of a composition of 25/75 acetonitrile/water.

5.5.2 Compensation Temperatures in Soil Systems

The enthalpy-entropy compensation model is a useful tool for investigating basic processes of interaction in a wide

variety of systems (Lumry and Rajender, 1970). It has been used to study the aqueous solvation of ions, proteins, and nonelectrolytes (Lumry and Rajender, 1970), and solute retention in reversed-phase (Melander et al., 1978, 1979, 1980; Sander and Field, 1980) and normal-phase chromatography (Knox and Vasvari, 1973). The chromatographic compensation model, Eqn. (3-48), was used in the previous section to examine the retention of various hydrophobic solutes in methanol/water and acetonitrile/water RPLC systems.

A fundamental premise of the RPLC experiments was to study the useful application of reversed-phase liquid chromatography as a model for solute sorption in natural soil/water/solvent systems. Thus, a thermodynamic solute sorption experiment was conducted on Webster soil to examine enthalpy-entropy compensation effects in an actual soil matrix. In this manner, retention mechanisms in RPLC could be compared to sorption interactions in the soil system. The design of this thermodynamic soil sorption experiment was outlined in Chapter IV, Section 4.8.5.

A plot of the natural logarithm of the Langmuir soil sorption coefficients (K) vs. inverse absolute temperature is shown in Figure 5-31 for biphenyl, anthracene, and pyrene solutes sorbed to Webster soil in a 30/70 methanol/water solution. The actual data appear in Appendix I. The linear nature of the three van't Hoff plots in Figure 5-31

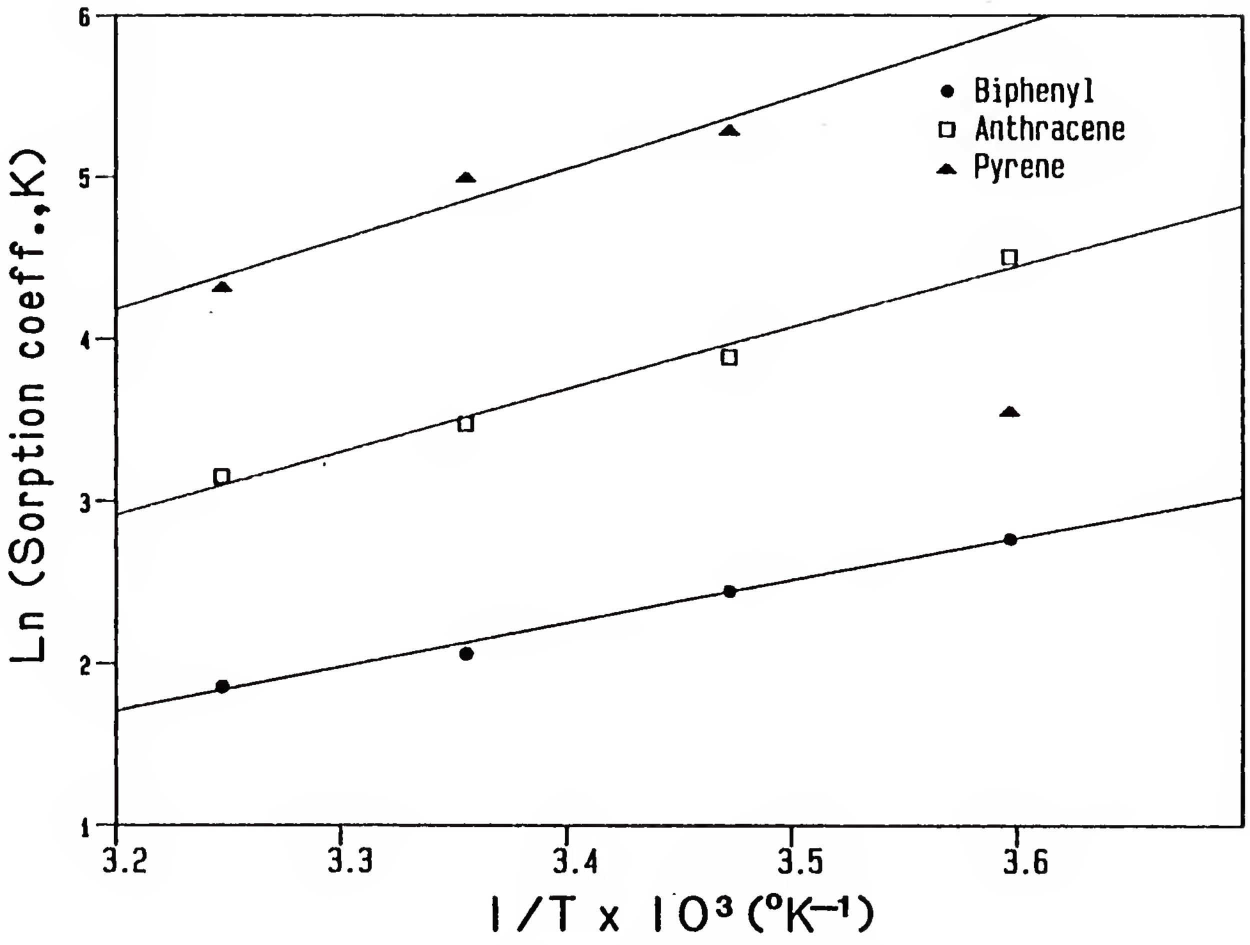

Figure 5-31. Ln (Soil sorption coefficient, K) at temperature T vs. 1/T for three aromatic solutes on Webster soil in a 30/70 methanol/water solution.

indicates that heat capacity effects are generally absent over the 5°C to 35°C temperature range used in the experiment. The 5°C data point for pyrene is an anomaly which may be attributed to solubilization difficulties at this temperature. This data point was omitted in the calculation of the linear regression line for pyrene shown in Figure 5-31.

From the slopes of the van't Hoff regression lines in Figure 5-31, the ΔH^{o}_{sorp} values for biphenyl, anthracene, and pyrene were calculated for sorption to Webster soil from a 30/70 methanol/water solution. These ΔH^{o}_{sorp} values are listed in Appendix I. An enthalpy-entropy compensation plot was developed from the soil sorption coefficients at 298°K and the ΔH^{o}_{sorp} values for the three compounds. This ln K vs. $-\Delta H^{o}_{sorp}/R$ plot is shown in Figure 5-32, and the compensation temperature for the Webster soil/methanol/water system was calculated at 573°K. This β value is remarkably similar to those developed for PAH compounds in RPLC methanol/water systems (Table 5-12). This finding indicates that the fundamental solute retention mechanism in the Webster soil/methanol/water environment is identical to the mechanism operating in methanol/water RPLC systems. Because of the paucity of data for the Webster soil system, this conclusion might be considered speculative, but it represents the first experimental evidence for comparing hydrophobic solute retention interactions in RPLC and

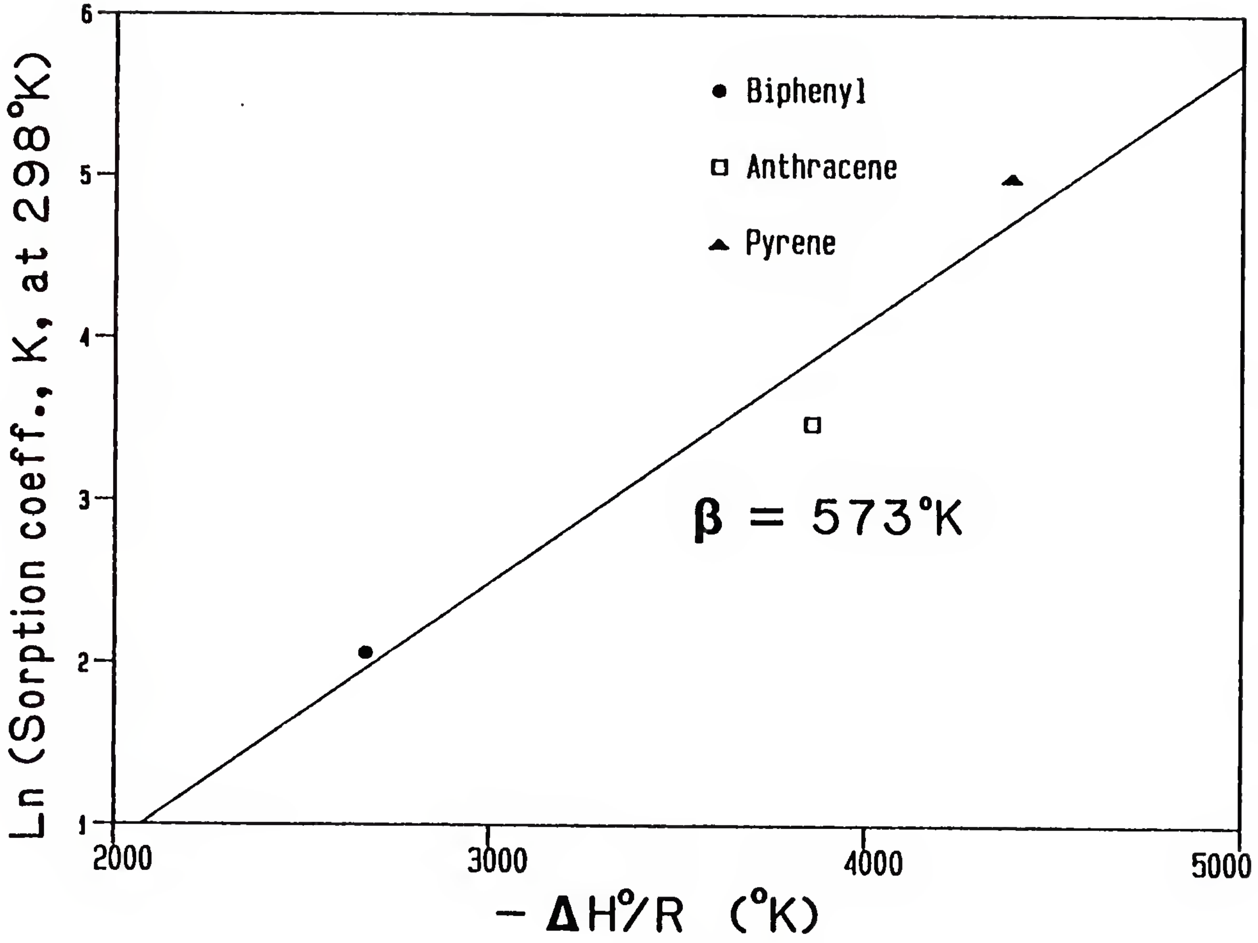

Figure 5-32. Ln (Soil Sorption coefficient, K) at 298°K vs. $-\Delta H^{O}/R$ for sorption of three aromatic solutes on Webster soil in a 30/70 methanol/water solution.

natural soil environments. Further experimentation is required to more fully understand sorption energetics in soil/water/solvent systems and the relationship of such systems to RPLC.

5.5.3 Compensation Effects in Reversed-Phase Chromatography

The previous two sections (Sections 5.5.1 and 5.5.2) examined the concept of the compensation temperature and its useful application for comparing and contrasting the solute retention mechanism in methanol/water and acetonitrile/water RPLC systems and the Webster soil/methanol/water environment. This section presents in greater detail the way in which the standard sorptive enthalpy and entropy changes compensate for one another and the manner in which thermodynamic compensation effects change with varying acetonitrile content.

In the overall standard sorptive free energy change, ΔG^{o}_{sorp}, there is an enthalpic contribution to retention (ΔH^{o}_{sorp}) and a contribution due to entropy effects ($T\Delta S^{o}_{sorp}$). A technique for comparing the relative importance of each term is to plot $T\Delta S^{o}_{sorp}$ vs. ΔH^{o}_{sorp}. A plot of this type also provides visual insight into enthalpy-entropy compensation effects. A sample plot of $T\Delta S^{o}$ vs. ΔH^{o} for solute sorption onto C-2 material in 35/65 methanol/water is shown in Figure 5-33. Two linear regression lines are drawn through the thermodynamic data, one for

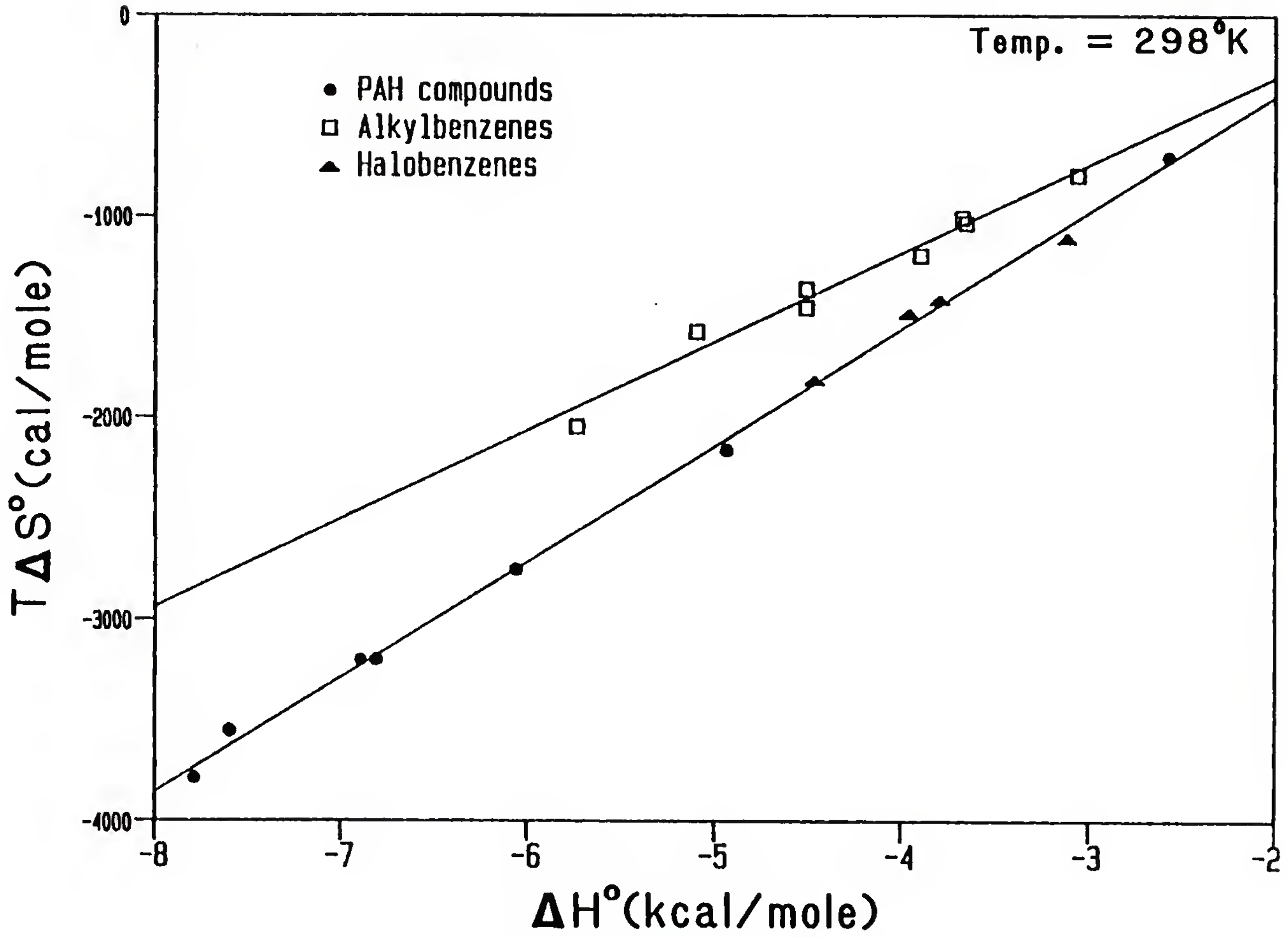

Figure 5-33. $T\Delta S^{o}$ vs. ΔH^{o} for sorption of the hydrophobic solutes on C-2 material in 35/65 methanol/water at 298°K.

the alkylbenzenes and one for the PAH compounds; also shown are data for the monohalobenzenes, which act in a manner similar to the PAH solutes. Compounds falling on either regression line involve the same relative contribution of ΔH^{o}_{sorp} and $T\Delta S^{o}_{sorp}$, i.e., the same enthalpy-entropy compensation effects. The entropic contribution to the standard free energy change is considerably greater for the alkylbenzenes in Figure 5-33 compared to the PAHs and halobenzenes. This conclusion agrees with the results of the earlier studies of ΔS^{o}_{sorp} vs. HSA for the hydrophobic solutes in methanol/water RPLC systems (Section 5.4.5).

Similar plots of $T\Delta S^{o}$ vs. ΔH^{o} for solute sorption on C-4 material in 50/50 and 75/25 methanol/water systems are shown in Figures 5-34 and 5-35, respectively. The separate enthalpy-entropy compensation trends noted in Figure 5-33 for the alkylbenzenes and the PAHs are also apparent in these plots. The relative thermodynamic difference between the two groups of compounds does not appear to change with RPLC chain length or methanol content. A listing of $T\Delta S^{o}$ vs. ΔH^{o} regression data for solute sorption on the C-2, C-4, and C-8 materials in a wide variety of methanol/water solutions is given in Table 5-14 for the PAHs and alkylbenzenes. The slopes of both the $T\Delta S^{o}_{sorp}$ vs. ΔH^{o}_{sorp} regression lines do not change significantly as the water content is decreased from 65% to 30% by volume or as the RPLC chain length is increased from C-2 to C-8. It may be concluded

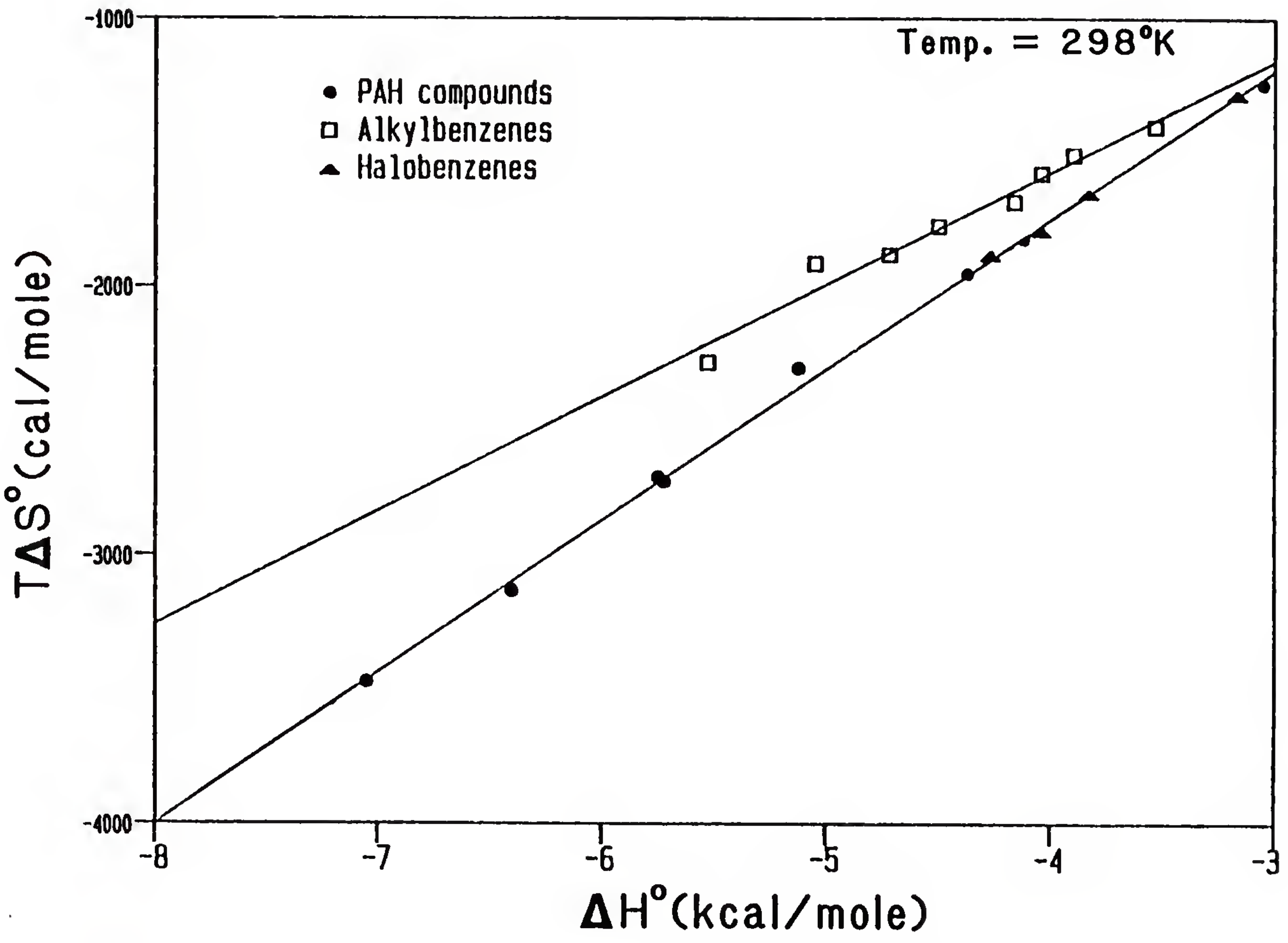

Figure 5-34. $T\Delta S^{o}$ vs. ΔH^{o} for sorption of the hydrophobic solutes on C-4 material in 50/50 methanol/water at 298°K.

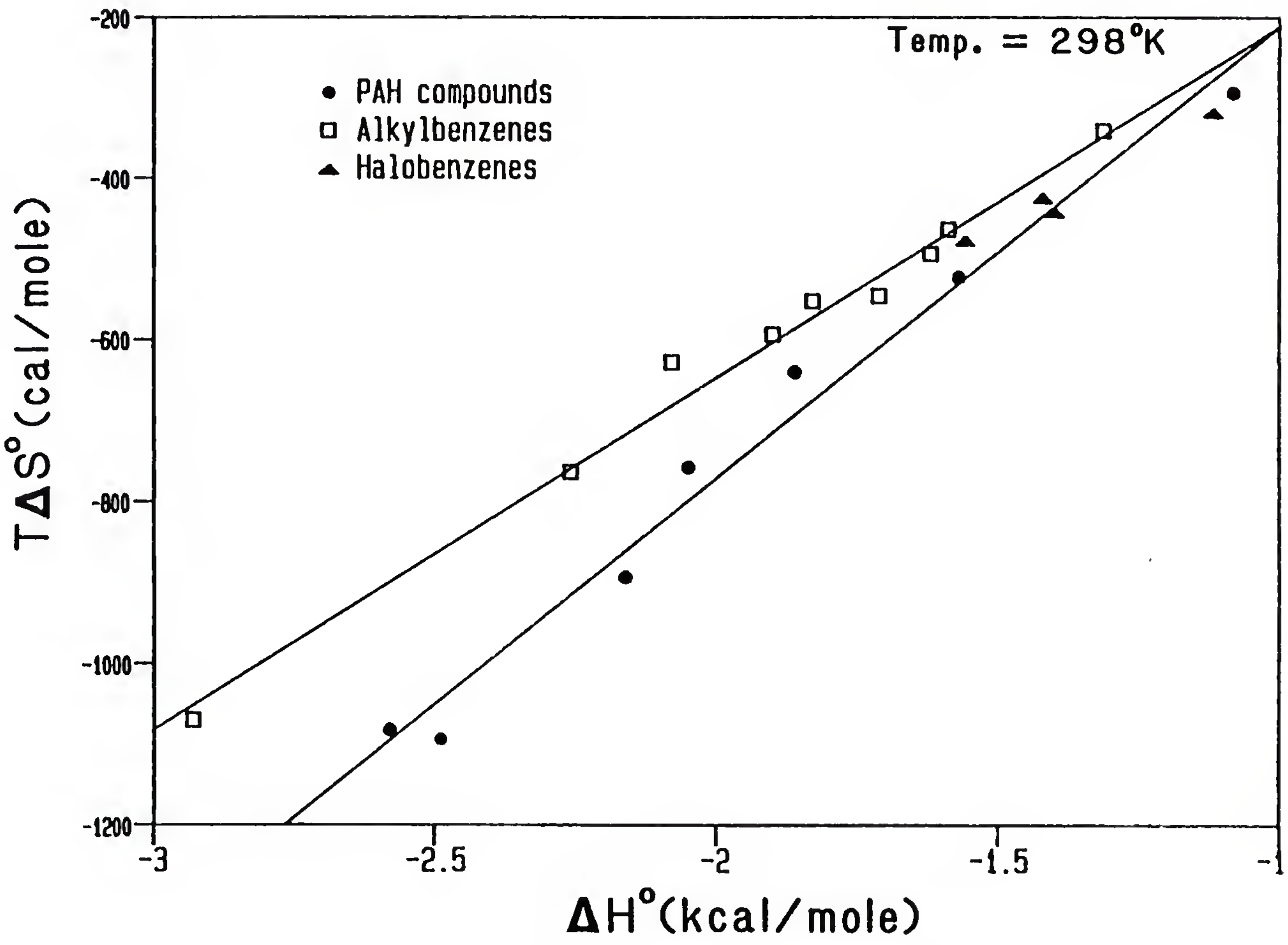

Figure 5-35. $T\Delta S^{o}$ vs. ΔH^{o} for sorption of the hydrophobic solutes on C-4 material in 75/25 methanol/water at 298°K.

Table 5-14. $T\Delta S^{o}$ vs. ΔH^{o} for sorption of hydrophobic solutes on C-2, C-4, and C-8 RPLC supports in various methanol/water eluents.

RPLC Support	Methanol/water mixture (v/v)	$T\Delta S^{o}$ vs. ΔH^{o} regression[a] for PAHs and benzene	$T\Delta S^{o}$ vs. ΔH^{o} regression[b] for alkylbenzenes
C-2	35/65	n = 7, R = 0.9990 Slope = 576.8 ± 29.5 Intercept = 748.6 ± 187.0	n = 8, R = 0.9877 Slope = 440.0 ± 69.5 Intercept = 568.6 ± 302.0
C-4	50/50	n = 7, R = 0.9985 Slope = 562.4 ± 35.9 Intercept = 501.0 ± 197.0	n = 8, R = 0.9835 Slope = 421.8 ± 77.7 Intercept = 112.3 ± 347.7
C-4	75/25	n = 7, R = 0.9905 Slope = 558.3 ± 89.3 Intercept = 344.1 ± 181.3	n = 9, R = 0.9834 Slope = 435.9 ± 67.2 Intercept = 222.9 ± 132.1
C-8	60/40	n = 8, R = 0.9984 Slope = 561.2 ± 31.6 Intercept = 446.2 ± 160.6	n = 9, R = 0.9932 Slope = 386.3 ± 40.4 Intercept = -22.4 ± 167.5
C-8	70/30	n = 8, R = 0.9986 Slope = 592.0 ± 31.5 Intercept = 385.7 ± 122.7	n = 8, R = 0.9890 Slope = 392.7 ± 58.5 Intercept = -17.3 ± 186.5

[a]Linear regression of $T\Delta S^{o}$ vs. ΔH^{o} for sorption of the PAH compounds and benzene; n is the number of data points; R is the correlation coefficient; slope and intercept values represent mean values ± 95% confidence limits.

[b]Linear regression of $T\Delta S^{o}$ vs. ΔH^{o} for sorption of the alkylbenzenes; n is the number of data points; R is the correlation coefficient; slope and intercept values represent mean values ± 95% confidence limits.

from the data in Table 5-14 that enthalpy-entropy compensation effects are independent of RPLC chain length and solution composition in methanol/water eluents. This result is the same as that demonstrated in the earlier study of compensation temperatures in methanol/water RPLC systems (Section 5.5.1).

In acetonitrile/water RPLC systems, solvent composition has a considerable impact upon enthalpy-entropy compensation effects; the situation is quite different from that observed in methanol/water eluents. A plot of $T\Delta S^{o}$ vs. ΔH^{o} for solute sorption on C-2 material in 25/75 acetonitrile/water is shown in Figure 5-36. The thermodynamic behavior of the hydrophobic solutes is similar in this solvent system to that noted in methanol/water eluents for the PAH compounds and the alkylbenzenes. This trend agrees with the previous ΔS^{o}_{sorp} vs. HSA studies (Section 5.4.5) and the results from Section 5.5.1 on compensation temperatures in various RPLC systems.

The earlier results (Section 5.5.1) on compensation temperatures in acetonitrile/water eluents indicated that the mechanisms/thermodynamics of solute retention changed with solution acetonitrile content. The change in system thermodynamics is demonstrated in Figure 5-37 as $T\Delta S^{o}$ is plotted vs. ΔH^{o} for solute sorption on the C-2 sorbent in 30/70 acetonitrile/water. The slope of the alkylbenzene regression line is dramatically different from that of the

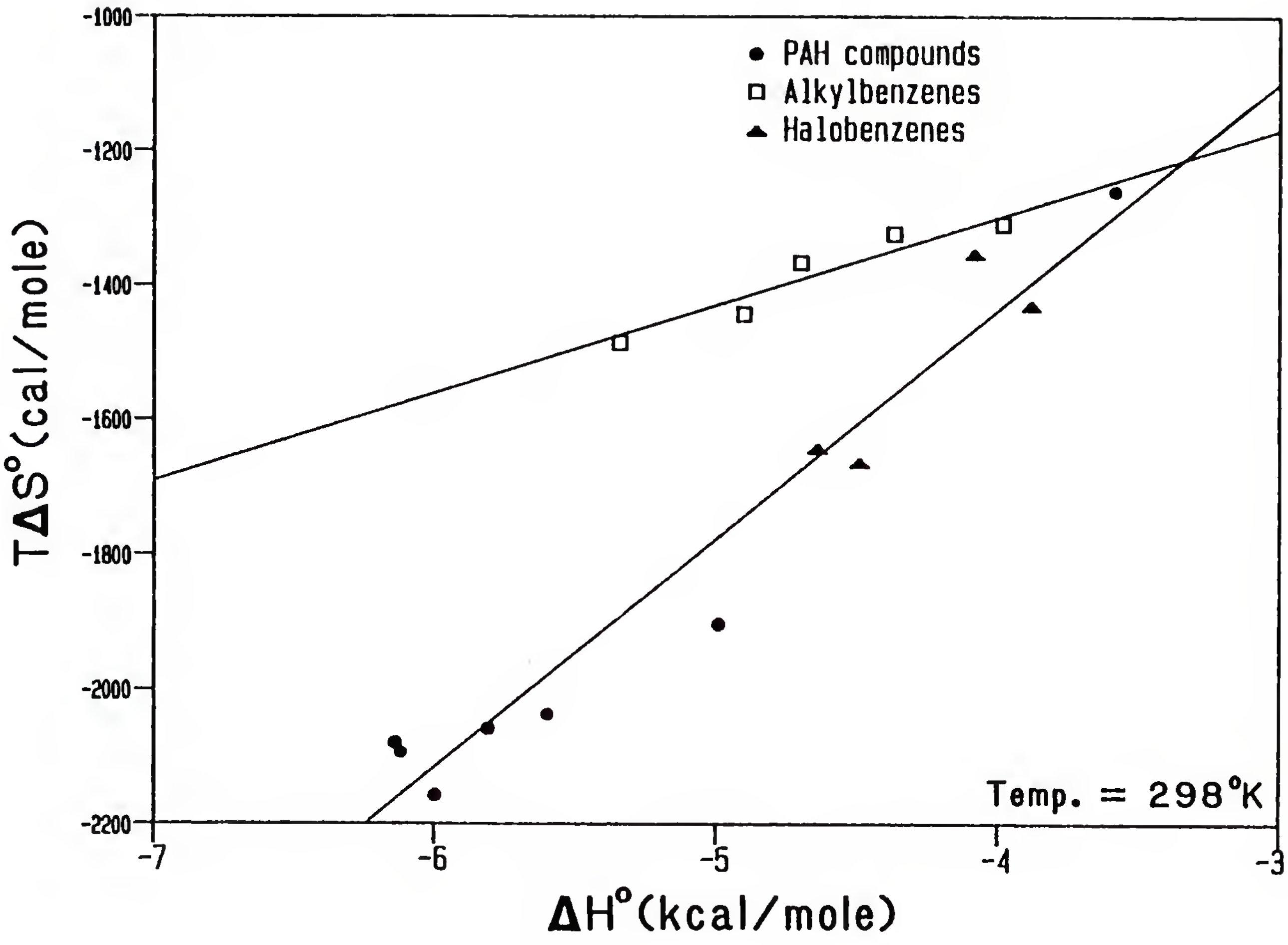

Figure 5-36. $T\Delta S^{o}$ vs. ΔH^{o} for sorption of the hydrophobic solutes on C-2 material in 25/75 acetonitrile/water at 298°K.

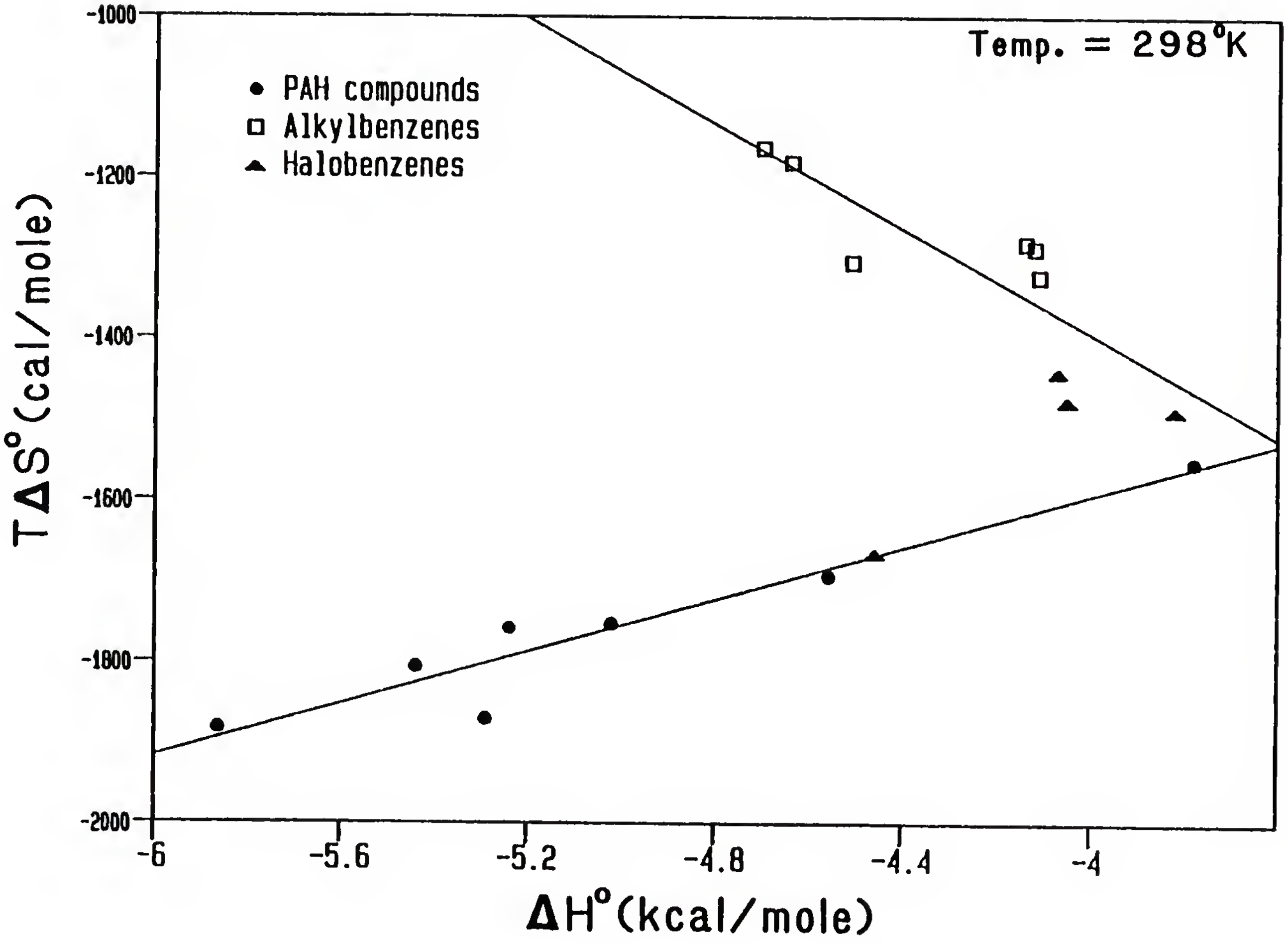

Figure 5-37. $T\Delta S^{o}$ vs. ΔH^{o} for sorption of the hydrophobic solutes on C-2 material in 30/70 acetonitrile/water at 298°K.

25/75 acetonitrile/water solution, i.e., the enthalpy-entropy compensation effects for these compounds have changed with only a relatively small change in acetonitrile content. For the 30/70 acetonitrile/water solution, as the standard sorptive enthalpy change for the alkylbenzenes decreases, the entropic contribution to the sorptive free energy change increases. This situation is considerably different in the 25/75 acetonitrile/water and methanol/water solutions, where an increasingly exothermic ΔH^{o} for alkylbenzenes produces a decrease in the $T\Delta S^{o}$ term.

The $T\Delta S^{o}$ vs. ΔH^{o} plot for solute C-2 sorption in 40/60 acetonitrile/water is shown in Figure 5-38. A decline in ΔH^{o}_{sorp} values correlates with an increase in $T\Delta S^{o}_{sorp}$ values for the PAH and halobenzene compounds, as well as for the alkylbenzenes. This solute behavior is a further extension of the $T\Delta S^{o}_{sorp}$ vs. ΔH^{o}_{sorp} trends noted in the 30/70 acetonitrile/water mixture (Figure 5-37) and is related to the large positive entropy change (ΔS^{o}_{2}) associated with release of the solute's solvation sphere molecules back to the 40/60 acetonitrile/water solution.

The addition of more acetonitrile to the 40/60 acetonitrile/water solvent mixture produces only minor changes in enthalpy-entropy compensation effects for the hydrophobic solutes. A plot of $T\Delta S^{o}_{sorp}$ vs. ΔH^{o}_{sorp} on C-4 material in 50/50 acetonitrile/water is shown in Figure 5-39. The slope of the linear regression line for the

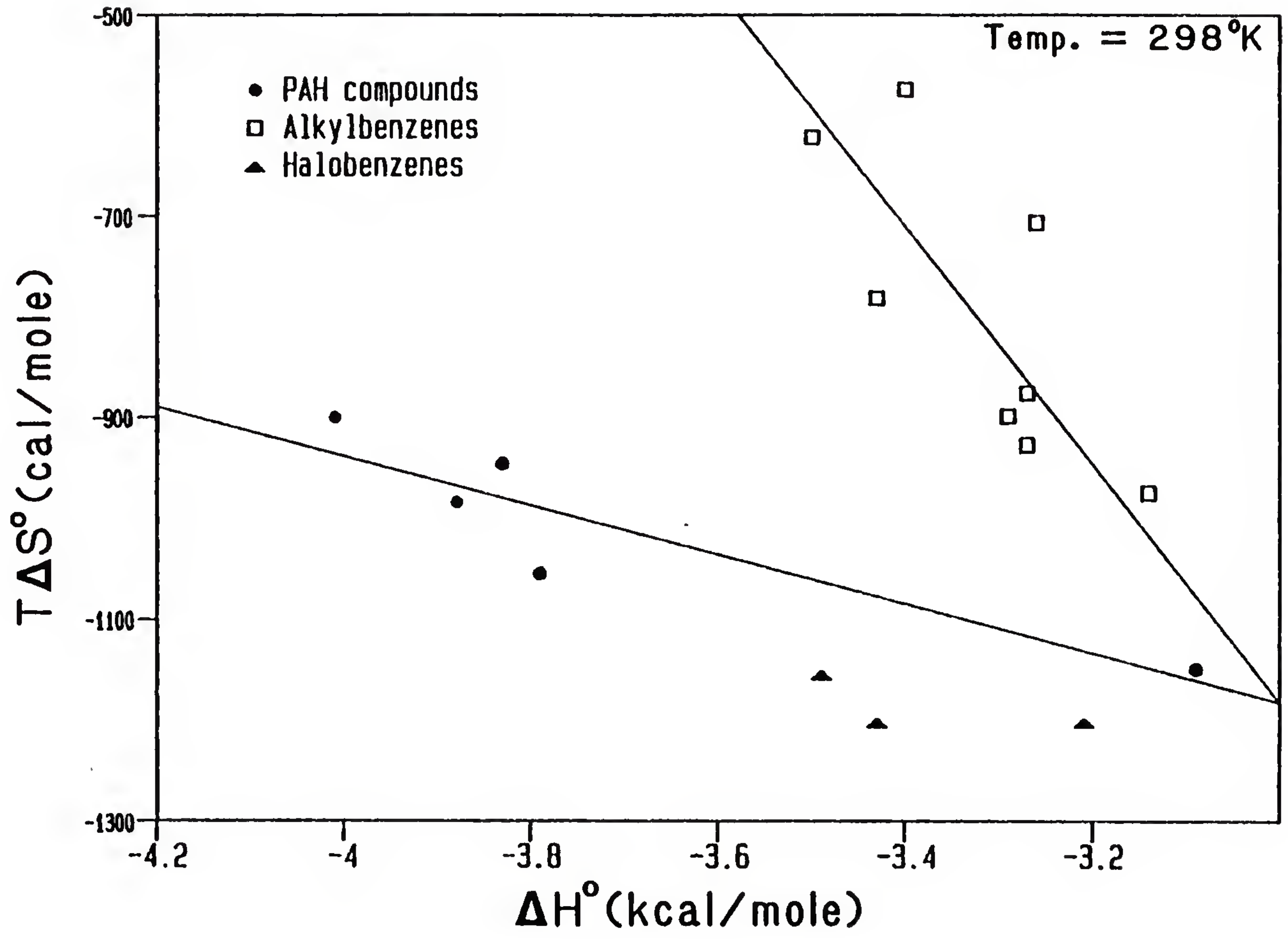

Figure 5-38. $T\Delta S^{o}$ vs. ΔH^{o} for sorption of the hydrophobic solutes on C-2 material in 40/60 acetonitrile/water at 298°K.

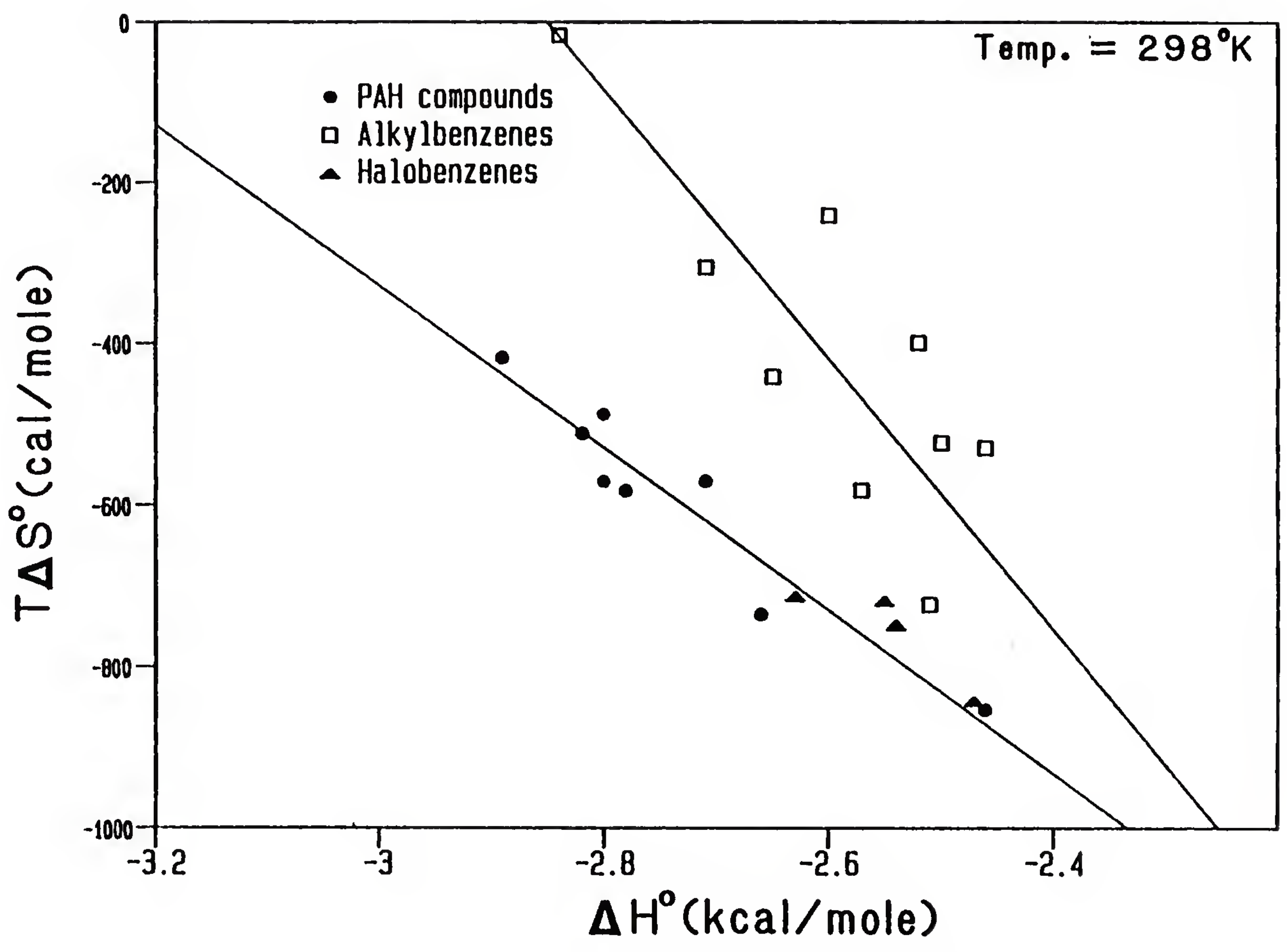

Figure 5-39. $T\Delta S^{o}$ vs. ΔH^{o} for sorption of the hydrophobic solutes on C-4 material in 50/50 acetonitrile/water at 298°K.

alkylbenzenes is almost identical in the two solvent systems, i.e., enthalpy-entropy compensation effects are approximately equivalent in 40/60 and 50/50 acetonitrile/water mobile phases. The PAHs and halobenzenes, however, show slightly greater entropic compensation in the 50/50 acetonitrile/water eluent system than the 40/60 acetonitrile/water mixture. In general, enthalpy-entropy compensation effects for the hydrophobic solutes change little as acetonitrile content is increased from 40 to 50% by volume in the RPLC systems under study.

Regression data from plots of $T\Delta S^{o}_{sorp}$ vs. ΔH^{o}_{sorp} for a variety of acetonitrile/water RPLC systems appear in Table 5-15. The data indicate that enthalpy-entropy compensation effects for the PAHs/halobenzenes and the alkylbenzenes change considerably as one goes from an acetonitrile content of 25 to 40% by volume. Over this range, the slopes of both $T\Delta S^{o}_{sorp}$ vs. ΔH^{o}_{sorp} regression lines change from positive to negative and then remain fairly constant at acetonitrile contents of 40% (v/v) and higher. A similar dependence on acetonitrile content of the ΔS^{o}_{sorp} vs. HSA plots was discussed in Section 5.3.5. This thermodynamic behavior indicates that the change in sorption thermodynamics is related to changes in solution surface tension and the concomitant effect upon the entropy term associated with release of the solute solvation sphere.

Table 5-15. $T\Delta S^o$ vs. ΔH^o for sorption of hydrophobic solutes on C-2, C-4, and C-8 RPLC supports in various acetonitrile/water eluents.

RPLC Support	Acetonitrile/water mixture (v/v)	$T\Delta S^o$ vs. ΔH^o regression[a] for PAHs and benzene	$T\Delta S^o$ vs. ΔH^o regression[b] for alkylbenzene
C-2	25/75	n = 7, R = 0.9722 Slope = 327.4 ± 90.6 Intercept = -152.8 ± 501.0	n = 6, R = 0.9691 Slope = 130.6 ± 46.0 Intercept = -780.9 ± 208.0
C-2	30/70	n = 7, R = 0.9554 Slope = 160.2 ± 57.0 Intercept = -954.5 ± 289.0	n = 7, R = -0.8712 Slope = -327.9 ± 212.5 Intercept = -2707. ± 913.2
C-2	40/60	n = 5, R = -0.9050 Slope = -245.0 ± 213.7 Intercept = -1918.5 ± 798.0	n = 9, R = -0.8512 Slope = -1173.9 ± 647.7 Intercept = -4702.9 ± 2135.4
C-4	50/50	n = 8, R = -0.9560 Slope = -1005.1 ± 307.7 Intercept = -3344.1 ± 844.0	n = 9, R = -0.8367 Slope = -1675.5 ± 979.0 Intercept = -4777.0 ± 2525.6
C-4	60/40	n = 6, R = -0.8591 Slope = -711.5 ± 587.3 Intercept = -2405.5 ± 1395.4	n = 7, R = -0.9040 Slope = -1640.1 ± 873.7 Intercept = -4270.0 ± 2006.7
C-8	60/40	n = 6, R = -0.9446 Slope = -206.4 ± 99.3 Intercept = -980.9 ± 228.3	n = 7, R = -0.8926 Slope = -1442.4 ± 890.4 Intercept = -3087.0 ± 2107.5

[a]Linear regression of $T\Delta S^o$ vs. ΔH^o for sorption of the PAH compounds and benzene; n is the number of data points; R is the correlation coefficient; slope and intercept values represent mean values ± 95% confidence limits.

[b]Linear regression of $T\Delta S^o$ vs. ΔH^o for sorption of the alkylbenzenes; n is the number of data points; R is the correlation coefficient; slope and intercept values represent mean values ± 95% confidence limits.

Although the scatter in the data given in Table 5-15 prevents a definitive conclusion concerning compensation dependence on the RPLC stationary phase, there is no systematic change in compensation effects with RPLC chain length. It has been assumed by this author that enthalpy-entropy compensation effects are independent of stationary phase chain length. The correlation coefficients are generally weaker for compensation effects in acetonitrile/water eluents (Table 5-15) than methanol/water RPLC systems (Table 5-14).

In summary, enthalpy-entropy compensation effects exist for hydrophobic solutes in methanol/water and acetonitrile/water systems of C-2, C-4, and C-8 stationary phases. The experimental data of this section and Section 5.5.1 indicate that the distinct trends of ln k' with HSA, log K_{ow}, and ^{1}X noted earlier (Section 5.3) for the alkylbenzenes and PAH/halobenzene compounds are due to differences in the sorptive thermodynamic behavior for these two sets of compounds. The alkylbenzenes consistently show greater input of the sorptive entropy change in the overall sorptive free energy change. Enthalpy-entropy compensation effects are independent of solution methanol content and RPLC chain length. The entropic compensation term, $T\Delta S^{o}_{sorp}$, increases with acetonitrile content for the alkylbenzenes and PAHs/halobenzenes, with compensation effects stabilizing in eluents of 40% or more acetonitrile by volume.

5.5.4 Application of the Enthalpy-Entropy Compensation Model

The presence of enthalpy-entropy compensation effects in reversed-phase liquid chromatographic systems may be examined with a simple expression relating ln k', ΔH^{o}_{sorp}, and β, i.e., Eqn. (3-48). Detailed expressions may be generated which explore compensation effects with more mathematical rigor. The three-parameter model (Eqn. 3-57) expressed RPLC compensation effects for a linear ln k' vs. θ relationship

$$\ln k' = A_1\theta(1 - \beta/T) + A_2/T + A_3$$

while a four-parameter model (Eqn. 3-58) may also be used to describe RPLC compensation effects for systems involving a quadratic ln k' vs. θ relationship

$$\ln k' = A_1\theta(1 - \beta/T) + A_2/T + A_3 + A_4\theta^2(1 - \beta/T)$$

A listing of the physical meaning of the compensation parameters (A_1, A_2, A_3, and A_4) may be found in Table 3-1 for fully compensated (Eqn. 3-54a) and partially compensated (Eqn. 3-54b) standard sorptive enthalpy changes.

The dependence of the natural logarithm of the solute retention factor (ln k') upon solvent composition (θ) was discussed in Section 5.4.1 for methanol/water and

acetonitrile/water RPLC systems. The retention data (Appendix A) indicate that a linear ln k' vs. θ model is appropriate for methanol/water eluents, while a quadratic expression adequately describes retention in acetonitrile/water RPLC systems. As a result, the three-parameter compensation model was applied to all methanol/water RPLC systems, and the four-parameter model was used for acetonitrile/water systems. For comparison purposes, the three-parameter expression was also applied to the acetonitrile/water eluents on all RPLC supports. The calculated regression parameters (A_1, A_2, A_3, and A_4) are listed in Appendix E for all methanol/water and acetonitrile/water RPLC systems.

For the hydrophobic solutes in methanol/water systems, the correlation coefficients (Appendix E) indicate that the three-parameter model provides an excellent description of solute retention as a function of solvent composition and temperature. Similar results were reported by Melander and Horvath (1984) and Melander et al. (1982) for the three-parameter model applied to alkylbenzene sorption on C-18 material in methanol/water eluents. The model may be interpreted for full or partial enthalpy compensation, according to Eqns. (3-54a) and (3-54b), respectively.

As discussed in Chapter III, Section 3.4.4, partial compensation effects are demonstrated by a nonzero intercept of an A_2 vs. A_1 linear regression for the methanol/water

RPLC system of interest. Partial enthalpy compensation effects were observed for all stationary phases with methanol/water mobile phases (Appendix E). The noncompensated portion of the standard enthalpy change in the reference solvent of 100% water is termed $\Delta H^o_n(0)$. A review of Table 3-1 may prove useful to the reader at this time.

The other important constant for the partial enthalpy compensation model, Eqn. (3-57), is the solvent parameter α (see Table 3-1). This parameter is specific for the organic solvent used in the RPLC system and may be calculated from the slope of an A_2 vs. A_1 linear regression line. If partial enthalpy compensation effects are present, Eqn. (3-60) describes the relationship of A_2 to A_1

$$A_2 = -\beta A_1/\alpha - \Delta H^o_n(0)/R$$

where β is the compensation temperature (°K), α is the solvent parameter for the binary system, and $\Delta H^o_n(0)$ is the noncompensated portion of the standard sorptive enthalpy change in 100% water. This equation was applied to the A_2 and A_1 data for the methanol/water RPLC systems and the calculated α values are listed in Appendix E. The data reveal that α is reasonably independent of RPLC chain length for the methanol/water eluent, averaging -1.07 at a β value of 625°K. The small increase in α with RPLC chain length may be an indication of increasing hydrophobicity of the

sorbent surface; the small rate of increase is not thought to be significant to the overall compensation model.

An inherent assumption of the three parameter compensation model is knowledge of the compensation temperature, β, for the RPLC system of interest. Melander et al. (1979, 1982, 1985) employed a compensation temperature of 625°K in their RPLC studies and this β value was adopted for general use in the calculations reported in Appendix E. The relative importance of the assumed compensation temperature to the computed $\Delta H^{o}_{n}(0)$ and α values was examined for the C-8, methanol/water system. The $\Delta H^{o}_{n}(0)$ and α terms did not vary significantly over a β range of 525 to 725°K in this RPLC system. These results are given in Appendix E.

The collected $\Delta H^{o}_{n}(0)$ and α values for the C-2, C-4, and C-8 stationary phases in methanol/water are listed in Table 5-16. As stated previously, the solvent parameter α is reasonably independent of RPLC chain length and neither α nor $\Delta H^{o}_{n}(0)$ vary significantly with β on the C-8 support. However, it appears that $\Delta H^{o}_{n}(0)$ increases directly with RPLC chain length. The calculated linear regression of $\Delta H^{o}_{n}(0)$ vs. stationary phase carbon number for a β value of 625°K is shown in Table 5-16.

The regression parameters A_1, A_2, and A_3 listed in Appendix E are specific for each solute in a given methanol/water RPLC system. These parameters are a function of either the sorptive enthalpy change, ΔH^{o}_{sorp}, or the

Table 5-16. Enthalpy-entropy compensation parameters on the C-2, C-4, and C-8 stationary phases in a methanol/water eluent system via the three-parameter compensation model, Eqn. (3-57).

RPLC Phase	β (°K)[a]	α[b]	$\Delta H^{o}_{n}(0)$ (kcal/mole)[c]
C-2	625	-1.18 ± 0.03	0.20 ± 0.33
C-4	625	-1.08 ± 0.03	0.23 ± 0.23
C-8	525	-1.02 ± 0.07	1.19 ± 0.87
C-8	625	-0.96 ± 0.05	1.09 ± 0.68
C-8	725	-0.90 ± 0.05	1.17 ± 0.76

[a]Compensation temperature.

[b]Mean value ± 95% confidence limits.

[c]Mean value ± 95% confidence limits. A plot of $\Delta H^{o}_{n}(0)$ vs. RPLC chain length at β of 625°K produces n = 3, R = 0.9542
Slope = 0.158 ± 0.630
Intercept = -0.23 ± 3.33

sorptive entropy change, ΔS^{o}_{sorp} (See Table 3-1). In Sections 5.4.4 and 5.4.5, the relationship of ΔH^{o}_{sorp} and ΔS^{o}_{sorp} to solute HSA was extensively discussed. It is therefore not surprising that A_1, A_2, and A_3 are also functions of the solute HSA value. A plot of A_1 vs. solute HSA is shown in Figure 5-40 for the methanol/water, C-4 system. Two regression lines were developed, one for the alkylbenzenes and one for the PAH and halobenzene compounds. A similar plot may be developed for any of the regression parameters (A_1, A_2, or A_3) in any methanol/water RPLC system. The linear regression equations developed between A_1, A_2, and A_3 and solute HSA are listed in Table 5-17 for the methanol/water, C-4 system.

In summary, the three-parameter enthalpy-entropy compensation model, Eqn (3-57)

$$\ln k' = A_1\theta(1 - \beta/T) + A_2/T + A_3$$

is an excellent analytical expression relating solute retention (k') with eluent composition (θ) and temperature (T). The regression parameters A_1, A_2, and A_3 are functions of solute HSA, with individual regression lines for the alkylbenzenes and PAH/halobenzene compounds. Partial compensation of the standard sorptive enthalpy change does occur in methanol/water RPLC systems, and the value of the noncompensated enthalpy residue in 100% water, $\Delta H^{o}_{n}(0)$, is a

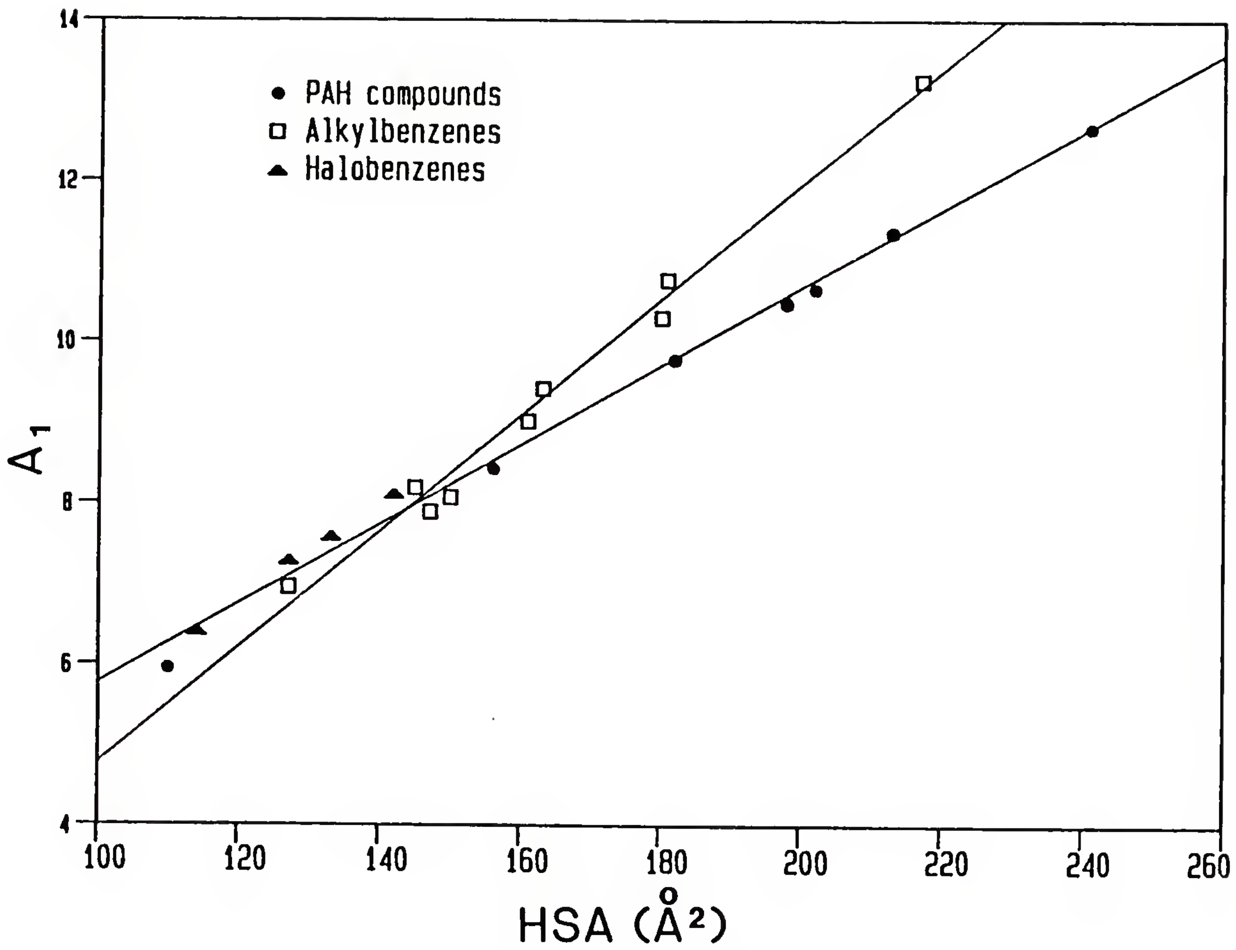

Figure 5-40. A_1 vs. solute HSA for sorption of the hydrophobic solutes on C-4 material in methanol/water eluents.

Table 5-17. Linear regression of the compensation parameters A_1, A_2, and A_3 vs. solute HSA for the alkylbenzenes and the PAH and halobenzene compounds on C-4 material in methanol/water at β of 625°K.

	Parameter vs. HSA for the PAHs, benzene, and halobenzenes*	Parameter vs. HSA for alkylbenzenes*
A_1	n = 11, R = 0.9967	n = 9, R = 0.9943
	Slope = 0.0489 ± 0.0030	Slope = 0.710 ± 0.0068
	Intercept = 0.907 ± 0.511	Intercept =-2.30 ± 1.13
A_2	n = 11, R = 0.9945	n = 9, R = 0.9935
	Slope = 29.09 ± 2.30	Slope = 42.55 ± 4.34
	Intercept = 281.7 ± 392.5	Intercept = -1686.4± 718.1
A3	n = 11, R = -0.9965	n = 9, R = -0.9908
	Slope = -0.0474 ± 0.0030	Slope = -0.0669 ± 0.0082
	Intercept = -2.12 ± 0.51	Intercept = 1.04 ± 1.35

*n is the number of data points; R is the correlation coefficient; slope and intercept values represent mean values ± 95% confidence limits.

function of RPLC chain length. The value of $\Delta H^{o}_{n}(0)$ is not significantly affected by the compensation temperature, β. The solvent parameter, α, is independent of RPLC chain length and the assumed β value. The physical meaning of the regression parameters was presented earlier in Table 3-1.

In acetonitrile/water RPLC systems, both the three- and four-parameter compensation models have been applied to the chromatographic data. The tabulated regression parameters (A_1, A_2, A_3, and A_4) are listed in Appendix E. The correlation coefficients indicate that the four-parameter model (Eqn. 3-58) does not offer a significant advantage relative to the three-parameter expression (Eqn. 3-57). The model constants $\Delta H^{o}_{n}(0)$, α, and Ψ in acetonitrile/water RPLC systems are listed in Tables 5-18 and 5-19 for the four-parameter and three-parameter models, respectively.

The model constants for the four-parameter equation are listed in Table 5-18 for the C-2, C-4, and C-8 supports in acetonitrile/water mobile phases. As demonstrated previously for the three-parameter model in methanol/water RPLC systems (Table 5-16), the value of $\Delta H^{o}_{n}(0)$ and the solvent parameters (α and Ψ) do not change appreciably with the RPLC compensation temperature, as shown for the C-8 stationary phase. At the β value of 625°K, an increase in RPLC chain does not produce any significant changes in α or Ψ until the C-8 support is reached. As theorized earlier for the methanol/water systems, this change may be related to a

Table 5-18. Enthalpy-entropy compensation parameters on the C-2, C-4, and C-8 (at three β levels) stationary phases in an acetronitrile/water eluent system via the four-parameter compensation model, Eqn. (3-58).

RPLC Phase	$\beta(°K)^{a}$	α^{b}	ψ^{b}	$\Delta H^{o}_{n}(0)$ (kcal/mol)[c]
C-2	625	-2.95 ± 0.11	2.18 ± 0.18	-5.13 ± 0.10
C-4	625	-2.99 ± 0.15	2.16 ± 0.14	-3.24 ± 0.34
C-8	525	-2.47 ± 0.11	1.50 ± 0.02	-2.12 ± 0.50
C-8	625	-2.41 ± 0.11	1.46 ± 0.04	-2.10 ± 0.40
C-8	725	-2.38 ± 0.12	1.44 ± 0.02	-2.11 ± 0.35

[a]Compensation temperature.

[b]Mean value $\pm$ 95% confidence limits.

[c]Mean value $\pm$ 95% confidence limits. A plot of $\Delta H^{o}_{n}(0)$ vs. RPLC chain length at β of 625°K produces

$$n = 3,\ R = 0.9513$$
$$\text{Slope} = 0.475 \pm 1.96$$
$$\text{Intercept} = -5.72 \pm 10.36$$

Table 5-19. Enthalpy-entropy compensation parameters on the C-2, C-4, and C-8 stationary phases in an acetonitrile/water eluent system via the three-parameter compensation model, Eqn. (3-57).

RLC Phase	$\beta(°K)$[a]	α[b]	$\Delta H^{o}_{n}(0)$ (kcal/mol)[c]
C-2	625	-1.89 ± 0.08	-2.17 ± 0.26
C-4	625	-1.77 ± 0.08	-1.95 ± 0.28
C-8	625	-1.57 ± 0.17	-1.32 ± 0.76

[a] Compensation temperature.

[b] Mean value $\pm$ 95% confidence limits.

[c] Mean value $\pm$ 95% confidence limits. A plot of $\Delta H^{o}_{n}(0)$ vs. RPLC chain length at β of 625°K produces

$$n = 3,\ R = 0.9967$$
$$\text{Slope} = 0.144 \pm 0.149$$
$$\text{Intercept} = -2.49 \pm 0.79$$

slight increase in the hydrophobicity of the sorbent surface as the RPLC chain length is increased. In a manner similar to that observed in the methanol/water RPLC systems, the noncompensated portion of the standard enthalpy change in 100% water, $\Delta H^{o}_{n}(0)$, increases with the RPLC chain length. The linear regression information for $\Delta H^{o}_{n}(0)$ vs. RPLC chain length is given in Table 5-18 for the four-parameter model in acetonitrile/water eluents.

The constants $\Delta H^{o}_{n}(0)$ and α for the three-parameter compensation model are listed in Table 5-19 for the C-2, C-4, and C-8 supports in the acetonitrile/water eluent system. Data presented in Tables 5-16 and 5-18 indicate that the value of the RPLC compensation temperature (β) is not integral to the determination of these model parameters. Therefore, the β value of 625°K (Melander et al., 1979) was applied. The solvent parameter α showed a small increase with RPLC chain length that may be attributed to the increasing hydrophobicity of the alkyl surface. This change was noted earlier in the methanol/water RPLC systems (Table 5-16) and for the four-parameter compensation model applied to acetonitrile/water systems. The small change observed is not significant for the successful application of the compensation model. The $\Delta H^{o}_{n}(0)$ values increase steadily with RPLC chain length, and the rate of increase in acetonitrile/water (Table 5-19) is similar to the increase noted in methanol/water eluents (Table 5-16), approximately

0.15 kcal/mole per RPLC carbon atom for the three-parameter model.

As in the methanol/water RPLC sytems, the compensation regression parameters A_1, A_2, A_3, and A_4 are related to solute structure, as expressed by HSA. Separate linear regression lines of the "A" parameters vs. solute HSA were developed for the alkylbenzenes and the PAHs/halobenzenes. The linear regression equations developed between A_1, A_2, A_3, and A_4 vs. HSA are listed in Table 5-20 for the C-8, acetonitrile/water system. Similar expressions may be derived for any acetonitrile/water RPLC system using either the three- or four-parameter compensation model.

In summarizing the application of the compensation model to acetonitrile/water RPLC systems, the four-parameter model does not offer a significant improvement over the three-parameter model in the fit of solute retention data to eluent composition and temperature. The regression parameters (A_1, A_2, A_3, and A_4) may be correlated with solute HSA, and separate regression lines exist for the alkylbenzenes and the PAH/halobenzene compounds. The solvent parameters (α and Ψ) show a small degree of dependence on RPLC chain length. The $\Delta H^o_n(0)$ values increase substantially with stationary phase chain length, and the rate of increase is similar to that noted for methanol/water RPLC systems. In view of the small decrease in error but considerable increase in complexity and data

Table 5-20. Linear regression of the compensation parameters A_1, A_2, A_3, and A_4 vs. solute HSA for the alkylbenzenes and the PAH, benzene, and halobenzene compounds on C-8 material in acetonitrile/water at a β of 625°K.

Parameter	Parameter vs. HSA for the PAHs, benzene, and halobenzenes*	Parameter vs. HSA for the alkylbenzenes*
A_1	n = 12, R = 0.9956	n = 9, R = 0.9900
	Slope = 0.102 ± 0.007	Slope = 0.147 ± 0.019
	Intercept = -1.40 ± 1.18	Intercept = -7.79 ± 3.08
A_2	n = 12, R = 0.9965	n = 9, R = 0.9875
	Slope = 27.67 ± 1.63	Slope = 36.32 ± 5.18
	Intercept = 552.0 ± 286.1	Intercept = -783.4 ± 855.8
A_3	n = 12, R = -0.9932	n = 9, R = -0.9870
	Slope = -0.039 ± 0.003	Slope = -0.044 ± 0.008
	Intercept = -2.53 ± 0.56	Intercept = -1.17 ± 1.37
A_4	n = 12, R = -0.9942	n = 9, R = -0.9873
	Slope = -0.062 ± 0.005	Slope = -0.089 ± 0.013
	Intercept = 2.97 ± 0.83	Intercept = 6.88 ± 2.11

*n is the number of data points; R is the correlation coefficient; slope and intercept values represent mean values ± 95% confidence limits.

collection, the three-parameter compensation model is recommended for general use in acetonitrile/water RPLC systems.

Summarizing the application of the enthalpy-entropy compensation model for RPLC binary systems of methanol or acetonitrile in water, the three-parameter model allows excellent correlation of solute retention factors to eluent composition and temperature. Partial compensation of the standard sorptive enthalpy change occurs in both methanol and acetonitrile systems, and the noncompensated portion of the sorptive enthalpy change increases in magnitude with increasing RPLC chain length. The solvent parameter α increases very slightly with stationary phase chain length, perhaps reflecting an increasing hydrophobicity of the RPLC surface as the sorbent's alkyl chain is lengthened. The RPLC compensation temperature used in these studies was 625°K (Melander et al., 1979), although deviations of $\pm$100°K have little influence upon the calculated model constants. The compensation regression parameters (A_1, A_2, and A_3) are linear functions of solute HSA, with separate correlations for the alkylbenzenes and the PAH, benzene, and halobenzene compounds. The distinct thermodynamic behavior of the alkylbenzenes compared to the PAHs/halobenzenes agrees with previous results of this chapter which indicated that these compounds differed in their mechanisms of hydrophobic retention.

5.6 Equilibrium Studies with RPLC Materials

The study of sorption thermodynamics implicitly assumes that an equilibrium condition exists between the sorbed and solution phases of the solute of interest. Two experiments were performed to test this assumption: one involved the measurement of the solute retention factor (k') as a function of RPLC column flow rate; the other determined batch equilibrium sorption coefficients on RPLC material and compared these values to the same coefficients determined in column experiments. The discussion of these experiments begins with the variation of k' with column flow rate.

The solute retention factor for pyrene was examined as a function of column flow rate for the C-8, 60/40 acetonitrile/water system. The k' of pyrene at 298°K was measured at flow rates of 0.10, 0.25, 0.50, and 1.00 mL/minute. If solution-phase kinetics are a limiting factor to reaching equilibrium, one would expect the k' value to increase as the flow rate is decreased. The k' data for the flow rate studies shown in Table 5-21 indicate that kinetic limitations are not present for the RPLC systems with flow rates of up to 1.00 mL/minute. These results suggest that the thermodynamic parameters under study for the RPLC systems (ΔH^{o}_{sorp}, ΔS^{o}_{sorp}, and ln k') were measured under equilibrium conditions.

The second series of experiments involved the measurement of solute k' values in batch RPLC systems to insure

Table 5-21. Study of the solute retention factor, k', of pyrene as a function of column flow rate on the C-8 material with a 60/40 acetonitrile/water eluent system at 298°K.

Flow rate (mL/min)	t_o (min)	t_{pyrene}(min)	k'_{pyrene}
1.00	0.51	3.77	6.39
0.50	1.03	7.47	6.25
0.25	2.06	15.01	6.29
0.10	5.15	37.50	6.28

RPLC Conditions: C-8 column, 5 cm.
60/40 acetonitrile/water eluent system
UV detector, 254 nm.
Pyrene at 29 mg/L in methanol, 25 µL injection loop.
Void volume measured with 25 g/L $NaNO_3$ in 60/40 acetonitrile/water solvent.
Temperature = 25°C.

determination of equilibrium sorption coefficients. All batch studies were performed at 22 $\pm$ 3°C and sorbent/ solution mixtures were shaken for 24 hours prior to analysis to allow equilibration to occur. The batch k' values were then compared to column k' values from RPLC column studies and examined for indications of kinetic processes involving solute sorption in RPLC column experiments. The batch systems studied were pyrene dissolved in 60/40 and 50/50 acetonitrile/water with C-8 RPLC material and biphenyl with C-8 material in a 50/50 acetonitrile/water solvent system. The details of the experimental design were given earlier in Chapter IV, Section 4.8.4.

The results of the batch and column k' experiments are listed in Table 5-22 for pyrene and biphenyl sorbed to C-8 RPLC materials in acetonitrile/water eluents. The data show good agreement between the batch and column determination of the solute retention factor, k'. The linear form of the Freundlich sorption constant (Eqn. 4-2) was employed in the batch studies as linear sorption isotherms are believed to operate in RPLC systems (Snyder and Kirkland, 1979), and the observed nonlinearity was minor (the exponential term, N, of Eqn. 4-2 was 0.80 to 1.24). The agreement of batch and column k' values is another indication that kinetic processes are not limiting factors in thermodynamic retention studies for RPLC column systems. Therefore, the

Table 5-22. Comparison of solute retention factors (k') of pyrene and biphenyl from batch and column acetonitrile/water RPLC systems at 298°K.

RPLC Phase	Solute	Acetonitrile/water (v/v) mixture	Linear Freundlich K (cm^3/g)[a]	k'_{batch}[b]	k'_{column}[b]
C-8	Pyrene	50/50	21.52 ± 3.30	15.49 ± 2.38	14.40 ± 0.14
C-8	Pyrene	60/40	8.98 ± 1.49	6.46 ± 1.07	5.24 ± 0.05
C-8	Biphenyl	50/50	10.77 ± 4.20	7.75 ± 3.02	7.89 ± 0.08

[a]Linear Freundlich K values (cm^3/g) converted to unitless k'_{batch} using column void volume (0.50 cm^3) and mass of C-8 material in column (0.360 g): k'_{batch} = K(0.360/0.50). Linear K values represent mean values ± 95% confidence limits.

[b]Mean value ± 95% confidence limits.

thermodynamic parameters measured in the course of this work were determined under equilibrium conditions.

5.7 Solvophobic Model of RPLC Retention

The solvophobic model describing the RPLC retention of hydrophobic compounds (Horvath et al., 1976) was extensively reviewed in Chapter III, Section 3.3. This theory was used to interpret the thermodynamics and mechanisms of solute retention on hydrophobic surfaces. As was discussed previously, the final form of the solvophobic equation (Eqn. 3-38) may be used to describe solute retention in terms of solvent properties such as molar volume (V), surface tension (γ), and the modified dielectric constant (Γ).

$$\ln k' - D(K^{e} - 1)V^{2/3}\gamma - \ln(RT/P_{o}V) = (A + E) + B\Gamma + C\gamma$$

This form of the solvophobic model was used by Wells and Clark (1982) and Wells et al. (1982) to study the mechanism for retention of n-alkylbenzamides on C-18 material in acetonitrile/water mixtures.

The above form of the solvophobic model was applied to the C-2, C-4, C-8, and C-18 acetonitrile/water systems at 298°K for the hydrophobic solutes under study. This application of the equation involved retention data (Appendix A) and physicochemical data (Appendix G). The left side of

Eqn. (3-38) was linearly regressed vs. Γ and γ for each hydrophobic solute, allowing the calculation of the regression parameters (A + E), B, and C. The regression parameters and correlation coefficient for each solute-ligand combination are tabulated in Appendix H.

The work of Wells (1981) indicated that Eqn. (3-38) was applicable to RPLC supports in acetonitrile/water eluents and that methanol/water eluent systems gave irregular results. Similar findings were noted for the RPLC systems under study, and only the correlations for acetonitrile/ water eluents are reported in Appendix H.

The (A + E) term of Eqn. (3-38) denotes the sum of the van der Waals solute-ligand interactions in the idealized gas phase and the solute-solvent interactions in the liquid phase (see Eqns. 3-33 and 3-37). The B term is an expression involving the molecular volume of the solute, v_s, and the proportionality constant (λ) relating the molecular volume of the solute-ligand complex, v_{sl}, and v_s (see Eqn. 3-34). Wells and Clark (1982) and Wells et al. (1982) plotted B vs. (A + E) as a means of studying RPLC retention mechanisms. These plots relate the molecular volume of the solute and solute-ligand complex to the total free energy change for van der Waals solute interactions.

A plot of B vs. (A + E) for the hydrophobic solutes in the C-2, acetonitrile/water system at 298°K is shown in Figure 5-41. All the solutes fall on a single linear

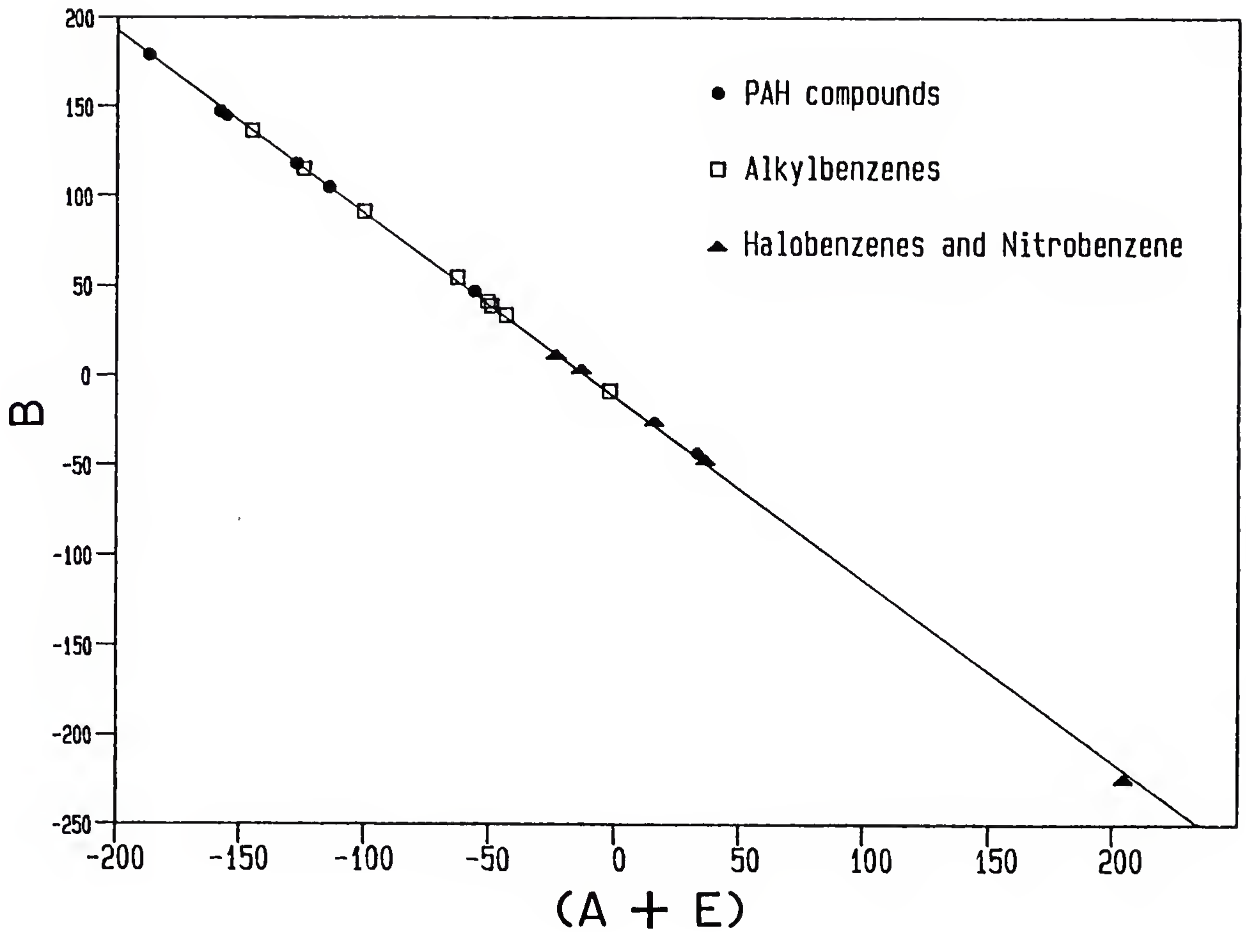

Figure 5-41. B vs. (A + E) from the solvophobic model applied to sorption of the hydrophobic solutes on C-2 material in acetonitrile/water eluents at 298°K.

regression line for B vs. (A + E). This indicates that the solutes undergo similar solute-ligand and solute-solvent interactions relative to the molecular volume of the solute and solute-ligand complex.

A similar B vs. (A + E) plot is shown in Figure 5-42 for the C-4, acetonitrile/water sytem at 298°K. A single linear regression line provides an excellent correlation for all solutes, with the exception of n-hexylbenzene. It is not known if the behavior of n-hexylbenzene is due to an actual change in retention interactions or merely a statistical variation.

The B vs. (A + E) plot for the hydrophobic solutes in the C-8, acetonitrile/water system is shown in Figure 5-43, where two linear regression lines were drawn through he retention data. The regression line for most of the compounds is unchanged from the C-2 and C-4 plots, while the second line relates B and (A + E) for the solutes phenanthrene, anthracene, pyrene, fluoranthene, chrysene, n-butylbenzene, and n-hexylbenzene. The increase in RPLC chain length has caused a change in the molecular volume of the solute-ligand complex relative to solute van der Waals interactions for solutes with larger HSA values and greater hydrophobicity.

The final B vs. (A + E) plot is shown in Figure 5-44 for the solutes in the C-18, acetonitrile/water system. The compounds have separated on the basis of chemical class, and

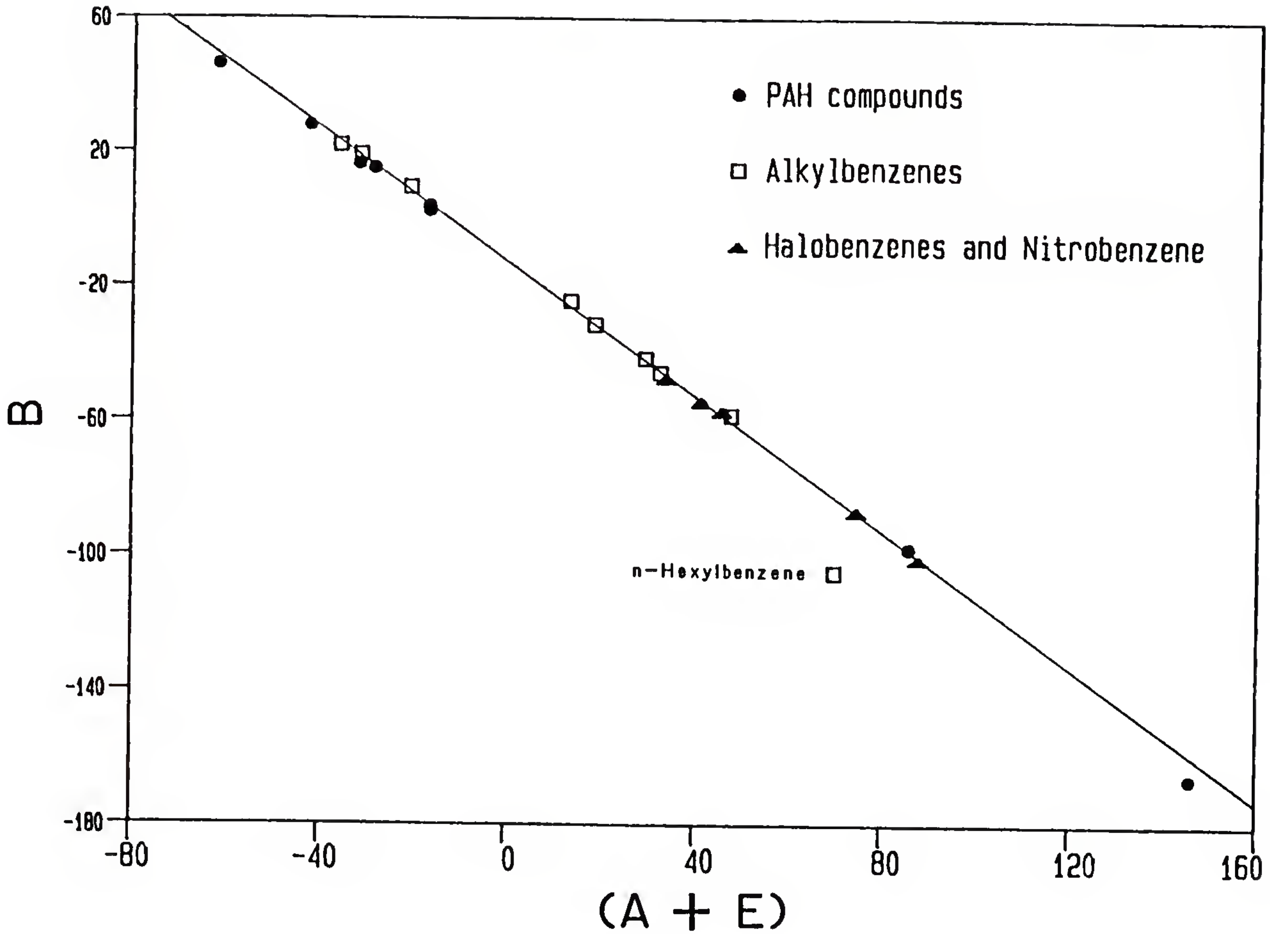

Figure 5-42. B vs. (A + E) from the solvophobic model applied to sorption of the hydrophobic solutes on C-4 material in acetonitrile/water eluents at 298°K.

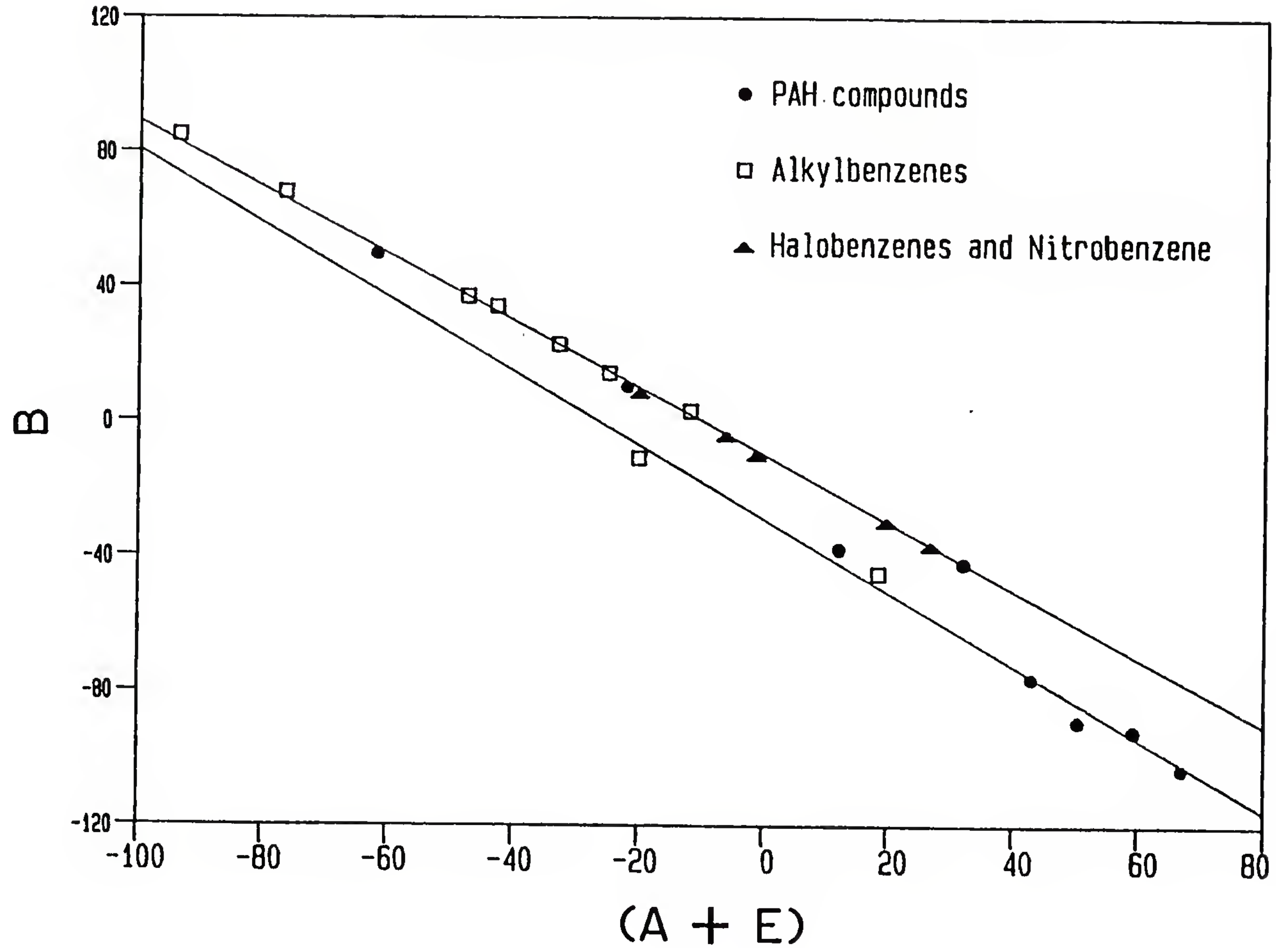

Figure 5-43. B vs. (A + E) from the solvophobic model applied to sorption of the hydrophobic solutes on C-8 material in acetonitrile/water eluents at 298°K.

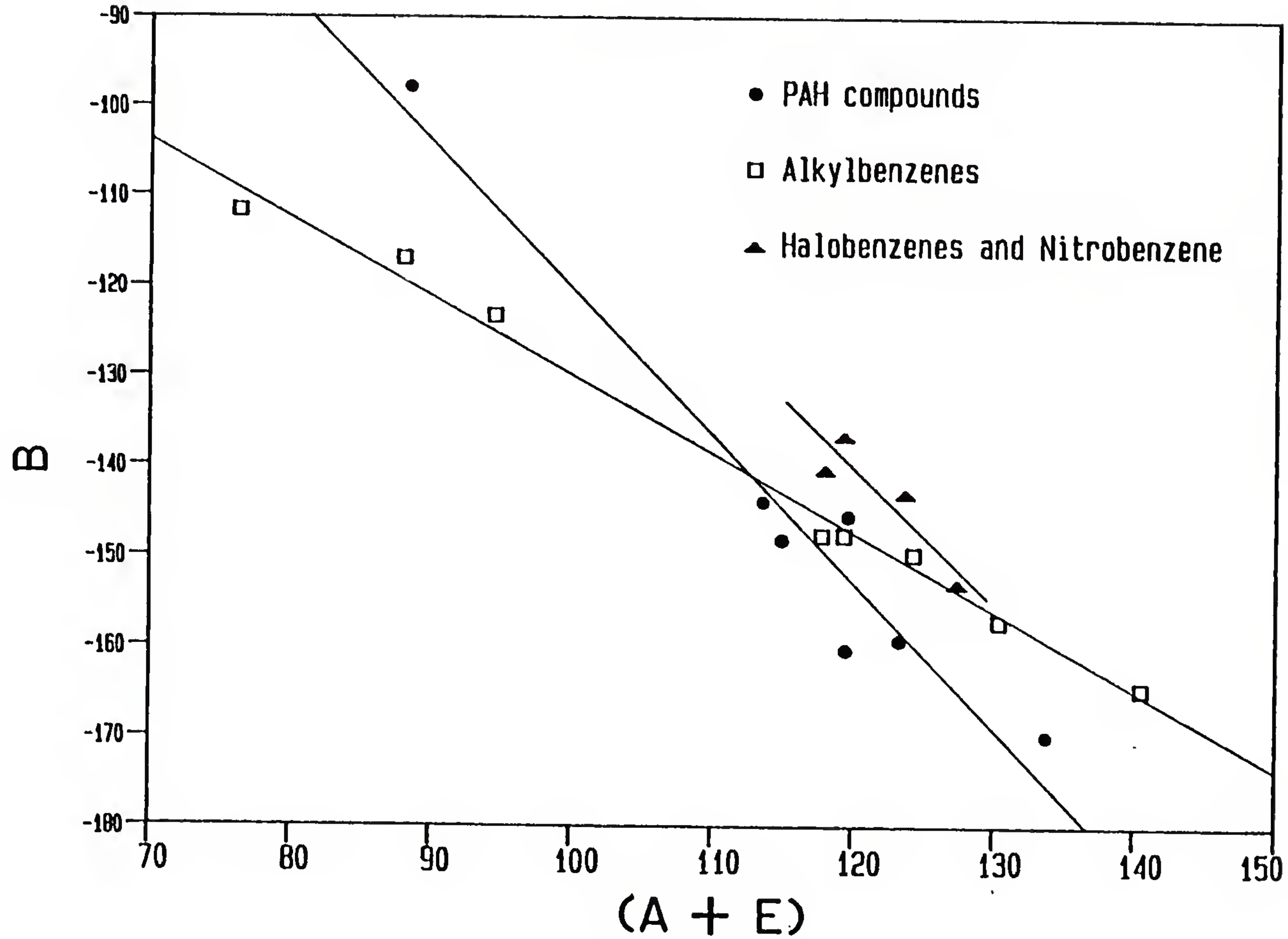

Figure 5-44. B vs. (A + E) from the solvophobic model applied to sorption of the hydrophobic solutes on C-18 material in acetonitrile/water eluents at 298°K.

three linear regression lines are drawn through the retention data: one for the alkylbenzenes, one for the substituted benzenes, and one for the PAH compounds and benzene. It appears that the increase in RPLC chain length has allowed greater differentiation of the relationship of solute-ligand molecular volume to the total free energy change of the solute van der Waals interactions.

The collected regression data for the C-2, C-4, C-8, and C-18 acetonitrile/water systems appear in Table 5-23. As noted in the table and in Figures 5-41 to 5-44, an increase in RPLC chain length produces a gradual change in solute behavior between the three classes of compounds under study. Since only the RPLC chain length was varied, the observed behavior cannot be explained by conformational changes in the solute molecules. The explanation must lie, therefore, in the changing nature of the solute-ligand interactions.

Berendsen and DeGalan (1980) have proposed the concept of a "critical chain length," which suggests that a solute molecule interacts with only a certain part of the bonded n-alkyl chains. The authors noted that the solute retention factor increased exponentially with RPLC chain length up to a certain, "critical" chain length, after which it remains essentially constant. The value of the critical chain length was independent of solution composition and increased with the size of the solute molecule.

Table 5-23. Linear regression of B vs. (A + E) model constants of the solvophobic theory for the hydrophobic solutes in C-2, C-4, C-8, and C-18 acetonitrile/water systems at 298°K.

RPLC Phase	B vs. (A + E)[a] Line #1	B vs. (A + E)[a] Line #2	B vs. (A + E)[a] Line #3
C-2	$n = 20$, $R = -0.9998$ Slope $= -1.02 \pm 0.01$ Intercept $= 11.89 \pm 1.00$	-------	-------
C-4	$n = 21$, $R = -0.9993$ Slope $= -1.00 \pm 0.02$ Intercept $= -13.55 \pm 0.99$	-------	-------
C-8	$n = 15$, $R = -0.9997$ Slope $= -1.00 \pm 0.02$ Intercept $= -10.37 \pm 0.65$	$n = 7$, $R = 0.9942$[b] Slope $= -1.09 \pm 0.14$ Intercept $= -29.07 \pm 5.89$	-------
C-18	$n = 8$, $R = -0.9950$[c] Slope $= -0.89 \pm 0.09$ Intercept $= -42.30 \pm 9.94$	$n = 7$, $R = -0.9730$[d] Slope $= -1.63 \pm 0.44$ Intercept $= 42.35 \pm 52.0$	$n = 4$, $R = 0.9020$[e] Slope $= 1.52 \pm 2.21$ Intercept $= 42.58 \pm 270.0$

[a] n is the number of data points; R is the correlation coefficient; slope and intercept values represent mean values $\pm$ 95% confidence limits.

[b] Data for the solutes phenanthrene, anthracene, pyrene, fluoranthene, chrysene, n-butylbenzene, and n-hexylbenzene.

[c] Data for the alkylbenzene compounds.

[d] Data for the PAH compounds and benzene.

[e] Data for the halobenzene compounds and nitrobenzene (except chlorobenzene).

The findings of Berendsen and DeGalan (1980) suggest that on short RPLC chains (C-2, C-4) hydrophobic solutes of various HSA values can penetrate the alkyl chains to only a limited extent. The larger molecules possess greater contact surface areas (ΔA), so they show stronger solute retention. If the chain length is increased, smaller solute molecules fully penetrate into the stationary phase, while larger molecules are still not totally encompassed by the alkyl chains. As the RPLC chain length is further increased, solutes of lower HSA do not exhibit greater penetration into the RPLC surface. Consequently, their retention with increasing chain length is unchanged, and they will show a lower critical carbon number. Solutes with larger HSA values need longer RPLC chains to become fully enclosed, and hence the critical carbon number is greater for these compounds.

In their work on solute-ligand interactions, Berendsen and DeGalan (1980) empirically defined the critical carbon number as the intercept of two tangent lines drawn on a ln k' vs. RPLC chain length retention curve. One tangent defines the initial rate of increase of solute retention with RPLC carbon number, while the second line is tangent to the plateau in solute sorption that occurs at elevated RPLC chain length values. A plot of ln k' vs. RPLC chain length is shown in Figure 5-45 for five compounds in 50/50 acetonitrile/water at 298°K. As noted in Figure 5-45, the

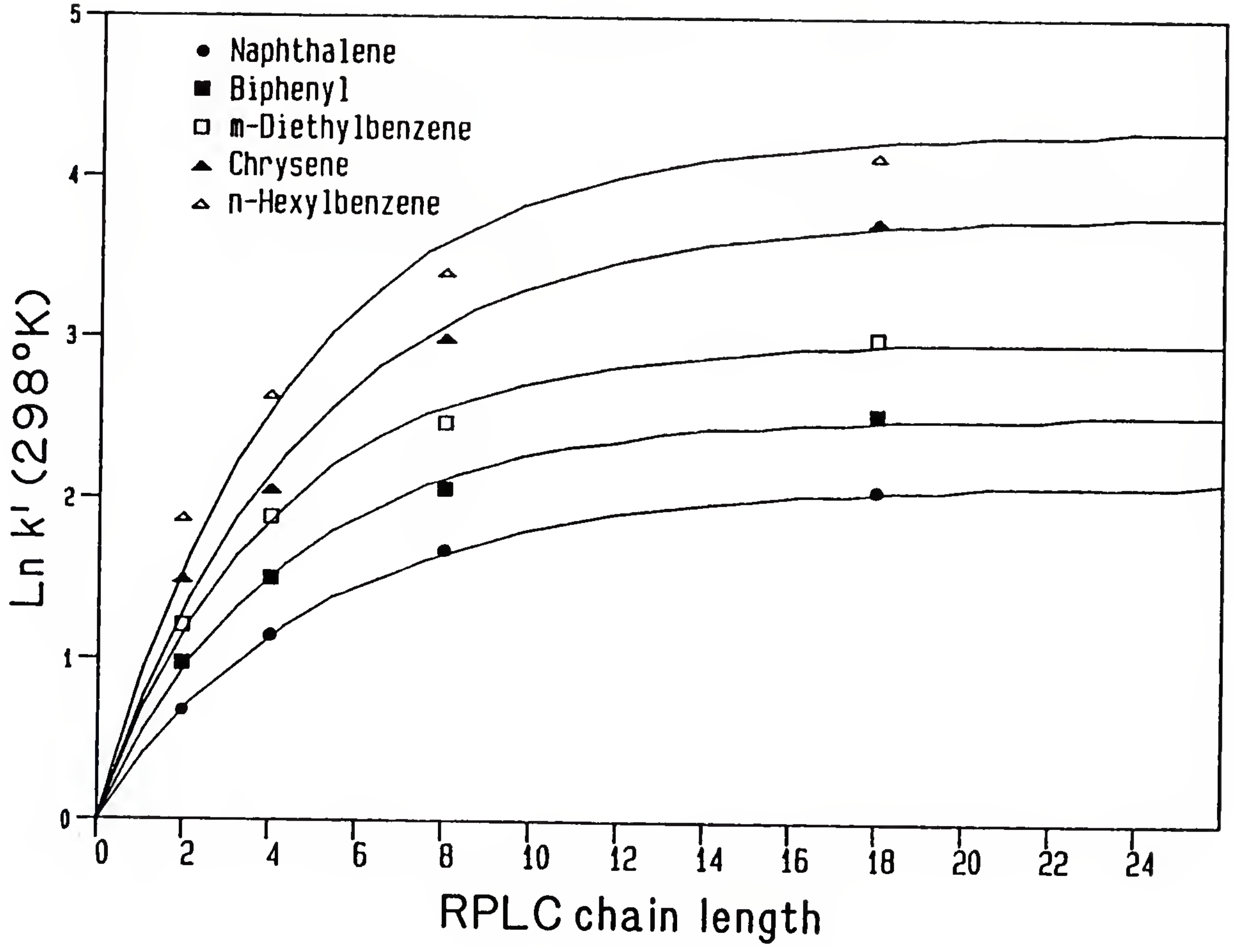

Figure 5-45. Ln k' vs. RPLC chain length for five hydrophobic solutes in 50/50 acetonitrile/water at 298°K.

RPLC carbon number at which the retention curve breaks into a plateau increases with the size and hydrophobicity of the solute molecule. These data are in general agreement with the critical carbon number retention theory of Berendsen and DeGalan (1980), which indicated that larger solutes need longer RPLC alkyl chains to become fully enclosed.

To properly evaluate the critical carbon number theory, a mathematical equation was analytically fitted to the ln k' vs. RPLC chain length data for the hydrophobic compounds. The following equation provides an excellent fit to the experimental data

$$Y = B[1 - \exp(-AX)] \tag{5-6}$$

where Y and X are the ln k' and RPLC carbon number values, respectively, and B is the maximum ln k' value for a given solute calculated from Eqn. (5-6).

Equation (5-6) was applied to the retention data of the hydrophobic solutes on the C-2, C-4, C-8, and C-18 supports in a 50/50 acetonitrile/water mobile phase at 298°K. The calculated regression parameters (A and B), the correlation coefficient, and the calculated critical carbon number (x_c) appear in Table 5-24 for each of the hydrophobic solutes. The critical carbon numbers were calculated using the retention maximum B and the ln k' data on the C-2 and C-4

Table 5-24. Regression parameters for fit of ln k' vs. RPLC chain length according to the equation $Y = B[1 - \exp(-AX)]$, where Y and X are the ln k' and RPLC carbon number values, respectively. The calculated critical carbon number (x_c) is also shown for each solute.

Compound[a]	A[b]	B[b]	R[c]	x_c[d]
Biphenyl	0.228	2.53	0.9998	7.8
Naphthalene	0.192	2.12	0.9999	8.0
Phenanthrene	0.207	2.90	0.9997	8.9
Anthracene	0.208	3.01	0.9997	8.8
Pyrene	0.198	3.39	0.9996	9.6
Chrysene	0.210	3.78	0.9991	10.0
Fluoranthene	0.243	3.03	0.9994	8.5
Benzene	0.138	1.36	0.9956	7.6
Toluene	0.172	1.79	0.9995	7.7
Ethylbenzene	0.205	2.18	0.9999	7.5
n-Propylbenzene	0.230	2.65	0.9997	7.6
n-Butylbenzene	0.249	3.10	0.9993	10.7
n-Hexylbenzene	0.225	4.30	0.9989	8.5
p-Xylene	0.193	2.22	0.9999	7.8
o-Xylene	0.190	2.13	0.9999	7.8
m-Diethylbenzene	0.244	2.99	0.9997	7.4
1,2,4-Trimethylbenzene	0.212	2.58	0.9997	8.2
Fluorobenzene	0.157	1.35	0.9972	7.4
Chlorobenzene	0.154	1.92	0.9995	8.4
Bromobenzene	0.178	1.92	0.9997	7.9
Iodobenzene	0.184	2.15	0.9999	8.0
Nitrobenzene	0.129	1.09	0.9991	7.8

[a]Eluent system was 50/50 acetonitrile/water at 298°K.

[b]Mean value

[c]Correlation coefficient

[d]Critical carbon number, calculated using the regression parameter B and the C-2 and C-4 ln k' data at 298°K.

supports to define the initial rate of solute retention with increasing RPLC carbon number.

The calculated values of the critical carbon number in Table 5-24 are in general agreement with the retention theory of Berendsen and DeGalan (1980). Although the x_c values do not increase sequentially with solute HSA, the larger HSA solutes generally require longer alkyl chains for full interaction, i.e., they have greater critical carbon number values. Considering solute behavior on the C-8 support (Figure 5-43), the seven compounds diverging from the main regression line (phenanthrene, anthracene, pyrene, fluoranthene, chrysene, n-butylbenzene, and n-hexylbenzene) all have x_c values greater than 8.0. Conversely, the solutes on the primary regression line generally have critical carbon numbers of 8.0 or less. The distinct solute-ligand interactions on the C-18 support cannot be explained at present by the retention theory of Berendsen and DeGalan (1980).

Although the critical carbon number theory of Berendsen and DeGalan (1980) does not fully explain the observed ligand effects on solute behavior, it does represent an attempt to understand the change in solute-ligand interactions as the RPLC chain length is increased. The solvophobic model (Eqn. 3-38) may also prove useful in this regard. The regression parameter "C," from the application of the solvophobic model to acetonitrile/water retention

data (Appendix H), may be used to calculate the solute-ligand contact area (ΔA) for a given solute-ligand combination. Recall Eqn. (3-35) from Chapter III, Section 3.3.

$$C = N \, \Delta A/RT$$

where N is Avogadro's number, ΔA is the solute-ligand contact area, R is the universal gas constant, and T is the absolute temperature. The collected ΔA values are listed in Table 5-25 for each hydrophobic solute on the C-2, C-4, C-8, and C-18 stationary phases in acetonitrile/water.

Although the ΔA values of Table 5-25 may not be explicitly accurate, an examination of their trends does prove enlightening. The ΔA values generally increase with solute HSA on a given RPLC support, as expected from solvophobic theory. For most of the hydrophobic solutes, the contact area values remain fairly constant with RPLC chain length until a sharp increase occurs with the C-18 support. For the seven divergent solutes of Figure 5-43, however, the increase in ΔA occurs on the C-8 stationary phase. The reason for this behavior is not clear, but it may be due to the critical carbon number effects discussed previously. The divergent solutes have larger HSA values and may require longer RPLC chains (C-8 and above) for complete interaction. The remaining solutes have smaller HSA values and may

Table 5-25. Contact areas of solute-ligand interaction calculated from the solvophobic model (Eqn. 3-35 and Appendix H) at 298°K.

	Contact Area (Å^2)* on RPLC Support			
Compound	C-2	C-4	C-8	C-18
Biphenyl	45	70	77	258
Naphthalene	30	99	50	189
Phenanthrene	57	92	301	333
Anthracene	47	88	228	305
Pyrene	69	107	346	337
Chrysene	--	131	397	---
Fluoranthene	69	99	332	413
Benzene	0	8	-1	-20
Toluene	12	16	6	159
Ethylbenzene	22	31	25	---
n-Propylbenzene	33	48	45	254
n-Butylbenzene	52	82	235	255
n-Hexylbenzene	--	351	329	362
o-Xylene	19	38	24	206
p-Xylene	15	41	38	182
m-Diethylbenzene	40	67	60	251
1,2,4-Trimethyl-benzene	40	60	51	231
Fluorobenzene	6	14	7	88
Chlorobenzene	10	21	24	---
Bromobenzene	21	30	28	140
Iodobenzene	70	40	39	189
Nitrobenzene	7	11	5	64

*Contact areas calculated from the regression parameter "C" of the solvophobic model:

$$\Delta A(\text{Å}^2) = \frac{C\times10^{16}(1.01325\times10^{6}\ \text{dynes/cm}^2)(82.06\ \text{cm}^3\text{-atm/mole-°K})(298\text{°K})}{6.023\times10^{23}\ \text{molecules/mole}}$$

Refer to Eqn. (3-35) and Appendix H for details.

interact fully with shorter RPLC chains and, therefore, demonstrate approximately constant ΔA values on the C-2, C-4, and C-8 supports. This retention theory does not explain, however, the increase in ΔA noted for the smaller solutes on the C-18 stationary phase.

One final statement concerns the solvophobic model and its useful application for understanding solute retention on hydrophobic surfaces. Earlier, in Section 5.5, it was noted that nitrobenzene exhibited stronger retention on RPLC surfaces than was expected given its HSA value and hydrophobic nature. This behavior was attributed to polar interactions of the nitro moiety with available silanol groups, and this compound was excluded from analysis of the thermodynamic and enthalpy-entropy compensation data. Nitrobenzene has been included, however, in the application of the solvophobic model (Eqn. 3-38) to acetonitrile/water RPLC systems, and its behavior correlates well with that of the other hydrophobic solutes. The reason for this is not currently known, but it may be due to the fact that the solvophobic model treats the modified dielectric constant of the solvent, Γ, as one of its regression variables. The solvophobic model is therefore capable of examining the retention of moderately polar solutes, as well as the hydrophobic solutes discussed previously. These results are supported by the work of Wells and Clark (1982) and Wells et al. (1982).

In summary, application of the solvophobic model of Horvath et al. (1976) to acetonitrile/water RPLC systems produces an excellent linear regression of ln k' vs. the solvent parameters γ and Γ for the hydrophobic solutes under study. Additionally, the model offers considerable insight into the variable nature of solute-ligand interactions. These interactions are approximately constant on the shorter C-2 and C-4 supports, but longer RPLC chains allow for differentiation on the basis of solute size and chemical class. These observations are supported by calculated solute-ligand contact areas, ΔA. The reason for the variable solute-ligand interactions is not clear, but it appears to be related to the critical carbon number theory of Berendsen and DeGalan (1980). This theory explains solute-ligand interactions based on the concept of solute penetration of the RPLC support.

CHAPTER VI
SUMMARY AND CONCLUSIONS

Reversed-phase liquid chromatography (RPLC) was used to study the thermodynamics and mechanisms of sorption for hydrophobic organic solutes retained on nonpolar RPLC and soil surfaces in polar solvent mixtures. Enthalpy-entropy compensation effects for a methanol/water mixture of three PAH solutes retained on a carbonaceous surface soil were identical to those measured for the PAH compounds in a methanol/water RPLC system. Therefore, the mechanism of retention was the same in these two systems; a similarity in retention mechanisms for hydrophobic solutes on RPLC and soil materials has not been previously reported in the literature. This finding should facilitate the study of sorption mechanisms for solutes transported in the soil or groundwater environment.

The standard sorptive enthalpy and entropy changes, ΔH^{o}_{sorp} and ΔS^{o}_{sorp}, respectively, were found to be linear functions of the eluent composition in methanol/water RPLC systems. Similar findings for methanol/water mobile phases were reported by Sander and Field (1980). These thermodynamic parameters were also linearly related to the hydrocarbonaceous surface area (HSA) of the solute

molecules. Hirata and Sumiya (1983) and Hornsby and Rao (1983) reported similar correlations between ΔH^{o}_{sorp} and solute size. In the methanol/water RPLC systems, different retention mechanisms were found to exist for the alkylbenzenes compared with the PAH and halobenzene compounds. The individual retention mechanisms were not affected by the methanol composition of the eluent. The energetically distinct retention behavior of alkylbenzenes from PAH and halobenzene compounds was related to differences in the standard sorptive entropy changes for these two groups of chemicals. The occurrence of distinct retention mechanisms for two groups of hydrophobic compounds on RPLC material has not been previously reported in the literature.

In acetonitrile/water RPLC sytems, ΔH^{o}_{sorp} and ΔS^{o}_{sorp} remained as linear functions of solute HSA, but unlike the methanol/water systems, the ΔS^{o}_{sorp} vs. HSA correlations were affected substantially by eluent composition. As acetonitrile content was increased, entropic effects assumed greater importance in controlling solute retention. The distinct retention mechanisms of the alkylbenzenes and the PAH/halobenzene compounds were noted in acetonitrile/water RPLC systems and were again related to differences in entropic behavior. As retention mechanisms are closely tied to sorption thermodyamics, the retention mechanism showed considerable variation with the acetonitrile composition of the mobile phase. Similar results were reported by Laub and

Madden (1985) concerning the solvent-dependent mechanism of retention for substituted phenols on C-18 material in tetrahydrofuran/water mixtures. It is clear, then, that retention interactions in acetonitrile/water RPLC systems are far more complex than originally assumed.

The solvophobic theory of Horvath et al. (1976) is generally regarded as an excellent model for describing hydrophobic interactions on RPLC surfaces (Berendsen and DeGalan, 1980; Wells and Clark, 1982). However, little work has been done concerning the application of the solvophobic model equation (Eqn. 3-38) to solute retention on RPLC stationary phases of various lengths. It was found in this work that the solvophobic model provides a useful technique for examining solute-ligand interactions as a function of RPLC chain length. The relationship of the solute-ligand molecular volume to the total solute van der Waals interactions remained constant on the shorter C-2 and C-4 RPLC supports. As the RPLC chain length was increased to C-8 and C-18, differentiation of solute behavior was observed on the basis of chemical class. The reason for this behavior is not clear, but it appears to be related to solute size and the ease of penetration of the RPLC support.

From the experimental and theoretical work performed for this dissertation, the following conclusions were reached:

(1) Solute retention data, expressed as ln k', were linearly correlated with solute descriptors such as the HSA, log K_{ow}, and the first-order molecular connectivity index (^1X), in methanol/water and acetonitrile/water RPLC systems with C-2, C-4, and C-8 stationary phases. These results indicate that solute hydrophobicity, size, and shape all play an important role in determining the retention of hydrophobic solutes on nonpolar surfaces. Differences in solute retention as a function of solute descriptor were present between the alkylbenzene solutes and the PAH and halobenzene compounds.

(2) The natural logarithm of the solute retention factor, ln k', was a linear function of methanol content (θ) on all three RPLC supports. In acetonitrile/water RPLC systems, the curvilinear response of ln k' to eluent composition required the use of a quadratic expression relating ln k' to θ_{ACN} for the solutes under study. These relationships were applied to the three- and four-parameter compensation equations modeling ln k' as a function of eluent composition (θ) and absolute temperature (T).

(3) The ΔH^o_{sorp} and ΔS^o_{sorp} values in methanol/water RPLC systems decreased as the water content of the mobile phase was increased. This indicates that as water is added to the methanol/water eluent, a more exothermic enthalpy change occurs, along with greater ordering of solute molecules on the RPLC stationary phase. Similar linear

results were noted for plots of ΔH^{o}_{sorp} vs. acetonitrile solution content by volume.

(4) In methanol/water and acetonitrile/water RPLC systems, a single linear regression line described the correlation of ΔH^{o}_{sorp} vs. solute HSA. The ΔH^{o}_{sorp} values in a given RPLC system decreased as HSA increased, indicating more exothermic sorptive enthalpy changes for the larger, more hydrophobic solutes.

(5) The ΔS^{o}_{sorp} values of the alkylbenzenes and the PAH/halobenzene compounds formed separate linear regression lines with solute HSA in methanol/water and acetonitrile/water RPLC systems. These differences in the correlation of ΔS^{o}_{sorp} vs. HSA accounted for the distinct retention behavior observed between these two groups of hydrophobic solutes.

(6) The observed increase in ln k' with RPLC chain length was attributed to enthalpic processes in methanol/water systems and entroptic effects in acetonitrile/water eluents.

(7) From the enthalpy-entropy compensation plots and system compensation temperatures (β), it was concluded that the hydrophobic sorptive mechanisms were different for the PAH/halobenzene compounds compared with the alkylbenzene solutes in methanol/water RPLC sytems. The two retention mechanisms were independent of methanol composition over the range of 35 to 80% methanol by volume.

(8) The enthalpy-entropy compensation plot of three PAH compounds in 30/70 methanol/water on a carbonaceous surface soil indicated that the mechanisms of interaction are the same for solutes retained on soil material and RPLC supports in methanol/water eluents. The compensation temperature for the soil/methanol/water environment, 573°K, compared favorably with β values obtained for PAH solutes in methanol/water RPLC systems.

(9) An analysis of enthalpy-entropy compensation plots and system β values revealed that the hydrophobic retention mechanisms differed for the alkylbenzenes compared with the PAH and halobenzene compounds in acetonitrile/water RPLC systems. This effect was related to differences in the standard sorptive entropy changes for these two groups of chemicals. Unlike the methanol/water system, however, these retention mechanisms were a function of acetonitrile composition of the mobile phase.

(10) At an acetonitrile content of 25% by volume, the retention mechanisms for the PAH/halobenzene compounds and the alkylbenzenes were similar to those observed in methanol/water RPLC systems. As the acetontrile content is increased, the retention mechanisms for both groups of compounds change rapidly and then become essentially constant at acetonitrile compositions of 50% (v/v) and higher.

(11) The solute nitrobenzene demonstrated greater RPLC retention than was anticipated given its small HSA value. These effects were attributed to polar interactions of the nitro moiety with available silanol groups on the RPLC surface and indicated that polar interactions can strongly influence the retention of hydrophobic compounds on RPLC surfaces.

(12) The three-parameter enthalpy-entropy compensation model provided an excellent description of solute retention ($\ln k'$) as a function of eluent composition (θ) and absolute temperature (T) over the θ range studied in acetonitrile/water and methanol/water RPLC systems.

(13) A comparison of solute retention factors determined from batch equilibrium isotherms on RPLC material and RPLC column experiments indicated that kinetic processes do not limit solute-sorbent interactions in RPLC column studies. These results were substantiated by RPLC flow experiments which found no dependence of k' on column flow rate.

(14) The solvophobic model of Horvath et al. (1976) provided an excellent description of solute retention in acetonitrile/water RPLC systems as a function of solvent surface tension (γ) and modified dielectric constant (Γ). The model indicated that solute-ligand interactions change considerably with RPLC chain length as one progresses from C-2 to C-18 carbon chains.

APPENDIX A
RPLC RETENTION DATA

Column: C-2, 5 cm.
Mobile Phase: 50/50 Acetonitrile/Water

Compound	HSA (Å^2)	ln k' at temperature T(°K) 298	308	318	328
Biphenyl	182	.9775	.8124	.6735	.5211
Naphthalene	156	.6665	.4805	.3612	.2193
Phenanthrene	198	1.0742	.9137	.7621	.6161
Anthracene	202	1.1158	.9645	.8267	.6637
Pyrene	213	1.2264	1.0899	.9445	.7673
Chrysene	241	1.4866	1.3226	1.1811	1.0069
Fluoranthene	218	1.2509	1.0789	.9545	.7687
n-Butylbenzene	181	1.3165	1.1365	1.0128	.8251
n-Hexylbenzene	217	1.8928	1.7095	1.5751	1.3897
Benzene	110	.1911	.0256	-.0741	-.2215
Toluene	127	.4526	.2812	.1615	.0166
Ethylbenzene	145	.7223	.5578	.4269	.2796
n-Propylbenzene	163	1.0235	.8380	.7123	.5733
p-Xylene	150	.7061	.5503	.4226	.2622
o-Xylene	147	.6560	.4964	.3702	.2193
m-Diethylbenzene	180	1.2092	1.0701	.9266	.8202
1,2,4-Trimethyl-benzene	161	.9495	.7530	.6329	.4700
Fluorobenzene	114	.2491	.0870	-.0263	-.1767
Chlorobenzene	127	.4733	.2958	.1834	.0380
Bromobenzene	133	.5213	.3567	.2309	.0924
Iodobenzene	142	.6425	.4724	.3383	.1983
Nitrobenzene	86	.1060	-.0741	-.1531	-.2921

Conditions: (1) Flow rate = 1.0 mL/min.
(2) UV detection, Wavelength = 254 nm.

Column: C-2, 5 cm #2.

Mobile Phase: 40/60 Acetonitrile/Water

Compound	HSA (Å^2)	ln k' at temperature T(°K) 298	308	318	328
Biphenyl	182	2.0970	1.8830	1.7079	1.5050
Naphthalene	156	1.6308	1.4271	1.2248	1.0734
Phenanthrene	198	2.2373	2.0351	1.8555	1.6456
Anthracene	202	2.3266	2.1098	1.9308	1.7198
Pyrene	213	2.4762	2.2728	2.0920	1.8792
Chrysene	241	2.8632	2.6514	2.4627	2.2378
Fluoranthene	218	2.5028	2.2871	2.1102	1.8958
n-Butylbenzene	181	2.4761	2.2803	2.1142	1.9307
n-Hexylbenzene	217	3.2950	3.0874	2.9049	2.6793
Benzene	110	0.8958	0.7129	0.5929	0.4055
Toluene	127	1.2708	1.0942	0.9508	0.7793
Ethylbenzene	145	1.6605	1.4755	1.3311	1.1471
n-Propylbenzene	163	2.0820	1.8941	1.7408	1.5442
p-Xylene	150	1.6666	1.4796	1.3218	1.1541
o-Xylene	147	1.5681	1.3913	1.2351	1.0583
m-Diethylbenzene	180	2.3838	2.2002	2.0488	1.8500
1,2,4-Trimethyl-benzene	161	1.9155	1.7322	1.6050	1.3983
Fluorobenzene	114	1.0141	0.8300	0.6799	0.5135
Chlorobenzene	127	1.3504	1.1140	0.9642	0.7892
Bromobenzene	133	1.3871	1.1919	1.0384	0.8492
Iodobenzene	143	1.5581	1.3593	1.2144	1.0068
Nitrobenzene	86	0.8199	0.6242	0.4733	0.2975

Conditions: (1) Flow rate = 1.0 mL/min.

(2) UV detection, Wavelength = 254 nm.

Column: C-2, 5 cm.

Mobile Phase: 30/70 Acetonitrile/Water

Compound	HSA (Å^2)	ln k' at temperature T(°K) 298	308	318	328
Biphenyl	182	3.1353	2.8514	2.6003	2.3585
Naphthalene	156	2.4649	2.2025	1.9748	1.7589
Phenanthrene	198	3.3844	3.1086	2.8287	2.5704
Anthracene	202	3.6093	3.2012	2.9373	2.6795
Pyrene	213	3.7421	3.4584	3.1730	2.9040
Chrysene	241	4.3225	4.0183	3.7137	3.4182
Fluoranthene	218	3.7834	3.4907	3.2101	2.9343
n-Butylbenzene	181	3.5728	3.3350	3.0905	2.8474
n-Hexylbenzene	217	---	---	---	---
Benzene	110	1.3895	1.1757	0.9832	0.8052
Toluene	127	1.8906	1.6917	1.4926	1.3167
Ethylbenzene	145	2.4335	2.2130	1.9950	1.7961
n-Propylbenzene	163	3.0275	2.7859	2.5505	2.3315
p-Xylene	150	2.4092	2.1704	1.9632	1.7713
o-Xylene	147	2.3123	2.0979	1.8777	1.6805
m-Diethylbenzene	180	3.4533	3.2021	2.9658	2.7359
1,2,4-Trimethyl-benzene	161	2.8011	2.5749	2.3562	2.1493
Fluorobenzene	114	1.5616	1.3477	1.1507	0.9723
Chlorobenzene	127	1.9691	1.7285	1.5418	1.3373
Bromobenzene	133	2.0702	1.8594	1.6360	1.4454
Iodobenzene	142	2.3324	2.0923	1.8639	1.6436
Nitrobenzene	86	1.3454	1.1340	0.9316	0.7433

Conditions: (1) Flow rate = 1.0 mL/min.

(2) UV detection, Wavelength = 254 nm.

Column: C-2, 5 cm.

Mobile Phase: 25/75 Acetonitrile/Water

Compound	HSA (Å^2)	ln k' at temperature T(°K) 298	308	318	328
Biphenyl	182	3.6392	3.3387	3.0547	2.7718
Naphthalene	156	2.8429	2.5649	2.3208	2.0675
Phenanthrene	198	3.9642	3.6478	3.3501	3.0660
Anthracene	202	4.1046	3.7830	3.4791	3.1767
Pyrene	213	4.4138	4.0790	3.7693	3.4669
Chrysene	241	---	---	---	---
Fluoranthene	218	4.4555	4.1481	3.8319	3.5055
n-Butylbenzene	181	4.1314	3.8475	3.5161	3.3274
n-Hexylbenzene	217	---	---	---	---
Benzene	110	1.5174	1.3426	1.1480	0.9681
Toluene	127	2.1303	1.9176	1.7013	1.5194
Ethylbenzene	145	2.7586	2.5229	2.3337	2.0699
n-Propylbenzene	163	3.4421	3.1899	2.9222	2.6906
p-Xylene	150	2.7064	2.4950	2.3214	2.0611
o-Xylene	147	2.6081	2.3734	2.2291	2.0124
m-Diethylbenzene	180	3.9438	3.6968	3.4125	3.1717
1,2,4-Trimethylbenzene	161	3.2315	3.0002	2.7331	2.5145
Fluorobenzene	114	1.7473	1.5359	1.3525	1.1420
Chlorobenzene	127	2.2243	2.0157	1.7552	1.6120
Bromobenzene	133	2.3752	2.1592	1.9063	1.6885
Iodobenzene	142	2.6649	2.4241	2.1816	1.9495
Nitrobenzene	86	1.5167	1.3227	1.1305	0.9213

Conditions: (1) Flow rate = 1.0 mL/min.

(2) UV detection, Wavelength = 254 nm.

Column: C-4, 5 cm.

Mobile Phase: 60/40 Acetonitrile/Water

Compound	HSA (Å^2)	ln k' at temperature T(°K)				
		288	298	308	318	328
Biphenyl	182	0.8074	0.7362	0.6049	0.4943	0.3666
Naphthalene	156	0.5583	0.4741	0.3443	0.2386	0.1187
Phenanthrene	198	0.8751	0.8047	0.6931	0.5739	0.4233
Anthracene	202	0.9434	0.8552	0.7472	0.6155	0.4751
Pyrene	213	1.0437	0.9509	0.8368	0.7251	0.5913
Chrysene	241	1.2044	1.1365	1.0266	0.8949	0.7522
Fluoranthene	218	1.0289	0.9491	0.8393	0.7113	0.5557
n-Butylbenzene	181	1.1820	1.1245	1.0074	0.8800	0.7556
n-Hexylbenzene	217	1.7248	1.6679	1.5464	1.4211	1.2836
Benzene	110	0.1722	0.0800	-0.0140	-0.1325	-0.2557
Toluene	127	0.3947	0.3252	0.1906	0.0999	-0.0135
Ethylbenzene	145	0.6404	0.5779	0.4592	0.3475	0.2219
n-Propylbenzene	163	0.9131	0.8552	0.7369	0.6271	0.4954
p-Xylene	150	0.6331	0.5649	0.4428	0.3475	0.2447
o-Xylene	147	0.5801	0.5136	0.4024	0.3024	0.1982
m-Diethylbenzene	180	1.1123	1.1017	0.9598	0.8315	0.6999
1,2,4-Trimethylbenzene	161	0.8249	0.7838	0.6602	0.5325	0.4383
Flurorobenzene	114	0.1797	0.1095	-0.0184	-0.1110	-0.2379
Chlorobenzene	127	0.3993	0.3083	0.2120	0.0832	-0.0414
Bromobenzene	133	0.4445	0.3677	0.2701	0.1443	0.0310
Iodobenzene	142	0.5687	0.4883	0.3579	0.2526	0.1148
Nitrobenzene	86	0.0138	-0.0671	-0.1823	-0.3015	-0.4539

Conditions: (1) Flow rate = 1.0 mL/min.

(2) UV detection, Wavelength = 254 nm.

Column: C-4, 5 cm.

Mobile Phase: 50/50 Acetonitrile/Water

Compound	HSA (Å^2)	ln k' at temperature T(°K)			
		298	308	318	328
Biphenyl	182	1.5133	1.3707	1.2377	1.0925
Naphthalene	156	1.1497	1.0072	0.8628	0.7421
Phenanthrene	198	1.6011	1.4663	1.3141	1.1748
Anthracene	202	1.6705	1.5240	1.3817	1.2363
Pyrene	213	1.7956	1.6617	1.5076	1.3620
Chrysene	241	2.0572	1.9211	1.7648	1.6131
Fluoranthene	218	1.8002	1.6551	1.5127	1.3667
n-Butylbenzene	181	1.9514	1.8221	1.6765	1.5336
n-Hexylbenzene	217	2.6493	2.5179	2.3680	2.2118
Benzene	110	0.6086	0.4827	0.3475	0.2313
Toluene	127	0.9200	0.7985	0.6583	0.5352
Ethylbenzene	145	1.2488	1.1290	0.9860	0.8551
n-Propylbenzene	163	1.6085	1.4875	1.3396	1.2026
p-Xylene	150	1.2287	1.1032	0.9670	0.8453
o-Xylene	147	1.1643	1.0431	0.9062	0.7868
m-Diethylbenzene	180	1.8732	1.7580	1.6131	1.4737
1,2,4-Trimethyl-benzene	161	1.4738	1.3510	1.2135	1.0863
Fluorobenzene	114	0.6602	0.5218	0.3886	0.2808
Chlorobenzene	127	0.9218	0.7878	0.6560	0.5298
Bromobenzene	133	0.9980	0.8565	0.7244	0.6049
Iodobenzene	142	1.1350	0.9939	0.8590	0.7290
Nitrobenzene	86	0.4418	0.2990	0.1639	0.0446

Conditions: (1) Flow rate = 1.0 mL/min.

(2) UV detection, Wavelength = 254 nm.

Column: C-4, 5 cm.

Mobile Phase: 40/60 Acetonitrile/Water

Compound	HSA (Å^2)	ln k' at temperature T(°K) 298	308	318	328
Biphenyl	182	2.3902	2.2242	2.0369	1.8611
Naphthalene	156	1.8894	1.7338	1.5532	1.3932
Phenanthrene	198	2.5282	2.3574	2.1664	1.9899
Anthracene	202	2.6143	2.4436	2.2523	2.0672
Pyrene	213	2.7809	2.6089	2.4171	2.2361
Chrysene	241	3.1656	2.9876	2.7855	2.5941
Fluoranthene	218	2.7982	2.6218	2.4282	2.2395
n-Butylbenzene	181	2.8957	2.7337	2.5622	2.3848
n-Hexylbenzene	217	3.8132	3.6428	3.4580	3.2595
Benzene	110	1.1194	0.9755	0.8317	0.6931
Toluene	127	1.5470	1.3881	1.2358	1.0815
Ethylbenzene	145	1.9873	1.8230	1.6628	1.4958
n-Propylbenzene	163	2.4623	2.2905	2.1224	1.9419
p-Xylene	150	1.9384	1.7198	1.6396	1.4885
o-Xylene	147	1.8653	1.7175	1.5523	1.4092
m-Diethylbenzene	180	2.8129	2.6441	2.4778	2.2900
1,2,4-Trimethyl-benzene	161	2.2606	2.1129	1.9593	1.8040
Fluorobenzene	114	1.2138	1.0733	0.9126	0.7732
Chlorobenzene	127	1.5544	1.4072	1.2395	1.0878
Bromobenzene	133	1.6576	1.5134	1.3377	1.1998
Iodobenzene	142	1.8410	1.6788	1.5082	1.3413
Nitrobenzene	86	0.9738	0.8187	0.6482	0.5025

Conditions: (1) Flow rate = 1.0 mL/min.

(2) UV detection, Wavelength = 254 nm.

Column: C-4, 5 cm.

Mobile Phase: 30/70 Acetonitrile/Water

Compound	HSA (Å^2)	ln k' at temperature T(°K) 298	308	318	328
Biphenyl	182	3.5605	3.3441	3.0910	2.9080
Naphthalene	156	2.8391	2.6457	2.4151	2.2438
Phenanthrene	198	3.8334	3.5604	3.3035	3.1130
Anthracene	202	3.9161	3.6713	3.4207	3.2294
Pyrene	213	4.2069	3.9264	3.6594	3.4650
Chrysene	241	4.7965	4.4931	4.2055	3.9969
Fluoranthene	218	4.1915	3.9795	3.6944	3.4965
n-Butylbenzene	181	4.1788	3.9227	3.7080	3.5240
n-Hexylbenzene	217	---	---	---	---
Benzene	110	1.7159	1.5337	1.3731	1.0912
Toluene	127	2.2573	2.1070	1.9154	1.7535
Ethylbenzene	145	2.8550	2.6964	2.4854	2.3012
n-Propylbenzene	163	3.5057	3.3368	3.1014	2.8974
p-Xylene	150	2.8423	2.6381	2.4558	2.2990
o-Xylene	147	2.7448	2.5469	2.3479	2.1957
m-Diethylbenzene	180	3.9802	3.8172	3.5737	3.3593
1,2,4-Trimethyl-benzene	161	3.2928	3.0741	2.8872	2.7265
Fluorobenzene	114	1.8658	1.7012	1.5183	1.3715
Chlorobenzene	127	2.3076	2.1579	1.9546	1.8007
Bromobenzene	133	2.4711	2.2807	2.0884	1.9139
Iodobenzene	142	2.7273	2.5555	2.3380	2.1491
Nitrobenzene	86	1.5749	1.4108	1.2328	1.0828

Conditions: (1) Flow rate = 1.0 mL/min.

(2) UV detection, Wavelength = 254 nm.

Column: C-8, 5 cm.

Mobile Phase: 80/20 Acetonitrile/Water

Compound	HSA (Å^2)	ln k' at temperature T(°K) 298	308	318	328
Biphenyl	182	-0.0864			
Naphthalene	156	-0.2513			
Phenanthrene	198	0.0831			
Anthracene	202	0.1144			
Pyrene	213	0.3791			
Chrysene	241	0.4618			
Fluoranthene	218	0.2785			
n-Butylbenzene	181	0.2711			
n-Hexylbenzene	217	0.7465			
Benzene	110	-0.5568			
Toluene	127	-0.3581			
Ethylbenzene	145	-0.1863			
n-Propylbenzene	163	0.0385			
p-Xylene	150	-0.1655			
o-Xylene	147	-0.2236			
m-Diethylbenzene	180	0.2113			
1,2,4-Trimethyl-benzene	161	0.0258			
Fluorobenzene	114	-0.5541			
Chlorobenzene	127	-0.3417			
Bromobenzene	133	-0.2928			
Iodobenzene	142	-0.2303			
Nitrobenzene	86	-0.7267			

Conditions: (1) Flow rate = 1.0 mL/min.

(2) UV detection, Wavelength = 254 nm.

Column: C-8, 5 cm.

Mobile Phase: 65/35 Acetonitrile/Water

Compound	HSA ($Å^2$)	ln k' at temperature T(°K) 288	298	308	318
Biphenyl	182	0.8433	0.7546	0.6450	0.5384
Naphthalene	156	0.5971	0.4995	0.3976	0.2718
Phenanthrene	198	1.0764	0.9738	0.8453	0.7376
Anthracene	202	1.1325	1.0323	0.9078	0.7705
Pyrene	213	1.4198	1.2903	1.1430	1.0024
Chrysene	241	1.6141	1.4835	1.3345	1.1763
Fluoranthene	218	1.3345	1.2124	1.0652	0.9389
n-Butylbenzene	181	1.2667	1.1725	1.0733	0.9443
n-Hexylbenzene	217	1.8929	1.8003	1.6854	1.5465
Benzene	110	0.1152	0.0278	-0.0580	-0.1671
Toluene	127	0.3785	0.3051	0.1994	0.0854
Ethylbenzene	145	0.6444	0.5632	0.4676	0.3655
n-Propylbenzene	163	0.9559	0.8672	0.7721	0.6539
p-Xylene	150	0.6646	0.5815	0.4706	0.3859
o-Xylene	147	0.5997	0.5248	0.4317	0.3204
m-Diethylbenzene	180	1.1841	1.1203	1.0120	0.8906
1,2,4-Trimethyl-benzene	161	0.8906	0.8208	0.7094	0.6093
Fluorobenzene	114	0.1068	0.0278	-0.0629	-0.1453
Chlorobenzene	127	0.4008	0.3051	0.2109	0.1068
Bromobenzene	133	0.4588	0.3913	0.2912	0.1788
Iodobenzene	142	0.6201	0.5331	0.4195	0.3120
Nitrobenzene	86	-0.0730	-0.1518	-0.2553	-0.3677

Conditions: (1) Flow rate = 1.0 mL/min.

(2) UV detection, Wavelength = 254 nm.

Column: C-8, 5 cm.

Mobile Phase: 60/40 Acetonitrile/Water

Compound	HSA (Å^2)	ln k' at temperature T(°K) 288	298	308	318
Biphenyl	182	1.1982	1.1002	0.9952	0.8573
Naphthalene	156	0.9188	0.8083	0.6903	0.5603
Phenanthrene	198	1.4449	1.3283	1.1978	1.0472
Anthracene	202	1.5125	1.3908	1.2597	1.1095
Pyrene	213	1.7893	1.6562	1.5096	1.3456
Chrysene	241	2.0101	1.8865	1.7368	1.5604
Fluoranthene	218	1.7096	1.5847	1.4512	1.2864
n-Butylbenzene	181	1.6389	1.5465	1.4312	1.3044
n-Hexylbenzene	217	2.3213	2.2316	2.1107	1.9473
Benzene	110	0.3810	0.2699	0.1776	0.0637
Toluene	127	0.6623	0.5555	0.4867	0.3425
Ethylbenzene	145	0.9681	0.8712	0.7612	0.6376
n-Propylbenzene	163	1.3045	1.2025	1.0977	0.9791
p-Xylene	150	0.9819	0.8771	0.7855	0.6718
o-Xylene	147	0.9249	0.8249	0.7235	0.6023
m-Diethylbenzene	180	1.5660	1.4814	1.3609	1.2180
1,2,4-Trimethyl-benzene	161	1.2283	1.1340	1.0032	0.9078
Fluorobenzene	114	0.3974	0.2877	0.1937	-0.0286
Chlorobenzene	127	0.7015	0.5835	0.4735	0.3623
Bromobenzene	133	0.7810	0.6646	0.5566	0.4408
Iodobenzene	142	0.9395	0.8249	0.7224	0.5868
Nitrobenzene	86	0.2047	0.0811	-0.0193	-0.1464

Conditions: (1) Flow rate = 1.0 mL/min.

(2) UV detection, Wavelength = 254 nm.

Column: C-8, 5 cm.

Mobile Phase: 50/50 Acetonitrile/Water

Compound	HSA (Å^2)	ln k' at temperature T(°K) 288	298	308	318
Biphenyl	182	2.1748	2.0653	1.8964	1.7612
Naphthalene	156	1.7806	1.6625	1.4966	1.3664
Phenanthrene	198	2.4400	2.3026	2.1255	1.9584
Anthracene	202	2.5988	2.3948	2.2029	2.0542
Pyrene	213	2.8524	2.6665	2.4728	2.2914
Chrysene	241	3.1472	2.9901	2.7893	2.5989
Fluoranthene	218	2.7313	2.6254	2.4216	2.2639
n-Butylbenzene	181	2.6411	2.5570	2.3928	2.2670
n-Hexylbenzene	217	3.4821	3.4204	3.2277	3.0823
Benzene	110	1.0923	0.9700	0.8151	0.7021
Toluene	127	1.4586	1.3577	1.1906	1.0689
Ethylbenzene	145	1.8322	1.7371	1.5675	1.4371
n-Propylbenzene	163	2.2543	2.1611	1.9876	1.8480
p-Xylene	150	1.8473	1.7170	1.5746	1.4471
o-Xylene	147	1.7669	1.6472	1.5025	1.3688
m-Diethylbenzene	180	2.5616	2.4794	2.3102	2.1680
1,2,4-Trimethyl-benzene	161	2.1445	2.0381	1.8879	1.7548
Fluorobenzene	114	1.1360	1.0222	0.8742	0.7581
Chlorobenzene	127	1.4956	1.3565	1.2136	1.0832
Bromobenzene	233	1.5941	1.4760	1.3031	1.1884
Iodobenzene	142	1.7830	1.6589	1.4966	1.3593
Nitrobenzene	86	0.9333	0.7936	0.6346	0.5052

Conditions: (1) Flow rate = 1.0 mL/min.

(2) UV detection, Wavelength = 254 nm.

Column: C-8, 5 cm.

Mobile Phase: 40/60 Acetonitrile/Water

Compound	HSA (Å^2)	ln k' at temperature T(°K) 298	308	318	328
Biphenyl	182	3.0163	2.8814	2.6792	2.5058
Naphthalene	156	2.4620	2.3321	2.1595	1.9759
Phenanthrene	198	3.3799	3.1617	2.9607	2.7476
Anthracene	202	3.4258	3.2718	3.0739	2.8549
Pyrene	213	3.8136	3.5772	3.3613	3.1279
Chrysene	241	4.2669	4.0225	3.7983	3.5489
Fluoranthene	218	3.7725	3.5461	3.3443	3.0991
n-Butylbenzene	181	3.6305	3.4406	3.2790	3.0731
n-Hexylbenzene	217	4.7074	4.5086	4.3332	4.0950
Benzene	110	1.5282	1.4104	1.2646	1.1173
Toluene	127	2.0559	1.8816	1.7425	1.5897
Ethylbenzene	145	2.5460	2.3653	2.2228	2.0643
n-Propylbenzene	163	3.0940	2.9040	2.7490	2.5768
p-Xylene	150	2.5171	2.3921	2.2350	2.0615
o-Xylene	147	2.4627	2.2867	2.1335	1.9681
m-Diethylbenzene	180	3.4949	3.3084	3.1557	2.9789
1,2,4-Trimethyl-benzene	161	2.9195	2.7861	2.6097	2.4502
Fluorobenzene	114	1.6203	1.5105	1.3627	1.2040
Chlorobenzene	127	2.0749	1.9394	1.7795	1.6059
Bromobenzene	133	2.1916	2.0603	1.8990	1.7283
Iodobenzene	142	2.4504	2.3022	2.1133	1.9472
Nitrobenzene	86	1.3968	1.2507	1.0729	0.9207

Conditions: (1) Flow rate = 1.0 mL/min.

(2) UV detection, Wavelength = 254 nm.

Column: C-8, 5 cm.

Mobile Phase: 30/70 Acetonitrile/Water

Compound	HSA (Å^2)	ln k' at temperature T(°K)			
		298	308	318	328
Biphenyl	182	4.3267	3.9885	3.8698	3.5489
Naphthalene	159	3.5335	3.2374	3.1214	2.8359
Phenanthrene	198	---	---	---	---
Anthracene	202	---	---	---	---
Pyrene	213	---	---	---	---
Chrysene	241	---	---	---	---
Fluoranthene	218	---	---	---	---
n-Butylbenzene	181	---	---	---	---
n-Hexylbenzene	217	---	---	---	---
Benzene	110	2.1909	2.0123	1.8830	1.7028
Toluene	127	2.8339	2.6929	2.5031	2.2877
Ethylbenzene	145	3.4966	3.3394	3.1308	2.9652
n-Propylbenzene	163	4.2285	4.0496	3.8270	3.5634
p-Xylene	150	3.5080	3.2309	3.1494	2.9086
o-Xylene	147	3.3771	3.1863	3.0191	2.7981
m-Diethylbenzene	180	4.7517	4.5820	4.3514	4.0768
1,2,4-Trimethyl-benzene	161	4.0349	3.8188	3.6518	3.3836
Fluorobenzene	114	2.3589	2.1513	2.0488	1.8222
Chlorobenzene	127	2.9410	2.7010	2.5939	2.3668
Bromobenzene	133	3.1018	2.9223	2.7439	2.5201
Iodobenzene	142	3.4448	3.2055	3.0231	2.7557
Nitrobenzene	86	2.0938	1.8917	1.7300	1.5197

Conditions: (1) Flow rate = 1.0 mL/min.

(2) UV detection, Wavelength = 254 nm.

Column: C-2, 5 cm.
Mobile Phase: 60/40 Methanol/Water

Compound	HSA ($\AA^2$)	ln k' at temperature T(°K) 298	308	318	328
Biphenyl	182	0.4055	0.1832	0.0163	-0.1757
Naphthalene	156	-0.0910	-0.2624	-0.4504	-0.5878
Phenanthrene	198	0.5500	0.3116	0.1383	-0.0530
Anthracene	202	0.6482	0.4217	0.2253	0.0328
Pyrene	213	0.8606	0.6290	0.4308	0.2121
Chrysene	241	1.2281	0.9727	0.7647	0.5335
Fluoranthene	218	0.8457	0.6111	0.4164	0.2052
n-Butylbenzene	181	0.8896	0.6709	0.4830	0.2877
n-Hexylbenzene	217	1.7871	1.5178	1.2852	1.0345
Benzene	110	-0.7497	-0.9245	-1.0144	-1.2040
Toluene	127	-0.3653	-0.5312	-0.7267	-0.8109
Ethylbenzene	145	0.0163	-0.1780	-0.3212	-0.4656
n-Propylbenzene	163	0.4569	0.2573	0.0943	-0.0810
p-Xylene	150	0.0377	-0.1469	-0.3238	-0.4138
o-Xylene	147	-0.0607	-0.2505	-0.3837	-0.5490
m-Diethylbenzene	180	0.7850	0.5494	0.3795	0.2007
1,2,4-Trimethyl-benzene	161	0.3457	0.1666	-0.0110	-0.1691
Fluorobenzene	114	-0.6286	-0.8690	-0.9135	-1.0018
Chlorobenzene	127	-0.3062	-0.4855	-0.6607	-0.8109
Bromobenzene	133	-0.2624	-0.4137	-0.5596	-0.7043
Iodobenzene	142	-0.0915	-0.2768	-0.4591	-0.6080
Nitrobenzene	86	-0.8602	-1.0405	-1.1436	-1.3218

Conditions: (1) Flow rate = 1.0 mL/min.
(2) UV detection, Wavelength = 254 nm.

Column: C-2, 5 cm.

Mobile Phase: 50/50 Methanol/Water

Compound	HSA (Å^2)	ln k' at temperature T(°K)			
		298	308	318	328
Biphenyl	182	1.6975	1.4326	1.2091	0.9794
Naphthalene	156	1.0678	0.8424	0.6551	0.4583
Phenanthrene	198	1.9524	1.6653	1.4230	1.1661
Anthracene	202	2.0802	1.7792	1.5305	1.2709
Pyrene	213	2.3948	2.0701	1.8022	1.5182
Chrysene	241	2.9327	2.5672	2.2752	1.9534
Fluoranthene	218	2.3701	2.0569	1.7860	1.5131
n-Butylbenzene	181	2.2525	1.9752	1.7507	1.4924
n-Hexylbenzene	217	3.4830	3.1220	2.8315	2.4960
Benzene	110	0.1076	-0.0722	-0.1754	-0.3112
Toluene	127	0.5916	0.4131	0.2703	0.1048
Ethylbenzene	145	1.0853	0.8788	0.7187	0.5258
n-Propylbenzene	163	1.6615	1.4216	1.2345	1.0116
p-Xylene	150	1.1118	0.9047	0.7353	0.5563
o-Xylene	147	0.9960	0.7968	0.6340	0.4472
m-Diethylbenzene	180	2.0608	1.8003	1.6014	1.3598
1,2,4-Trimethyl-benzene	161	1.5129	1.2808	1.1005	0.8880
Fluorobenzene	114	0.2676	0.1088	-0.0351	-0.1777
Chlorobenzene	127	0.6960	0.5177	0.3381	0.1608
Bromobenzene	133	0.8008	0.6278	0.4612	0.2370
Iodobenzene	142	0.9991	0.7864	0.6030	0.4055
Nitrobenzene	86	0.0390	-0.1418	-0.2992	-0.4380

Conditions: (1) Flow rate = 1.0 mL/min.

(2) UV detection, Wavelength = 254 nm.

Column: C-2, 5 cm.

Mobile Phase: 40/60 Methanol/Water

Compound	HSA (Å^2)	ln k' at temperature T(°K) 298	308	318	328
Biphenyl	182	2.7326	2.4338	2.1441	1.8335
Naphthalene	156	1.9057	1.6599	1.4188	1.1588
Phenanthrene	198	3.1352	2.7985	2.4897	2.1523
Anthracene	202	3.2992	2.9472	2.6133	2.2525
Pyrene	213	3.7518	3.3703	3.0187	2.6336
Chrysene	241	4.4976	4.0384	3.6501	3.2176
Fluoranthene	218	3.7314	3.3545	2.9833	2.5919
n-Butylbenzene	181	3.3525	3.0863	2.7861	2.4534
n-Hexylbenzene	217	---	---	---	---
Benzene	110	0.5998	0.4613	0.3048	0.1508
Toluene	127	1.1988	1.0271	0.8740	0.6960
Ethylbenzene	145	1.8173	1.6243	1.4476	1.2326
n-Propylbenzene	163	2.5556	2.3281	2.1154	1.8510
p-Xylene	150	1.9031	1.7427	1.4551	1.2478
o-Xylene	147	1.7100	1.5256	1.3422	1.1254
m-Diethylbenzene	180	3.0584	2.8302	2.6082	2.3164
1,2,4-Trimethyl-benzene	161	2.3805	2.1707	1.9352	1.6670
Fluorobenzene	114	0.8198	0.6581	0.4969	0.3121
Chlorobenzene	127	1.3571	1.1707	0.9722	0.7579
Bromobenzene	133	1.5155	1.3102	1.0928	0.8711
Iodobenzene	142	1.7841	1.5648	1.3347	1.0928
Nitrobenzene	86	0.5968	0.4207	0.2346	0.0674

Conditions: (1) Flow rate = 1.0 mL/min.

(2) UV detection, Wavelength = 254 nm.

Column: C-2, 5 cm.

Mobile Phase: 35/65 Methanol/Water

Compound	HSA (Å^2)	ln k' at temperature T(°K) 298	308	318	328
Biphenyl	182	3.2170	2.8901	2.5642	2.2857
Naphthalene	156	2.2823	2.0164	1.7522	1.5251
Phenanthrene	198	3.7040	3.3453	2.9879	2.6539
Anthracene	202	3.8659	3.4828	3.1231	2.8037
Pyrene	213	4.4016	4.0078	3.5962	3.2366
Chrysene	241	---	---	---	---
Fluoranthene	218	4.3915	3.9670	3.5671	3.1879
n-Butylbenzene	181	3.8559	3.5729	3.2701	2.9706
n-Hexylbenzene	217	---	---	---	---
Benzene	110	0.7679	0.6370	0.4969	0.3740
Toluene	127	1.4326	1.2707	1.0998	0.9640
Ethylbenzene	145	2.1251	1.9319	1.7248	1.5630
n-Propylbenzene	163	2.9511	2.7195	2.4697	2.2598
p-Xylene	150	2.1713	1.9734	1.7748	1.5681
o-Xylene	147	2.0225	1.8330	1.6406	1.4592
m-Diethylbenzene	180	3.5642	3.3064	3.0456	2.7751
1,2,4-Trimethyl-benzene	161	2.7869	2.5529	2.3068	2.0945
Fluorobenzene	114	1.0251	0.8644	0.7046	0.5429
Chlorobenzene	127	1.6265	1.4271	1.2277	1.0411
Bromobenzene	133	1.7994	1.5850	1.3819	1.1876
Iodobenzene	142	2.1140	1.8780	1.6502	1.4234
Nitrobenzene	86	0.7968	0.6124	0.4232	0.2949

Conditions: (1) Flow rate = 1.0 mL/min.

(2) UV detection, Wavelength = 254 nm.

Column: C-4, 15 cm.

Mobile Phase: 75/25 Methanol/Water

Compound	HSA (Å^2)	ln k' at temperature T(°K) 288	298	308	318
Biphenyl	182	0.06760	-0.02387	-0.12840	-0.23915
Naphthalene	156	-0.25435	-0.32312	-0.42679	-0.50733
Phenanthrene	198	0.14350	0.06676	-0.08981	-0.2004
Anthracene	202	0.19449	0.09163	-0.02912	-0.14156
Pyrene	213	0.38336	0.28893	0.11440	-0.01552
Chrysene	241	0.55089	0.45046	0.27239	0.13750
n-Butylbenzene	181	0.54795	0.43532	0.30748	0.17614
n-Hexylbenzene	217	1.20588	1.05327	0.88937	0.72309
Benzene	110	-0.70818	-0.72736	-0.82622	-0.88819
Toluene	127	-0.4083	-0.45198	-0.54335	-0.61804
Ethylbenzene	145	-0.11631	-0.18032	-0.28356	-0.37382
n-Propylbenzene	163	0.21172	0.1293	0.01143	-0.09849
p-Xylene	150	-0.10712	-0.17027	-0.27378	-0.37063
o-Xylene	147	-0.14122	-0.19249	-0.32310	-0.41189
m-Diethylbenzene	172	0.46367	0.36538	0.24287	0.12239
1,2,4-Trimethylbenzene		0.14975	0.06987	-0.04144	-0.14908
Fluorobenzene	114	-0.70142	-0.73439	-0.81690	-0.87924
Chlorobenzene	127	-0.41008	-0.45732	-0.55338	-0.63582
Bromobenzene	133	-0.34414	-0.41055	-0.50634	-0.57252
Iodobenzene	142	-0.22922	-0.28883	-0.38787	-0.48272
Nitrobenzene	86	-0.89850	-0.94018	-1.03479	-1.11932

Conditions: (1) Flow rate = 1.0 mL/min.

(2) UV detection, Wavelength = 254 nm.

Column: C-4, 15 cm.

Mobile Phase: 70/30 Methanol/Water

Compound	HSA (Å^2)	ln k' at temperature T(°K) 288	298	308	318
Biphenyl	182	0.6787	0.5068	0.3813	0.2442
Naphthalene	156	0.2940	0.1305	0.0293	-0.0848
Phenanthrene	198	0.7732	0.5900	0.4537	0.3234
Anthracene	202	0.8444	0.6611	0.5243	0.3736
Pyrene	213	1.0503	0.8523	0.6973	0.5477
Chrysene	241	1.2803	1.0727	0.9027	0.7397
n-Butylbenzene	181	1.1753	0.9969	0.8567	0.7055
n-Hexylbenzene	217	1.9664	1.7480	1.5579	1.3642
Benzene	110	-0.2513	-0.4086	-0.4814	-0.5412
Toluene	127	0.0870	-0.0768	-0.1379	-0.2474
Ethylbenzene	145	0.4255	0.2559	0.1745	0.0537
n-Propylbenzene	163	0.8038	0.6255	0.5197	0.3801
p-Xylene	150	0.4375	0.2696	0.1643	0.0636
o-Xylene	147	0.3666	0.2143	0.1084	0.01400
m-Diethylbenzene	180	1.0924	0.9076	0.7863	0.6350
1,2,4-Trimethyl-benzene	161	0.7206	0.5470	0.4228	0.3044
Fluorobenzene	114	-0.2173	-0.3721	-0.4342	-0.5154
Chlorobenzene	127	0.1054	-0.0613	-0.1551	-0.2388
Bromobenzene	133	0.1895	0.0207	-0.0846	-0.1771
Iodobenzene	142	0.3139	0.1398	0.0373	-0.0660
Nitrobenzene	86	-0.4207	-0.6192	-0.7044	-0.7816

Conditions: (1) Flow rate = 1.0 mL/min.

(2) UV detection, Wavelength = 254 nm.

Column: C-4, 15 cm.

Mobile Phase: 60/40 Methanol/Water

Compound	HSA (Å^2)	ln k' at temperature T(°K)				
		288	298	308	318	328
Biphenyl	182	1.7822	1.5862	1.3810	1.1981	
Naphthalene	156	1.2404	1.0862	0.8957	0.7381	
Phenanthrene	198	1.9741	1.7515	1.5338	1.3274	
Anthracene	202	2.0592	1.8437	1.6080	1.4043	
Pyrene	213	2.3562	2.1078	1.8610	1.6310	
Chrysene	241	2.7478	2.4671	2.1965	1.9463	
n-Butylbenzene	181	---	2.1697	1.9560	1.7429	1.5454
n-Hexylbenzene	217	---	3.2107	2.9349	2.6631	2.4032
Benzene	110	0.4411	0.3346	0.2040	0.0817	
Toluene	127	0.8838	0.7390	0.6105	0.4806	
Ethylbenzene	145	1.3408	1.1786	1.0264	0.8773	
n-Propylbenzene	163	1.8550	1.6745	1.4929	1.3189	
p-Xylene	150	1.3439	1.1762	1.0230	0.8706	
o-Xylene	147	1.2602	1.0943	0.9489	0.7990	
m-Diethylbenzene	180	2.2428	2.0756	1.8462	1.6579	
1,2,4-Trimethylbenzene	161	1.7226	1.5448	1.3630	1.2020	
Fluorobenzene	114	0.5277	0.4020	0.2716	0.1540	
Chlorobenzene	127	0.9388	0.7915	0.6391	0.4969	
Bromobenzene	133	1.0519	0.9131	0.7351	0.5910	
Iodobenzene	142	1.2314	1.0640	0.8940	0.7471	
Nitrobenzene	86	0.2874	0.1368	-0.0106	-0.1328	

Conditions: (1) Flow rate = 1.0 mL/min.

(2) UV detection, Wavelength = 254 nm.

Column: C-4 column.

Mobile Phase: 50/50 Methanol/Water

Compound	HSA (Å^2)	ln k' at temperature T(°K) 298	308	318	328
Biphenyl	182	2.6739	2.3749	2.1214	1.8803
Naphthalene	156	1.9822	1.7230	1.5082	1.3051
Phenanthrene	198	2.9374	2.6107	2.3287	2.0508
Anthracene	202	3.0448	2.7106	2.4238	2.1536
Pyrene	213	3.4130	3.0477	2.7330	2.4204
Chrysene	241	3.9343	3.5402	3.1887	2.8421
n-Butylbenzene	181	3.3727	3.0586	2.7875	2.5143
n-Hexylbenzene	217	---	---	---	---
Benzene	110	0.9460	0.7516	0.6102	0.4712
Toluene	127	1.4935	1.2821	1.1132	0.9450
Ethylbenzene	145	2.0595	1.8191	1.6255	1.4309
n-Propylbenzene	163	2.7075	2.4318	2.1990	1.9761
p-Xylene	150	2.0691	1.8152	1.6119	1.4241
o-Xylene	147	1.9383	1.7150	1.5264	1.3329
m-Diethylbenzene	180	3.1794	2.8839	2.6403	2.3950
1,2,4-Trimethyl-benzene	161	2.5209	2.2553	2.0358	1.8223
Fluorobenzene	114	1.0785	0.8894	0.7366	0.5868
Chlorobenzene	127	1.5777	1.3501	1.1594	0.9848
Bromobenzene	133	1.7195	1.4682	1.2734	1.0921
Iodobenzene	142	1.9445	1.6916	1.4835	1.2817
Nitrobenzene	86	0.7915	0.5809	0.4159	0.2545

Conditions: (1) Flow rate = 1.0 mL/min.

(2) UV detection, Wavelength = 254 nm.

Column: C-4, 15 cm.

Mobile Phase: 40/60 Methanol/Water

		ln k' at temperature T(°K)			
Compound	HSA (Å^2)	298	308	318	328
Biphenyl	182	---	---	---	---
Naphthalene	156	2.8940	2.6062	2.3461	2.1055
Phenanthrene	198	---	---	---	---
Anthracene	202	---	---	---	---
Pyrene	213	---	---	---	---
Chrysene	241	---	---	---	---
n-Butylbenzene	181	---	---	---	---
n-Hexylbenzene	217	---	---	---	---
Benzene	110	1.4749	1.3083	1.1441	0.9944
Toluene	127	2.1598	1.9770	1.7724	1.5936
Ethylbenzene	145	2.8968	2.6780	2.4423	2.2298
n-Propylbenzene	163	---	---	---	---
p-Xylene	150	2.8701	2.6477	2.4088	2.1948
o-Xylene	147	---	---	---	---
m-Diethylbenzene	180	---	---	---	---
1,2,4-Trimethyl-benzene	161	3.4822	3.2044	2.9418	2.7024
Fluorobenzene	114	1.6694	1.4938	1.3200	1.1620
Chlorobenzene	127	2.2852	2.0778	1.8576	1.6595
Bromobenzene	133	2.4585	2.2444	2.0063	1.7941
Iodobenzene	142	2.8027	2.5288	2.2738	2.0461
Nitrobenzene	86	1.3931	1.1861	0.9946	0.8275

Conditions: (1) Flow rate = 1.0 mL/min.

(2) UV detection, Wavelength = 254 nm.

Column: C-8, 5 cm.

Mobile Phase: 80/20 Methanol/Water

Compound	HSA (Å^2)	ln k' at temperature T(°K) 288	298	308	318
Biphenyl	182	0.2102	0.0800	-0.0203	-0.1301
Naphthalene	156	-0.0854	-0.1919	-0.2870	-0.3873
Phenanthrene	198	0.5361	0.3795	0.2418	0.0931
Anthracene	202	0.6128	0.4469	0.3032	0.1472
Pyrene	213	0.9996	0.8024	0.6320	0.4583
Chrysene	241	1.2315	1.0078	0.8116	0.6216
n-Butylbenzene	181	0.6344	0.5013	0.3844	0.2472
n-Hexylbenzene	217	1.3177	1.1426	0.9846	0.8100
Benzene	110	-0.7089	-0.7493	-0.7834	-0.8514
Toluene	127	-0.3272	-0.4234	-0.4765	-0.5636
Ethylbenzene	145	-0.0640	-0.1682	-0.2404	-0.3348
n-Propylbenzene	163	0.2819	0.1643	0.0663	-0.0458
p-Xylene	150	0.0382	-0.0741	-0.1802	-0.2796
o-Xylene	147	-0.0395	-0.1303	-0.2097	-0.3013
m-Diethylbenzene	180	0.5805	0.4495	0.3359	0.2150
1,2,4-Trimethyl-benzene	161	0.3325	0.2326	0.1216	0.0040
Fluorobenzene	114	-0.7391	-0.7932	-0.8287	-0.8804
Chlorobenzene	127	-0.3513	-0.4357	-0.5015	-0.5709
Bromobenzene	133	-0.2903	-0.3422	-0.4125	-0.5149
Iodobenzene	142	-0.1277	-0.2015	-0.2829	-0.3814
Nitrobenzene	86	-0.9350	-0.9621	-1.0284	-1.0745

Conditions: (1) Flow rate = 1.0 mL/min.

(2) UV detection, Wavelength = 254 nm.

Column: C-8, 5 cm.
Mobile Phase: 70/30 Methanol/Water

Compound	HSA (Å^2)	ln k' at temperature T(°K) 288	298	308	318
Biphenyl	182	1.2917	1.1266	0.9195	0.7581
Naphthalene	156	0.8405	0.7013	0.5196	0.3696
Phenanthrene	198	1.6753	1.4626	1.2233	1.0328
Anthracene	202	1.7643	1.5511	1.3000	1.1027
Pyrene	213	2.1990	1.9448	1.6711	1.4417
Chrysene	241	2.5711	2.2803	1.9770	1.7187
Fluoranthene	218	2.0954	---	1.5668	1.3459
n-Butylbenzene	181	1.8053	1.6419	1.4169	1.2625
n-Hexylbenzene	217	2.7477	2.5304	2.2527	2.2094
Benzene	110	0.0392	-0.0496	-0.1575	-0.2636
Toluene	127	0.5108	0.3864	0.2351	0.1331
Ethylbenzene	145	0.9058	0.7651	0.5984	0.4736
n-Propylbenzene	163	1.3588	1.1959	1.0032	0.8628
p-Xylene	150	0.9564	0.8269	0.6611	0.5157
o-Xylene	147	0.8819	0.7530	0.5815	0.4192
m-Diethylbenzene	180	1.7353	1.5565	1.3474	1.1892
1,2,4-Trimethyl-benzene	161	1.3563	1.1975	1.0154	0.8525
Fluorobenzene	114	0.0465	-0.0287	-0.1664	-0.2688
Chlorobenzene	127	0.4900	0.3864	0.2435	0.1151
Bromobenzene	133	0.6184	0.4954	0.3543	0.2183
Iodobenzene	142	0.8090	0.6809	0.5245	0.3724
Nitrobenzene	86	-0.1465	-0.2677	-0.4046	-0.5424

Conditions: (1) Flow rate = 1.0 mL/min.
(2) UV detection, Wavelength = 254 nm.

Column: C-8, 5 cm.

Mobile Phase: 60/40 Methanol/Water

Compound	HSA (Å^2)	ln k' at temperature T(°K)			
		298	308	318	328
Biphenyl	182	2.2178	1.9748	1.7625	1.5378
Naphthalene	156	1.6346	1.4228	1.2288	1.0457
Phenanthrene	198	2.6194	2.3439	2.0702	1.8288
Anthracene	202	2.7412	2.4471	2.1796	1.9206
Pyrene	213	3.1928	2.8665	2.5500	2.2885
Chrysene	241	3.6851	3.3179	2.9685	2.6599
Fluoranthene	218	3.0838	2.7760	2.4718	2.1999
n-Butylbenzene	181	2.8186	2.5859	2.3396	2.1203
n-Hexylbenzene	217	4.0073	3.6994	3.3938	3.1084
Benzene	110	0.6406	0.4987	0.3634	0.2472
Toluene	127	1.1922	1.0154	0.8542	0.7132
Ethylbenzene	145	1.6877	1.4900	1.3069	1.1475
n-Propylbenzene	163	2.2564	2.0264	1.8169	1.6288
p-Xylene	150	1.7505	1.5439	1.3518	1.1857
o-Xylene	147	1.6318	1.4514	1.2755	1.1043
m-Diethylbenzene	180	2.7131	2.4663	2.2327	2.0257
1,2,4-Trimethyl-benzene	161	2.2144	1.9875	1.7836	1.5839
Fluorobenzene	114	0.7021	0.5533	0.4214	0.2908
Chlorobenzene	127	1.2310	1.0379	0.8693	0.7243
Bromobenzene	133	1.3593	1.1746	1.0006	0.8420
Iodobenzene	142	1.6005	1.3903	1.1964	1.0356
Nitrobenzene	86	0.4167	0.2415	0.0840	-0.0500

Conditions: (1) Flow rate = 1.0 mL/min.

(2) UV detection, Wavelength = 254 nm.

Column: C-8, 5 cm.

Mobile Phase: 50/50 Methanol/Water

Compound	HSA (Å^2)	ln k' at temperature T(°K) 298	308	318	328
Biphenyl	182	3.4383	3.0809	2.8579	2.5747
Naphthalene	156	2.6340	2.3582	2.1668	1.9216
Phenanthrene	198	3.9206	3.5617	3.2847	2.9572
Anthracene	202	4.0593	3.7184	3.4054	3.0900
Pyrene	213	4.6294	4.2420	3.8581	3.5426
Chrysene	241	---	---	---	---
Fluoranthene	218	4.5332	4.1448	3.7757	3.4695
n-Butylbenzene	181	4.1283	3.8496	3.5663	3.3157
n-Hexylbenzene	217	---	---	---	---
Benzene	110	1.3207	1.1426	1.0259	0.8679
Toluene	127	2.0107	1.8275	1.6372	1.4803
Ethylbenzene	145	2.6441	2.4361	2.2205	2.0376
n-Propylbenzene	163	3.3783	3.1357	2.8870	2.6688
p-Xylene	150	2.6788	2.4520	2.2847	2.0582
o-Xylene	147	2.5579	2.3656	2.1715	1.9533
m-Diethylbenzene	180	3.9370	3.6779	3.4094	3.1751
1,2,4-Trimethyl-benzene	161	3.2557	3.0329	2.8104	2.5653
Fluorobenzene	114	1.4422	1.2873	1.1437	0.9788
Chlorobenzene	127	2.0680	1.8601	1.7044	1.5014
Bromobenzene	133	2.2481	2.0117	1.8490	1.6338
Iodobenzene	142	2.5346	2.3026	2.1239	1.8877
Nitrobenzene	86	1.1100	0.8873	0.7453	0.5707

Conditions: (1) Flow rate = 1.0 mL/min.
(2) UV detection, Wavelength = 254 nm.

Column: C-18, 5 cm.

Temperature: 298°K

Compound	ln k' in Acetonitrile/Water (v/v) mixture, ACN/Water 70/30	60/40	55/45	50/50
Biphenyl	1.0801	1.7328	2.0917	2.5161
Naphthalene	0.7789	1.3666	1.6798	2.0564
Phenanthrene	1.3598	2.0273	2.4101	2.8577
Anthracene	1.4466	2.1358	2.5148	2.9710
Pyrene	1.7679	2.4656	2.8541	3.3223
Chrysene	2.0270	2.7926	3.2228	3.7446
Fluoranthene	---	---	---	---
n-Butylbenzene	1.5964	2.3005	2.6845	3.1339
n-Hexylbenzene	2.3582	3.1724	3.6241	4.1559
Benzene	0.2221	0.7048	0.9495	1.2164
Toluene	0.5640	1.0829	1.3626	1.6952
Ethylbenzene	0.8626	1.4457	1.7627	2.1364
n-Propylbenzene	1.2317	1.8734	2.2246	2.6431
p-Xylene	0.9050	1.4759	1.8021	2.1661
o-Xylene	0.8251	1.3902	1.7104	2.0657
m-Diethylbenzene	1.4955	2.1827	2.5577	2.9976
1,2,4-Trimethylbenzene	1.1947	1.8098	2.1577	2.5512
Fluorobenzene	0.1865	0.6800	0.9471	1.2453
Chlorobenzene	---	---	---	---
Bromobenzene	0.6459	1.1914	1.4924	1.8288
Iodobenzene	0.8251	1.3915	1.7076	2.0677
Nitrobenzene	-0.0800	0.4020	0.6614	0.9471

Conditions: (1) Flow rate = 1.0 mL/min.

(2) UV detector; 254 nm.

(3) Column void volume determined with 25 g/L $NaNO_3$.

APPENDIX B
LINEAR REGRESSION ANALYSIS OF RETENTION DATA

Column: C-2, 5 cm.
Mobile Phase: 50/50 Acetonitrile/Water

Compound	HSA(Å^2)	ln k' versus 1/T(°K) slope	95% CL[a]	intercept	95% CL[b]	R[c]
Biphenyl	182	1474.0	123.3	-3.97	0.39	0.9996
Naphthalene	156	1429.9	312.5	-4.14	1.00	0.9974
Phenanthrene	198	1491.5	34.0	-3.93	0.11	1.0000
Anthracene	202	1458.8	233.5	-3.77	0.75	0.9986
Pyrene	213	1484.9	405.2	-3.74	1.30	0.9960
Chrysene	241	1543.4	258.4	-3.69	0.83	0.9985
Fluoranthene	218	1533.8	392.3	-3.89	1.26	0.9965
n-Butylbenzene	181	1560.8	399.6	-3.92	1.23	0.9965
n-Hexylbenzene	217	1605.6	331.8	-3.49	1.06	0.9977
Benzene	110	1307.7	335.1	-4.20	1.07	0.9965
Toluene	127	1396.3	232.6	-4.24	0.74	0.9985
Ethylbenzene	145	1426.3	146.3	-4.07	0.47	0.9994
n-Propylbenzene	163	1445.1	282.5	-3.84	0.90	0.9979
p-Xylene	150	1425.3	235.8	-4.07	0.76	0.9985
o-Xylene	147	1367.5	131.0	-3.94	0.42	0.9995
m-Diethylbenzene	180	1282.2	164.5	-3.09	0.53	0.9991
1,2,4-Trimethyl-benzene	161	1524.7	363.1	-4.18	1.16	0.9970
Fluorobenzene	114	1353.5	248.4	-4.30	0.80	0.9982
Chlorobenzene	127	1387.5	303.6	-4.19	0.97	0.9974
Bromobenzene	133	1381.5	159.8	-4.12	0.51	0.9993
Iodobenzene	142	1434.6	143.3	-4.18	0.46	0.9995
Nitrobenzene	86	1246.5	504.4	-4.09	1.62	0.9913

[a]95% Confidence limit on the slope.

[b]95% Confidence limit on the intercept.

[c]Correlation coefficient.

Column: C-2, 5 cm #2.

Mobile Phase: 40/60 Acetonitrile/Water

		ln k' versus 1/T(°K)				
Compound	HSA(Å^2)	slope	95% CL[a]	intercept	95% CL[b]	R[c]
Biphenyl	182	1906.6	215.4	-4.30	0.69	0.9993
Naphthalene	156	1834.3	241.1	-4.53	0.77	0.9991
Phenanthrene	198	1909.0	266.2	-4.16	0.85	0.9989
Anthracene	202	1953.5	242.5	-4.23	0.78	0.9992
Pyrene	213	1925.6	279.5	-3.98	0.89	0.9989
Chrysene	241	2016.3	314.2	-3.90	1.00	0.9987
Fluoranthene	218	1951.8	275.3	-4.04	0.88	0.9989
n-Butylbenzene	181	1761.4	154.3	-3.43	0.49	0.9996
n-Hexylbenzene	217	1981.5	353.5	-3.35	1.13	0.9983
Benzene	110	1553.8	418.5	-4.32	1.34	0.9961
Toluene	127	1580.8	207.1	-4.03	0.66	0.9991
Ethylbenzene	145	1645.7	272.1	-3.86	0.87	0.9985
n-Propylbenzene	163	1725.3	308.9	-3.70	0.99	0.9983
p-Xylene	150	1657.3	114.3	-3.90	0.37	0.9997
o-Xylene	147	1646.6	186.5	-3.95	0.60	0.9993
m-Diethylbenzene	180	1711.3	342.0	-3.35	1.09	0.9978
1,2,4-Trimethylbenzene	161	1638.5	499.0	-3.58	1.60	0.9950
Fluorobenzene	114	1614.8	148.3	-4.41	0.47	0.9995
Chlorobenzene	127	1794.8	414.7	-4.69	1.33	0.9971
Bromobenzene	133	1726.7	252.3	-4.41	0.81	0.9988
Iodobenzene	142	1756.7	403.2	-4.33	1.29	0.9972
Nitrobenzene	86	1679.6	204.6	-4.82	0.65	0.9992

[a]95% Confidence limit on the slope.

[b]95% Confidence limit on the intercept.

[c]Correlation coefficient.

Column: C-2, 5 cm.

Mobile Phase: 30/70 Acetonitrile/Water

Compound	HSA(Å^2)	ln k' versus 1/T(°K) slope	95% CL[a]	intercept	95% CL[b]	R[c]
Biphenyl	182	2524.4	88.9	-5.34	0.28	0.9999
Naphthalene	156	2294.3	126.9	-5.24	0.41	0.9998
Phenanthrene	198	2659.9	140.9	-5.54	0.45	0.9998
Anthracene	202	2634.7	381.7	-5.35	1.20	0.9999
Pyrene	213	2735.8	152.1	-5.43	0.49	0.9998
Chrysene	241	2948.1	201.4	-5.56	0.64	0.9997
Fluoranthene	218	2763.5	129.0	-5.49	0.41	0.9999
n-Butylbenzene	181	2364.3	242.6	-4.35	0.78	0.9994
n-Hexylbenzene	217	---	---	---	---	---
Benzene	110	1902.6	74.5	-5.00	0.24	0.9999
Toluene	127	1877.7	73.8	-4.41	0.24	0.9999
Ethylbenzene	145	2082.2	65.1	-4.55	0.21	0.9999
n-Propylbenzene	163	2271.0	58.5	-4.59	0.19	1.00
p-Xylene	150	2074.7	138.8	-4.56	0.44	0.9998
o-Xylene	147	2067.7	110.9	-4.62	0.35	0.9998
m-Diethylbenzene	180	2334.5	64.9	-4.38	0.21	1.00
1,2,4-Trimethyl-benzene	161	2124.9	58.9	-4.33	0.19	1.00
Fluorobenzene	114	1921.6	69.5	-4.89	0.22	0.9999
Chlorobenzene	127	2036.2	218.7	-4.87	0.70	0.9994
Bromobenzene	133	2050.4	145.6	-4.81	0.47	0.9997
Iodobenzene	142	2242.9	63.7	-5.19	0.20	1.00
Nitrobenzene	86	1963.6	25.5	-5.24	0.08	1.00

[a]95% Confidence limit on the slope.

[b]95% Confidence limit on the intercept.

[c]Correlation coefficient.

Column: C-2, 5 cm.

Mobile Phase: 25/75 Acetonitrile/Water

Compound	HSA($Å^2$)	ln k' versus 1/T(°K) slope	95% CL[a]	intercept	95% CL[b]	R[c]
Biphenyl	182	2820.5	134.5	-5.82	0.43	0.9999
Naphthalene	156	2512.3	134.9	-5.59	0.43	0.9998
Phenanthrene	198	2925.0	40.8	-5.85	0.13	1.000
Anthracene	202	3017.3	141.3	-6.02	0.45	0.9999
Pyrene	213	3079.5	70.5	-5.92	0.23	1.000
Chrysene	241	---	---	---	---	---
Fluoranthene	218	3091.7	395.3	-5.90	1.26	0.9991
n-Butylbenzene	181	2685.7	696.6	-4.89	2.23	0.9964
n-Hexylbenzene	217	---	---	---	---	---
Benzene	110	1799.5	217.9	-4.51	0.70	0.9992
Toluene	127	2003.5	120.7	-4.59	0.39	0.9998
Ethylbenzene	145	2201.4	519.5	-4.62	1.66	0.9970
n-Propylbenzene	163	2465.0	176.0	-4.82	0.56	0.9997
p-Xylene	150	2057.7	623.3	-4.19	1.99	0.9951
o-Xylene	147	1887.9	482.6	-3.73	1.54	0.9965
m-Diethylbenzene	180	2540.7	303.9	-4.57	0.97	0.9992
1,2,4-Trimethyl-benzene	161	2362.8	282.3	-4.69	0.90	0.9992
Fluorobenzene	114	1953.1	229.2	-4.80	0.73	0.9993
Chlorobenzene	127	2052.8	568.1	-4.66	1.82	0.9959
Bromobenzene	133	2259.3	302.9	-5.19	0.97	0.9990
Iodobenzene	142	2333.9	150.6	-5.16	0.48	0.9998
Nitrobenzene	86	1931.6	274.2	-4.96	0.88	0.9989

[a]95% Confidence limit on the slope.

[b]95% Confidence limit on the intercept.

[c]Correlation coefficient.

Column: C-4, 5 cm.

Mobile Phase: 60/40 Acetonitrile/Water

Compound	HSA(Å^2)	ln k' versus 1/T(°K) slope	95% CL[a]	intercept	95% CL[b]	R[c]
Biphenyl	182	1191.4	136.0	-3.26	0.44	0.9993
Naphthalene	156	1145.4	116.7	-3.37	0.37	0.9994
Phenanthrene	198	1231.7	372.9	-3.32	1.19	0.9951
Anthracene	202	1240.5	326.8	-3.29	1.05	0.9963
Pyrene	213	1161.7	242.6	-2.94	0.78	0.9977
Chrysene	241	1252.7	329.0	-3.06	1.05	0.9963
Fluoranthene	218	1275.0	416.3	-3.31	1.33	0.9943
n-Butylbenzene	181	1205.1	159.0	-2.91	0.51	0.9991
n-Hexylbenzene	217	1247.6	216.1	-2.51	0.69	0.9984
Benzene	110	1097.7	296.0	-3.59	0.95	0.9961
Toluene	127	1082.5	201.5	-3.31	0.645	0.9981
Ethylbenzene	145	1152.0	157.9	-3.28	0.51	0.9990
n-Propylbenzene	163	1160.8	209.6	-3.03	0.67	0.9982
p-Xylene	150	1032.7	107.2	-2.90	0.34	0.9994
o-Xylene	147	1019.9	87.4	-2.91	0.28	0.9996
m-Diethylbenzene	180	1303.5	65.6	-3.27	0.21	0.9999
1,2,4-Trimethyl-benzene	161	1139.1	149.3	-3.04	0.48	0.9991
Fluorobenzene	114	1108.6	223.7	-3.61	0.72	0.9978
Chlorobenzene	127	1148.8	308.9	-3.53	0.99	0.9961
Bromobenzene	133	1108.6	235.6	-3.34	0.75	0.9976
Iodobenzene	142	1197.0	228.2	-3.52	0.73	0.9980
Nitrobenzene	86	1247.6	365.8	-4.24	1.17	0.9954

[a]95% Confidence limit on the slope.

[b]95% Confidence limit on the intercept.

[c]Correlation coefficient.

Column: C-4, 5 cm.

Mobile Phase: 50/50 Acetonitrile/Water

Compound	HSA($\AA^2$)	ln k' versus 1/T(°K) slope	95% CL[a]	intercept	95% CL[b]	R[c]
Biphenyl	182	1362.9	149.5	-3.06	0.48	0.9994
Naphthalene	156	1336.9	83.7	-3.34	0.27	0.9999
Phenanthrene	198	1397.7	177.6	-3.08	0.57	0.9991
Anthracene	202	1411.5	117.0	-3.06	0.37	0.9996
Pyrene	213	1420.5	219.8	-2.96	0.70	0.9987
Chrysene	241	1453.1	242.5	-2.81	0.78	0.9985
Fluoranthene	218	1409.4	129.6	-2.92	0.41	0.9995
n-Butylbenzene	181	1365.7	217.4	-2.62	0.70	0.9986
n-Hexylbenzene	217	1427.0	291.7	-2.13	0.93	0.9977
Benzene	110	1238.3	96.6	-3.54	0.31	0.9997
Toluene	127	1264.5	162.5	-3.32	0.52	0.9991
Ethylbenzene	145	1292.7	215.0	-3.08	0.69	0.9985
n-Propylbenzene	163	1332.9	250.3	-2.85	0.80	0.9981
p-Xylene	150	1256.8	114.2	-2.98	0.36	0.9996
o-Xylene	147	1240.1	139.3	-2.99	0.45	0.9993
m-Diethylbenzene	180	1310.8	295.1	-2.51	0.94	0.9973
1,2,4-Trimethyl-benzene	161	1269.6	159.4	-2.78	0.51	0.9991
Fluorobenzene	114	1243.8	113.9	-3.52	0.36	0.9995
Chlorobenzene	127	1278.0	60.6	-3.36	0.19	0.9999
Bromobenzene	133	1282.4	36.8	-3.31	0.12	0.99996
Iodobenzene	142	1322.3	41.2	-3.30	0.13	0.99995
Nitrobenzene	86	1297.4	50.9	-3.91	0.16	0.9999

[a]95% Confidence limit on the slope.

[b]95% Confidence limit on the intercept.

[c]Correlation coefficient.

Column: C-4, 5 cm.
Mobile Phase: 40/60 Acetonitrile/Water

Compound	HSA(Å^2)	ln k' versus 1/T(°K) slope	95% CL[a]	intercept	95% CL[b]	R[c]
Biphenyl	182	1732.9	238.3	-3.41	0.76	0.9990
Naphthalene	156	1630.2	220.2	-3.57	0.70	0.9990
Phenanthrene	198	1763.7	219.0	-3.38	0.70	0.9992
Anthracene	202	1789.2	264.8	-3.38	0.85	0.9988
Pyrene	213	1783.3	234.8	-3.19	0.75	0.9991
Chrysene	241	1871.4	273.7	-3.10	0.88	0.9988
Fluoranthene	218	1825.6	250.3	-3.32	0.80	0.9990
n-Butylbenzene	181	1663.8	247.5	-2.68	0.79	0.9988
n-Hexylbenzene	217	1801.4	343.6	-2.22	1.10	0.9980
Benzene	110	1390.1	87.5	-3.54	0.28	0.9998
Toluene	127	1513.2	103.6	-3.53	0.33	0.9997
Ethylbenzene	145	1596.7	159.6	-3.36	0.51	0.9995
n-Propylbenzene	163	1688.7	209.6	-3.20	0.67	0.9992
p-Xylene	150	1466.8	159.1	-2.98	0.51	0.9994
o-Xylene	147	1498.3	155.8	-3.16	0.50	0.9994
m-Diethylbenzene	180	1693.6	282.1	-2.86	0.90	0.9985
1,2,4-Trimethyl-benzene	161	1487.6	180.6	-2.72	0.58	0.9992
Fluorobenzene	114	1448.2	173.1	-3.64	0.55	0.9992
Chlorobenzene	127	1530.9	197.5	-3.58	0.63	0.9991
Bromobenzene	133	1513.6	227.3	-3.41	0.73	0.9988
Iodobenzene	142	1630.7	177.4	-3.62	0.57	0.9994
Nitrobenzene	86	1548.3	142.1	-4.22	0.45	0.9995

[a] 95% Confidence limit on the slope.
[b] 95% Confidence limit on the intercept.
[c] Correlation coefficient.

Column: C-4, 5 cm.

Mobile Phase: 30/70 Acetonitrile/Water

Compound	HSA(Å^2)	ln k' versus 1/T(°K) slope	95% CL[a]	intercept	95% CL[b]	R[c]
Biphenyl	182	2161.4	323.4	-3.69	1.04	0.9988
Naphthalene	156	1971.1	291.6	-3.77	0.93	0.9988
Phenanthrene	198	2367.2	375.8	-4.12	1.20	0.9986
Anthracene	202	2260.5	253.9	-3.67	0.81	0.9993
Pyrene	213	2440.2	403.0	-3.99	1.29	0.9985
Chrysene	241	2630.1	445.6	-4.04	1.43	0.9985
Fluoranthene	218	2316.0	492.9	-3.57	1.58	0.9976
n-Butylbenzene	181	2133.1	295.3	-3.99	0.945	0.9990
n-Hexylbenzene	217	---	---	---	---	---
Benzene	110	1624.8	363.8	-3.74	1.18	0.9998
Toluene	127	1662.8	308.4	-3.31	0.99	0.9981
Ethylbenzene	145	1827.4	406.8	-3.26	1.30	0.9973
n-Propylbenzene	163	2010.3	503.7	-3.22	1.61	0.9966
p-Xylene	150	1773.2	161.6	-3.11	0.52	0.99955
o-Xylene	147	1806.4	206.9	-3.32	0.66	0.9993
m-Diethylbenzene	180	2054.1	616.2	-2.89	1.97	0.9952
1,2,4-Trimethylbenzene	161	1845.7	225.6	-2.91	0.72	0.9992
Fluorobenzene	114	1628.3	166.4	-3.59	0.53	0.9994
Chlorobenzene	127	1683.7	355.2	-3.33	1.14	0.9976
Bromobenzene	133	1821.7	81.35	-3.64	0.26	0.9999
Iodobenzene	142	1905.8	358.5	-3.65	1.15	0.9981
Nitrobenzene	86	1616.8	135.9	-3.85	0.435	0.9996

[a]95% Confidence limit on the slope.

[b]95% Confidence limit on the intercept.

[c]Correlation coefficient.

Column: C-8, 5 cm.

Mobile Phase: 65/35 Acetonitrile/Water

Compound	HSA(Å^2)	ln k' versus 1/T(°K) slope	95% CL[a]	intercept	95% CL[b]	R[c]
Biphenyl	182	936.4	207.3	-2.40	0.68	0.9974
Naphthalene	156	884.3	357.6	-2.47	1.20	0.9995
Phenanthrene	198	1047.5	182.6	-2.55	0.60	0.9984
Anthracene	202	1105.6	332.3	-2.69	1.10	0.9952
Pyrene	213	1280.2	197.3	-3.02	0.65	0.9987
Chrysene	241	1336.8	293.5	-3.02	0.97	0.9974
Fluoranthene	218	1220.6	188.5	-2.90	0.62	0.9987
n-Butylbenzene	181	973.9	311.7	-2.10	1.03	0.9945
n-Hexylbenzene	217	1053.5	383.2	-1.75	1.27	0.9929
Benzene	110	852.3	222.4	-2.84	0.73	0.9963
Toluene	127	899.0	340.8	-2.73	1.13	0.9923
Ethylbenzene	145	852.0	208.2	-2.31	0.69	0.9968
n-Propylbenzene	163	914.5	269.8	-2.21	0.89	0.9953
p-Xylene	150	866.6	175.7	-2.34	0.58	0.9978
o-Xylene	147	849.9	303.2	-2.34	1.00	0.9932
m-Diethylbenzene	180	901.5	449.0	-1.93	1.48	0.9869
1,2,4-Trimethyl-benzene	161	872.5	306.0	-2.13	1.01	0.9934
Fluorobenzene	114	775.0	107.4	-2.58	0.36	0.9990
Chlorobenzene	127	893.0	135.9	-2.70	0.45	0.9988
Bromobenzene	133	857.7	361.6	-2.50	1.20	0.9905
Iodobenzene	142	948.7	232.4	-2.66	0.77	0.9968
Nitrobenzene	86	901.8	294.0	-3.19	0.97	0.9943

[a]95% Confidence limit on the slope.

[b]95% Confidence limit on the intercept.

[c]Correlation coefficient.

Column: C-8, 5 cm, #2.

Mobile Phase: 60/40 Acetronitrile/Water

Compound	HSA(Å^2)	ln k' versus 1/T(°K) slope	95% CL[a]	intercept	95% CL[b]	R[c]
Biphenyl	182	1148.8	1417.2	-2.75	4.61	0.9953
Naphthalene	156	1091.2	219.8	-2.86	0.73	0.9978
Phenanthrene	198	1209.4	320.9	-2.74	1.06	0.9962
Anthracene	202	1224.8	288.7	-2.73	0.96	0.9970
Pyrene	213	1350.6	314.0	-2.89	1.04	0.9971
Chrysene	241	1393.8	398.9	-2.81	1.32	0.9956
Fluoranthene	218	1281.8	368.9	-2.73	1.22	0.9956
n-Butylbenzene	181	1021.9	308.1	-1.90	1.02	0.9951
n-Hexylbenzene	217	1133.1	561.9	-1.59	1.86	0.9870
Benzene	110	955.5	151.4	-2.93	0.50	0.9986
Toluene	127	938.9	446.6	-2.59	1.48	0.988
Ethylbenzene	145	1006.5	256.8	-2.52	0.85	0.9965
n-Propylbenzene	163	988.4	194.4	-2.12	0.64	0.9979
p-Xylene	150	934.8	170.0	-2.26	0.56	0.9982
o-Xylene	147	977.3	225.4	-2.46	0.75	0.9971
m-Diethylbenzene	180	1062.3	460.5	-2.10	1.52	0.9900
1,2,4-Trimethyl-benzene	161	999.6	224.2	-2.23	0.74	0.9973
Fluorobenzene	114	1249.0	906.4	-3.92	3.00	0.973
Chlorobenzene	127	1032.4	55.6	-2.88	0.18	0.998
Bromobenzene	133	1033.0	99.0	-2.80	0.33	0.9995
Iodobenzene	142	1061.0	258.0	-2.74	0.85	0.9968
Nitrobenzene	86	1055.7	180.0	-3.46	0.59	0.9984

[a]95% Confidence limit on the slope.

[b]95% Confidence limit on the intercept.

[c]Correlation coefficient.

Column: C-8, 5 cm.

Mobile Phase: 50/50 Acetonitrile/Water

Compound	HSA(Å^2)	ln k' versus 1/T(°K) slope	95% CL[a]	intercept	95% CL[b]	R[c]
Biphenyl	182	1442.1	828	-2.78	2.69	0.9990
Naphthalene	156	1404.3	906	-3.05	2.94	0.9987
Phenanthrene	198	1630.8	41	-3.17	0.13	0.99999
Anthracene	202	1674.3	214	-3.22	0.71	0.9991
Pyrene	213	1717.9	140	-3.11	0.46	0.9996
Chrysene	241	1853.5	80	-3.23	0.26	0.99999
Fluoranthene	218	1714.6	1194	-3.13	3.88	0.9985
n-Butylbenzene	181	1375.6	1007	-2.06	3.27	0.9983
n-Hexylbenzene	217	1603.8	1248	-1.97	4.06	0.9981
Benzene	110	1215.4	236	-3.12	.78	0.9980
Toluene	127	1370.2	1252	-3.25	4.07	0.9974
Ethylbenzene	145	1423.0	1024	-3.04	3.33	0.9984
n-Propylbenzene	163	1484.7	825	-2.83	2.68	0.9990
p-Xylene	150	1279.1	213	-2.58	0.69	0.9999
o-Xylene	147	1319.2	68	-2.78	0.22	0.99999
m-Diethylbenzene	180	1476.3	587	-2.48	1.91	0.9995
1,2,4-Trimethyl-benzene	161	1342.7	274	-2.47	0.89	0.9999
Fluorobenzene	114	1252.5	810	-3.18	2.63	0.9987
Chlorobenzene	127	1295.1	126	-2.99	0.41	0.9999
Bromobenzene	133	1365.2	1698	-3.11	5.51	0.9952
Iodobenzene	142	1420.3	531	-3.11	1.72	0.9996
Nitrobenzene	86	1321.6	149	-3.65	0.49	0.9993

[a]95% Confidence limit on the slope.

[b]95% Confidence limit on the intercept.

[c]Correlation coefficient.

Column: C-8, 5 cm.

Mobile Phase: 40/60 Acetonitrile/Water

Compound	HSA($\AA^2$)	ln k' versus 1/T(°K) slope	95% CL[a]	intercept	95% CL[b]	R^c
Biphenyl	182	1691.1	496	-2.64	1.59	0.9954
Naphthalene	156	1589.8	505	-2.85	1.62	0.9946
Phenanthrene	198	2049.6	167	-3.49	0.53	0.9996
Anthracene	202	1862.3	599	-2.80	1.92	0.9945
Pyrene	213	2220.6	204	-3.63	0.65	0.9995
Chrysene	241	2322.8	269	-3.52	0.86	0.9993
Fluoranthene	218	2169.4	371	-3.50	1.19	0.9984
n-Butylbenzene	181	1790.4	337	-2.37	1.08	0.9981
n-Hexylbenzene	217	1963.6	501	-1.87	1.60	0.9964
Benzene	110	1344.7	323	-2.97	1.04	0.9969
Toluene	127	1503.4	143	-2.99	0.46	0.9995
Ethylbenzene	145	1552.2	159	-2.67	0.51	0.9994
n-Propylbenzene	163	1668.2	154	-2.50	0.49	0.9995
p-Xylene	150	1485.6	454	-2.45	1.45	0.9950
o-Xylene	147	1599.8	122	-2.90	0.39	0.9997
m-Diethylbenzene	180	1661.9	187	-2.08	0.60	0.9993
1,2,4-Trimethylbenzene	161	1545.9	357	-2.25	1.14	0.9971
Fluorobenzene	114	1361.3	451	-2.93	1.44	0.9941
Chlorobenzene	127	1528.3	388	-3.04	1.24	0.9965
Bromobenzene	133	1512.8	399	-2.87	1.28	0.9963
Iodobenzene	142	1658.0	326	-3.10	1.04	0.9979
Nitrobenzene	86	1568.5	248	-3.86	0.79	0.9987

[a]95% Confidence limit on the slope.

[b]95% Confidence limit on the intercept.

[c]Correlation coefficient.

Column: C-8, 5 cm.

Mobile Phase: 30/70 Acetonitrile/Water

		ln k' versus 1/T(°K)				
Compound	HSA($\AA^2$)	slope	95% CL[a]	intercept	95% CL[b]	R[c]
Biphenyl	182	2396.6	1252.9	-3.73	4.01	0.9856
Naphthalene	156	2158.5	1042.1	-3.72	3.34	0.9876
Phenanthrene	198	---	---	---	---	---
Anthracene	202	---	---	---	---	---
Pyrene	213	---	---	---	---	---
Chrysene	241	---	---	---	---	---
Fluoranthene	218	---	---	---	---	---
n-Butylbenzene	181	---	---	---	---	---
n-Hexylbenzene	217	---	---	---	---	---
Benzene	110	1556.2	329.2	-3.03	1.05	0.9976
Toluene	127	1781.4	653.8	-3.12	2.09	0.9928
Ethylbenzene	145	1760.5	352.6	-2.40	1.13	0.9978
n-Propylbenzene	163	2161.2	751.5	-3.00	2.41	0.9935
p-Xylene	150	1838.6	1055.0	-2.68	3.38	0.9827
o-Xylene	147	1858.3	427.5	-2.85	1.37	0.9971
m-Diethylbenzene	180	2196.5	890.5	-2.59	2.85	0.9912
1,2,4-Trimethyl-benzene	161	2068.6	688.1	-2.89	2.20	0.9941
Fluorobenzene	114	1671.9	730.8	-3.25	2.34	0.9898
Chlorobenzene	127	1788.3	751.89	-3.07	2.41	0.9906
Bromobenzene	133	1876.2	477.3	-3.18	1.53	0.9965
Iodobenzene	142	2195.9	563.4	-3.92	1.80	0.9965
Nitrobenzene	86	1836.9	339.8	-4.07	1.09	0.9982

[a]95% Confidence limit on the slope.

[b]95% Confidence limit on the intercept.

[c]Correlation coefficient.

Column: C-2, 5 cm.

Mobile Phase: 60/40 Methanol/Water

Compound	HSA(Å^2)	slope	95% CL[a]	intercept	95% CL[b]	R[c]
		ln k' versus 1/T(°K)				
Biphenyl	182	1868.2	239.1	-5.87	0.76	0.9991
Naphthalene	156	1641.6	219.3	-5.60	0.70	0.9990
Phenanthrene	198	1939.4	283.2	-5.97	0.91	0.9989
Anthracene	202	1997.4	90.8	-6.06	0.29	0.9999
Pyrene	213	2094.9	183.7	-6.17	0.59	0.9996
Chrysene	241	2240.3	208.5	-6.29	0.67	0.9995
Fluoranthene	218	2068.7	165.6	-6.10	0.53	0.9996
n-Butylbenzene	181	1948.9	110.8	-5.65	0.35	0.9998
n-Hexylbenzene	217	2433.9	181.2	-6.38	0.58	0.9997
Benzene	110	1418.3	589.6	-5.51	1.89	0.9908
Toluene	127	1501.8	590.1	-5.41	1.89	0.9918
Ethylbenzene	145	1555.2	248.9	-5.21	0.80	0.9986
n-Propylbenzene	163	1737.1	142.5	-5.37	0.46	0.9996
p-Xylene	150	1507.0	602.0	-5.03	1.93	0.9915
o-Xylene	147	1562.7	262.2	-5.31	0.84	0.9985
m-Diethylbenzene	180	1881.9	305.8	-5.54	0.98	0.9986
1,2,4-Trimethyl-benzene	161	1683.4	57.1	-5.30	0.18	0.9999
Fluorobenzene	114	1237.9	1291.0	-4.79	4.11	0.9966
Chlorobenzene	127	1652.0	82.1	-5.85	0.26	0.9999
Bromobenzene	133	1437.9	81.8	-5.08	0.26	0.9998
Iodobenzene	142	1693.9	133.2	-5.78	0.43	0.9997
Nitrobenzene	86	1453.7	464.0	-5.74	1.48	0.9945

[a]95% Confidence limit on the slope.

[b]95% Confidence limit on the intercept.

[c]Correlation coefficient.

Column: C-2, 5 cm.

Mobile Phase: 50/50 Methanol/Water

Compound	HSA(Å^2)	ln k' versus 1/T(°K) slope	95% CL[a]	intercept	95% CL[b]	R[c]
Biphenyl	182	2325.0	140.9	-6.11	0.45	0.9998
Naphthalene	156	1970.9	139.1	-5.55	0.44	0.9997
Phenanthrene	198	2542.9	173.1	-6.58	0.55	0.9997
Anthracene	202	2617.2	189.2	-6.71	0.61	0.9997
Pyrene	213	2833.2	212.9	-7.12	0.68	0.9997
Chrysene	241	3157.9	301.7	-7.67	0.97	0.9995
Fluoranthene	218	2778.6	129.3	-6.96	0.41	0.9999
n-Butylbenzene	181	2448.0	267.3	-5.96	0.86	0.9994
n-Hexylbenzene	217	3177.9	354.0	-7.18	1.13	0.9993
Benzene	110	1330.9	367.6	-4.37	1.18	0.9959
Toluene	127	1566.9	177.8	-4.67	0.57	0.9993
Ethylbenzene	145	1796.9	241.3	-4.95	0.77	0.9990
n-Propylbenzene	163	2088.5	268.5	-5.35	0.86	0.9991
p-Xylene	150	1795.2	140.7	-4.92	0.45	0.9997
o-Xylene	147	1768.1	190.2	-4.94	0.61	0.9994
m-Diethylbenzene	180	2249.8	313.8	-5.49	1.00	0.9990
1,2,4-Trimethyl-benzene	161	2008.7	250.0	-5.23	0.80	0.9992
Fluorobenzene	114	1446.5	41.8	-4.59	0.13	0.9999
Chlorobenzene	127	1743.9	145.7	-5.15	0.47	0.9997
Bromobenzene	133	1811.8	532.1	-5.26	1.70	0.9954
Iodobenzene	142	1919.7	141.7	-5.44	0.45	0.9997
Nitrobenzene	86	1554.2	144.6	-5.18	0.46	0.9995

[a]95% Confidence limit on the slope.

[b]95% Confidence limit on the intercept.

[c]Correlation coefficient.

Column: C-2, 5 cm.

Mobile Phase: 40/60 Methanol/Water

Compound	HSA(Å^2)	ln k' versus 1/T(°K) slope	95% CL[a]	intercept	95% CL[b]	R[c]
Biphenyl	182	2917.1	342.6	-7.05	1.10	0.9993
Naphthalene	156	2423.4	312.2	-6.22	1.00	0.9991
Phenanthrene	198	3182.0	324.8	-7.54	1.04	0.9994
Anthracene	202	3393.0	376.0	-8.08	1.20	0.9994
Pyrene	213	3620.2	384.5	-8.39	1.23	0.9994
Chrysene	241	4132.1	380.7	-9.37	1.22	0.9995
Fluoranthene	218	3701.0	424.2	-8.67	1.36	0.9993
n-Butylbenzene	181	2923.9	696.7	-6.43	2.23	0.9969
n-Hexylbenzene	217	---	---	---	---	---
Benzene	110	1467.7	239.4	-4.32	0.77	0.9986
Toluene	127	1622.6	222.4	-4.24	0.71	0.9990
Ethylbenzene	145	1884.7	348.6	-4.50	1.12	0.9982
n-Propylbenzene	163	2270.4	483.4	-5.05	1.55	0.9976
p-Xylene	150	2198.3	799.3	-5.44	2.56	0.9929
o-Xylene	147	1890.3	392.6	-4.62	1.26	0.9977
m-Diethylbenzene	180	2387.4	668.5	-4.93	2.14	0.9958
1,2,4-Trimethyl-benzene	161	2317.3	590.3	-5.37	1.89	0.9965
Fluorobenzene	114	1643.9	304.5	-4.69	0.97	0.9982
Chlorobenzene	127	1948.1	355.1	-5.17	1.14	0.9982
Bromobenzene	133	2099.8	293.0	-5.52	0.94	0.9990
Iodobenzene	142	2249.2	346.0	-5.75	1.11	0.9987
Nitrobenzene	86	1733.7	127.8	-5.22	0.41	0.9997

[a]95% Confidence limit on the slope.

[b]95% Confidence limit on the intercept.

[c]Correlation coefficient.

Column: C-2, 5 cm.

Mobile Phase: 35/65 Methanol/Water

Compound	HSA(Å^2)	ln k' versus 1/T(°K) slope	95% CL[a]	intercept	95% CL[b]	R[c]
Biphenyl	182	3050.5	154.4	-7.02	0.49	0.9999
Naphthalene	156	2479.5	117.8	-6.04	0.38	0.9999
Phenanthrene	198	3428.0	1521.1	-7.79	0.49	0.9999
Anthracene	202	3468.1	134.5	-7.78	0.43	0.9999
Pyrene	213	3818.2	238.8	-8.40	0.76	0.9998
Chrysene	241	---	---	---	---	---
Fluoranthene	218	3920.6	40.0	-8.76	0.13	1.0000
n-Butylbenzene	181	2889.1	368.6	-5.82	1.18	0.9991
n-Hexylbenzene	217	---	---	---	---	---
Benzene	110	1291.7	100.2	-3.56	0.32	0.9997
Toluene	127	1541.8	139.7	-3.74	0.45	0.9996
Ethylbenzene	145	1851.5	185.7	-4.09	0.59	0.9995
n-Propylbenzene	163	2271.2	184.8	-4.67	0.59	0.9996
p-Xylene	150	1961.2	229.9	-4.40	0.74	0.9993
o-Xylene	147	1839.2	115.2	-4.14	0.37	0.9998
m-Diethylbenzene	180	2566.4	308.1	-5.04	0.99	0.9992
1,2,4-Trimethyl-benzene	161	2270.8	150.4	-4.83	0.48	0.9999
Fluorobenzene	114	1569.1	143.2	-4.23	0.46	0.9996
Chlorobenzene	127	1911.1	91.2	-4.78	0.29	0.9999
Bromobenzene	133	1992.5	31.8	-4.89	0.13	1.0000
Iodobenzene	142	2246.9	135.4	-5.42	0.43	0.9998
Nitrobenzene	86	1659.1	302.9	-4.78	0.97	0.9982

[a]95% Confidence limit on the slope.

[b]95% Confidence limit on the intercept.

[c]Correlation coefficient.

Column: C-4, 15 cm.

Mobile Phase: 75/25 Methanol/Water

Compound	HSA($Å^2$)	ln k' versus 1/T(°K) slope	95% CL[a]	intercept	95% CL[b]	R[c]
Biphenyl	182	936.7	205.4	-3.18	0.68	0.997
Naphthalene	156	788.7	217.8	-2.98	0.72	0.996
Phenanthrene	198	1085.4	468.6	-3.61	1.55	0.990
Anthracene	202	1032.6	170.0	-3.38	0.56	0.998
Pyrene	213	1252.7	483.6	-3.95	1.60	0.992
Chrysene	241	1295.9	474.1	-3.93	-1.60	0.992
n-Butylbenzene	181	1136.7	221.5	-3.39	0.73	0.998
n-Hexylbenzene	217	1474.8	219.5	-3.91	0.72	0.999
Benzene	110	545.2	250.7	-2.60	0.82	0.999
Toluene	127	657.6	310.3	-2.68	-1.03	0.988
Ethylbenzene	145	799.9	277.6	-2.88	0.98	0.994
n-Propylbenzene	163	957.9	285.3	-3.10	0.94	0.995
p-Xylene	150	816.2	312.9	-2.93	1.03	0.992
o-Xylene	147	860.4	460.3	-3.11	1.5	0.985
m-Diethylbenzene	180	1047.8	244.3	-3.16	0.81	0.997
1,2,4-Trimethyl-benzene	161	920.7	274.5	-3.03	0.91	0.995
Fluorobenzene	114	561.9	304.5	-2.64	1.007	0.984
Chlorobenzene	127	705.6	332.7	-2.85	1.1	0.988
Bromobenzene	133	714.7	177.3	-2.82	0.59	0.997
Iodobenzene	142	784.5	315.2	-2.90	1.04	0.991
Nitrobenzene	86	690.3	373.6	-3.28	-1.2	0.984

[a]95% Confidence limit on the slope.

[b]95% Confidence limit on the intercept.

[c]Correlation coefficient.

Column: C-4, 15 cm.

Mobile Phase: 70/30 Methanol/Water

Compound	HSA(Å^2)	ln k' versus 1/T(°K) slope	95% CL[a]	intercept	95% CL[b]	R[c]
Biphenyl	182	1310.0	187.4	-3.877	0.62	0.9989
Naphthalene	156	1135.6	294.2	-3.661	0.97	0.9964
Phenanthrene	198	1363.0	235.2	-3.969	0.78	0.9984
Anthracene	202	1419.9	181.9	-4.092	0.60	0.9991
Pyrene	213	1524.8	193.5	-4.252	0.64	0.9991
Chrysene	241	1642.6	154.0	-4.430	0.51	0.9995
n-Butylbenzene	181	1419.9	140.6	-3.759	0.46	0.9995
n-Hexylbenzene	217	1829.0	85.9	-4.385	0.28	0.9999
Benzene	110	868.6	565.2	-3.291	1.87	0.9770
Toluene	127	977.5	487.9	-3.324	1.61	0.9868
Ethylbenzene	145	1098.3	408.7	-3.402	1.35	0.9926
n-Propylbenzene	163	1262.6	320.2	-3.590	1.06	0.9965
p-Xylene	150	1127.2	355.2	-3.491	1.17	0.9947
o-Xylene	147	1068.6	281.4	-3.356	0.93	0.9963
m-Diethylbenzene	180	1369.0	271.7	-3.669	0.90	0.9979
1,2,4-Trimethylbenzene	161	1259.8	259.7	-3.665	0.86	0.9977
Fluorobenzene	114	879.9	490.0	-3.293	1.62	0.9837
Chlorobenzene	127	1035.9	458.0	-3.511	1.52	0.9896
Bromobenzene	133	1107.6	400.8	-3.673	1.33	0.9930
Iodobenzene	142	1141.2	393.1	-3.665	1.30	0.9937
Nitrobenzene	86	769.9	94.8	-3.20	0.30	0.9999

[a]95% Confidence limit on the slope.

[b]95% Confidence limit on the intercept.

[c]Correlation coefficient.

Column: C-4, 15 cm.

Mobile Phase: 60/40 Methanol/Water

Compound	HSA(Å^2)	ln k' versus 1/T(°K) slope	95% CL[a]	intercept	95% CL[b]	R[c]
Biphenyl	182	1792.4	121.0	-4.44	0.40	0.9997
Naphthalene	156	1553.3	253.4	-4.14	0.84	0.9986
Phenanthrene	198	1975.9	79.6	-4.88	0.26	1.000
Anthracene	202	2014.6	184.1	-4.93	0.61	0.9995
Pyrene	213	2218.2	96.7	-5.34	0.32	1.000
Chrysene	241	2450.2	45.1	-5.76	0.15	1.000
n-Butylbenzene	181	2038.7	84.8	-4.67	0.27	1.000
n-Hexylbenzene	217	2632.9	126.5	-5.62	0.40	0.9999
Benzene	110	1105.4	218.5	-3.39	0.72	0.9979
Toluene	127	1225.6	49.9	-3.37	0.16	0.9999
Ethylbenzene	145	1412.7	48.2	-3.56	0.16	0.9999
n-Propylbenzene	163	1638.6	110.2	-3.83	0.36	0.9998
p-Xylene	150	1440.7	49.1	-3.66	0.16	0.9999
o-Xylene	147	1400.4	71.8	-3.60	0.24	0.9999
m-Diethylbenzene	180	1814.6	414.0	-4.04	1.37	0.9972
1,2,4-Trimethyl-benzene	161	1596.8	82.0	-3.82	0.27	0.9999
Fluorobenzene	114	1145.9	73.2	-3.45	0.242	0.9998
Chlorobenzene	127	1355.5	104.8	-3.76	0.35	0.9997
Bromobenzene	133	1428.0	262.1	-3.90	0.87	0.9982
Iodobenzene	142	1486.6	74.8	-3.93	0.25	0.9999
Nitrobenzene	86	1290.4	88.3	-4.19	0.29	0.9997

[a]95% Confidence limit on the slope.
[b]95% Confidence limit on the intercept.
[c]Correlation coefficient.

Column: C-4, 15 cm.

Mobile Phase: 50/50 Methanol/Water

Compound	HSA(Å^2)	ln k' versus 1/T(°K) slope	95% CL[a]	intercept	95% CL[b]	R[c]
Biphenyl	182	2576.9	186.2	-5.98	0.60	0.9997
Naphthalene	156	2197.6	204.4	-5.40	0.65	0.9995
Phenanthrene	198	2876.7	137.2	-6.72	0.44	0.9999
Anthracene	202	2895.8	194.0	-6.68	0.62	0.9998
Pyrene	213	3219.6	155.1	-7.396	0.497	0.9999
Chrysene	241	3547.1	105.7	-7.97	0.34	0.9999
n-Butylbenzene	181	2783.0	132.3	-5.97	0.42	0.9999
Benzene	110	1533.1	277.1	-4.21	0.89	0.9982
Toluene	127	1775.1	179.7	-4.47	0.57	0.9994
Ethylbenzene	145	2034.1	188.3	-4.77	0.60	0.9995
n-Propylbenzene	163	2374.1	172.4	-5.27	0.55	0.9997
p-Xylene	150	2092.9	276.5	-4.96	0.88	0.9990
o-Xylene	147	1960.2	117.4	-4.64	0.38	0.9998
m-Diethylbenzene	180	2539.8	191.5	-5.35	0.61	0.9997
1,2,4-Trimethylbenzene	161	2264.96	188.6	-5.09	0.60	0.9996
Fluorobenzene	114	1592.7	155.9	-4.27	0.50	0.9995
Chlorobenzene	127	1927.1	193.9	-4.90	0.62	0.9994
Bromobenzene	133	2033.3	314.3	-5.12	1.01	0.9987
Iodobenzene	142	2148.8	188.7	-5.27	0.60	0.9996
Nitrobenzene	86	1738.0	214.0	-5.05	0.68	0.9992

[a]95% Confidence limit on the slope.

[b]95% Confidence limit on the intercept.

[c]Correlation coefficient.

Column: C-4, 15 cm.

Mobile Phase: 40/60 Methanol/Water

Compound	HSA(Å^2)	ln k' versus 1/T(°K) slope	95% CL[a]	intercept	95% CL[b]	R[c]
Biphenyl	182	---	---	---	---	---
Naphthalene	156	2567.7	92.7	-5.726	0.30	0.9999
Phenanthrene	198	---	---	---	---	---
Anthracene	202	---	---	---	---	---
Pyrene	213	---	---	---	---	---
Chrysene	241	---	---	---	---	---
Benzene	110	1569.6	45.8	-3.791	0.15	0.9999
Toluene	127	1859.3	198.2	-4.072	0.63	0.9994
Ethylbenzene	145	2185.3	192.8	-4.429	0.62	0.9996
n-Propylbenzene	163	---	---	---	---	---
p-Xylene	150	2212.8	186.7	-4.548	0.60	0.9996
o-Xylene	147	---	---	---	---	---
1,2,4-Trimethyl-benzene		2544.1	44.5	-5.056	0.14	0.9999
Fluorobenzene	114	1657.8	52.3	-3.891	0.17	0.9999
Chlorobenzene	127	2049.0	158.2	-4.585	0.51	0.9997
Bromobenzene	133	2179.7	233.6	-4.847	0.75	0.9994
Iodobenzene	142	2469.2	97.1	-5.486	0.31	0.9999
Nitrobenzene	86	1847.1	108.9	-4.808	0.35	0.9998

[a]95% Confidence limit on the slope.

[b]95% Confidence limit on the intercept.

[c]Correlation coefficient.

Column: C-8, 5 cm.

Mobile Phase: 80/20 Methanol/Water

Compound	HSA($Å^2$)	ln k' versus 1/T(°K) slope	95% CL[a]	intercept	95% CL[b]	R[c]
Biphenyl	182	1027.4	113.2	-3.36	0.37	0.9993
Naphthalene	156	916.4	62.3	-3.27	0.21	0.99975
Phenanthrene	198	1282.5	112.7	-4.12	0.36	0.99965
Anthracene	202	1410.5	113.7	-4.28	0.38	0.99965
Pyrene	213	1643.6	80.6	-4.71	0.27	0.99987
Chrysene	241	1856.5	70.3	-5.22	0.23	0.99992
n-Butylbenzene	181	1169.9	164.2	-3.42	0.54	0.99894
n-Hexylbenzene	217	1538.7	162.8	-4.02	0.54	0.9994
Benzene	110	420.8	237.45	-2.16	0.78	0.9833
Toluene	127	698.3	213.5	-2.75	0.71	0.995
Ethylbenzene	145	810.2	149.8	-2.88	0.50	0.9982
n-Propylbenzene	163	989.8	106.9	-3.15	0.35	0.9994
p-Xylene	150	970.5	7.5	-3.33	0.02	0.999997
o-Xylene	147	791.5	99.5	-2.79	0.33	0.99915
m-Diethylbenzene	180	1108.2	76.0	-3.27	0.25	0.9997
1,2,4-Trimethyl-benzene	161	1002.4	200.9	-3.14	0.66	0.9978
Fluorobenzene	114	420.6	98.8	-2.20	0.33	0.9970
Chlorobenzene	127	664.1	69.3	-2.66	0.23	0.9994
Bromobenzene	133	677.9	377.5	-2.63	1.25	0.9837
Iodobenzene	142	769.6	224.5	-2.79	0.74	0.9858
Nitrobenzene	86					
	n=4	442.5	228.3	-2.46	0.76	0.9858
	n=3	533.4	575.0	-2.75	1.87	0.9964

[a]95% Confidence limit on the slope.

[b]95% Confidence limit on the intercept.

[c]Correlation coefficient.

Column: C-8, 5 cm.

Mobile Phase: 70/30 Methanol/Water

Compound	HSA($Å^2$)	ln k' versus 1/T(°K) slope	95% CL[a]	intercept	95% CL[b]	R[c]
Biphenyl	182	1654.8	277.7	-4.44	0.92	0.9985
Naphthalene	156	1458.6	288.6	-4.21	0.95	0.9979
Phenanthrene	198	1984.4	217.7	-5.21	0.72	0.9993
Anthracene	202	2047.3	273.1	-5.34	0.90	0.9990
Pyrene	213	2331.3	190.5	-5.89	0.63	0.9996
Chrysene	241	2620.0	168.6	-6.52	0.56	0.9998
Fluoranthene	218	2297.4	543.6	-5.88	1.79	0.9998
n-Butylbenzene	181	1696.8	384.0	-4.08	1.27	0.9972
n-Hexylbenzene	217	2226.0	401.9	-4.97	1.33	0.9982
Benzene	110	929.1	200.5	-3.18	0.66	0.9975
Toluene	127	1176.8	217.3	-3.57	0.72	0.9982
Ethylbenzene	145	1340.2	193.0	-3.74	0.64	0.9989
n-Propylbenzene	163	1539.6	231.8	-3.98	0.77	0.9988
p-Xylene	150	1360.8	273.5	-3.76	0.90	0.9978
o-Xylene	147	1447.8	314.3	-4.12	1.04	0.9975
m-Diethylbenzene	180	1692.0	230.8	-4.13	0.76	0.9990
1,2,4-Trimethyl-benzene	161	1549.7	204.7	-4.02	0.68	0.9991
Fluorobenzene	114	990.0	377.0	-3.38	1.25	0.9923
Chlorobenzene	127	1158.6	300.1	-3.52	0.99	0.9964
Bromobenzene	133	1226.9	202.7	-3.63	0.67	0.9985
Iodobenzene	142	1340.5	285.8	-3.83	0.945	0.9975
Nitrobenzene	86	1211.3	216.7	-4.34	0.72	0.9983

[a]95% Confidence limit on the slope.

[b]95% Confidence limit on the intercept.

[c]Correlation coefficient.

Column: C-8, 5 cm.

Mobile Phase: 60/40 Methanol/Water

Compound	HSA(Å^2)	ln k' versus 1/T(°K) slope	95% CL[a]	intercept	95% CL[b]	R[c]
Biphenyl	182	2201.3	142.3	-5.17	0.46	0.9998
Naphthalene	156	1917.1	29.5	-4.80	0.09	1.000
Phenanthrene	198	2569.1	121.3	-6.00	0.39	0.9999
Anthracene	202	2668.3	48.9	-6.21	0.16	1.000
Pyrene	213	2958.1	169.7	-6.74	0.54	0.9998
Chrysene	241	3349.3	123.5	-7.56	0.39	0.9999
Fluoranthene	218	2889.7	91.6	-6.61	0.29	0.9999
n-Butylbenzene	181	2287.8	166.4	-4.85	0.53	0.9997
n-Hexylbenzene	217	2934.2	120.8	-5.83	0.39	0.9999
Benzene	110	1286.6	71.6	-3.68	0.23	0.9998
Toluene	127	1563.4	103.5	-4.06	0.33	0.9998
Ethylbenzene	145	1764.3	105.7	-4.24	0.34	0.9998
n-Propylbenzene	163	2046.5	100.9	-4.61	0.32	0.9999
p-Xylene	150	1845.3	115.2	-4.44	0.37	0.9998
o-Xylene	147	1718.2	88.3	-4.13	0.28	0.9999
m-Diethylbenzene	180	2245.1	82.2	-4.82	0.26	0.9999
1,2,4-Trimethyl-benzene	161	2048.6	52.1	-4.66	0.17	1.00
Fluorobenzene	114	1335.3	44.2	-3.78	0.14	0.9999
Chlorobenzene	127	1652.6	176.2	-4.32	0.56	0.9994
Bromobenzene	133	1687.6	31.8	-4.30	0.10	1.00
Iodobenzene	142	1847.9	176.1	-4.61	0.56	0.9995
Nitrobenzene	86	1524.1	142.9	-4.70	0.46	0.9995

[a]95% Confidence limit on the slope.

[b]95% Confidence limit on the intercept.

[c]Correlation coefficient.

Column: C-8, 5 cm.

Mobile Phase: 50/50 Methanol/Water

Compound	HSA($\AA^2$)	ln k' versus 1/T(°K)				
		slope	95% CL[a]	intercept	95% CL[b]	R[c]
Biphenyl	182	2753.1	627.25	-5.82	2.01	0.9972
Naphthalene	156	2276.4	406.4	-5.01	1.30	0.9983
Phenanthrene	198	3095.9	392.6	-6.47	1.26	0.9991
Anthracene	202	3147.9	134.0	-6.50	0.43	0.9999
Pyrene	213	3564.3	261.0	-7.33	0.83	0.9997
Chrysene	241	3482.8	279.0	-7.16	0.89	0.9996
Fluoranthene	218	3482.8	279.0	-7.16	0.89	0.9996
n-Butylbenzene	181	2659.8	124.1	-4.79	0.40	0.9999
n-Hexylbenzene	217	---	---	---	---	---
Benzene	110	1442.2	302.8	-3.52	0.97	0.9976
Toluene	127	1741.9	125.9	-3.83	0.40	0.9997
Ethylbenzene	145	1989.5	123.7	-4.03	0.40	0.9998
n-Propylbenzene	163	2323.6	120.0	-4.42	0.38	0.9999
p-Xylene	150	1982.2	388.6	-3.97	1.24	0.9979
o-Xylene	147	1959.8	348.4	-4.01	1.11	0.9983
m-Diethylbenzene	180	2496.6	144.1	-4.44	0.46	0.9998
1,2,4-Trimethyl-benzene	161	2239.2	349.0	-4.25	1.12	0.9987
Fluorobenzene	114	1497.7	218.1	-3.58	0.70	0.9989
Chlorobenzene	127	1812.9	318.1	-4.02	1.02	0.9983
Bromobenzene	133	1960.5	372.8	-4.34	1.19	0.9980
Iodobenzene	142	2070.1	386.4	-4.41	1.24	0.9981
Nitrobenzene	86	1722.2	374.5	-4.68	1.20	0.9975

[a]95% Confidence limit on the slope.

[b]95% Confidence limit on the intercept.

[c]Correlation coefficient.

APPENDIX C
ΔH° AS A FUNCTION OF ORGANIC SOLVENT CONTENT

Column: C-2, 5 cm.
Mobile phase: Methanol/Water (v/v) mixtures, % MeOH given

Compound	$\Delta H°$ (kcal/mol) at given volume fraction of organic solvent			
	0.60	0.50	0.40	0.35
Biphenyl	-3.71	-4.62	-5.80	-6.06
Naphthalene	-3.26	-3.92	-4.82	-4.93
Phenanthrene	-3.85	-5.05	-6.32	-6.81
Anthracene	-3.97	-5.20	-6.74	-6.89
Pyrene	-4.16	-5.63	-7.19	-7.59
Chrysene	-4.45	-6.27	-8.21	---
Fluorathene	-4.11	-5.52	-7.35	-7.79
Benzene	-2.82	-2.64	-2.92	-2.57
Toluene	-2.98	-3.11	-3.22	-3.06
Ethylbenzene	-3.09	-3.57	-3.75	-3.68
n-Propylbenzene	-3.45	-4.15	-4.51	-4.51
n-Butylbenzene	-3.87	-4.86	-5.81	-5.74
n-Hexylbenzene	-4.84	-6.31	---	---
p-Xylene	-2.99	-3.57	-4.37	-3.90
o-Xylene	-3.11	-3.51	-3.76	-3.65
m-Diethylbenzene	-3.74	-4.47	-4.74	-5.10
1,2,4-Trimethyl-benzene	-3.35	-3.99	-4.60	-4.51
Fluorobenzene	-2.46	-2.87	-3.27	-3.12
Chlorobenzene	-3.28	-3.46	-3.87	-3.80
Bromobenzene	-2.86	-3.60	-4.17	-3.96
Iodobenzene	-3.37	-3.81	-4.47	-4.47
Nitrobenzene	-2.89	-3.09	-3.45	-3.30

Conditions: (1) Flow rate = 1.0 mL/min.
(2) UV detector, 254 nm.
(3) Column void volume determined with 25 g/L $NaNO_3$.

Column: C-4, 15 cm.
Mobile phase: Methanol/Water (v/v) mixtures, % MeOH given

Compound	ΔH° (kcal/mol) at given volume fraction of organic solvent				
	0.75	0.70	0.60	0.50	0.40
Biphenyl	-1.86	-2.60	-3.56	-5.12	---
Naphthalene	-1.57	-2.26	-3.09	-4.37	-5.10
Phenanthrene	-2.16	-2.71	-3.93	-5.72	---
Anthracene	-2.05	-2.82	-4.00	-5.75	---
Pyrene	-2.49	-3.03	-4.41	-6.40	---
Chrysene	-2.58	-3.23	-4.87	-7.05	---
Benzene	-1.08	-1.73	-2.20	-3.05	-3.12
Toluene	-1.31	-1.94	-2.44	-3.53	-3.69
Ethylbenzene	-1.59	-2.18	-2.81	-4.04	-4.34
n-Propylbenzene	-1.90	-2.51	-3.26	-4.72	---
n-Butylbenzene	-2.26	-2.82	-4.05	-5.53	---
n-Hexylbenzene	-2.93	-3.63	-5.23	---	---
p-Xylene	-1.62	-2.24	-2.86	-4.16	-4.40
o-Xylene	-1.71	-2.12	-2.78	-3.90	---
m-Diethylbenzene	-2.08	-2.72	-3.61	-5.05	---
1,2,4-Trimethyl-benzene	-1.83	-2.50	-3.17	-4.50	-5.06
Fluorobenzene	-1.12	-1.75	-2.28	-3.17	-3.29
Chlorobenzene	-1.40	-2.06	-2.69	-3.83	-4.07
Bromobenzene	-1.42	-2.20	-2.84	-4.04	-4.33
Iodobenzene	-1.56	-2.27	-2.95	-4.27	-4.91
Nitrobenzene	-1.37	-1.53	-2.56	-3.45	-3.67

Conditions: (1) Flow rate = 1.0 mL/min.

(2) UV detector, 254 nm.

(3) Column void volume determined with 25 g/L $NaNO_3$.

Column: C-8, 5 cm.
Mobile phase: Methanol/Water (v/v) mixtures, % MeOH given

	ΔH° (kcal/mol) at given volume fraction of organic solvent			
Compound	0.80	0.70	0.60	0.50
Biphenyl	-2.04	-3.29	-4.37	-5.47
Naphthalene	-1.82	-2.90	-3.81	-4.52
Phenanthrene	-2.55	-3.94	-5.11	-6.15
Anthracene	-2.80	-4.07	-5.30	-6.26
Pyrene	-3.27	-4.63	-5.88	-7.08
Chrysene	-3.69	-5.21	-6.66	-6.92
Fluorathene	---	-4.56	-5.74	-6.92
Benzene	-0.84	-1.85	-2.56	-2.87
Toluene	-1.39	-2.34	-3.11	-3.46
Ethylbenzene	-1.61	-2.66	-3.51	-3.95
n-Propylbenzene	-1.97	-3.06	-4.07	-4.62
n-Butylbenzene	-2.32	-3.37	-4.55	-5.29
n-Hexylbenzene	-3.06	-4.42	-5.83	---
p-Xylene	-1.93	-2.70	-3.67	-3.94
o-Xylene	-1.57	-2.88	-3.41	-3.90
m-Diethylbenzene	-2.02	-3.36	-4.46	-4.96
1,2,4-Trimethylbenzene	-1.99	-3.08	-4.07	-4.45
Fluorobenzene	-0.84	-1.97	-2.65	-2.98
Chlorobenzene	-1.32	-2.30	-3.28	-3.60
Bromobenzene	-1.35	-2.44	-3.35	-3.90
Iodobenzene	-1.53	-2.66	-3.67	-4.11
Nitrobenzene	-0.88	-2.41	-3.03	-3.42

Conditions: (1) Flow rate = 1.0 mL/min.
(2) UV detector, 254 nm.
(3) Column void volume determined with 25 g/L $NaNO_3$.

Column: C-2, 5 cm.
Mobile phase: Acetonitrile/Water (v/v) mixtures, % ACN given

Compound	ΔH° (kcal/mol) at given volume fraction of organic solvent			
	0.50	0.40	0.30	0.25
Biphenyl	-2.93	-3.79	-5.02	-5.60
Naphthalene	-2.84	-3.64	-4.56	-4.99
Phenanthrene	-2.96	-3.79	-5.29	-5.81
Anthracene	-2.90	-3.88	-5.24	-6.00
Pyrene	-2.95	-3.83	-5.44	-6.12
Chrysene	-3.07	-4.01	-5.86	---
Fluorathene	-3.05	-3.88	-5.49	-6.14
Benzene	-2.60	-3.09	-3.78	-3.58
Toluene	-2.77	-3.14	-3.73	-3.98
Ethylbenzene	-2.83	-3.27	-4.14	-4.37
n-Propylbenzene	-2.87	-3.43	-4.51	-4.90
n-Butylbenzene	-3.10	-3.50	-4.70	-5.34
n-Hexylbenzene	-3.19	-3.94	---	---
p-Xylene	-2.83	-3.29	-4.12	-4.09
o-Xylene	-2.72	-3.27	-4.11	-3.75
m-Diethylbenzene	-2.55	-3.40	-4.64	-5.05
1,2,4-Trimethylbenzene	-3.03	-3.26	-4.22	-4.70
Fluorobenzene	-2.69	-3.21	-3.82	-3.88
Chlorobenzene	-2.76	-3.57	-4.05	-4.08
Bromobenzene	-2.75	-3.43	-4.07	-4.49
Iodobenzene	-2.85	-3.49	-4.46	-4.64
Nitrobenzene	-2.48	-3.34	-3.90	-3.84

Conditions: (1) Flow rate = 1.0 mL/min.
(2) UV detector, 254 nm.
(3) Column void volume determined with 25 g/L $NaNO_3$.

Column: C-4
Mobile phase: Acetonitrile/Water (v/v) mixtures, % ACN given

Compound	$\Delta H°$ (kcal/mol) at given volume fraction of organic solvent 0.60	0.50	0.40	0.30
Biphenyl	-2.37	-2.71	-3.44	-4.30
Naphthalene	-2.28	-2.66	-3.24	-3.92
Phenanthrene	-2.45	-2.78	-3.50	-4.70
Anthracene	-2.47	-2.80	-3.56	-4.49
Pyrene	-2.31	-2.82	-3.54	-4.85
Chrysene	-2.49	-2.89	-3.72	-5.23
Fluorathene	-2.53	-2.80	-3.63	-4.60
Benzene	-2.18	-2.46	-2.76	-3.23
Toluene	-2.15	-2.51	-3.01	-3.30
Ethylbenzene	-2.29	-2.57	-3.17	-3.63
n-Propylbenzene	-2.31	-2.65	-3.36	-4.00
n-Butylbenzene	-2.39	-2.71	-3.31	-4.24
n-Hexylbenzene	-2.48	-2.84	-3.58	---
p-Xylene	-2.05	-2.50	-2.91	-3.52
o-Xylene	-2.03	-2.46	-2.98	-3.59
m-Diethylbenzene	-2.59	-2.60	-3.37	-4.08
1,2,4-Trimethyl-benzene	-2.26	-2.52	-2.96	-3.67
Fluorobenzene	-2.20	-2.47	-2.88	-3.24
Chlorobenzene	-2.28	-2.54	-3.04	-3.35
Bromobenzene	-2.20	-2.55	-3.01	-3.62
Iodobenzene	-2.38	-2.63	-3.24	-3.79
Nitrobenzene	-2.48	-2.58	-3.08	-3.21

Conditions: (1) Flow rate = 1.0 mL/min.
(2) UV detector, 254 nm.
(3) Column void volume determined with 25 g/L $NaNO_3$.

Column: C-8, 5 cm.
Mobile phase: Acetonitrile/Water (v/v) mixtures, % ACN given

Compound	ΔH° (kcal/mol) at given volume fraction of organic solvent				
	0.65	0.60	0.50	0.40	0.30
Biphenyl	-1.86	-2.28	-2.87	-3.36	-4.76
Naphthalene	-1.76	-2.17	-2.79	-3.16	-4.29
Phenanthrene	-2.08	-2.40	-3.24	-4.07	---
Anthracene	-2.20	-2.43	-3.33	-3.70	---
Pyrene	-2.54	-2.68	-3.41	-4.41	---
Chrysene	-2.66	-2.77	-3.68	-4.62	---
Fluorathene	-2.43	-2.55	-3.41	-4.31	---
Benzene	-1.69	-1.90	-2.41	-2.67	-3.09
Toluene	-1.79	-1.87	-2.72	-2.99	-3.54
Ethylbenzene	-1.69	-2.00	-2.83	-3.08	-3.50
n-Propylbenzene	-1.82	-1.96	-2.95	-3.32	-4.29
n-Butylbenzene	-1.94	-2.03	-3.73	-3.56	---
n-Hexylbenzene	-2.09	-2.25	-3.19	-3.90	---
p-Xylene	-1.72	-1.86	-2.54	-2.95	-3.40
o-Xylene	-1.69	-1.94	-2.62	-3.18	-3.69
m-Diethylbenzene	-1.79	-2.11	-2.93	-3.30	-4.36
1,2,4-Trimethylbenzene	-1.73	-1.99	-2.67	-3.07	-4.11
Fluorobenzene	-1.54	-2.48	-2.49	-2.70	-3.32
Chlorobenzene	-1.77	-2.05	-2.57	-3.04	-3.55
Bromobenzene	-1.70	-2.05	-2.71	-3.01	-3.73
Iodobenzene	-1.89	-2.11	-2.82	-3.30	-4.36
Nitrobenzene	-1.79	-21.0	-2.63	-3.12	-3.65

Conditions: (1) Flow rate = 1.0 mL/min.

(2) UV detector, 254 nm.

(3) Column void volume determined with 25 g/L $NaNO_3$.

APPENDIX D
ΔS° AS A FUNCTION OF ORGANIC SOLVENT CONTENT

Column: C-2, 5 cm.
Mobile phase: Methanol/Water (v/v) mixtures, % MeOH given

Compound	ΔS° (cal/mol-°K) at given volume fraction of organic solvent			
	0.60	0.50	0.40	0.35
Biphenyl	-6.94	-7.41	-9.28	-9.22
Naphthalene	-6.40	-6.30	-7.63	-7.27
Phenanthrene	-7.13	-8.35	-10.25	-10.75
Anthracene	-7.31	-8.60	-11.33	-10.73
Pyrene	-7.53	-9.42	-11.94	-11.96
Chrysene	-7.77	-10.51	-13.89	---
Fluoranthene	-7.39	-9.10	-12.50	-12.68
Benzene	-6.22	-3.95	-3.86	-2.34
Toluene	-6.02	-4.55	-3.70	-2.70
Ethylbenzene	-5.62	-5.11	-4.21	-3.40
n-Propylbenzene	-5.94	-5.90	-5.31	-4.55
n-Butylbenzene	-6.50	-7.11	-8.05	-6.84
n-Hexylbenzene	-7.95	-9.54	---	---
p-Xylene	-5.27	-5.05	-6.08	-4.01
o-Xylene	-5.82	-5.09	-4.45	-3.50
m-Diethylbenzene	-6.28	-6.18	-5.07	-5.29
1,2,4-Trimethyl-benzene	-5.80	-5.66	-5.94	-4.87
Fluorobenzene	-4.79	-4.39	-4.59	-4.77
Chlorobenzene	-6.90	-5.50	-5.54	-4.77
Bromobenzene	-5.37	-5.72	-6.24	-4.99
Iodobenzene	-6.76	-6.08	-6.70	-6.04
Nitrobenzene	-6.68	-5.56	-5.64	-4.77

Conditions: (a) Flow rate = 1.0 mL/min.
(b) UV detector, 254 nm.
(c) Void volume measured with 25 g/L $NaNO_3$.
(d) Calculated phase ratio = 0.0926.

Column: C-4, 15 cm

Mobile phase: Methanol/Water (v/v) mixtures, % MeOH given

Compound	ΔS° (cal/mol-°K) at given volume fraction of organic solvent				
	0.75	0.70	0.60	0.50	0.40
Biphenyl	-2.15	-3.54	-4.65	-7.71	---
Naphthalene	-1.75	-3.10	-4.05	-6.56	-7.21
Phenanthrene	-3.00	-3.72	-5.52	-9.18	---
Anthracene	-2.54	-3.95	-5.62	-9.10	---
Pyrene	-3.68	-4.27	-6.44	-10.53	---
Chrysene	-3.64	-4.63	-7.27	-11.66	---
Benzene	-0.99	-2.36	-2.56	-4.19	-3.36
Toluene	-1.15	-2.42	-2.52	-4.71	-3.91
Ethylbenzene	-1.55	-2.58	-2.90	-5.31	-4.63
n-Propylbenzene	-1.99	-2.96	-3.44	-6.30	---
n-Butylbenzene	-2.56	-3.30	-5.11	-7.69	---
n-Hexylbenzene	-3.60	-4.54	-6.99	---	---
p-Xylene	-1.65	-2.76	-3.10	-5.68	-4.86
o-Xylene	-2.01	-2.50	-2.98	-5.05	---
m-Diethylbenzene	-2.11	-3.12	-3.86	-6.46	---
1,2,4-Trimethylbenzene	-1.85	-3.11	-3.42	-5.94	-5.87
Fluorobenzene	-1.07	-2.37	-2.68	-4.31	-3.56
Chlorobenzene	-1.49	-2.80	-3.30	-5.56	-4.94
Bromobenzene	-1.43	-3.13	-3.58	-6.00	-5.46
Iodobenzene	-1.59	-3.11	-3.64	-6.30	-6.73
Nitrobenzene	-2.34	-2.19	-4.15	-5.86	-5.38

Conditions: (a) Flow rate = 1.0 mL/min.
(b) UV detector, 254 nm.
(c) Void volume measured with 25 g/L $NaNO_3$.
(d) Calculated phase ratio = 0.1224.

Column: C-8, 5 cm

Mobile phase: Methanol/Water (v/v) mixtures, % MeOH given

	ΔS° (cal/mol-°K) at given volume fraction of organic solvent			
Compound	0.80	0.70	0.60	0.50
Biphenyl	-2.84	-4.99	-6.44	-7.73
Naphthalene	-2.66	-4.53	-5.70	-6.12
Phenanthrene	-4.35	-6.52	-8.09	-9.02
Anthracene	-4.67	-6.78	-8.51	-9.08
Pyrene	-5.52	-7.87	-9.56	-10.73
Chrysene	-6.54	-9.12	-11.19	---
Fluoranthene	---	-7.85	-9.30	-10.27
Benzene	-0.46	-2.48	-3.48	-3.16
Toluene	-1.63	-3.26	-4.23	-3.78
Ethylbenzene	-1.89	-3.60	-4.59	-4.17
n-Propylbenzene	-2.42	-4.07	-5.33	-4.95
n-Butylbenzene	-2.96	-4.27	-5.80	-5.68
n-Hexylbenzene	-4.15	-6.04	-7.75	---
p-Xylene	-2.78	-3.64	-4.99	-4.05
o-Xylene	-1.71	-4.35	-4.37	-4.13
m-Diethylbenzene	-2.66	-4.37	-5.74	-4.99
1,2,4-Trimethylbenzene	-2.40	-4.15	-5.43	-4.61
Fluorobenzene	-0.54	-2.88	-3.68	-3.28
Chlorobenzene	-1.45	-3.16	-4.75	-4.15
Bromobenzene	-1.39	-3.38	-4.71	-4.79
Iodobenzene	-1.71	-3.78	-5.33	-4.93
Nitrobenzene	-1.05	-4.79	-5.50	-5.46

Conditions: (a) Flow rate = 1.0 mL/min.

(b) UV detector, 254 nm.

(c) Void volume measured with 25 g/L $NaNO_3$.

(d) Calculated phase ratio = 0.1454.

Column: C-2, 5 cm

Mobile phase: Acetonitrile/Water (v/v) mixtures, % ACN given

	$\Delta S°$ (cal/mol-°K) at given volume fraction of organic solvent			
Compound	0.50	0.40	0.30	0.25
Biphenyl	-3.16	-3.82	-5.88	-6.84
Naphthalene	-3.50	-4.27	-5.68	-6.38
Phenanthrene	-3.08	-3.54	-6.28	-6.90
Anthracene	-2.76	-3.68	-5.90	-7.23
Pyrene	-2.70	-3.18	-6.06	-7.03
Chrysene	-2.60	-3.02	-6.32	---
Fluoranthene	-3.00	-3.30	-6.18	-6.99
Benzene	-3.62	-3.86	-5.21	-4.23
Toluene	-3.70	-3.28	-4.03	-4.39
Ethylbenzene	-3.36	-2.94	-4.31	-4.45
n-Propylbenzene	-2.90	-2.62	-4.39	-4.85
n-Butylbenzene	-3.06	-2.09	-3.91	-4.99
n-Hexylbenzene	-2.21	-1.93	---	---
p-Xylene	-3.36	-3.02	-4.33	-3.60
o-Xylene	-3.10	-3.12	-4.45	-2.68
m-Diethylbenzene	-1.41	-1.93	-3.97	-4.35
1,2,4-Trimethylbenzene	-3.58	-2.38	-3.88	-4.59
Fluorobenzene	-3.82	-4.03	-4.99	-4.81
Chlorobenzene	-3.60	-4.59	-4.95	-4.53
Bromobenzene	-3.46	-4.03	-4.83	-5.58
Iodobenzene	-3.58	-3.88	-5.58	-5.52
Nitrobenzene	-3.40	-4.85	-5.68	-5.13

Conditions: (a) Flow rate = 1.0 mL/min.

(b) UV detector, 254 nm.

(c) Void volume measured with 25 g/L $NaNO_3$.

(d) Calculated phase ratio = 0.0926.

Column: C-4, 5 cm.

Mobile phase: Acetonitrile/Water (v/v) mixtures, % ACN given

Compound	$\Delta S°$ (cal/mol-°K) at given volume fraction of organic solvent 0.60	0.50	0.40	0.30
Biphenyl	-2.21	-1.81	-2.50	-3.06
Naphthalene	-2.42	-2.36	-2.82	-3.22
Phenanthrene	-2.33	-1.85	-2.44	-3.91
Anthracene	-2.27	-1.81	-2.44	-3.02
Pyrene	-1.57	-1.61	-2.07	-3.66
Chrysene	-1.81	-1.31	-1.89	-3.76
Fluoranthene	-2.31	-1.53	-2.32	-2.82
Benzene	-2.86	-2.76	-2.76	-3.16
Toluene	-2.31	-2.33	-2.74	-2.30
Ethylbenzene	-2.25	-1.85	-2.40	-2.21
n-Propylbenzene	-1.75	-1.39	-2.09	-2.13
n-Butylbenzene	-1.51	-0.93	-1.05	-1.67
n-Hexylbenzene	-0.72	+0.04	-0.14	---
p-Xylene	-1.49	-1.65	-1.65	-2.01
o-Xylene	-1.51	-1.67	-2.01	-2.32
m-Diethylbenzene	-2.23	-0.72	-1.41	-1.47
1,2,4-Trimethylbenzene	-1.77	-1.25	-1.13	-1.51
Fluorobenzene	-2.90	-2.72	-2.96	-2.86
Chlorobenzene	-2.74	-2.40	-2.84	-2.34
Bromobenzene	-2.36	-2.31	-2.50	-2.96
Iodobenzene	-2.72	-2.29	-2.92	-2.98
Nitrobenzene	-4.15	-3.50	-4.11	-3.38

Conditions: (a) Flow rate = 1.0 mL/min.
(b) UV detector, 254 nm.
(c) Void volume measured with 25 g/L $NaNO_3$.
(d) Calculated phase ratio = 0.1170.

Column: C-8, 5 cm.

Mobile phase: Acetonitrile/Water (v/v) mixtures, % ACN given

Compound	$\Delta S°$ (cal/mol-°K) at given volume fraction of organic solvent				
	0.65	0.60	0.50	0.40	0.30
Biphenyl	-0.93	-1.63	-1.69	-1.41	-3.58
Naphthalene	-1.07	-1.85	-2.23	-1.83	-3.56
Phenanthrene	-1.23	-1.61	-2.46	-3.10	---
Anthracene	-1.51	-1.59	-2.56	-1.73	---
Pyrene	-2.17	-1.91	-2.34	-3.38	---
Chrysene	-2.17	-1.75	-2.58	-3.16	---
Fluoranthene	-1.93	-1.59	-2.38	-3.12	---
Benzene	-1.81	-1.99	-2.36	-2.07	-2.19
Toluene	-1.59	-1.31	-2.62	-2.11	-2.36
Ethylbenzene	-0.76	-1.17	-2.21	-1.47	-0.93
n-Propylbenzene	-0.56	-0.38	-1.79	-1.13	-2.13
n-Butylbenzene	-0.34	+0.06	-0.26	-0.87	---
n-Hexylbenzene	+0.36	+0.68	-0.08	+0.12	---
p-Xylene	-0.81	-0.66	-1.29	-1.03	-1.49
o-Xylene	-0.81	-1.05	-1.69	-1.93	-1.83
m-Diethylbenzene	0.00	-0.34	-1.09	-0.30	-1.31
1,2,4-Trimethyl-benzene	-0.40	-0.60	-1.07	-0.64	-1.91
Fluorobenzene	-1.29	-3.95	-2.48	-1.99	-2.62
Chlorobenzene	-1.53	-1.89	-2.11	-2.21	-2.27
Bromobenzene	-1.13	-1.73	-2.34	-1.87	-2.48
Iodobenzene	-1.45	-1.61	-2.34	-2.33	-3.95
Nitrobenzene	-2.50	-3.04	-3.42	-3.84	-4.25

Conditions: (a) Flow rate = 1.0 mL/min.

(b) UV detector, 254 nm.

(c) Void volume measured with 25 g/L $NaNO_3$.

(d) Calculated phase ratio = 0.1454.

APPENDIX E
REGRESSION COEFFICIENTS FOR THE ENTHALPY-ENTROPY COMPENSATION MODEL

Column: C-2, 5 cm.
Mobile phase: Methanol/Water
Compensation temperature (β) = 625°K
Compensation model: $\ln k' = A_1\theta\ (1 - \beta/T) + A_2/T + A_3$

Compound	A_1	A_2	A_3	R
Biphenyl	10.74	5567.4	-11.35	0.9976
Naphthalene	8.90	4701.3	- 9.97	0.9951
Phenanthrene	11.70	6154.3	-12.38	0.9987
Anthracene	11.90	6308.9	-12.66	0.9987
Pyrene	13.07	6869.8	-13.56	0.9994
Chrysene	14.89	7830.4	-15.22	0.9996
Fluoranthene	13.00	6873.7	-13.63	0.9994
Benzene	6.09	3138.4	- 7.26	0.9837
Toluene	7.13	3620.1	- 7.81	0.9886
Ethylbenzene	8.24	4153.2	- 8.50	0.9929
n-Propylbenzene	9.62	4873.7	- 9.56	0.9958
n-Butylbenzene	11.28	5814.3	-11.19	0.9979
n-Hexylbenzene	15.76	8223.4	-15.45	0.9998
p-Xylene	8.33	4272.2	- 8.80	0.9932
o-Xylene	8.12	4113.4	- 8.51	0.9929
m-Diethylbenzene	10.72	5368.8	-10.21	0.9973
1,2,4-Trimethylbenzene	9.34	4769.3	- 9.50	0.9963
Fluorobenzene	6.49	3326.9	- 7.51	0.9872
Chlorobenzene	7.51	3585.9	- 8.71	0.9904
Bromobenzene	7.82	4096.9	- 8.80	0.9921
Iodobenzene	8.45	4468.9	- 9.50	0.9941
Nitrobenzene	6.44	3463.1	- 8.21	0.9875

Regression Analysis: A_2 vs. A_1

n = 22, R = 0.9979
Slope = 530.6 $\pm$ 16.1 = $-\beta/\alpha$
Intercept = -101.6 $\pm$ 163.9 = $-\Delta H^{o}_{n}(0)/R$

where R is the correlation coefficient and the regression values represent mean values $\pm$ 95% confidence limits.

Assuming β = 625°K, from the slope: $\alpha = -1.17 \pm 0.03$

From the y-intercept: $\Delta H^{o}_{n}(0)$ = 0.20 kcal/mol $\pm$ 0.33

For details, refer to Table 3-1.

Column: C-4, 15 cm.
Mobile phase: Methanol/Water
Compensation temperature (β) = 625°K
Compensation model: $\ln k' = A_1\theta\ (1 - \beta/T) + A_2/T + A_3$

Compound	A_1	A_2	A_3	R
Biphenyl	9.78	5549.4	-10.60	0.9999
Naphthalene	8.40	4762.3	- 9.39	0.9999
Phenanthrene	10.47	5989.3	-11.45	0.9999
Anthracene	10.67	6085.4	-11.55	0.9999
Pyrene	11.37	6565.2	-12.42	0.9998
Chrysene	12.67	7250.6	-13.50	0.9989
Benzene	5.92	3353.6	- 7.09	0.9982
Toluene	6.97	3895.0	- 7.78	0.9993
Ethylbenzene	8.17	4540.4	- 8.70	0.9997
n-Propylbenzene	9.43	5324.4	- 9.99	0.9998
n-Butylbenzene	10.74	6125.2	-11.30	0.9999
n-Hexylbenzene	13.26	7634.1	-13.67	0.9999
p-Xylene	8.08	4535.4	- 8.74	0.9997
o-Xylene	7.91	4494.0	- 8.78	0.9996
m-Diethylbenzene	10.31	5807.6	-10.65	0.9998
1,2,4-Trimethylbenzene	9.00	5050.4	- 9.48	0.9998
Fluorobenzene	6.42	3565.8	- 7.40	0.9987
Chlorobenzene	7.29	4126.7	- 8.30	0.9994
Bromobenzene	7.58	4316.5	- 8.63	0.9995
Iodobenzene	8.11	4612.7	- 9.10	0.9998
Nitrobenzene	6.20	3645.6	- 8.06	0.9990

Regression Analysis: $A_2(y)$ vs. $A_1(x)$

n = 21, R = 0.9990
Slope = 581.0 $\pm$ 12.8 = $-\beta/\alpha$
Intercept = -115.6 $\pm$ 117.6 = $-\Delta H^{o}_{n}(0)/R$

where R is the correlation coefficient and the regression values represent mean values $\pm$ 95% confidence limits.

Assuming β = 625°K, from the slope: $\alpha = 1.08 \pm 0.03$

From the intercept: $\Delta H^{o}_{n}(0)$ = 0.23 kcal/mol $\pm$ 0.23

For details, refer to Table 3-1.

Column: C-8, 5 cm.
Mobile phase: Methanol/Water
Compensation temperature (β) = 525°K
Compensation model: $\ln k' = A_1\theta\ (1 - \beta/T) + A_2/T + A_3$

Compound	A_1	A_2	A_3	R
Biphenyl	14.83	6972.4	-14.33	0.9985
Naphthalene	12.61	5944.1	-12.51	0.9986
Phenanthrene	15.76	7639.1	-15.73	0.9980
Anthracene	16.13	7830.9	-16.08	0.9977
Pyrene	17.00	8438.4	-17.25	0.9972
Chrysene	17.69	9040.8	-18.58	0.9988
Fluoranthene	18.31	8730.2	-17.76	0.9980
Benzene	9.26	4185.3	- 9.16	0.9991
Toluene	10.91	5026.1	-10.66	0.9988
Ethylbenzene	12.63	5800.7	-11.97	0.9987
n-Propylbenzene	14.46	6674.0	-13.47	0.9984
n-Butylbenzene	16.32	7356.8	-14.92	0.9980
n-Hexylbenzene	19.03	9028.8	-17.59	0.9985
p-Xylene	12.46	5799.3	-11.98	0.9985
o-Xylene	12.16	5627.8	-11.65	0.9985
m-Diethylbenzene	15.73	7267.2	-14.42	0.9981
1,2,4-Trimethylbenzene	13.72	6401.8	-12.95	0.9984
Fluorobenzene	10.04	4490.8	- 9.76	0.9991
Chlorobenzene	11.22	5154.2	-10.92	0.9988
Bromobenzene	11.62	5358.6	-11.29	0.9991
Iodobenzene	12.31	5712.3	-11.92	0.9987
Nitrobenzene	9.21	4374.4	-10.05	0.9994

Regression Analysis: $A_2(y)$ vs. $A_1(x)$

n = 22, R = 0.9916
Slope = 514.1 $\pm$ 31.2 = $-\beta/\alpha$
Intercept = -596.8 $\pm$ 439.2 = $-\Delta H^{o}_{n}(0)/R$

where R is the correlation coefficient and the regression values represent mean values $\pm$ 95% confidence limits.

Assuming β = 525°K, from the slope: $\alpha = -1.02 \pm 0.07$

From the intercept: $\Delta H^{o}_{n}(0)$ = 1.19 kcal/mol $\pm$ 0.87

For details, refer to Table 3-1.

Column: C-8, 5 cm.
Mobile phase: Methanol/Water
Compensation temperature (β) = 625°K
Compensation model: $\ln k' = A_1\theta (1 - \beta/T) + A_2/T + A_3$

Compound	A_1	A_2	A_3	R
Biphenyl	10.18	6043.1	-11.31	0.9989
Naphthalene	8.65	5154.9	- 9.94	0.9991
Phenanthrene	10.81	6652.2	-12.51	0.9985
Anthracene	11.07	6820.3	-12.79	0.9983
Pyrene	11.66	7374.1	-13.78	0.9978
Chrysene	12.14	7856.5	-14.72	0.9992
Fluoranthene	12.55	7663.8	-14.30	0.9987
Benzene	6.35	3604.5	- 7.27	0.9997
Toluene	7.48	4343.4	- 8.44	0.9994
Ethylbenzene	8.67	5010.3	- 9.39	0.9994
n-Propylbenzene	9.92	5769.4	-10.52	0.9990
n-Butylbenzene	11.20	6516.3	-11.60	0.9986
n-Hexylbenzene	13.05	7753.0	-13.44	0.9990
p-Xylene	8.55	5020.0	- 9.45	0.9992
o-Xylene	8.34	4867.1	- 9.17	0.9991
m-Diethylbenzene	10.80	6283.5	-11.21	0.9989
1,2,4-Trimethylbenzene	9.42	5543.2	-10.15	0.9990
Fluorobenzene	6.88	3861.9	- 7.71	0.9995
Chlorobenzene	7.70	4451.1	- 8.63	0.9993
Bromobenzene	7.97	4630.3	- 8.92	0.9995
Iodobenzene	8.44	4941.3	- 9.41	0.9993
Nitrobenzene	6.32	3796.0	- 8.17	0.9994

Regression Analysis: $A_2(y)$ vs. $A_1(x)$

$n = 22$, $R = 0.9934$
Slope = $652.6 \pm 35.1 = -\beta/\alpha$
Intercept = $-549.4 \pm 339.4 = -\Delta H^o_n(0)/R$

where R is the correlation coefficient and the regression values represent mean values ± 95% confidence limits.

Assuming β = 625°K, from the slope: $\alpha = -0.96 \pm 0.05$

From the intercept: $\Delta H^o_n(0)$ = 1.09 kcal/mol ± 0.68

For details, refer to Table 3-1.

Column: C-8, 5 cm.
Mobile phase: Methanol/Water
Compensation temperature (β) = 725°K
Compensation model: $\ln k' = A_1\theta\,(1 - \beta/T) + A_2/T + A_3$

Compound	A_1	A_2	A_3	R
Biphenyl	7.74	5556.0	- 9.72	0.9985
Naphthalene	6.58	4741.0	- 8.59	0.9992
Phenanthrene	8.23	6134.9	-10.83	0.9986
Anthracene	8.42	6290.8	-11.06	0.9985
Pyrene	8.88	6816.2	-11.96	0.9980
Chrysene	9.24	7236.0	-12.70	0.9994
Fluoranthene	9.55	7106.2	-12.48	0.9988
Benzene	4.84	3300.2	- 6.28	0.9997
Toluene	5.70	3985.5	- 7.28	0.9996
Ethylbenzene	6.59	4596.0	- 8.04	0.9995
n-Propylbenzene	7.55	5295.1	- 8.98	0.9992
n-Butylbenzene	8.52	5981.2	- 9.86	0.9988
n-Hexylbenzene	9.93	7084.5	-11.26	0.9991
p-Xylene	6.51	4611.4	- 8.12	0.9995
o-Xylene	6.35	4468.3	- 7.87	0.9992
m-Diethylbenzene	8.22	5767.8	- 9.53	0.9990
1,2,4-Trimethylbenzene	7.17	5093.1	- 8.69	0.9992
Fluorobenzene	5.24	3532.3	- 6.64	0.9996
Chlorobenzene	5.86	4082.6	- 7.43	0.9995
Bromobenzene	6.06	4248.7	- 7.67	0.9996
Iodobenzene	6.43	4537.2	- 8.09	0.9994
Nitrobenzene	4.80	3492.9	- 7.18	0.9994

Regression Analysis: $A_2(y)$ vs. $A_1(x)$

$n = 22$, $R = 0.9904$
Slope = $801.1 \pm 52.1 = -\beta/\alpha$
Intercept = $-588.4 \pm 383.0 = -\Delta H^{o}_{n}(0)/R$

where R is the correlation coefficient and the regression values represent mean values $\pm$ 95% confidence limits.

Assuming β = 725°K, from the slope: $\alpha = -0.90 \pm 0.05$

From the y-intercept: $\Delta H^{o}_{n}(0)$ = 1.17 kcal/mol $\pm$ 0.76

For details, refer to Table 3-1.

Column: C-2, 5 cm.
Mobile phase: Acetronitrile/Water
Compensation temperature (β) = 625°K
Compensation model: $\ln k' = A_1\theta\,(1 - \beta/T) + A_2/T + A_3$

Compound	A_1	A_2	A_3	R
Biphenyl	9.79	4400.3	-8.41	0.9995
Naphthalene	8.06	3843.6	-7.80	0.9985
Phenanthrene	10.62	4653.6	-8.72	0.9998
Anthracene	10.98	4843.2	-9.10	0.9997
Pyrene	11.65	4946.4	-8.99	0.9998
Chrysene	13.09	5442.6	-9.62	0.9998
Fluoranthene	11.83	5015.3	-9.12	0.9998
Benzene	5.05	2784.3	-6.34	0.9905
Toluene	6.35	3153.9	-6.62	0.9940
Ethylbenzene	7.68	3577.8	-7.06	0.9968
n-Propylbenzene	9.08	4035.0	-7.53	0.9982
n-Butylbenzene	10.50	4472.2	-7.95	0.9991
n-Hexylbenzene	13.47	5581.8	-9.48	0.9991
p-Xylene	7.58	3521.7	-6.93	0.9959
o-Xylene	7.44	3436.5	-6.79	0.9966
m-Diethylbenzene	10.27	4302.0	-7.60	0.9985
1,2,4-Trimethylbenzene	8.63	3866.9	-7.32	0.9985
Fluorobenzene	5.64	2989.5	-6.65	0.9927
Chlorobenzene	6.58	3310.0	-6.99	0.9954
Bromobenzene	6.91	3420.7	-7.14	0.9971
Iodobenzene	7.54	3651.4	-7.45	0.9978
Nitrobenzene	5.31	2909.0	-6.70	0.9947

Regression Analysis: $A_2(y)$ vs. $A_1(x)$

$n = 22$, $R = 0.9957$
Slope = $350.5 \pm 14.3 = -\beta/\alpha$
Intercept = $+1092.3 \pm 130.6 = -\Delta H^{o}_{n}(0)/R$

where R is the correlation coefficient and the regression values represent mean values ± 95% confidence limits.

Assuming β = 625°K, from the slope: $\alpha = -1.89 \pm 0.08$

From the intercept: $\Delta H^{o}_{n}(0) = -2.17$ kcal/mol ± 0.26

For details, refer to Table 3-1.

lumn: C-2, 5 cm.
bile phase: Acetronitrile/Water
mpensation temperature (β) = 625°K
mpensation model: $\ln k' = A_1\theta\,(1 - \beta/T) + A_2/T + A_3 + A_4\theta^2(1-\beta/T)$

mpound	A_1	A_2	A_3	A_4	R
phenyl	6.66	4057.2	-7.86	4.16	0.9999
phthalene	3.26	3317.6	-6.95	6.38	0.9999
enanthrene	9.29	4507.5	-8.49	1.77	0.9997
thracene	9.42	4672.4	-8.83	2.07	0.9999
rene	12.05	4990.4	-9.06	-0.53	0.9998
rysene	13.64	5507.9	-9.72	-0.68	0.9998
uoranthene	12.60	5100.1	-9.26	-1.03	0.9998
nzene	-3.06	1895.7	-4.92	10.78	0.9994
luene	-1.48	2294.6	-5.25	10.43	0.9995
hylbenzene	1.16	2863.3	-5.91	8.67	0.9995
Propylbenzene	3.39	3410.5	-6.53	7.58	0.9997
Butylbenzene	7.16	4105.6	-7.37	4.45	0.9995
Hexylbenzene	---	---	---	---	---
Xylene	0.43	2736.90	-5.67	9.52	0.9992
Xylene	1.34	2767.9	-5.72	8.11	0.9991
Diethylbenzene	5.23	3766.6	-6.78	6.70	0.9994
2,4-Trimethyl-benzene	4.47	3411.7	-6.59	5.52	0.9994
uorobenzene	-2.25	2124.6	-5.26	10.50	0.9997
lorobenzene	-0.34	2551.1	-5.78	9.21	0.9994
omobenzene	1.01	2773.2	-6.10	7.86	0.9998
iobenzene	2.14	3058.6	-6.50	7.19	0.9997
trobenzene	-1.02	2214.5	-5.59	8.43	0.9997

gression Analysis: (1) A_2 vs. A_1

$n = 21$, $R = 0.9971$
Slope = $212.2 \pm 7.8 = -\beta/\alpha$
Intercept = $2581.4 \pm 49.6 = -\Delta H^{o}_{n}(0)/R$

ere R is the correlation coefficient and the regression values present mean values $\pm$ 95% confidence limits.

suming β = 625°K, from the slope: $\alpha = -2.95 \pm 0.11$

om the intercept: $\Delta H^{o}_{n}(0) = -5.13$ kcal/mol $\pm$ 0.10

(2) A_4 vs. A_1

$n = 21$, $R = -0.9803$
Slope = $-0.74 \pm 0.06 = \Psi/\alpha$
Intercept = 9.10 ± 0.40

suming $\alpha = -2.95$, from the slope: $\Psi = 2.18 \pm 0.18$
details, refer to Table 3-1.

Column: C-4, 5 cm.
Mobile phase: Acetonitrile/Water
Compensation temperature (β) = 625°K
Compensation model: $\ln k' = A_1\theta\ (1 - \beta/T) + A_2/T + A_3$

Compound	A_1	A_2	A_3	R
Biphenyl	8.84	4097.9	-7.33	0.9955
Naphthalene	7.42	3607.1	-6.85	0.9970
Phenanthrene	9.35	4318.9	-7.68	0.9945
Anthracene	9.54	4357.2	-7.64	0.9945
Pyrene	10.03	4523.4	-7.79	0.9935
Chrysene	11.29	4977.8	-8.33	0.9925
Fluoranthene	10.15	4561.7	-7.85	0.9935
Benzene	5.01	2837.4	-6.15	0.9990
Toluene	6.15	3109.6	-6.13	0.9985
Ethylbenzene	7.22	3498.6	-6.50	0.9975
n-Propylbenzene	8.38	3903.9	-6.85	0.9965
n-Butylbenzene	9.56	4279.3	-7.10	0.9950
n-Hexylbenzene	10.29	4709.1	-7.43	0.9980
p-Xylene	7.12	3369.7	-6.15	0.9965
o-Xylene	6.96	3350.7	-6.23	0.9975
m-Diethylbenzene	9.21	4180.9	-7.03	0.9955
1,2,4-Trimethylbenzene	7.91	3660.5	-6.42	0.9960
Fluorobenzene	5.55	2920.1	-6.09	0.9985
Chlorobenzene	6.33	3190.5	-6.30	0.9980
Bromobenzene	6.58	3282.0	-6.39	0.9980
Iodobenzene	6.71	3502.0	-6.71	0.9970
Nitrobenzene	5.22	2894.5	-6.40	0.9980

Regression Analysis: A_2 vs. A_1

$n = 22$, $R = 0.9944$
Slope = $352.4 \pm 17.5 = -\beta/\alpha$
Intercept = $979.7 \pm 142.6 = -\Delta H^o_n(0)/R$

where R is the correlation coefficient and the regression values represent mean values $\pm$ 95% confidence limits.

Assuming β = 625°K, from the slope: $\alpha = -1.77 \pm 0.08$

From the intercept: $\Delta H^o_n(0) = -1.95$ kcal/mol $\pm$ 0.28

For details, refer to Table 3-1.

Column: C-4, 5 cm.
Mobile phase: Acetronitrile/Water
Compensation temperature (β) = 625°K
Compensation model: $\ln k' = A_1 \theta (1 - \beta/T) + A_2/T + A_3 + A_4 \theta^2 (1-\beta/T)$

Compound	A_1	A_2	A_3	A_4	R
Biphenyl	16.61	5123.0	- 8.97	- 8.63	0.9993
Naphthalene	12.98	4340.7	- 8.02	- 6.18	0.9994
Phenanthrene	18.99	5590.8	- 9.72	-10.71	0.9994
Anthracene	19.34	5650.5	- 9.71	-10.89	0.9993
Pyrene	21.26	6004.8	-10.16	-12.47	0.9994
Chrysene	24.91	6774.3	-11.21	-15.13	0.9993
Fluoranthene	21.39	6044.3	-10.22	-12.48	0.9991
Benzene	5.67	2923.5	- 6.29	- 0.73	0.9991
Toluene	8.78	3456.9	- 6.69	- 2.92	0.9992
Ethylbenzene	11.48	4060.0	- 7.40	- 4.73	0.9992
n-Propylbenzene	14.57	4720.8	- 8.15	- 6.88	0.9993
n-Butylbenzene	18.24	5425.4	- 8.93	- 9.65	0.9992
n-Hexylbenzene	17.82	5853.9	- 9.26	- 7.53	0.9991
p-Xylene	12.21	4041.7	- 7.23	- 5.66	0.9990
o-Xylene	11.50	3949.4	- 7.19	- 5.04	0.9994
m-Diethylbenzene	17.01	5209.4	- 8.67	- 8.66	0.9990
1,2,4-Trimethyl-benzene	14.30	4503.9	- 7.77	- 7.10	0.9991
Fluorobenzene	7.63	3194.8	- 6.53	- 2.31	0.9992
Chlorobenzene	9.69	3633.3	- 7.01	- 3.73	0.9990
Bromobenzene	10.39	3785.3	- 7.19	- 4.24	0.9994
Iodobenzene	12.12	4168.6	- 7.77	- 5.61	0.9992
Nitrobenzene	7.48	3193.5	- 6.88	- 2.52	0.9989

Regression Analysis: (1) A_2 vs. A_1

n = 22, R = 0.9935
Slope = 201.1 ± 11.2 = $-\beta/\alpha$
Intercept = 1632.7 ± 168.9 = $-\Delta H^o_n(0)/R$

where R is the correlation coefficient and the regression values represent mean values ± 95% confidence limits.

Assuming β = 625°K, from the slope: $\alpha = -2.99 \pm 0.15$

From the intercept: $\Delta H^o_n(0) = -3.24$ kcal/mol ± 0.34

(2) A_4 vs. A_1

n = 22, R = 0.9909
Slope = -0.72 ± 0.05 = Ψ/α
Intercept = 3.34 ± 0.69

Assuming $\alpha = -2.99$, from the slope: $\Psi = 2.16 \pm 0.14$
For details, refer to Table 3-1.

Column: C-8, 5 cm.
Mobile phase: Acetonitrile/Water
Compensation temperature (β) = 625°K
Compensation model: $\ln k' = A_1\theta\,(1 - \beta/T) + A_2/T + A_3$

Compound	A_1	A_2	A_3	R
Biphenyl	8.76	4070.0	-6.67	0.9884
Naphthalene	7.53	3669.3	-6.45	0.9905
Phenanthrene	8.18	4041.6	-6.73	0.9874
Anthracene	8.37	4148.6	-6.90	0.9879
Pyrene	8.57	4350.9	-7.18	0.9859
Chrysene	9.46	4653.8	-7.37	0.9859
Fluoranthene	8.68	4264.1	-6.88	0.9859
Benzene	5.54	2867.8	-5.62	0.9940
Toluene	6.49	3218.1	-5.87	0.9920
Ethylbenzene	7.45	3511.9	-5.91	0.9910
n-Propylbenzene	8.44	3911.3	-6.24	0.9894
n-Butylbenzene	8.40	3913.7	-5.95	0.9869
n-Hexylbenzene	9.93	4488.1	-6.16	0.9854
p-Xylene	7.34	3463.5	-5.81	0.9915
o-Xylene	7.23	3461.9	-5.94	0.9920
m-Diethylbenzene	9.15	4125.3	-6.23	0.9884
1,2,4-Trimethylbenzene	8.07	3737.7	-5.99	0.9894
Fluorobenzene	5.93	3037.3	-5.92	0.9915
Chlorobenzene	6.62	3284.6	-5.99	0.9915
Bromobenzene	6.86	3368.5	-6.03	0.9910
Iodobenzene	7.29	3613.5	-6.40	0.9920
Nitrobenzene	5.70	3057.2	-6.33	0.9930

Regression Analysis: A_2 vs. A_1

$n = 22$, $R = 0.9669$
Slope = $398.0 \pm 48.9 = -\beta/\alpha$
Intercept = $663.9 \pm 382.4 = -\Delta H^o_n(0)/R$

where R is the correlation coefficient and the regression values represent mean values $\pm$ 95% confidence limits.

Assuming β = 625°K, from the slope: $\alpha = -1.57 \pm 0.17$

From the intercept: $\Delta H^o_n(0) = -1.32$ kcal/mol $\pm$ 0.76

For details, refer to Table 3-1.

Column: C-8, 5 cm.
Mobile phase: Acetonitrile/Water
Compensation temperature (β) = 525°K
Compensation model: $\ln k' = A_1\theta(1 - \beta/T) + A_2/T + A_3 + A_4\theta^2(1-\beta/T)$

Compound	A_1	A_2	A_3	A_4	R
Biphenyl	25.99	6453.1	-12.20	-12.88	0.9990
Naphthalene	21.02	5538.9	-10.84	- 9.79	0.9986
Phenanthrene	28.28	7187.5	-13.81	-14.37	0.9992
Anthracene	28.23	7258.0	-13.92	-14.09	0.9986
Pyrene	30.43	7771.3	-14.84	-15.76	0.9991
Chrysene	33.70	8447.6	-15.86	-17.50	0.9990
Fluoranthene	30.64	7698.9	-14.58	-15.80	0.9990
Benzene	13.20	3936.4	- 8.24	- 5.00	0.9973
Toluene	16.90	4665.0	- 9.32	- 7.25	0.9980
Ethylbenzene	20.52	5323.5	-10.18	- 9.41	0.9984
n-Propylbenzene	24.22	6096.5	-11.35	-11.61	0.9988
n-Butylbenzene	29.98	7135.5	-13.19	-14.72	0.9987
n-Hexylbenzene	35.55	8496.9	-15.13	-18.53	0.9985
p-Xylene	19.87	5202.6	- 9.93	- 8.94	0.9984
o-Xylene	19.41	5152.9	- 9.95	- 8.65	0.9987
m-Diethylbenzene	26.94	6585.2	-11.95	-13.24	0.9987
1,2,4-Trimethylbenzene	23.19	5831.2	-10.88	-11.14	0.9987
Fluorobenzene	15.04	4304.2	- 8.96	- 6.24	0.9965
Chlorobenzene	17.80	4836.8	- 9.67	- 7.95	0.9982
Bromobenzene	18.74	5017.2	- 9.92	- 8.53	0.9985
Iodobenzene	19.74	5341.6	-10.49	- 8.88	0.9990
Nitrobenzene	14.30	4255.0	- 9.22	- 5.84	0.9977

Regression Analysis: (1) A_2 vs. A_1

$n = 22$, $R = 0.9946$
Slope = $212.4 \pm 10.4 = -\beta/\alpha$
Intercept = $1065.3 \pm 251.0 = -\Delta H^o_n(0)/R$

where R is the correlation coefficient and the regression values represent mean values ± 95% confidence limits.

Assuming β = 525°K, from the slope: $\alpha = -2.47 \pm 0.11$

From the intercept: $\Delta H^o_n(0) = -2.12$ kcal/mol ±

(2) A_4 vs. A_1

$n = 22$, $R = 0.9991$
Slope = $-0.60 \pm 0.01 = \Psi/\alpha$
Intercept = 2.94 ± 0.28

Assuming $\alpha = -2.47$, from the slope: $\Psi = 1.50 \pm 0.02$
For details, refer to Table 3-1.

Column: C-8, 5 cm.
Mobile phase: Acetonitrile/Water
Compensation temperature (β) = 625°K
Compensation model: $\ln k' = A_1\theta(1 - \beta/T) + A_2/T + A_3 + A_4\theta^2(1-\beta/T)$

Compound	A_1	A_2	A_3	A_4	R
Biphenyl	17.58	5506.6	- 9.18	- 8.57	0.9994
Naphthalene	14.19	4756.0	- 8.35	- 6.48	0.9991
Phenanthrene	19.07	6085.8	-10.31	- 9.55	0.9996
Anthracene	19.04	6151.0	-10.40	- 9.36	0.9991
Pyrene	20.53	5697.0	-11.10	-10.50	0.9995
Chrysene	22.75	7149.2	-11.73	-11.66	0.9995
Fluoranthene	20.67	6513.9	-10.82	-10.51	0.9995
Benzene	8.88	3412.5	- 6.58	- 3.25	0.9980
Toluene	11.40	4018.0	- 7.26	- 4.77	0.9985
Ethylbenzene	13.86	4556.9	- 7.74	- 6.24	0.9990
n-Propylbenzene	16.37	5204.1	- 8.51	- 7.72	0.9994
n-Butylbenzene	19.55	6006.8	- 9.60	- 9.78	0.9992
n-Hexylbenzene	24.00	7130.4	-10.78	-12.35	0.9991
p-Xylene	13.41	4454.5	- 7.55	- 5.91	0.9990
o-Xylene	13.10	4419.2	- 7.61	- 5.71	0.9992
m-Diethylbenzene	18.22	5603.1	- 8.81	- 8.82	0.9992
1,2,4-Trimethylbenzene	15.67	4977.3	- 8.16	- 7.40	0.9992
Fluorobenzene	10.13	3722.8	- 7.12	- 4.09	0.9971
Chlorobenzene	12.01	4164.8	- 7.53	- 5.25	0.9987
Bromobenzene	12.66	4313.8	- 7.68	- 5.64	0.9990
Iodobenzene	13.32	4596.5	- 8.12	- 5.87	0.9994
Nitrobenzene	9.63	3698.5	- 7.46	- 3.83	0.9982

Regression Analysis: (1) A_2 vs. A_1

n = 22, R = 0.9947
Slope = 259.6 ± 12.6 = $-\beta/\alpha$
Intercept = 1055.0 ± 204.7 = $-\Delta H^o_n(0)/R$

where R is the correlation coefficient and the regression values represent mean values ± 95% confidence limits.

Assuming β = 625°K, from the slope: α = 2.41 ± 0.11

From the intercept: $\Delta H^o_n(0)$ = -2.10 kcal/mol ± 0.40

(2) A_4 vs. A_1

n = 22, R = -0.9995
Slope = -0.61 ± 0.01 = Ψ/α
Intercept = 2.11 ± 0.15

Assuming α = -2.41, from the slope: Ψ = 1.46 ± 0.04
For details, refer to Table 3-1.

Column: C-8, 5 cm.
Mobile phase: Acetonitrile/Water
Compensation temperature (β) = 725°K
Compensation model: $\ln k' = A_1\theta(1 - \beta/T) + A_2/T + A_3 + A_4\theta^2(1-\beta/T)$

Compound	A_1	A_2	A_3	A_4	R
Biphenyl	13.24	5016.7	- 7.62	- 6.42	0.9995
Naphthalene	10.71	4351.1	- 7.06	- 4.84	0.9992
Phenanthrene	14.37	5517.6	- 8.51	- 7.14	0.9997
Anthracene	14.35	5579.9	- 8.59	- 6.99	0.9992
Pyrene	15.48	5991.0	- 9.18	- 7.85	0.9997
Chrysene	17.15	6479.0	- 9.61	- 8.73	0.9996
Fluoranthene	15.58	5902.4	- 8.88	- 7.86	0.9996
Benzene	6.69	3142.0	- 5.72	- 2.40	0.9981
Toluene	8.59	3683.6	- 6.20	- 3.55	0.9987
Ethylbenzene	10.46	4160.2	- 6.48	- 4.65	0.9992
n-Propylbenzene	12.36	4742.3	- 7.04	- 5.77	0.9995
n-Butylbenzene	14.73	5424.5	- 7.76	- 7.31	0.9994
n-Hexylbenzene	18.10	6424.8	- 8.54	- 9.24	0.9993
p-Xylene	10.12	4067.6	- 6.32	- 4.41	0.9991
o-Xylene	9.88	4039.8	- 6.41	- 4.26	0.9994
m-Diethylbenzene	13.75	5094.7	- 7.20	- 6.60	0.9995
1,2,4-Trimethyl-benzene	11.83	4535.6	- 6.75	- 5.53	0.9994
Fluorobenzene	7.64	3422.4	- 6.13	- 3.04	0.9972
Chlorobenzene	9.06	3817.3	- 6.42	- 3.91	0.9990
Bromobenzene	9.54	3950.0	- 6.52	- 4.21	0.9991
Iodobenzene	10.05	4211.3	- 6.90	- 4.37	0.9995
Nitrobenzene	7.25	3411.0	- 6.54	- 2.84	0.9983

Regression Analysis: (1) A_2 vs. A_1

n = 22, R = 0.9938
Slope = 305.1 $\pm$ 15.9 = $-\beta/\alpha$
Intercept = 1060.8 $\pm$ 195.0 = $-\Delta H^{o}_{n}(0)/R$

where R is the correlation coefficient and the regression values represent mean values $\pm$ 95% confidence limits.

Assuming β = 725°K, from the slope: $\alpha = -2.38 \pm 0.12$

From the intercept: $\Delta H^{o}_{n}(0) = -2.11$ kcal/mol $\pm$ 0.38

(2) A_4 vs. A_1

n = 22, R = -0.9994
Slope = -0.60 $\pm$ 0.01 = Ψ/α
Intercept = 1.61 $\pm$ 0.11

Assuming α = -2.38, from the slope: $\Psi = 1.44 \pm 0.02$
For details, refer to Table 3-1.

APPENDIX F
PHYSICOCHEMICAL CONSTANTS OF METHANOL/WATER SOLUTIONS[a]

% v/v MeOH	d^b	R.I.[c]	ε^d	$V\times10^{3\,e}$	γ^f	$k^{e\,g}$	Γ^h
0	0.9971	1.3325	78.5	18.07	72.00	1.28	0.981
5	0.9903	1.3334	76.7	18.52	61.33	1.54	0.980
10	0.9836	1.3342	75.0	18.99	55.75	1.78	0.980
15	0.9771	1.3353	73.0	19.48	52.42	1.97	0.980
20	0.9703	1.3362	70.9	20.01	49.33	2.10	0.979
25	0.9634	1.3373	68.8	20.58	46.46	2.17	0.978
30	0.9563	1.3384	66.6	21.19	43.79	2.21	0.978
35	0.9495	1.3394	64.4	21.83	41.50	2.23	0.977
40	0.9415	1.3400	62.2	22.54	39.50	2.21	0.976
45	0.9321	1.3405	59.9	23.34	37.42	2.18	0.975
50	0.9229	1.3408	57.7	24.19	35.42	2.13	0.974
55	0.9148	1.3408	55.5	25.09	33.50	2.08	0.973
60	0.9037	1.3407	53.1	25.14	31.17	2.04	0.972
65	0.8924	1.3403	50.4	27.29	30.17	2.00	0.970
70	0.8801	1.3396	47.7	28.58	28.92	1.97	0.969
75	0.8662	1.3386	44.8	30.05	27.67	1.94	0.967
80	0.8519	1.3370	42.0	31.68	26.46	1.91	0.965
85	0.8363	1.3352	39.3	33.54	25.21	1.87	0.962
90	0.8210	1.3330	36.7	35.60	24.00	1.84	0.960
95	0.8044	1.3301	34.1	37.98	22.83	1.81	0.957
100	0.7867	1.3274	31.5	40.73	21.75	1.78	0.953

[a]Taken with permission after Wells (1981).

[b]Density at 25°C (g/cm^3).

[c]Refractive index at 25°C.

[d]Dielectric constant at 25°C.

[e]Molar volume at 25°C (lit/mole).

[f]Surface tension at 25°C (dyne/cm).

[g]Kappa (K^e) at 25°C; see Horvath et al. (1976) and Eqn. (3-39).

[h]Function of ε at 25°C, $\Gamma = 2(\varepsilon - 1)/(2\varepsilon + 1)$.

APPENDIX G

PHYSICOCHEMICAL CONSTANTS OF ACETONITRILE/WATER SOLUTIONS[a]

% v/v ACN	d^b	R.I.[c]	ε^d	$Vx10^{3}$ [e]	γ^f	K^{e} [g]	Γ^h
0	0.9971	1.3325	78.5	18.07	72.00	1.28	0.981
2.5	0.9928	1.3338	78.0	18.35	63.92	1.35	0.981
5	0.9889	1.3347	77.4	18.63	58.00	1.43	0.981
10	0.9812	1.3367	75.9	19.22	50.33	1.58	0.980
15	0.9739	1.3386	74.2	19.84	44.83	1.72	0.980
20	0.9661	1.3402	72.4	20.52	40.08	1.84	0.979
25	0.9572	1.3412	70.4	21.28	36.33	1.93	0.979
30	0.9477	1.3424	68.2	22.11	33.92	1.99	0.978
35	0.9367	1.3432	65.8	23.03	32.25	1.94	0.977
40	0.9264	1.3442	63.4	24.06	31.33	1.86	0.976
45	0.9149	1.3448	60.8	25.18	30.83	1.78	0.976
50	0.9034	1.3450	58.4	26.34	30.50	1.70	0.974
55	0.8919	1.3454	56.1	27.80	30.31	1.61	0.973
60	0.8800	1.3454	53.8	29.33	29.96	1.53	0.972
70	0.8542	1.3454	49.2	33.04	29.58	1.38	0.970
80	0.8287	1.3446	44.7	37.78	29.17	1.22	0.967
90	0.8009	1.3432	40.2	44.19	28.92	1.06	0.963
100	0.7743	1.3412	36.0	53.02	28.83	0.90	0.959

[a]Taken with permission after Wells (1981).

[b]Density at 25°C (g/cm^3).

[c]Refractive index at 25°C.

[d]Dielectric constant at 25°C.

[e]Molar volume at 25°C (lit mole).

[f]Surface tension at 25°C (dyne/cm).

[g]Kappa (K^e) at 25°C; see Horvath et al. (1976) and Eqn. (3-39).

[h]Function of ε at 25°C, $\Gamma = 2(\varepsilon - 1)/(2\varepsilon + 1)$.

APPENDIX H
REGRESSION COEFFICIENTS FOR THE SOLVOPHOBIC MODEL OF RPLC RETENTION

Column: C-2, 5 cm.
Mobile phase: Acetonitrile/Water
Temperature: 298°K
Solvophobic model: $X = (A + E) + B\Gamma + C\gamma$

where $X = \ln k' - D(K^e - 1)V^{2/3}\gamma - \ln(RT/P_oV)$

Compound	n[a]	(A + E)	B	C	R[b]
Biphenyl	4	-114.87	105.35	0.1091	0.984
Naphthalene	4	- 55.80	45.51	0.0734	0.957
Phenanthrene	4	-127.60	117.59	0.1388	0.989
Anthracene	4	-187.02	179.39	0.1143	0.997
Pyrene	4	-155.65	145.67	0.1668	0.992
Chrysene	-	---	---	---	---
Fluoranthene	4	-158.30	148.38	0.1681	0.992
Benzene	4	32.68	-43.54	-3E-5	0.767
Toluene	4	- 2.39	- 8.21	0.0306	0.617
Ethylbenzene	4	- 50.52	40.76	0.0535	0.932
n-Propylbenzene	4	-100.16	91.21	0.0798	0.977
n-Butylbenzene	4	-124.87	115.42	0.1267	0.986
n-Hexylbenzene	-	---	---	---	---
p-Xylene	4	- 63.26	54.37	0.0362	0.911
o-Xylene	4	- 43.41	33.65	0.0452	0.912
m-Diethylbenzene	4	-145.42	137.33	0.0971	0.985
1,2,4-Trimethyl-benzene	4	- 49.32	38.41	0.0969	0.970
Fluorobenzene	4	15.26	-26.03	0.0143	0.270
Chlorobenzene	4	- 23.13	13.30	0.0245	0.683
Bromobenzene	4	- 13.73	2.86	0.0509	0.844
Iodobenzene	4	203.95	-223.74	0.1714	0.997
Nitrobenzene	4	35.83	- 47.38	0.0168	0.606

[a]Number of data points used to fit solvophobic model.

[b]Correlation coefficient for X vs. Γ and γ.

Regression Analysis: (1) B vs. (A + E)

n = 20, R = -0.9998
Slope = -1.02 ± 0.01
Intercept = -11.89 ± 1.00

where R is the correlation coefficient and the regression parameters represent mean values ± 95% confidence limits.

For further study, refer to Eqns. (3-32) and (3-38), and to Appendices F and G.

Note: $\ln(RT/P_oV)$ at 298°K = $\ln(0.08205 * 298)/(1\text{ atm} * V)$, where V is the molar volume (L/mol) of the solvent.

<u>Column</u>: C-4
<u>Mobile phase</u>: Acetonitrile/Water
<u>Temperature</u>: 298°K
<u>Solvophobic model</u>: $X = (A + E) + B\Gamma + C\gamma$
where $X = \ln k' - D(K^e - 1)V^{2/3}\gamma - \ln (RT/P_oV)$

Compound	n[a]	(A + E)	B	C	R[b]
Biphenyl	4	-16.95	3.45	0.1701	0.996
Naphthalene	4	145.79	-166.10	0.2396	0.856
Phenanthrene	4	-17.07	1.96	0.2246	0.997
Anthracene	4	-28.99	14.61	0.2136	0.997
Pyrene	4	-32.08	16.46	0.2600	0.998
Chrysene	4	-61.98	45.58	0.3192	0.998
Fluoranthene	4	-42.81	28.13	0.2395	0.997
Benzene	4	85.54	-98.04	0.0205	0.999
Toluene	4	47.37	-59.07	0.0382	0.977
Ethylbenzene	4	13.42	-25.02	0.0748	0.943
n-Propylbenzene	4	-21.07	9.42	0.1178	0.991
n-Butylbenzene	4	-35.96	22.49	0.1997	0.997
n-Hexylbenzene	3	69.74	-105.77	0.8517	1.000
p-Xylene	4	29.26	-42.08	0.1000	0.974
o-Xylene	4	32.68	-45.46	0.0932	0.956
m-Diethylbenzene	4	-31.88	19.40	0.1627	0.991
1,2,4-Trimethyl-benzene	4	18.51	-32.20	0.1447	0.988
Fluorobenzene	4	74.32	-86.91	0.0347	0.997
Chlorobenzene	4	45.45	-57.54	0.0521	0.975
Bromobenzene	4	41.19	-53.74	0.0728	0.944
Iodobenzene	4	33.81	-46.79	0.0975	0.954
Nitrobenzene	4	87.64	-100.58	0.0276	0.996

[a] Number of data points used to fit solvophobic model.

[b] Correlation coefficient for X vs. Γ and γ.

<u>Regression Analysis</u>: (1) B vs. (A + E)

n = 21, R = -0.9993
Slope = -1.00 ± 0.02
Intercept = -13.55 ± 0.99

where R is the correlation coefficient and the regression parameters represent mean values ± 95% confidence limits.

For further study, refer to Eqns. (3-32) and (3-38), and to Appendices F and G.

<u>Note</u>: $\ln(RT/P_oV)$ at 298°K = ln (0.08205 * 298)/(1 atm * V), where V^o is the molar volume (L/mol) of the solvent.

Column: C-8, 5 cm.
Mobile phase: Acetonitrile/Water
Temperature: 298°K
Solvophobic model: $X = (A + E) + B\Gamma + C\gamma$
where $X = \ln k' - D(K^e - 1)V^{2/3}\gamma - \ln(RT/P_oV)$

Compound	n[a]	(A + E)	B	C	R[b]
Biphenyl	5	-61.83	49.53	0.1872	0.998
Naphthalene	5	-22.10	10.39	0.1212	0.995
Phenanthrene	4	59.35	-91.67	0.7305	0.999
Anthracene	4	12.12	-37.56	0.5540	0.998
Pyrene	4	66.87	-102.44	0.8397	0.999
Chrysene	4	50.50	-89.20	0.9639	0.999
Fluoranthene	4	42.82	-75.95	0.7810	0.999
Benzene	5	31.75	-41.74	-0.0032	0.985
Toluene	5	-11.99	3.00	0.0153	0.710
Ethylbenzene	5	-42.79	33.64	0.0597	0.990
n-Propylbenzene	5	-76.67	67.34	0.1083	0.995
n-Butylbenzene	4	18.40	-45.87	0.6184	0.999
n-Hexylbenzene	4	-19.82	-11.41	0.7993	0.999
p-Xylene	5	-24.73	14.10	0.0910	0.989
o-Xylene	5	-32.60	23.14	0.0587	0.982
m-Diethylbenzene	5	-93.75	84.04	0.1458	0.997
1,2,4-Trimethyl-benzene	5	-47.44	36.73	0.1237	0.994
Fluorobenzene	5	19.60	-29.84	0.0171	0.943
Chlorobenzene	5	- 1.25	- 9.38	0.0589	0.957
Bromobenzene	5	- 6.28	- 4.42	0.0689	0.970
Iodobenzene	5	-20.04	9.07	0.0958	0.994
Nitrobenzene	5	26.57	-37.04	0.0114	0.962

[a] Number of data points used to fit solvophobic model.
[b] Correlation coefficient for X vs. Γ and γ.

Regression Analysis: (1) B vs. (A + E) for pyrene, phenanthrene, chrysene, fluoranthene, n-butylbenzene, n-hexylbenzene and anthracene.
$n = 7$, $R = -0.9942$
Slope = -1.09 ± 0.14
Intercept = -29.07 ± 5.89

(2) B vs. (A + E) for remaining compounds.
$n = 15$, $R = -0.9997$
Slope = -1.00 ± 0.02
Intercept = -10.37 ± 0.65

where R is the correlation coefficient and the regression parameters represent mean values $\pm$ 95% confidence limits. For further study, refer to Eqns. (3-32) and (3-38) and to Appendices F and G.

Note: $\ln(RT/P^oV)$ at 298°K = $\ln(0.08205 * 298)/(1 \text{ atm} * V)$, where V is the molar volume (L/mol) of the solvent.

Column: C-18, 5 cm.
Mobile phase: Acetonitrile/Water
Temperature: 298°K
Solvophobic model: $X = (A + E) + B\Gamma + C\gamma$
where $X = \ln k' - D(K^e - 1)V^{2/3}\gamma - \ln(RT/P_oV)$

Compound	n[a]	(A + E)	B	C	R[b]
Biphenyl	4	113.62	-143.92	0.6270	0.999
Naphthalene	4	119.67	-145.39	0.4603	0.999
Phenanthrene	4	133.79	-169.97	0.8090	0.999
Anthracene	4	114.91	-148.35	0.7411	0.998
Pyrene	4	123.32	-159.12	0.8207	0.999
Chrysene	4	119.54	-160.53	1.0034	0.999
Benzene	4	88.38	- 98.16	-0.0490	0.999
Toluene	4	140.46	-164.80	0.3870	0.999
Ethylbenzene	-	---	---	---	---
n-Propylbenzene	4	117.76	-147.70	0.6164	0.998
n-Butylbenzene	4	88.06	-116.80	0.6194	0.999
n-Hexylbenzene	4	76.33	-111.88	0.8801	0.999
p-Xylene	4	130.37	-157.50	0.5000	0.998
o-Xylene	4	124.27	-149.56	0.4432	0.998
m-Diethylbenzene	4	94.56	-123.30	0.6092	0.999
1,2,4-Trimethyl-benzene	4	119.38	-147.70	0.5601	0.997
Fluorobenzene	4	123.72	-142.68	0.2148	0.999
Bromobenzene	4	118.05	-140.15	0.3388	0.999
Iodobenzene	4	127.36	-153.26	0.4600	0.999
Nitrobenzene	4	119.37	-136.64	0.1544	0.999

[a]Number of data points used to fit solvophobic model.
[b]Correlation coefficient for X vs. Γ and γ.

Regression Analysis: (1) B vs. (A + E) for all PAHs and benzene.
$n = 7$, $R = -0.973$
Slope = -1.63 ± 0.44
Intercept = 42.35 ± 52.00

(2) B vs. (A + E) for alkylbenzenes
$n = 8$, $R = -0.995$
Slope = -0.88 ± 0.09
Intercept = -42.30 ± 9.94

(3) b vs. (A + E) for nitrobenzene and halobenzenes
$n = 4$, $R = -0.902$
Slope = -1.52 ± 2.21
Intercept = 42.6 ± 270.0

where R is the correlation coefficient and the regression parameters represent mean values $\pm$ 95% confidence limits.

For further study, refer to Eqns. (3-32) and (3-38) and to Appendices F and G.

Note: $\ln(RT/P_o/V)$ at 298°K = $\ln(0.08205 * 298)/(1 \text{ atm.} * V)$, where V is the molar volume (L/mol) of the solvent.

APPENDIX I
BATCH EQUILIBRIUM SORPTION DATA FROM SOIL THERMODYNAMIC STUDIES

(A) Sorption conditions:

(1) Soil type--Webster (sandy clay loam; Typic Haplaquolls; 3.9% organic carbon), air-dired, 2 mm sieved.

(2) Solvent--30/70 methanol/water (v/v) mixture.

(3) Solutes--Biphenyl, anthracene, and pyrene.

(4) Temperature--5, 15, 25, and 35°C. Shaken 16-24 hours and centrifuged for 1 hour at 1000 rpm prior to sampling and analysis.

(5) Soil/solvent ratio--1g/5mL initial ratio at 5°C. Samples run in duplicate.

(B) Solution phase analysis:

From each sample at each temperature, 50 L aliquots were taken from the solution phase for quantitative analysis by HPLC. A 15 cm, 10 m, C-8 Zorbax column was used with a mobile phase of 65/35 acetonitrile/water at 1.5 mL/min. For the solute biphenyl, UV detection at 254 nm was employed, while anthracene and pyrene solutions required use of the filter fluorometer. Solution data were interpreted with the aid of Eqn. (4-1) and the Freundlich equation, Eqn. (4-2).

(C) Sorption data:

(1) Biphenyl: Samples at 5°C

Sample #	C_o(μg/mL)	C_e(μg/mL)	V(mL)	m(g)	S_e(μg/g)
8	2.08	0.4175	5	1.01	8.2302
7	2.08	0.4303	5	0.99	8.3318
6	3.46	0.7925	5	1.00	13.3375
5	3.46	0.7969	5	1.00	13.3155
4	5.54	1.3537	5	0.99	21.1429
3	5.54	1.4225	5	1.00	20.5875
2	6.92	1.8208	5	1.00	25.4960
1	6.92	1.8578	5	1.00	25.3110

From the Freundlich equation, $S_e = KC_e^N$

n = 8, R = 0.9990
N = 0.77 ± 0.03
K = 16.01 (15.70, 16.32)
95% conf. limit on Ln K = ± 0.02
Linear K = 14.66 ± 2.68

where R is the correlation coefficient and regression parameters represent mean values ± 95% confidence limits.

(2) Biphenyl--Samples at 15°C

Sample #	C_o(μg/mL0	C_e(μg/mL)	V(mL)	M(g)	S_e(μg/g)
8	2.08	0.5540	4.65	1.01	7.0256
7	2.08	0.5562	4.65	0.99	7.1572
6	3.46	1.0512	4.65	1.00	11.2010
5	3.46	0.9773	4.65	1.00	11.5448
4	5.54	1.7421	4.65	0.99	17.8385
3	5.54	1.7082	4.65	1.00	17.8179
2	6.92	2.2134	4.65	1.00	21.8857
1	6.92	2.1401	4.65	1.00	22.2264

From the Freundlich equation, $S_e = KC_e^N$

n = 8, R = 0.9979
N = 0.83 ± 0.05
K = 11.43 (11.09, 11.78)
95% conf. limit on Ln K = ± 0.03
Linear K = 10.41 ± 1.32

(3) Biphenyl--Samples at 25°C

Sample #	C_o(µg/mL)	C_e(µg/mL)	V(mL)	m(g)	S_e(µg/g)
8	2.08	0.6941	4.55	1.01	6.2434
7	2.08	0.7921	4.55	0.99	5.9193
6	3.46	1.3441	4.55	1.00	9.6272
5	3.46	1.2563	4.55	1.00	10.0268
4	5.54	2.1371	4.55	0.99	15.6395
3	5.54	2.1085	4.55	1.00	15.6134
2	6.92	2.8360	4.55	1.00	18.5821
1	6.92	2.6910	4.55	1.00	19.2421

From the Freundlich equation, $S_e = KC_e^N$

n = 8, R = 0.9921
N = 0.87 $\pm$ 0.11
K = 7.92 (7.36, 8.52)
95% conf. limit on Ln K = $\pm$ 0.07
Linear K = 7.13 $\pm$ 1.01

(4) Biphenyl--Samples at 35°C

Sample #	C_o(µg/mL)	C_e(µg/mL)	V(mL)	m(g)	S_e(µg/g)
8	2.08	0.9195	4.45	1.01	5.1131
7	2.08	0.7990	4.45	0.99	5.7582
6	3.46	1.4338	4.45	1.00	9.0167
5	3.46	1.3844	4.45	1.00	9.2365
4	5.54	2.4502	4.45	0.99	13.8884
3	5.54	2.4862	4.45	1.00	13.5892
2	6.92	3.0506	4.45	1.00	17.2188
1	6.92	2.9649	4.45	1.00	17.6003

From the Freundlich equation, $S_e = KC_e^N$

n = 8, R = 0.9861
N = 0.89 $\pm$ 0.15
K = 6.41 (5.74, 7.16)
95% conf. limit on Ln K = $\pm$ 0.11
Linear K = 5.81 $\pm$ 0.78

(5) Anthracene--Samples at 5°C

Sample #	C_o(μg/mL)	C_e(μg/mL)	V(mL)	m(g)	S_e(μg/g)
8	1.68	0.1424	5.0	1.01	7.6121
7	1.68	0.1387	5.0	1.01	7.6303
6	2.80	0.1811	5.0	1.00	13.0945
5	2.80	0.1790	5.0	1.02	12.8482
4	4.48	0.2634	5.0	1.03	20.4687
3	4.48	0.2557	5.0	1.04	20.3091
2	5.60	0.3801	5.0	1.02	25.5878
1	5.60	0.3801	5.0	1.02	25.5878

From the Freundlich equation, $S_e = KC_e^N$

$n = 8$, $R = 0.9676$

$N = 1.19 \pm 0.31$

$K = 89.80$ (55.57, 145.10)

95% conf. limit on Ln $K = \pm 0.48$

Linear $K = 69.78 \pm 16.24$

(6) Anthracene--Samples at 15°C

Sample #	C_o(μg/mL)	C_e(μg/mL)	V(mL)	m(g)	S_e(μg/g)
8	1.68	0.0605	4.65	1.01	7.4560
7	1.68	0.0521	4.65	1.01	7.4946
6	2.80	0.1166	4.65	1.00	12.4776
5	2.80	0.1131	4.65	1.02	12.2492
4	4.48	0.2274	4.65	1.03	19.1986
3	4.48	0.2201	4.60	1.04	18.8420
2	5.60	0.3521	4.60	1.02	23.6671
1	5.60	0.3226	4.55	1.02	23.5413

From the Freundlich equation, $S_e = KC_e^N$

$n = 8$, $R = 0.9966$

$N = 0.64 \pm 0.05$

$K = 48.68$ (43.70, 54.22)

95% conf. limit on Ln $K = \pm 0.11$

Linear $K = 77.92 \pm 23.56$

(7) Anthracene--Samples at 25°C

Sample #	C_o (µg/mL)	C_e (µg/mL)	V(mL)	m(g)	S_e (µg/g)
8	1.68	0.1112	4.55	1.01	7.0674
7	1.68	0.0957	4.55	1.01	7.1371
6	2.80	0.2037	4.55	1.00	11.8133
5	2.80	0.1952	4.55	1.02	11.6193
4	4.48	0.4124	4.55	1.03	17.9684
3	4.48	0.3955	4.50	1.04	17.6733
2	5.60	0.6297	4.50	1.02	21.9276
1	5.60	0.5354	4.45	1.02	22.5922

From the Freundlich equation, $S_e = KC_e^N$

$n = 8$, $R = 0.9932$
$N = 0.65 \pm 0.08$
$K = 32.05$ (28.71, 35.78)
95% conf. limit on Ln $K = \pm 0.11$
Linear $K = 41.81 \pm 13.07$

(8) Anthracene--Samples at 35°C

Sample #	C_o (µg/mL)	C_e (µg/mL)	V(mL)	m(g)	S_e (µg/g)
8	1.68	0.1571	4.45	1.01	6.7097
7	1.68	0.1341	4.45	1.01	6.8112
6	2.80	0.2926	4.45	1.00	11.1579
5	2.80	0.2664	4.45	1.02	11.0535
4	4.48	0.5822	4.45	1.03	16.8393
3	4.48	0.5068	4.40	1.04	16.8099
2	5.60	0.9385	4.40	1.02	20.1085
1	---	Sample leaked	--	--	---

From the Freundlich equation, $S_e = KC_e^N$

$n = 7$, $R = 0.9842$
$N = 0.61 \pm 0.13$
$K = 23.12$ (19.70, 27.13)
95% conf. limit on Ln $K = \pm 0.16$
Linear $K = 27.07 \pm 12.74$

(9) Pyrene--Samples at 5°C

Sample #	C_o(μg/mL)	C_e(μg/mL)	V(mL)	m(g)	S_e(μg/g)
8	1.98	0.0584	5.0	1.05	9.1505
7	1.98	0.0642	5.0	1.03	9.3000
6	3.30	0.1237	5.0	1.06	14.9825
5	3.30	0.1333	5.0	1.06	14.9373
4	5.28	0.2945	5.0	1.03	24.2015
3	5.28	0.3718	5.0	1.07	22.9355
2	6.60	0.6997	5.0	1.03	28.6422
1	6.60	0.8315	5.0	1.00	28.8425

From the Freundlich equation, $S_e = KC_e^N$

n = 8, R = 0.9750
N = 0.45 $\pm$ 0.10
K = 35.18 (29.20, 42.39)
95% conf. limit on Ln K = $\pm$ 0.19
Linear K = 44.70 $\pm$ 25.24

(10) Pyrene--Samples at 15°C

Sample #	C_o(μg/mL)	C_e(μg/mL)	V(mL)	m(g)	S_e(μg/g)
8	1.98	0.0349	4.65	1.05	8.6139
7	1.98	0.0308	4.65	1.03	8.7997
6	3.30	0.0517	4.65	1.06	14.2497
5	3.30	0.0513	4.65	1.06	14.2514
4	5.28	0.0860	4.65	1.03	23.4485
3	5.28	0.0815	4.60	1.07	22.3486
2	6.60	0.1236	4.65	1.03	29.2379
1	6.60	0.1325	4.65	1.00	30.0739

From the Freundlich equation, $S_e = KC_e^N$

n = 8, R = 0.9906
N = 0.90 $\pm$ 0.12
K = 201.64 (286.14, 142.09)
95% conf. limit on Ln K = $\pm$ 0.35
Linear K = 247.98 $\pm$ 43.24

(11) Pyrene--Samples at 25°C

Sample #	C_o(μg/mL)	C_e(μg/mL)	V(mL)	m(g)	S_e(μg/g)
8	1.98	0.0409	4.55	1.05	8.4029
7	1.98	0.0404	4.55	1.03	8.5682
6	3.30	0.0642	4.55	1.06	13.8893
5	3.30	0.0647	4.55	1.06	13.8873
4	5.28	0.1060	4.55	1.03	22.8559
3	5.28	0.1055	4.50	1.07	21.7621
2	6.60	0.1633	4.55	1.03	28.4339
1	6.60	0.1719	4.55	1.00	29.2476

From the Freundlich equation, $S_e = KC_e^N$

n = 8, R = 0.9911
N = 0.87 $\pm$ 0.12
K = 146.69 (108.67, 198.01)
95% conf. limit on Ln K = $\pm$ 0.30
Linear K = 187.03 $\pm$ 38.52

(12) Pyrene--Samples at 35°C

Sample #	C_o(μg/mL)	C_e(μg/mL)	V(mL)	m(g)	S_e(μg/g)
8	1.98	0.0471	4.45	1.05	8.1918
7	1.98	0.0423	4.45	1.03	8.3716
6	3.30	0.0769	4.45	1.06	13.5309
5	3.30	0.0865	4.45	1.06	13.4906
4	---	Sample leaked	--	--	---
3	5.28	0.1548	4.40	1.07	21.0757
2	6.60	0.2442	4.45	1.03	27.4597
1	6.60	0.2576	4.45	1.00	28.2236

From the Freundlich equation, $S_e = KC_e^N$

n = 7, R = 0.9952
N = 0.70 $\pm$ 0.08
K = 74.66 (61.74, 90.28)
95% conf. limit on Ln K = $\pm$ 0.19
Linear K = 120.62 $\pm$ 35.55

(D) <u>Determination of $\Delta H^{o}_{sorption}$</u>:

(1) Biphenyl--Regress Ln K vs. T^{-1}(°K^{-1})

n = 4, R = 0.9963
Slope = 2670 ± 687 = $-\Delta H^{o}_{sorp}/R$
Intercept = -6.84 ± 2.35

where R is the correlation coefficient and regression parameters represent mean values ± 95% confidence limits.

From the slope: ΔH^{o}_{sorp} = -5.31 kcal/lmol ± 1.36

(2) Anthacene--Regress Ln K vs. T^{-1}(°K^{-1})

n = 4, R = 0.9936
Slope = 3858 ± 1332 = $\Delta H^{o}_{sorp}/R$
Intercept = -9.44 ± 4.56

where R is the correlation coefficient and regression parameters represent mean values ± 95% confidence limits.

From the slope: ΔH^{o}_{sorp} = -7.66 kcal/lmol ± 2.65

(3) Pyrene--Regress Ln K vs. T^{-1}(°K^{-1})

n = 3 (Omit 278°K data point)
R = 0.9750
Slope = 4387 ± 12702 = $-\Delta H^{o}_{sorp}/R$
Intercept = -9.86 ± 42.67

where R is the correlation coefficient and regression parameters represent mean values ± 95% confidence limits.

From the slope: ΔH^{o}_{sorp} = -8.72 kcal/mol ± 25.24

(E) <u>Enthalpy-entropy compensation model</u>:

(1) For the 3 solutes, regress Ln K_{298} vs. $-\Delta H_{sorp}/R$

n = 3, R = 0.9707
Slope = 1.61E-3 ± 5.05E-3
Intercept = -2.36 ± 18.74

From the slope: β = 573°K ± 425

where R is the correlation coefficient and regression parameters represent mean valus ± 95% confidence limits.

REFERENCES

Abbott, S.R., Berg, J.R., Achener, P., and Stevenson, R.L., 1976. Chromatographic reproducibility in high-performance liquid chromatographic gradient elution. J. Chromatogr., 126: 421-437.

Adams, J., and Giam, C.S., 1984. Polynuclear azaarenes in wood preservative wastewater. Environ. Sci. Technol., 18: 391-394.

Akerlof, G., 1932. Dielectric constants of some organic solvent-water mixtures at various temperatures. J. Amer. Chem. Soc., 54: 4125-4139.

Belfort, G., 1982. Personal communication.

Berendsen, G.E., and DeGalan, L., 1980. Role of the chain length of chemically bonded phases and the retention mechanisms in reversed-phase liquid chromatography. J. Chromatogr., 196: 21-37.

Berendsen, G.E., Schoenmakers, P.J., and DeGalan, L., 1980. On the determination of the hold-up time in reversed phase chromatography. J. Liq. Chromatogr., 3: 1669-1686.

Boehm, P.D., and Farrington, J.W., 1984. Aspects of the polycyclic aromatic hydrocarbon geochemistry of recent sediments. Environ. Sci. Technol., 18: 840-845.

Bojarski, J., and Ekiert, L., 1982. Relationship between molecular connectivity indices of barbiturates and chromatographic parameters. Chromatographia, 15: 172-176.

Bondi, A., 1964. Van der Waals volumes and radii. J. Phys. Chem., 68: 441-451.

Boumahraz, M., Davydov, V.Y., Gonzalez, M.E., and Kiselev, A.V., 1983. Intermolecular interactions in liquid adsorption chromatography. Chromatographia, 17: 143-148.

Bruggeman, W.A., van der Steen, J., and Hutzinger, O., 1982. Reversed-phase thin-layer chromatography of polynuclear aromatic hydrocarbons and chlorinated biphenyls. Relationship with hydrophobicity as measured by aqueous solubility and octanol-water partition coefficient. J. Chromatogr., 238: 335-346.

Brunauer, S., Emmett, D.H., and Teller, E., 1938. Adsorption of gases in multimolecular layers. J. Amer. Chem. Soc., 60:309-319.

Buytenhuys, F.A., and van der Maeden, F.P.B., 1978. Gel permeation chromatography on unmodified silica using aqueous solvents. J. Chromatogr., 149: 489-500.

Carr, C., and Riddick, J.A., 1951. Physical properties of methanol-water system. Ind. Eng. Chem., 43: 692-696.

Castellan, G.W., 1971. Physical Chemistry. Addison-Wesley, Reading, Mass., 866 pp.

Chang, C.A., and Huang, C.S., 1985. Effects of solvent composition and temperature on the separation of anilines with silica, amino, and diamine bonded phase columns. Anal. Chem., 57: 997-1005.

Chiou, C.T., 1985. Partition coefficients of organic compounds in lipid-water systems and correlations with fish bioconcentration factors. Environ. Sci. Technol., 19: 57-62.

Chiou, C.T., Peters, L.S., and Freed,V.H., 1979. A physical concept of soil-water equilibria for nonionic organic compounds. Science, 206: 831-832.

Chiou, C.T., Porter, P.E., and Schmedding, D.W., 1983. Partition dequilibria of nonionic organic compounds between soil organic matter and water. Environ. Sci. Technol., 17: 227-231.

Chmielowiec, J., and Sawatzky, H., 1979. Entropy dominated high performance liquid chromatographic separations of polynuclear aromatic hydrocarbons. Temperature as a separation parameter. J. Chromatog. Sci., 17: 245-252.

Colin, H., Diez-Masa, J.C., Guiochon, G., Czajkowska, T., and Miedziak, I., 1978. The role of the temperature in reversed-phase high-performance liquid chromatography using pyrocarbon-containing adsorbents. J. Chromatogr., 167: 41-65.

Colin, H., Krstulovic, A.M., Gonnord, M.F., Guiochon, G., Yun, Z., and Jandera, P., 1983. Investigation of selectivity in reversed-phase liquid chromatography--Effects of stationary and mobile phases on retention of homologous series. Chromatographia, 17: 9-15.

Davidson, J.M., and McDougal, J.R., 1973. Experimental and predicted movement of herbicides in a water-saturated soil. J. Environ. Qual., 2: 428-433.

Davydov, V.Y., Gonzalez, M.E., Kiselev, A.V., and Lenda, K., 1981. Physico-chemical applications of liquid chromatography II. Investigations of the surface properties of chemically modified silica gels and of the adsorption of cardiac glycosides from solutions. Chromatographia, 14: 13-18.

DiPaolo, T., Kier, L.B., and Hall, L.H., 1977. Molecular connectivity and structure-activity relationship of general anesthetics. Molec. Pharmacol., 13: 31-37.

Donnan, F.G., 1924. The theory of membrane equilibria. Chem. Rev., 1: 73-90.

Dorsey, J.G., 1984. Personal communication.

Dorsey, J.G., DeEchegaray, M.T., and Landy, J.S., 1983. Efficiency enhancement in micellar liquid chromatography. Anal. Chem., 55: 924-928.

Douheret, G., and Morenas, M., 1967. Sur les constantes dielectriques de quelques melanges hydroorganiques. C.R. Aca. Sci., Ser. C, 264: 729-731.

Dzombak, D.A., and Luthy, R.G., 1984. Estimating adsorption of polycyclic aromatic hydrocarbons on soils. Soil Science, 137: 292-308.

Edward, J.T., 1970. Molecular volumes and the Stokes-Einstein equation. J. Chem. Ed., 47: 261-270.

Engelhardt, H., Dreyer, B., and Schmidt, H., 1982. Properties and diversity of C18 bonded phases. Chromatographia, 16: 11-17.

Gale, R.L., and Beebe, R.A., 1964. Determination of heats of adsorption on carbon blacks and bone mineral by chromatography using the eluted pulse technique. J. Phys. Chem., 68: 555-567.

Gilpin, R.K., and Gangoda, M.E., 1984. Nuclear magnetic resonance of alkyl ligands immobilized on reversed-phase liquid chromatographic surfaces. Anal. Chem., 56: 1470-1473.

Grant, J.R., Dolan, J.W., and Snyder, L.R., 1979. Systematic approach to optimizing resolution in reversed-phase liquid chromatography, with emphasis on the role of temperature. J. Chromatogr., 185: 153-177.

Greene, S.S.A., and Pust, H., 1958. The determination of heats of adsorption by gas-solid chromatography. J. Phys. Chem., 62: 55-58.

Hafkenscheid, T.L., and Tomlinson, E., 1983. Observations on capacity factor determination for reversed-phase liquid chromatography with aqueous methanol eluents using the solubility parameter concept model and its derivatives. J. Chromatogr., 264: 47-62.

Halicioglu, T., and Sinanoglu, O., 1969. Solvent effects on cis-trans azobenzene isomerization: A detailed application of a theory of solvent effects on molecular association. Ann. N.Y. Acad. Sci., 158: 308-317.

Hall, L.H., Kier, L.B., and Murray, W.J., 1975. Molecular connectivity II: Relationship to water solubility and boiling point. J. Pharm. Sci., 64: 1974-1977.

Hammers, W.E., Muers, G.J., and DeLigny, C.L., 1982. Correlations between liquid chromatographic capacity ratio data on Lichrosorb RP-18 and partition coefficients in the octanol-water system. J. Chromatogr., 247: 1-13.

Hanai, T., and Hubert, J., 1984. Retention versus van der Waals volume and π energy in liquid chromatography. J. Chromatogr., 290: 197-206.

Handa, T., Yamauchi, T., Sawai, K., Yamamura, T., Koseki, Y., and Ishii, T., 1984. In situ emission levels of carcinogenic and mutagenic compounds from diesel and gasoline engine vehicles on an expressway. Environ. Sci. Technol., 18: 895-902.

Harkov, R., Greenberg, A., Darack, F., Daisey, J.M., and Lioy, P.J., 1984. Summertime variations in polycyclic aromatic hydrocarbons at four sites in New Jersey. Environ. Sci. Technol., 18: 287-291.

Harnisch, M., Mockel, H.J., and Schulze, G., 1983. Relationship between log P_{ow} from reversed-phase values and capacity factors derived from reversed-phase high-performance liquid chromatography for n-alkylbenzenes and some OECD reference substances. J. Chromatogr., 282: 315-332.

Hasan, M.N., and Jurs., P.C., 1983. Computer-assisted prediction of liquid chromatographic retention indexes of polycyclic aromatic hydrocarbons. Anal. Chem., 55: 263-269.

Hase, A., and Hites, R.A., 1976. On the origin of polycyclic aromatic hydrocarbons in the aqueous environment. In: L.H. Keith (Editor), Identification and Analysis of Organic Pollutants in Water. Ann Arbor Science, Ann Arbor, Michigan, pp. 205-214.

Helling, C.S., 1971. Pesticide mobility in soils II. Application of soil thin-layer chromatography. Soil Sci. Soc. Amer. Proc., 35: 737-743.

Hermann, R.B., 1972. Theory of hydrophobic bonding. II. The correlation of hydrocarbon solubility in water with solvent cavity surface area. J. Phys. Chem., 76: 2754-2759.

Hirata, Y., and Sumiya, E., 1983. Temperature-programmed reversed-phase liquid chromatography with packed fused-silica columns. J. Chromatogr., 267: 125-131.

Hornsby, A.G., and Rao, P.S.C., 1983. Energetics of sorption. In "Sorption and transport of toxic organic substances in soils: Evaluation of protocols and effects of solvent-mixtures." EPA CR-806744.

Horvath, C., and Melander, W., 1977. Liquid chromatography with hydrocarbonaceous bonded phases; Theory and practice of reversed phase chromatography. J. Chromatog. Sci., 15: 393-404.

Horvath, C., Melander, W., and Molnar, I., 1976. Solvophobic interactions in liquid chromatography with nonpolar stationary phases. J. Chromatogr., 125: 129-156.

Horvath, C., Melander, W., and Molnar, I., 1977. Liquid chromatography of ionogenic substances with nonpolar stationary phases. Anal. Chem., 49: 142-154.

Jandera, P., Colin, H., and Guiochon, G., 1982a. Interaction indexes for prediction of retention in reversed-phase liquid chromatography. Anal. Chem., 54: 435-441.

Jandera, P., Colin, H., and Guiochon, G., 1982b. Optimization of separation conditions in reversed phase liquid chromatography using complex solvent mixtures. Chromatographia, 16: 132-137.

Jinno, K., and Kawasaki, K., 1983a. Correlation between the retention data of polycyclic aromatic hydrocarbons and several descriptors in reversed-phase HPLC. Chromatographia, 17: 445-449.

Jinno, K., and Kawasaki, K., 1983b. Correlations between retention data of isomeric alkylbenzenes and physical parameters in reversed-phase micro high-performance liquid chromatography. Chromatographia, 17: 337-340.

Jinno, K., and Kawasaki, K., 1984a. Retention prediction of substituted benzenes in reversed-phase HPLC. Chromatographia, 18: 90-95.

Jinno, K., and Kawasaki, K., 1984b. The correlation between molecular polarizability of PAHs and their retention data on various stationary phases in reversed-phase HPLC. Chromatographia, 18: 103-105.

Jinno, K., and Ozaki, N., 1984. Enthalpy-entropy compensation of octylsilica stationary phase in reversed-phase HPLC. J. Liq. Chromatogr., 7: 877-882.

Jinno, K., Ozaki, N., and Sato, T., 1983. Elution characteristics of some solutes used to measure the column void time on reversed-phase stationary phases in micro-HPLC. Chromatographia, 17: 341-344.

Kamens, R., Bell, D., Dietrich, A., Perry, J., Goodman, R., Claxton, L., and Tejada, S., 1985. Mutagenic transformations of dilute wood smoke systems in the presence of ozone and nitrogen dioxide. Analysis of selected high-pressure liquid chromatography fractions from wood smoke particle extracts. Environ. Sci. Technol., 19: 63-69.

Karger, B.L., Gant, J.R., Hartfopf, A., and Weiner, P.H., 1976. Hydrophobic effects in reversed-phase liquid chromatography. J. Chromatogr., 128: 65-78.

Karickhoff, S.W., 1981. Semi-empirical estimation of sorption of hydrophobic pollutants on natural sediments and soils. Chemosphere, 10: 833-846.

Karickhoff, S.W., Brown, D.S., and Scott, T.A., 1979. Sorption of hydrophobic pollutants on natural sediments. Water Res., 13: 241-248.

Kay, B.D., and Elrick, D.E., 1967. Adsorption and movement of lidane in soils. Soil Sci., 104: 314-322.

Kenega, E.E., and Goring, C.A.I., 1980. Relationship between water solubility, soil sorption, octanol/water partitioning, and concentration of chemicals in biota. In: J.G. Eaton, P.R. Parrish, and A.C. Hendricks (Editors), Aquatic Toxicology. American Society of Testing Material, STP 707, pp. 78-115.

Kier, L.B., and Hall, L.H., 1976. Molecular Connectivity in Chemistry and Drug Research. Academic Press, New York, 257 pp.

Kikta, E.J., and Grushka, E., 1976. Retention behavior on alkyl bonded stationary phases in liquid chromatography. Anal. Chem., 48: 1098-1104.

Knox, J.H., and Vasvari, G., 1973. The performance of packings in high-speed liquid chromatography III. Chemicaly bonded pellicular materials. J. Chromatogr., 83: 181-194.

Koopmans, R.E., and Rekker, R.F., 1984. High-performance liquid chromatography of alkylbenzenes. Relationship with lipophilicities as determined from octanol-water partition coefficients or calculated from hydrophobic fragmental data and connectivity indices; Lipophilicity predictions for polyaromatics. J. Chromatogr., 285: 267-279.

Krstulovic, A.M., Colin, H., and Guiochon, G., 1982. Comparison of methods used for the determination of void volume in reversed-phase liquid chromatography. Anal. Chem., 54: 2438-2443.

Lamparczyk, H., Wilczynska, D., and Radecki, A., 1983. Relationship between the average molecular polarizabilities of polycyclic aromatic hydrocarbons and their retention indices determined on various stationary phases. Chromatographia, 17: 300-302.

Laub, R.J., and Madden, S.J., 1985. Solute retention in column liquid chromatography. VI. Enthalpy-entropy compensation: The column temperature and mobile-phase composition. J. Liq. Chromatogr., 8: 187-205.

Leffler, J., and Grunwald, E., 1963. Rates and Equilibria of Organic Reactions. Wiley, New York, 458 pp.

Leo, A., Hansch, C., and Elkins, D., 1971. Partition coefficients and their uses. Chem. Rev., 71: 525-616.

Lewis, G.N., and Randall, M., 1961. Thermodynamics. McGraw-Hill, New York, 723 pp.

Lumry, R., and Rajender, S., 1970. Enthalpy-entropy compensation phenomena in water solutions of proteins and small molecules: A ubiquitous property of water. Biopolymers, 9: 1125-1227.

Martin, A.J.P., and Synge, R.L.M., 1941. A new form of chromatogram employing two liquid phases. 1. A theory of chromatography. 2. Application to a micro-determination of the higher monoamino-acids in proteins. Biochem. J., 35: 1358-1368.

Martire, D.E., and Boehm, R.E., 1983. Unified theory of retention and selectivity in liquid chromatography. 2. Reversed-phase liquid chromatography with chemically bonded phases. J. Phys. Chem., 84: 1045-1062.

Mast, T.J., Hsieh, D.P.H., and Seiber, J.N., 1984. Mutagenicity and chemical characterization of organic constituents in rice staw smoke particulate matter. Environ. Sci. Technol., 18: 338-348.

McCall, P.J., Swann, R.L., Laskowski, D.A., Unger, S.M., Vrona, S.A., and Dishburger, H., 1980. Estimation of chemical mobility in soil from liquid chromatographic retention times. Bull. Environm. Contam. Toxicol., 24: 190-195.

Means, J.C., Wood, S.G., Hassett, J.J., and Banwart, W.L., 1980. Sorption of polynuclear aromatic hydrocarbons by sediments and soils. Environ. Sci. Technol., 14: 1524-1528.

Melander, W., Campbell, D.E., and Horvath, C., 1978. Enthalpy-entropy compensation in reversed-phase chromatography. J. Chromatogr., 158: 215-225.

Melander, W., Chen, B.K., and Horvath, C., 1979. Mobile phase effects in reversed-phase chromatography I. Concomitant dependence of retention on column temperature and eluent composition. J. Chromatogr., 185: 99-109.

Melander, W.R., Chen, B.K., Horvath, C., 1985. Mobile phase effects in reversed-phase chromatography VII. Dependence of retention of mobile phase composition and column temperature. J. Chromatogr., 318: 1-10.

Melander, W.R., Erard, J.F., and Horvath, C., 1983. Movement of components in reversed-phase chromatography I. Mobile phase space with multi-component eluents. J. Chromatogr., 282: 211-228.

Melander, W., and Horvath, C., 1980. Reversed-Phase Chromatography. In: C. Horvath (Editor), High-Performance Liquid Chromatography, Advances and Perspectives , Vol. 2. Academic Press, New York, pp. 114-319.

Melander, W.R., and Horvath, C., 1984. Mobile phase effects in reversed-phase chromatography VI. Thermodynamic models for retention and its dependence on mobile phase composition and temperature. Chromatographia, 18: 353-361.

Melander, W., Mannan, C.A., and Horvath, C., 1982. Mobile phase effects in reversed-phase chromatography IV. Retention by n-alkylbenzenes as a function of column temperature and the nature and concentration of organic co-solvent. Chromatographia, 15: 611-615.

Melander, W., Stoveken, J., and Horvath, C., 1980. Stationary phase effects in reversed-phase chromatography I. Comparison of energetics of retention on alkyl-silica bonded phases. J. Chromatogr., 199: 35-56.

Miller, M.L., Linton, R.W., Bush, S.G., and Jorgenson, J.W., 1984. Correlation of retention behavior with quantitative surface analysis of octadecyl bonded chromatographic supports. Anal. Chem., 56: 2204-2210.

Mills, A.C., and Biggar, J.W., 1969. Adsorption of 1,2,3,4,5,6-hexachlorocyclohexane from solution: The differential heat of adsorption applied to adsorption from dilute solutions on organic and inorganic surfaces. J. Coll. Interface Sci., 29: 720-731.

Mingelgrin, J., and Gerstl, Z., 1983. Reevaluation of partitioning as a mechanism of nonionic chemicals adsorption in soils. J. Environ. Qual., 12: 1-11.

Mizushima, S.I., 1954. Structure of Molecules and Internal Rotation. Academic Press, New York, 244 pp.

Murray, W.J., Hall, L.H., and Kier, L.B., 1975. Molecular connectivity III: Relationship to partition coefficients. J. Pharm. Sci., 64: 1978-1981.

Neff, J.M., 1979. Polycyclic Aromatic Hydrocarbons in the Aquatic Environment. Applied Science Publishers, Ltd., Essex, England, 262 pp.

Nemethy, G., and Scheraga, H.A., 1962. Structure of water and hydrophobic bonding in proteins. II. Model for the thermodynamic properties of aqueous solutions of hydrocarbons. J. Chem. Phys., 36: 3401-3417.

Nkedi-Kizza, P., Rao, P.S.C., and Hornsby, A.G., 1985. Influence of organic co-solvents on sorption of hydrophobic organic chemicals by soils. Environ. Sci. Tech. (in press).

Nkedi-Kizza, P., Rao, P.S.C., and Johnson, J.W., 1983. Adsorption of diuron and 2,4,5-T on soil particle-size separates. J. Environ. Qual., 12: 195-197.

Nys, G.G., and Rekker, R.F., 1973. Statistical analysis of a series of partition coefficients with special reference to the predictability of foding of drug molecules. The introduction of hydrophobic fragmental constants (f values). Chimie Therapeutique, 5: 521-538.

Pankow, J.F., Isabelle, L.M., and Asher, W.E., 1984. Trace organic compounds in rain. 1. Sampler design and analysis by adsorption/thermal desorption (ATD). Environ. Sci. Technol., 18: 310-318.

Prahl, R.G., Crecelius, E., and Carpenter, R., 1984. Polycyclic aromatic hydrocarbons in Washington coastal sediments: An evaluation of atmosperhic and riverine routes of introduction. Environ. Sci. Technol., 18: 687-693.

Pye, V.I., and Patrick, R., 1983. Ground water contamination in the United States. Science, 221: 713-718.

Randic, M., 1975. On characterization of molecular branching. J. Am. Chem. Soc., 97: 6609-6615.

Rao, P.S.C., and Davidson, J.M., 1979. Adsorption and movement of selected pesticides at high concentrations in soils. Water Res., 13: 375-380.

Rao, P.S.C., Hornsby, A.G., Kilcrease, D.P., and Nkedi-Kizza, P., 1985. Sorption and transport of toxic organic substances in aqueous and mixed-solvent systems. Jour. Environ. Qual. (in press).

Rao, P.S.C., and Nkedi-Kizza, P., 1983. Pesticide sorption on whole soils and soil-size separates. In: Estimation of parameters for modeling the behavior of selected pesticides and orthophosphate. EPA-600/11-83-XXX.

Reinhard, M., Goodman, N.L., and Barker, J.F., 1984. Occurrence and distribution of organic chemicals in two landfill leachate plumes. Environ. Sci. Technol., 18: 953-961.

Sabljic, A., 1984. Predictions of the nature and strength of soil sorption of organic pollutants by molecular topology. J. Agric. Food Chem., 32: 243-246.

Sadek, P.C., and Carr, P.W., 1984. Study of solute retention in reversed-phase high-performance liquid chromatography on hydrocarbonaceous and three fluorinated bonded phases. J. Chromatogr., 288: 25-41.

Sander, L.C., and Field, L.R., 1980. Effect of eluent composition on thermodynamic properties in high-performance liquid chromatography. Anal. Chem., 52: 2009-2013.

Sander, L.C., and Wise, S.A., 1984. Synthesis and characterization of polymeric C_{18} stationary phases for liquid chromatography. Anal. Chem., 56: 504-510.

Schoenmakers, P.J., Billiet, H.A.H., and DeGalan, L., 1983. Description of solute retention over the full range of mobile phase compositions in reversed-phase liquid chromatography. J. Chromatogr., 282: 107-121.

Schoenmaker, P.J., Billiet, H.A., Tijssen, R., and DeGalan, L., 1978. Gradient selection in reversed-phase liquid chromatography. J. Chromatogr., 149: 519-537.

Scott, R.P.W., and Kucera, P., 1977. Examination of five commercially available liquid chromatographic reversed phases (including the nature of the solute-solvent-stationary phase interactions associated with them). J. Chromatogr., 142: 213-232.

Scott, R.P.W., and Simpson, C.F., 1980. Solute-solvent interactions on the surface of reversed phases. I. Stationary phase interactions and their dependence on bonding characteristics. J. Chromatogr., 197: 11-20.

Sinanoglu, O., 1968. Solvent Effects on Molecular Associations. In: B. Pullman (Editor), Molecular Associations in Biology. Academic Press, New York, pp. 427-445.

Snyder, L.R., 1979. Temperature-induced selectivity in separations by reversed-phase liquid chromatography. J. Chromatogr., 179: 167-172.

Snyder, L.R., Dolan, J.W., and Gant, J.R., 1979. Gradient elution in high-performance liquid chromatography I. Theoretical basis for reversed-phase systems. J. Chromatogr., 165: 3-30.

Snyder, L.R., and Kirkland, J.J., 1979. Introduction to Modern Liquid Chromatography. John Wiley and Sons, New York, 863 pp.

Stahlberg, J., and Almgren, M., 1985. Polarity of chemically modified silica surfaces and its dependence on mobile-phase composition by fluorescence spectrometry. Anal. Chem., 57: 817-821.

Swann, R.L., McCall, P.J., Laskowski, D.A., Unger, S.M., and Dishburger, H.J., 1979. Fourth ASTM Symposium on Aquatic Toxicology, Chicago: ASTM Philadelphia.

Tanaka, N., Goodell, H., and Karger, B.L., 1978. The role of organic modifiers on polar group selectivity in reversed-phase liquid chromatography. J. Chromatogr., 158: 233-248.

Tchapla, A., Colin, H., and Guiochon, G., 1984. Linearity of homologous series retention plots in reversed-phase liquid chromatography. Anal. Chem., 56: 621-625.

Testa, B., 1979. Principles of Organic Stereochemistry. Marcel Dekker, New York, 248 pp.

Timmermans, J., 1960. Physiochemical Constants of Binary Systems in Concentrated Solutions, Vol. 4. Interscience, New York, 1326 pp.

Todd, D.K., 1980. Groundwater Hydrology. John Wiley and Sons, New York, 535 pp.

Valvani, S.C., Yalkowsky, S.H., and Amidon, G.L., 1976. Solubility of nonelectrolytes in polar solvents. VI. Refinements in molecular surface area computations. J. Phys. Chem., 80: 829-836.

Veith, G.D., Austin, N.M., and Morris, R.T., 1979. A rapid method for estimating log P for organic chemicals. Water Res., 13: 43-47.

Walters, R.W., and Luthy, R.G., 1984. Equilibrium adsorption of polycyclic aromatic hydrocarbons from water onto activated carbon. Environ. Sci. Technol., 18: 395-403.

Wasik, S.P., Tewari, Y.B., Miller, M.M., and Martire, D.E., 1981. Octanol/water partition coefficients and aqueous solubilities of organic compounds. National Bureau of Standards, NBSIR 81-2406.

Wauchope, R.D., Savage, K.E., and Koskinen, W.C., 1983. Adsorption-desorption equilibria of herbicides in soil: Naphthalene as a model compound for entropy-enthalpy effects. Weed Science, 31: 744-751.

Wells, M.J.M., 1981. Ph.D. thesis, Auburn University.

Wells, M.J.M., and Clark C.R., 1981. Liquid chromatographic elution characteristics of some solutes used to measure column void colume on C_{18} bonded phases. Anal. Chem., 53: 1341-1345.

Wells, M.J.M., and Clark, C.R., 1982. Investigation of n-alkylbenzamides by reversed-phase liquid chromatography IV. The study of a homologous series of n-alkylbenzamides using the solvophobic theory and molecular connectivity. J. Chromatogr., 243: 263-277.

Wells, M.J.M., and Clark, C.R., 1984. Study of the relationship between dynamic and static equilibrium methods for the measurement of hydrophobicity. Comparison of capacity factors and partition coefficients for some 5,5-disubstituted barbituric acids. J. Chromatogr., 284: 319-335.

Wells, M.J.M., Clark, C.R., and Patterson, R.M., 1982. Investigation of n-alkylbenzamides by reversed-phase liquid chromatography III. Correlation of chromatographic parameters with molecular connectivity indices for the C_1-C_5 n-alkylbenzamides. J. Chromatogr., 235: 61-74.

Wise, S.A., Bonnett, W.J., Guenther, F.R., and May, W.E., 1981. A relationship between reversed-phase C18 liquid chromatographic retention and the shape of polycyclic aromatic hydrocarbons. J. Chromatogr. Sci., 19: 457-465.

Wise, S.A., and May, W.E., 1983. Effect of C_{18} surface coverage on selectivity in reversed-phase liquid chromatography of polycyclic aromatic hydrocarbaons. Anal. Chem., 55: 1479-1485.

Woodburn, K.B., Rao, P.S.C., Fukui, M., and Nkedi-Kizza, P., 1985. Solvophobic approach for predicting sorption of hydrophobic organic chemicals on synthetic sorbents and soils. Contam. Hydrology (in press).

Yalkowsky, S.H., Orr, R.J., and Valvani, S.C., 1979. Solubility and partitioning. 3. The solubility of halobenzenes in water. Ind. Eng. Chem. Fundam., 18: 351-353.

Yalkowsky, S.H., and Valvani, S.C., 1979. Solubilities and partitioning. 2. Relationships between aqueous solubilities, partition coefficients, and molecular surface areas of rigid aromatic hydrocarbons. J. Chem. Eng. Data, 24: 127-129.

BIOGRAPHICAL SKETCH

Kent B. Woodburn was born on May 3, 1956, in Hyattsville, Maryland, and grew up in nearby College Park, Maryland. In 1978, he received a B.S. degree in chemistry from the University of Maryland in College Park. An interest in the chemistry of natural water systems led Mr. Woodburn to the University of Wisconsin-Madison, where he received an M.S. degree in water chemistry in the spring of 1982. Later that year he was married to his wife, Janet, and began his Ph.D. studies at the University of Florida under the direction of Dr. Joseph Delfino. Mr. Woodburn is currently a Ph.D. candidate in the Department of Environmental Engineering Sciences at the University of Florida, specializing in the field of environmental chemistry.

I certify that I have read this study and that in my opinion it conforms to acceptable standards of scholarly presentation and is fully adequate, in scope and quality, as a dissertation for the degree of Doctor of Philosophy.

Joseph J. Delfino, Chairman
Professor of Environmental
Engineering Sciences

I certify that I have read this study and that in my opinion it conforms to acceptable standards of scholarly presentation and is fully adequate, in scope and quality, as a dissertation for the degree of Doctor of Philosophy.

Eric R. Allen
Professor of Environmental
Engineering Sciences

I certify that I have read this study and that in my opinion it conforms to acceptable standards of scholarly presentation and is fully adequate, in scope and quality, as a dissertation for the degree of Doctor of Philosophy.

Palakurthi S. Rao
Associate Professor of Soil
Science

I certify that I have read this study and that in my opinion it conforms to acceptable standards of scholarly presentation and is fully adequate, in scope and quality, as a dissertation for the degree of Doctor of Philosophy.

Arthur G. Hornsby

Arthur G. Hornsby
Associate Professor of Soil Science

I certify that I have read this study and that in my opinion it conforms to acceptable standards of scholarly presentation and is fully adequate, in scope and quality, as a dissertation for the degree of Doctor of Philosophy.

John G. Dorsey

John G. Dorsey
Assistant Professor of Chemistry

This dissertation was submitted to the Graduate Faculty of the College of Engineering and to the Graduate School and was accepted as partial fulfillment of the requirements for the degree of Doctor of Philosophy.

August 1985

Hubert A. Bevis

Dean, College of Engineering

Dean, Graduate School